Deciphering the Interlink between STAT3 and MAPKs in Ischemia/Reperfusion and Ischemic Conditioning

Zeina Harhous

N°d'ordre NNT: 2019LYSE1145

THESE de DOCTORAT DE L'UNIVERSITE DE LYON
opérée au sein de
l'Université Claude Bernard Lyon 1
en Cotutelle avec
L'Université Libanaise-LIBAN

Ecole Doctorale ED 205
Ecole Doctorale Interdisciplinaire Sciences- Santé (EDISS)
Spécialité de doctorat : Biologie

Discipline : Physiologie, Biologie des organismes, populations, interactions

Soutenue publiquement le 20/09/2019, par :

Zeina HARHOUS

Deciphering the Interlink between STAT3 and MAPKs in Ischemia/Reperfusion and Ischemic Conditioning

---

Devant le jury composé de :

Mme. ELSIBAI Mirvat, Prof., Lebanese American University	Rapporteure
Mme. PINET Florence, Prof., Institut de Pasteur de Lille, Lille	Rapporteure
Mme. ITANI Hana, PhD, American University of Beirut, Beyrouth	Examinatrice
M. VAN-COPPENOLLE Fabien, Prof., Université Claude Bernard Lyon1, Lyon	President
M. BIDAUX Gabriel, PhD, Université Claude Bernard Lyon 1, Lyon	Directeur de thèse
M. KURDI Mazen, Prof., Université Libanaise, Beyrouth	Co-directeur de thèse
Mme. SOULAS Emmanuelle, Prof., Université Claude Bernard Lyon 1, Lyon	Invitée

Acknowledgements

A thesis is a life-changing experience, during which we move out of our comfort zones to pursue our goals. I'm very grateful for the people who crossed my path during these three years and left their own impact. I hereby extend my sincere gratitude to:

***The respected jury members,** thank you for dedicating your time and energy to read and attend my thesis.*

***Prof. Ovize**, thank you for welcoming me as a member in your team and giving me the opportunity to learn from you and all the team members.*

***Dr. Gabriel**, it's basically you who truly knows the ups, downs and challenges of this work. Thank you for pushing me to the limits and provoking me to give the best of what I have. Thank you for the remarkable impact you made in my life on the scientific and personal levels. Thank you for being a brilliant researcher to whom I will always look up. Thank you for all our discussions and all what you have taught me. I am privileged to be your student and will forever be!*

***Prof. Mazen**, thank you for being the first with whom my journey began and for opening up the first door. Thank you for believing in my potentials and for supporting me from the very beginning up till now. Thank you for the good times, good knowledge and good memories. Thank you for investing in me and trusting me ever since I've been your student. You will always have your special place and I will also always be your student.*

***Prof. Emannuelle**, thank you for accepting to be my co-supervisor and for the help you offered once needed.*

***Sally**, our friendship started in the second year of our BS. Since then, we became companions of the ups and downs, of the new beginnings, of the successes, of the changes, of the challenges, of the laughter, of the tears, of the talks and journeys. Thank you for being my "home" here and for being a very special person in my life. We started all together and we're going to end it up together. Cheers for all the upcoming bright days that we're going to share ... Love you <3.*

***Maya**, your presence made our days brighter and our hearts warmer. You are not less than a baby sister. Thank you for what you've brought to my life and to all what we've shared together. You are a building block of our home here. Our Saturday nights, talks, walks and memories will forever be a remarkable beautiful part of my memories in Lyon. Love you <3*

***Nolwenn**, my fara ..kifik? we shared a lot of beautiful times in the lab and outside it. Thank you for all the beautiful memories we made together, for the help you offered when needed, for the cute Lebanese words you keep on using, for loving me, for hiding and scaring me always :p, for being a true "majnune". Ra7 ishta2lik and Bhibbik <3.*

***Mallory**, « tick tick tick yammi Sleiman » … I know you will never forget this song. Thank you for your peaceful giving spirit and for always offering your kind help. I wish you all the best dear ☺*

***Alex** .. « Alexandre le Grand » .. your presence added a special touch to our life in the lab. Thank you for the fun and the happy ambiance that you add. Thank you for the beautiful moments that you left in our memory. I will truly miss you!*

***Camille and Ribal**, thank you for being there from the very beginning. Camille, thank you for all what you have taught me since the beginning of my thesis and for the beautiful times we shared inside the lab and outside it. I'm always ready to offer Lebanese courses, with pleasure ;). Ribal, no words are enough to thank you dear. Thank you for being a true brother and for everything you have done for us. Thank you for the beautiful memories we created. You were an important part of our lives here in Lyon and we will always miss you. I wish you and Camille the best of what you both truly deserve :)!*

***Claire**, I can't describe how special you are to my heart. Thank you for always listening and supporting. Thank you for your care and love. Thank you for being uniquely special just the way you are! We are lucky to have someone like you in the lab. I deeply and truly love you <3*

***Melanie and Ludo**, thank you for all what you taught me throughout these three years. Melanie, thank you for your positive vibes, energy and smile that always bright up the lab! Ludo, thank you for all the discussions we had about science and life, for always being ready to teach and help, for making the lab a better place, for always reminding me of the lab coat :p … and now I can finally tell you "I finishhhhheddddd".*

***Noelle**, it's because of you that I started speaking French .. "Je jeté?". Thank you for all what you have taught me and for all the help you offered during this period. You've been a caring mother here, and your presence was heart-warming.*

***Delphine**, thank you for your kindness and all the help you offer whenever needed.*

***Lionel**, thank you for all the help and fun spirit you have. You always draw a smile on my face :). Don't forget that I've been once your assistant for the "couchon":p.*

***Bruno**, bonsoiiiirrrrrr, I am very grateful for all the work we have done together. Thank you for always finding time for my urgent experiments and for always managing my work "perfectly: p".*

***Yves**, thank you for the good joyful vibes you always spread around, for State of art of inspection and for the perfect blots that I have never seen :p!*

***Fabrice**, thank you for all what you taught me from your long experience in the world of molecular biology.*

***René, Joe, Christophe, Fabien, Sylvie** thank you for all the shared moments in the lab, and for being ready to help when needed.*

***Mumu**, thank you for always managing all our administrative stuff and always helping us to solve any issue. Thank you also for caring about everyone and handling all the laboratory responsibilities :)*

***Andrea, Marie, Jenny, Christelle and Megane**, thank you for the good times and all the help.*

***Maher**, you were and will always be a unique irreplaceable friend. Thank you for always being there, as a wise listener, supporter and an advisor. Thank you for all what we have learned and shared together. Regardless the distance, you were a major part of this period abroad :)*

***Dana, Malak, Salma, Shireen, Sylva**: our friendship started back from the elementary classes. Here we are today, standing as young women and witnessing each other's growth and development. Thank you for what we have lived together and for all what we are gonna share in the upcoming days. I love you <3*

*Finally, I'm all I am because of my loving **family** which God have blessed me with. I am forever grateful for the support and unconditional love which I have received ever since I was young. You will always come first, wherever I go and whatever I do. I love you <3*

"The pursuit of knowledge is a never-ending journey. The day we stop seeking knowledge is the day we stop growing".

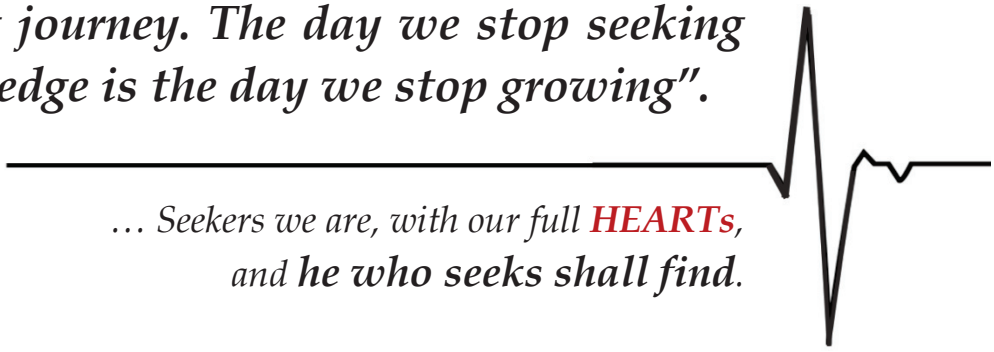

… Seekers we are, with our full ***HEARTs****,*
and ***he who seeks shall find****.*

Résumé

Les maladies cardiovasculaires sont une des principales causes de morbidité et de mortalité au monde. La plus courante est l'infarctus du myocarde définit pathologiquement par la mortalité cellulaire dû à une ischémie prolongée d'une partie du ventricule gauche. L'ischémie est caractérisée par un apport sanguin insuffisant causé par une obstruction d'une artère coronaire. La restauration, en clinique, du flux sanguin, appelée reperfusion, est considérée comme la méthode la plus efficace contre les dommages ischémiques. Paradoxalement, cette restauration du flux sanguin est associée à une exacerbation de la lésion tissulaire, entraînant alors des lésions d'ischémie-reperfusion (I/R). Dans le but de limiter ces lésions, le conditionnement ischémique myocardique est une avancée majeure dans le domaine de la cardioprotection. Ce protocole confère ses effets cardioprotecteurs via le recrutement de divers mécanismes endogènes suivant l'activation de deux voies intracellulaires : la voie RISK (Reperfusion Injury Salvage Kinase) et/ou la voie SAFE (Survivor Activator Factor Enhancer). Ces voies impliquent l'activation de différentes cascades de signalisation et de protéines kinases. En particulier, concernant la voie SAFE, le transducteur de signal et l'activateur de transcription-3 STAT3, a été identifié comme un acteur clé dans le postconditionnement ischémique (PostCI). Il est suggéré que les effets cardioprotecteurs attribués à STAT3 soient liés à ses effets en tant que facteur de transcription et en tant que régulateur de l'activité mitochondriale, mais tout n'est pas encore connu. En revanche, il est admis que STAT3 est activé par la phosphorylation ciblant les résidus tyrosine 705 et sérine 727.

Dans nos travaux actuels, nous avions initialement pour objectif d'étudier les rôles cardioprotecteurs mitochondriaux de STAT3 après une I/R et un PostCI. Cependant, nous n'avons pas été en mesure de détecter STAT3 dans les mitochondries de cardiomyocytes adultes de souris, dans des conditions basales et de stress, en utilisant différentes approches. Fait intéressant, nous avons montré une localisation exclusive de STAT3 dans les myocytes cardiaques adultes, le long des tubules T, et nous avons mis en évidence les inconvénients des techniques précédemment utilisées.

Outre les rôles putatifs de STAT3 dans les mitochondries, nous avons ciblé ses effets dans la signalisation et la génomique au cours de l'I/R et du PostCI. Nous avons tout d'abord cherché à déterminer, pendant l'I/R et le PostCI, la cinétique temporelle d'activation de STAT3 et des autres kinases de la voie RISK, notamment Akt et les MAPK ERK1 / 2, JNK et p38. En outre, nous avions pour objectif d'étudier les liens entre les voies SAFE et RISK en déchiffrant les liens entre STAT3 et les kinases RISK au cours du PostCI. Nous avons montré qu'après une ischémie et un temps court de reperfusion, STAT3 et ERK1/2 sont activés, et que l'utilisation d'un PostCI active d'autant plus STAT3 en induisant exclusivement la phosphorylation de sa tyrosine. Nous avons également montré que l'interconnexion entre les voies SAFE et RISK, dans le protocole PostCI utilisé, se fait par STAT3 et ERK1/2. À partir de ces résultats, nous nous sommes dirigés vers la génomique grâce à laquelle nous avons étudié l'activité de STAT3 au cours de l'IPoC. À cet égard, nous avons montré que STAT3 est impliqué dans la régulation de la réponse inflammatoire au cours de la PostCI.

Dans l'ensemble, cette étude présente une approche globale des fonctions mitochondriales, de signalisation et génomiques de STAT3 dans le contexte de la protection cardiaque.

Abstract

Cardiovascular diseases are leading causes of morbidity and mortality worldwide. Among the mostly prevailing cardiovascular diseases is myocardial infarction, which is pathologically defined as myocardial death due to a prolonged ischemia. Ischemia is an insufficient supply of blood caused by a blockade in the coronary arteries. The early restoration of blood flow is considered the most effective method against the ischemic lesions. Paradoxically, this blood flow restoration is associated with an exacerbation of the tissue injury, leading to the ischemia-reperfusion (I/R) injury. To avoid this injury, the myocardial ischemic conditioning protocol has rejuvenated the field of cardioprotection. This protocol confers its cardioprotective effects via recruiting various endogenous mechanisms following the activation of two intracellular pathways: the reperfusion injury salvage kinase (RISK) or survivor activator factor enhancer (SAFE) pathways. These pathways involve the activation of different signaling cascades and protein kinases. Zooming in through the SAFE pathway, the signal transducer and activator of transcription-3, STAT3, has been identified as a prominent key player in ischemic postconditioning (IPoC). The cardioprotective effects attributed to STAT3 are suggested to be linked to its roles as a transcription factor and as a regulator of the mitochondrial activity, but these are not well studied and elaborated. STAT3 is activated by phosphorylation, which targets the tyrosine 705 and serine 727 residues.

In our current work, we initially aimed to investigate the mitochondrial cardioprotective roles of STAT3 following I/R and IPoC. However, we were not able to detect STAT3 in the mitochondria of adult mouse cardiomyocytes under various

basal and stress conditions using different approaches. Interestingly, we showed an exclusive STAT3 pattern in adult cardiac myocytes, along the T-tubules, and highlighted drawbacks of previously used techniques.

Aside from the mitochondrial roles of STAT3, we targeted its signaling and genomic roles during I/R and IPoC. We first aimed to determine, during I/R and IPoC, the temporal kinetics of activation of STAT3 and the other kinases of the RISK pathway including Akt and the MAPKs ERK1/2, JNK and p38. In addition, we aimed to decipher the interlink between the SAFE and RISK pathways through deciphering the interlink between STAT3 and the RISK kinases following IPoC. We showed that a short reperfusion time activates STAT3 and ERK1/2 following ischemia, and that the application of IPoC further activates STAT3 through inducing its tyrosine phosphorylation. We also showed that the interlink between SAFE and RISK pathways, in the IPoC protocol we used, is through STAT3 and ERK1/2. From this signaling level, we moved toward the genomic level whereby we investigated the genomic activity of STAT3 during IPoC. In this regard, we have shown that STAT3 is involved in the regulation of the inflammatory response during IPoC.

Overall, this study presents a global approach of STAT3's mitochondrial, signaling and genomic functions in the context of cardiac protection.

Table of Contents

List of Publications and Communications i
List of Figures and Tables iii
List of Abbreviations vi
Introduction 1
Chapter 1: The Cardiovascular System 3
1. Definition of the Cardiovascular System 3
2. Components of the Cardiovascular System 3
2.1. Blood Vessels 3
2.2. Blood 4
2.3. The Heart 4
2.3.1. Heart Anatomy 4
2.3.2. Heart Function 9
3. Cardiovascular diseases 12
Chapter 2: Myocardial Infarction 13
1. Myocardial Infarction Definition 13
2. The Ischemic Lesions 15
3. Reperfusion Lesions 18
3.1. The Reperfusion Injury Features 19
3.2. Cell death mechanisms of Reperfusion injury 21
Chapter 3: Post-myocardial Infarction Inflammatory Response 24
1. Activation of Inflammatory Response 24
2. Mediators of the Inflammatory Response 25
2.1. Endothelial Cells 25
2.2. Neutrophils 26
2.3. Monocytes and Macrophages 27
2.4. Lymphocytes 27
2.5. Dendritic Cells (DCs) 28
2.6. Cardiac Fibroblasts 28
2.7. Inflammasomes 29
Chapter 4: The Mitochondria in Ischemia Reperfusion 31
1. Mitochondrial Structure 31
2. Mitochondrial Function 31
2.1. Oxidative Phosphorylation (OxPhos) 32

2.2. The Membrane Potential (ΔΨm) 33
2.3. ROS Generation 33
2.4. Calcium Handling and mPTP opening 34
3. Mitochondria in IRI 35
Chapter 5: Cardioprotection against Myocardial infarction 36
1. Ischemic Preconditioning (IPC) 37
2. Ischemic Postconditioning (IPoC) 38
3. Cardioprotective Signaling pathways 39
3.1. The RISK pathway 41
3.1.1. The signaling cascades 41
3.1.2. Activation and downstream signal 42
3.1.3. Mechanisms of cardioprotection 42
3.1.4. Controversial Issues of RISK pathway 43
3.2. The SAFE pathway 43
3.2.1. Signaling cascades 43
3.2.2. Activation and downstream signal 44
3.2.3. Mechanisms of cardioprotection 44
3.2.4. Controversial Issues of SAFE pathway 45
3.3. Interlink RISK-SAFE 46
Chapter 6: STAT3 47
1. Definition and Structure 47
2. Post-translational modifications and Activation 47
2.1. Phosphorylation 48
2.1.1. Tyrosine Phosphorylation 48
2.1.2. Serine Phosphorylation 49
2.2. Acetylation 50
3. Pharmacological inhibition 50
4. Cellular STAT3 pools 51
51
4.1. Nuclear STAT3 51
4.2. Mitochondrial STAT3 52
5. STAT3 in Cardioprotection 52
5.1. STAT3 in IRI 53
5.2. STAT3 in Ischemic Conditioning 53
6. STAT3 in Cardiac Inflammation 54
6.1. STAT3 in Inflammatory Cytokine Signaling 54

6.2. STAT3 in neutrophils/macrophages recruitment ... 55
6.3. STAT3 in macrophages Polarization ... 55
MATERIALS and METHODS ... 59
1. Biological Models ... 60
1.1. In Vivo Models ... 60
1.1.1. Animals ... 60
1.1.2. Acute Myocardial Ischemia-Reperfusion (IR) Injury ... 60
1.1.3. Ischemic Post-Conditioning (IPoC) ... 61
1.1.4. In Vivo Inhibitors ... 61
1.1.5. Infarct Size Measurement ... 62
1.2. *In vitro* Models ... 63
1.2.1. Culture of H9C2 ... 63
1.2.2. Experimental groups of H9C2 ... 63
1.3. Ex vivo Model of Cardiomyocytes ... 65
1.3.1. Cardiomyocytes Isolation ... 65
1.3.2. Hypoxia-Reoxygenation of cardiomyocytes ... 65
1.3.3. Stattic treatment of cardiomyocytes ... 66
2. Biochemical Analysis ... 66
2.1. Western Blotting ... 66
2.1.1. Principle ... 66
2.1.2. Protocol ... 66
2.2. Immunofluorescence (IF): ... 70
2.2.1. Principle ... 70
2.2.2. Protocol of immuno-labeling ... 70
2.3. Mass spectrometry ... 72
3. Mitochondrial Activity ... 72
3.1. Mitochondrial Extraction ... 72
3.1.1. Crude Mitochondrial Extraction ... 72
3.1.2. Pure Mitochondrial Extraction ... 73
3.2. Mitochondrial Functioning ... 74
3.2.1. Aerobic Respiration (Oxidative phosphorylation) ... 74
3.2.2. Calcium Retention Capacity (CRC) ... 75
4. Molecular Biology Techniques ... 76
4.1. RNA Extraction ... 76
4.2. cDNA Synthesis ... 76
4.3. Polymerase Chain Reaction (PCR) ... 77

4.4. Gene Ontology (GO) Enrichment Analysis ... 79
5. Statistical Analysis ... 81
RESULTS ... 87
Section I: Mitochondrial STAT3 ... 87
Section II: STAT3 in signaling and transcription ... 110
Part I. Signaling ... 111
1. The in vitro Interlink ... 111
1.1. The MEK/ERK – STAT3 Interlink ... 111
1.2. The PI3/Akt - STAT3 Interlink ... 112
1.3. The JNK – STAT3 Interlink ... 112
1.4. The P38 – STAT3 Interlink ... 113
1.5. A Competitive Relationship Exists between PY705 and PS727 STAT3 phosphorylation ... 113
2. The in vivo Kinetics and Correlation during I/R and IPoC ... 115
2.1. Kinetics of Phosphorylation of STAT3 following I/R and IPoC ... 116
2.2. Kinetics of Phosphorylation of ERK1/2 MAPK following IR and IPoC ... 117
2.3. Kinetics of Phosphorylation of the MAPKs JNK and P38 during IR and IPoC 118
2.4. Kinetics of Phosphorylation of Akt during IR and IPoC ... 119
2.5. The *in vivo* ratios of PS727/PY705 following IR and IPoC ... 120
Part II. Genomics ... 123
1. In vivo Drug Efficiency ... 125
2. Necrotic Area Determination ... 126
3. Gene Analysis ... 127
3.1. Selection of time point ... 128
3.2. Selection of genes ... 129
3.3. Significant STAT3-dependent genes ... 130
3.4. Significant STAT3-dependent genes ... 130
3.5. Inflammatory approach ... 133
Section III: Collaborative work ... 139
DISCUSSION ... 145
CONCLUSION and PERSPECTIVES ... 158
REFERENCES ... 159

List of Publications and Communications

Publications

Critical appraisal of STAT3 pattern in adult cardiomyocytes.
Zeina Harhous, Sally Badawi, Noelle Gallo Bona, Bruno Pillot, Lionel Augeul, Melanie Paillard, George W. Booz, Emmanuelle Canet-Soulas, Michel Ovize, Mazen Kurdi**, Gabriel Bidaux*. Journal of Molecular and Cellular Cardiology 131 (2019) 91–100 https://doi.org/10.1016/j.yjmcc.2019.04.021.

Deciphering the crosslink between STAT3 and MAPKs in ischemia-reperfusion and ischemic postconditioning.
Zeina Harhous, Sally Badawi, Alex Pacallet, Bruno Pillot, Lionel Augeul, Fabrice Gonnot, Michel Ovize, Mazen Kurdi, Gabriel Bidaux. (In preparation)

An Update on the multifaceted Roles of STAT3 in the Heart
Zeina Harhous, George Booz, Gabriel Bidaux, Mazen Kurdi.
(Review Article – To be submitted end of June 2019)

A dynamic transcriptional analysis reveals IL-6 axis as a prominent mediator of surgical acute response in non-ischemic mouse heart.
Sally Badawi, Alexandre Paccalet, *Zeina Harhous*, Bruno Pillot, Lionel Augeul, Fabien Van Coppenolle, Joel Lachuer, Mazen Kurdi, Claire Crola da Silva, Michel Ovize and Gabriel Bidaux*. (Under revision in *Frontiers in Physiology*)

Loss of MFN2 induces metabolic reprogramming and confers resistance to hypoxia.
Gouriou Y, Alam MR, *Harhous Z*, Crola C, Baetz D, Badawi S, Lefai E, Rieusset J, Durand A, Harisseh R, Gharib A, Bidaux G§ & Ovize M§. (In preparation)

Multilabeling analysis by flow cytometry of mouse adult cardiac myocytes in suspension exposed to hypoxia-reoxygenation
Alexandre Paccalet•[1], Nolwenn Tessier•[1], Melanie Paillard[1], Lucille Païta[1], Ludovic Gomez[1], Noëlle Gallo Bona[1], Christophe Chouabe[1], Christelle Léon[1], Sally Badawi[1], Zeina Harhous[1], Michel Ovize[1,2] and Claire Crola Da Silva[1]* (Under revision in *Scientific Reports).*

Decreased mitochondrial deacetylase activity with age, independently of SIRT3, compromises the beneficial effect of heart ischemic post-conditioning in mice.
Villedieu C, Pillot B, Harisseh R, Augeul L, Gallo-Bona N, *Harhous Z*, Al-Mawla R, Bochaton T, Gharib A, Ovize M & Baetz D (In preparation)

Communications

2019 - GRRC
Lille - International session oral presentation

2019 - Les 29es Journées Européennes de la Société Française de Cardiologie
Paris - Poster

2018 - International Society of Heart Research (ISHR-EU)
Amsterdam - Poster

2018 - GRRC
Montpellier - Poster

2018 - Sante Fédération de Recherche
Lyon - Oral presentation

(2016-2018) EDISS and EDST Scientific days

Lyon and Beirut - Oral presentations and posters

List of Figures and Tables

Figure 1. The main blood circuits entering and leaving the heart 4

Figure 2. The different heart chambers 5

Figure 3. The cardiac valves 6

Figure 4. Structure of cardiomyocytes 8

Figure 5. The cardiac Cycle 10

Figure 6. The cardiac filaments 11

Figure 7. The cardiac excitation-contraction coupling 12

Figure 8. Myocardial infarction 14

Figure 9. The area at risk representation 15

Figure 10.The main proponents of acute myocardial IRI 17

Figure 11. Cell death during ischemia and reperfusion 18

Figure 12. The pro-inflammatory response induced by DAMPs 25

Figure 13. Diverse roles of inflammatory cells in the pathophysiology of MI 28

Figure 14. NLRP3 Formation in Cardiomyocytes 29

Figure 15. The Electron transport chain 33

Figure 16. The three types of Ischemic Conditioning 37

Figure 17. Ischemic post conditioning decreases the reperfusion injury lesions 39

Figure 18. Schematic mechanisms of cardioprotection by ischemic postconditioning 40

Figure 19. The different STAT3 domains. 47

Figure 20. The JAK-STAT pathway activation 49

Figure 21. STAT3 nuclear and mitochondrial pools 51

Figure 22. The different used in vivo animal groups 62

Figure 23. The scheme of the different inhibitors used in vitro 64

Figure 24: Scatter plots of the three used reference genes 78

Figure 25: Illustration of STRING function 80

Figure 26: Illustration of the predictive networks in STRING 80

Figure 27: The effect of MEK/ERK inhibition on STAT3 phosphorylation 111

Figure 28. The effect of PI3K inhibition on STAT3 phosphorylation 112

Figure 29. The effect of JNK inhibition on STAT3 phosphorylation 112

Figure 30. The effect of P38 inhibition on STAT3 phosphorylation 113

Figure 31. The competitive relationship between PY705 and PS727 STAT3 114

Figure 32. The in vitro interlink between STAT3 and MAPKS 114

Figure 33. Representative scheme of the different in vivo conditions 115

Figure 34. Kinetics of variation in STAT3 phosphorylation level following I/R and IPoC 116

Figure 35. Kinetics of variation in ERK1/2 phosphorylation levels following I/R and IPoC 117

Figure 36. Kinetics of variation in JNK and P38 phosphorylation levels following I/R and IPoC 118

Figure 37. Kinetics of variation in Akt phosphorylation levels following I/R and IPoC .. 119

Figure 38. The ratios of phosphorylation levels of S727-STAT3 to Y705-STAT3 120

Figure 39. Representative plots for the kinetics of phosphorylation of STAT3 and ERK1/2 under I/R and IPoC 121

Figure 40. The investigation of STAT3's transcriptional activity under inhibitory conditions. 122

Figure 41. Representative scheme of the in vivo experiments of the genomics section 123

Figure 42. The time points of the dynamic transcriptomic analysis 124

Figure 43. The in vivo validation of the inhibitors doses 125

Figure 44. Percentages of necrotic areas to healthy areas under different conditions 126

Figure 45. PCA plot of STAT3-induced genes clustered over time 128

Figure 46. STEM analysis clustering profiles at the different time points 129

Figure 47. The families of biological functions for Stattic-dependent genes. 131

Figure 48. The families of biological functions for PD-dependent genes 132

Figure 49. The families of biological functions of the common GO terms 132

Figure 50. The Shell of interacting proteins obtained from Stattic-dependent genes. 134

Figure 51. The expression levels of some inflammatory markers under DMSO treatment during IR and IPoC 136

Figure 52. The expression levels of STAT3 and Cxcl-1 during IPoC, under DMSO and Stattic treatment 137

Figure 53. The network of transcription factors retrieved from the enrichment analysis of DEGs in the sham model 140

Figure 54. IL-6 increases in plasma of sham mice following 45 mins of surgery 141

Figure 55. The phosphorylation levels in the remote areas 143

Figure 56. The expression levels of Socs3 during IR, under DMSO and Stattic treatment 144

Figure 57. The Inflammatory GO Terms regulated by Stattic and PD98059 152

Figure 58. The IL6-STAT3-Socs3 loop effect during I/R 156

Table 1. The list of the used reagents for the in vitro studies 64

Table 2: The list of primary antibodies used in Western blotting 69

Table 3: The list of secondary antibodies used in Western blotting 69

Table 4 : The list of primary Antibodies used in immunofluorescence 71

Table 5: The list of secondary antibodies used in immuno fluorescence 71

Table 6: List 1 of PCR Primers 82

Table 7: List 2 of PCR Primers 83

Table 8: List 3 of PCR Primers 84

Table 9: List 4 of PCR Primers 86

List of Abbreviations

AAR: Area at Risk

ATP: Adenosine Triphosphate

CMs: Cardiomyocytes

CRC: Calcium Retention Capacity

DAMPS: Damage Associated Molecular Pattern

DMSO: Dimethyl Sulfoxide

ERK: Extracellular Signal Regulated Kinase

ETC: Electron Transport Chain

FACS: Fluorescence Activated Cell Sorting

GO: Gene Ontology

IF: Immuno Fluorescence

IL6/10: Interleukin 6/10

IPoC: Ischemic Post Conditioning

IR: Ischemia Reperfusion

IRI: Ischemia Reperfusion Injury

JAK: Janus Kinase

JNK: c-Jun Kinase

KO: Knock Out

LIF: Leukemia Inhibitory Factor

M1/2: Macrophages Type1/2

MAPKs: Mitogen Activated Protein Kinase

MI: Myocardial Infarction

mPTP: mitochondrial Permeability Transition Pore

PCR: Polymerase Chain Reaction

PD: PD98059

PI3K: Phospho Inositol-3 Kinase

RISK: Reperfusion Injury Salvage Kinase

ROS: Reactive Oxygen Species

S727: Serine 727 residue

SAFE: Survivor Activator Factor Enhancer

SOCS3: Suppressor of Cytokine Signaling 3

STAT3: Signal Transducer and Activator of Transcription 3

STRING: Search Tool for the Retrieval of Interacting Genes/Proteins

WB: Western Blotting

Y705: Tyrosine 705 residue

ΔΨm: Membrane Potential

Introduction

Human life is nothing less than a miracle, dwelling through a single-celled zygote and growing up to a system of organs forming our embryos. In human embryology, the 22nd day marks the first heartbeat, the beat of life. Standing as the core organ of life, the human heart is the earliest functioning organ. Ironically, this core organ of life lies as a core organ of death, whereby cardiac diseases are the leading causes for morbidity and mortality worldwide.

According to the World Health Organization (WHO), cardiovascular diseases result in 17.5 million global deaths per year. Financially speaking, the American Heart Association estimated the global cost of cardiovascular diseases in 2010 to be around 863 billion dollars. This alarming situation represents a crushing health and economic burden for the nations. Therefore, a pressing need is recognized for increasing awareness and taking bold actions to scale up the prevention and management of risk factors. In order to build an improved health, we primarily need to understand the causes and mechanisms underlying these diseases, along with finding preventive and treatment molecules and protocols. Here lies the importance of cardiovascular research, manifested by a huge number of studies conducted in this field.

Among the mostly prevailing cardiovascular diseases is myocardial infarction, which is thoroughly studied in cardiovascular research. It is pathologically defined as myocardial death due to a prolonged ischemia, an insufficient supply of blood caused by a blockade in the coronary arteries. The early restoration of blood flow is considered the most effective method against the ischemic lesions. Paradoxically, this blood flow restoration is associated with an exacerbation of the tissue injury, leading to the ischemia-reperfusion injury. To avoid this injury, the myocardial ischemic conditioning protocol have rejuvenated the field of cardioprotection. This protocol confers its cardioprotective effects via recruiting various endogenous mechanisms following the activation of two intracellular pathways: the reperfusion injury salvage kinase (RISK) or survivor activator factor enhancer (SAFE) pathways. These pathways involve the activation of different signaling cascades and protein kinases. Zooming in through the SAFE pathway, the signal transducer and activator of transcription-3, STAT3, has been identified as a prominent key player in the

cardioprotective effects of ischemic conditioning. As a signaling molecule and a transcription factor, its plays various cardioprotective roles.

In our current work, we aimed to study the kinetics of activation of STAT3 and other different kinases activated following cardiac ischemia reperfusion and ischemic conditioning, in addition to deciphering the interlink between the different activated signaling kinases and STAT3. From this proteomic level, we moved to the genomic level whereby we aimed to study the involvement of STAT3, as a transcription factor, in regulating the expression of selective genes during ischemic conditioning.

Chapter 1: The Cardiovascular System

The human body is a system of systems, functioning in synchrony and harmonization to keep us living. To understand the human body as a whole, we need to decipher the complexity of its harmonized systems, passing through the organs, tissues and cellular levels. Among the different systems lies the cardiovascular one, a central system which contains the heart, the vital organ standing as "the heart of life".

1. Definition of the Cardiovascular System

The cardiovascular system, also called the circulatory system or vascular system, is a multi-organ system which permits blood circulation throughout the body. It has three main components: The heart, blood and vessels. The heart is the pump which pushes blood into organs, tissues and cells. The vessels are the delivery routes used to carry the blood to its destination. They include a complex network of arteries, veins and capillaries. The blood is responsible for delivering oxygen and nutrients to every cell in the body, and it collects the carbon dioxide and wastes made by these cells [1], [2].

2. Components of the Cardiovascular System

2.1. Blood Vessels

Blood vessels include veins, arteries and capillaries which deliver blood throughout the body. Veins carry blood from the body back to the heart, while arteries carry blood from the heart to the body. The capillaries are microscopic blood vessels which connect arteries and veins together. Among all these vessels, few main blood ones connect to the different chambers of the heart. They include the aorta, pulmonary arteries/veins and vena cava (Inferior and superior). Like all your muscles, the heart needs oxygen to work. This oxygen is brought to the heart by the coronary arteries **Fig. 1** [1], [2]

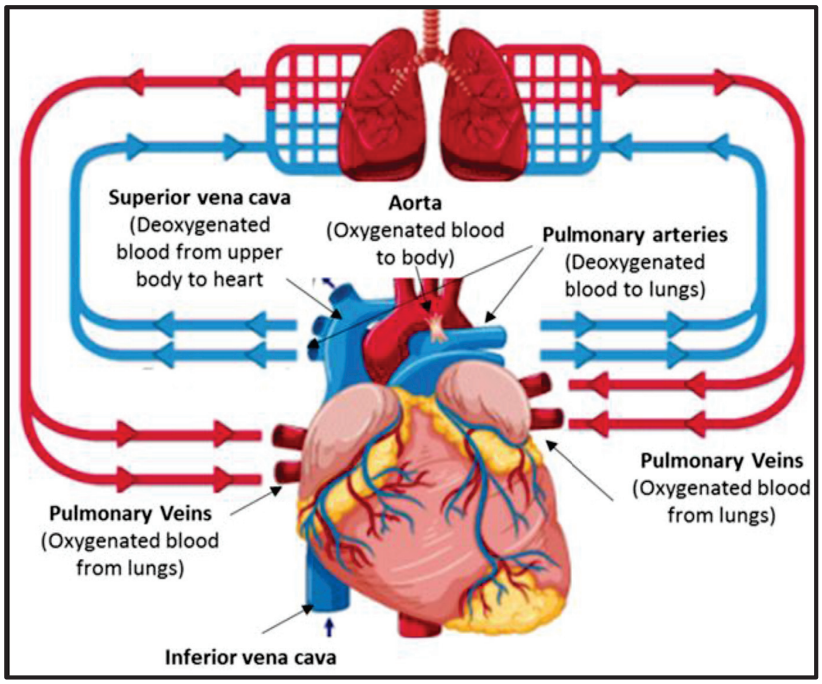

Figure 1. The main blood circuits entering and leaving the heart

A representative scheme showing blood circulation from and to the heart. The blue circuit indicates deoxygenated blood, while the red one indicates oxygenated blood [3].

2.2. Blood

The blood is both a tissue and a fluid. It is considered a tissue since it is a collection of similar specialized cells (45%) which serve particular functions. It is a fluid, because these cells are suspended in a liquid matrix, plasma (55%). The plasma is largely water, containing proteins, nutrients, hormones, antibodies, and dissolved waste products. The blood cells include erythrocytes (red blood cells), leukocytes (white blood cells) and thrombocytes (platelets) [3], [4].

2.3. The Heart

2.3.1. Heart Anatomy

The heart is a muscular organ which pumps blood throughout the body, permitting the body cells to receive oxygen and nutrients. In most people, it is located on the left side of the chest in the thoracic cavity between the lungs [5], [6].

A- **Cardiac chambers**

The heart contains four chambers which contract in a specific order to allow the efficient pumping through both circuits. It is divided into two parts, the left and right sides, separated by a septum and containing an atrium and a ventricle each. The right and left atria are the smaller chambers of the heart, and they have thinner, less muscular walls. While the right and left ventricles are larger chambers with stronger, thicker walls. They pump blood to the organs at high pressures.

The right atrium receives de-oxygenated blood, collected from the body, through the inferior and superior vena cava and pump it into the right ventricle. The latter pumps blood through the pulmonary artery to the lungs, where the blood is oxygenated, at high pressure. The oxygenated blood then returns, through the pulmonary veins, to the left atrium, which pumps this blood into the left ventricle. The left ventricle finally pumps oxygenated blood throughout the rest of the body **Fig. 2** [1], [5].

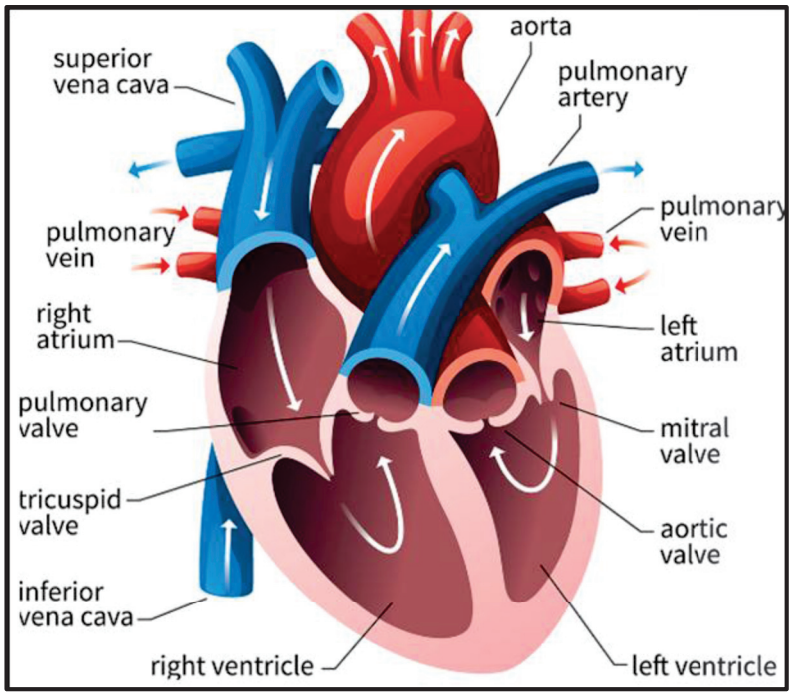

Figure 2. The different heart chambers

A schematic representation of the different cardiac chambers, along with the main arteries and veins.

B- **Cardiac Valves**

Heart valves are fibrous flaps of tissues presented in the heart to ensure that the blood flows in the right direction between the chambers and in blood vessels. They are gates which prevent the back flow of blood in the wrong direction. They are located between the atria and ventricles (atrioventricular), and between ventricles and the main arteries (semilunar) **Fig. 3**.

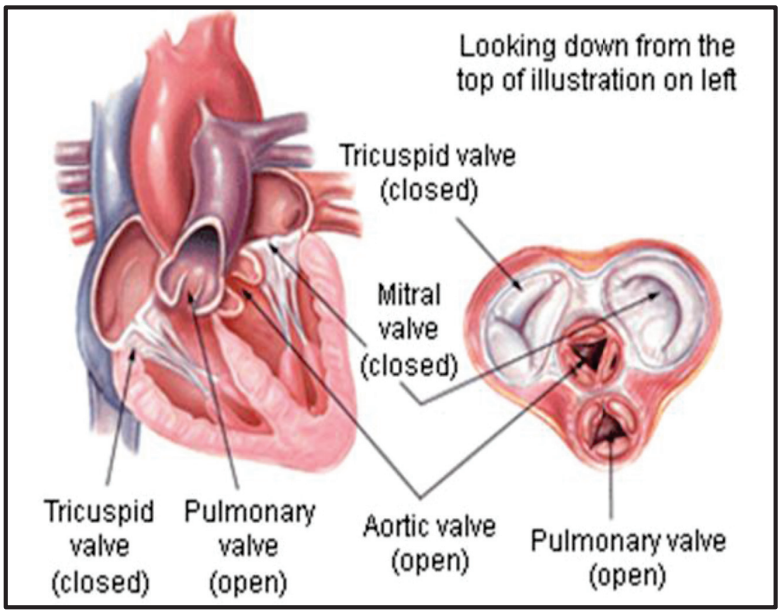

Figure 3. The cardiac valves

A representative scheme of the different cardiac valves including the mitral, tricuspid, aortic and pulmonary valves [8].

C- **The Cardiac Muscle**

The heart is composed of four layers: The pericardium, epicardium, myocardium, endocardium. Each layer has its own function, which primarily helps the pumping action of the heart. The epicardium is the outermost layer of the heart wall. It is a thin layer of serous membrane that helps to lubricate and protect the outside of the heart. As for the endocardium, it is the innermost squamous endothelium layer, which lines the inside of the heart. It is in direct contact with the lumen and consists of an endothelium that lines each chamber. In between these two layers lies the myocardium, which is the middle muscular layer of the heart wall composed of the cardiac muscle [7], [8].

The cardiac muscle is very unique, being striated and having an exceptional ability to initiate and spread an electrical potential that triggers the contractile mechanism [9]. Two types of cardiac muscle cells exist: myocardial contractile cells (cardiomyocytes) and myocardial conducting cells. The myocardial contractile cells constitute the majority of the cells in the atria and ventricles (99%). They are responsible for contractions that pump blood through the body. While the myocardial conducting cells (1%) form the conduction system of the heart. They initiate and propagate the action potential that triggers cardiac contraction [10]. The blood to this myocardium is supplied by the coronary arteries. Any occlusion in these arteries can lead to diseases due to the cut of the oxygen supply [11].

D- **Cardiac Cells**

Multiple resident cells contribute to maintain the structure and function of the heart over the life-time. The adult mammalian heart is composed mainly of cardiomyocytes, fibroblasts (FBs), endothelial cells (ECs) and peri-vascular cells. In addition, neurons, stem cells and immune cells are also presented [12].

- **Cardiomyocytes (CMs)**

Given the function of the heart in contracting and pumping blood, cardiac muscle cells, also called cardiomyocytes, are key resident cells. However, the majority of myocardial cells are non-cardiomyocytes. CMs account for 30-40% of cardiac mammalian cells, but they occupy 70–85% of the mammalian heart volume [13]. Each cardiac myocyte is surrounded by a lipid bilayer constituting the cell membrane, called the sarcolemma. The sarcolemma contains membrane proteins, which include receptors, pumps, and channels. It forms two specialized regions of the myocyte, the intercalated disks and the transverse tubular system. The intercalated disks are cell-cell junctions, serving as a strong mechanical linkage among myocytes and as a path which allows rapid conduction of action potential between myocytes. Transverse tubules, or T tubules, are invaginations of the sarcolemma into the myocyte, forming a barrier between the intracellular and extracellular spaces. These extensions closely bring L-type Ca2+ channels and the sarcoplasmic reticulum Ca2+ discharge system, rendering the T-tubular system an important structural component in excitation-contraction coupling **Fig. 4** [14]–[16].

CMs have a high mitochondrial content essential for the steady supply of ATP required to sustain cardiac contraction. They also contain the contractile proteins actin (thin filaments) and myosin (thick filaments) together with the regulatory proteins troponin and tropomyosin. The detailed contraction machinery is described later on in this chapter [10].

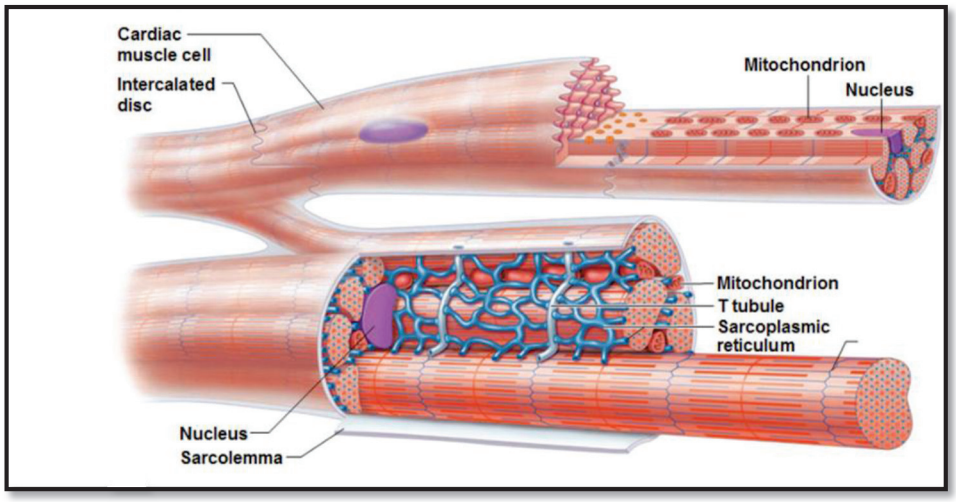

Figure 4. Structure of cardiomyocytes

A representative scheme showing the general internal structure and organization of a cardiomyocyte. Adapted from [19]

- **Endothelial Cells (ECs)**

Endothelial cells (ECs) make up the largest proportion (60%) of non-myocytes in the adult heart. They are squamous cells forming the endothelium. They form a single cell layer that lines all blood vessels and regulates the exchanges between the bloodstream and the surrounding tissues. Overall, ECs play important roles in heart development, in vascular homeostasis, in cardiomyocyte organization promotion and survival, in addition to roles in healing and regeneration after cardiac injury. Vascular ECs are also a key site for regulation of inflammatory cell recruitment following myocardial infarction (described later) [12].

- **Fibroblasts (FBs)**

Fibroblasts are responsible for the production of interstitial collagen. They are distributed throughout the cardiac tissue, surrounding myocytes and bridging ''the spaces'' between myocardial tissue layers, such that every cardiomyocyte is closely related to a fibroblast in a normal cardiac tissue. Overall, FBs contribute to cardiac development, myocardial structure, cell signaling, and electro-mechanical function in healthy and diseased myocardium. Pathological cardiac states are frequently associated with myocardial remodeling involving fibrosis. The growth of the fibrous tissue content is based on the proliferative potential of FBs and their ability to synthesize the extra-cellular matrix proteins [17].

2.3.2. Heart Function

A- The Cardiac Cycle

The cardiac cycle is the term used to describe the relaxation and contraction occurring when the heart pumps blood through the body. The period of contraction is called the systole, while that of relaxation, is called diastole, the phase during which the chambers are filled with blood**.** This cycle represents a heartbeat. Every single heartbeat includes three major stages: atrial systole, ventricular systole, and complete cardiac diastole **Fig. 5** [18], [19].

- **Atrial systole**

During this phase, the atria contract causing blood pumping into the ventricles. It lasts approximately 100 ms and ends prior to ventricular systole, as the atrial muscles relax.

- **Ventricular systole**

During this phase, ventricles contract and eject blood into the pulmonary artery or aorta, depending on the side. This phase lasts around 270 msec.

- **Complete cardiac diastole**

During this phase, the four cardiac chambers relax and are filled with blood once again, ensuring the repetition of the cycle. This phase lasts around 430 msec.

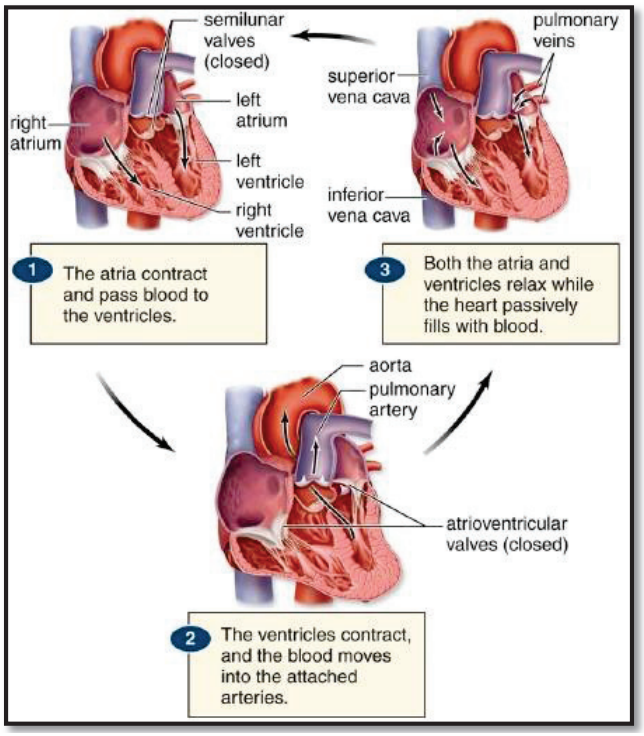

Figure 5. The cardiac Cycle

A representative scheme showing the three main steps of the cardiac cycle, and representing heartbeat [23]

B- Cardiac Contractility

The global heart contraction starts at the level of a single cardiomyocyte through the excitation-contraction coupling. This coupling is triggered by an action potential and is achieved by converting a chemical signal into mechanical energy via the action of contractile proteins. Calcium is the crucial mediator which couples electrical excitation to physical contraction through cycling from and to the myocyte's cytosol during each action potential [20].

- **Contractile Apparatus**

In order to understand the mechanism of contractility of a cardiomyocyte, it is important to have in mind the components of the contractile apparatus. The basic contractile unit in the myocyte is the sarcomere. It is composed of the contractile proteins myosin, actin, tropomyosin and troponin. Myosin is the thick filament, which has a filamentous tail and a globular head region. Actin, tropomyosin and troponin make up the thin filament. The interaction between the myosin globular head and actin in the presence of ATP results in

cross-bridge formation, allowing the sliding of the thick filaments on the fine filaments and sarcomere shortening. This sarcomere shortening resembles the cardiomyocyte contraction **Fig. 6** [14].

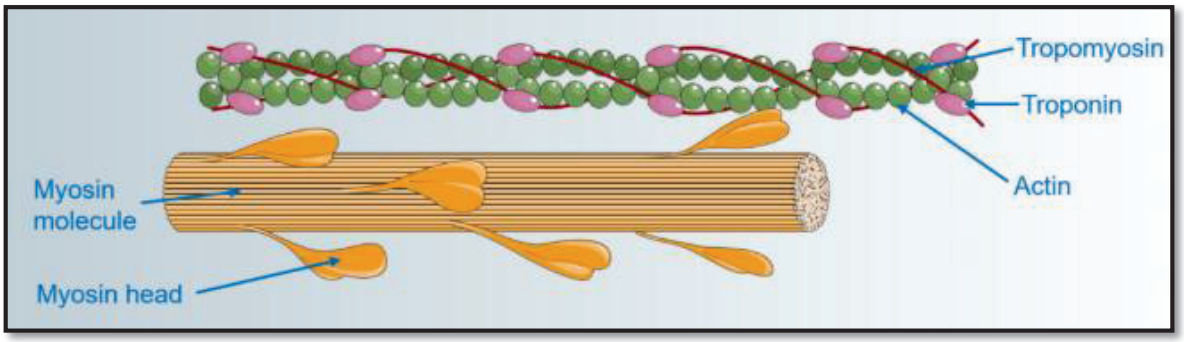

Figure 6. The cardiac filaments

A representative scheme showing the different cardiac filaments, including the thin and the thick ones.

- **Excitation-contraction coupling**

As an action potential travels along the sarcolemma and down into the T-tubule system, it induces local cell membrane depolarization. This causes L-type calcium channels to open, permitting calcium entrance to the cells. The increase in the cytosolic concentration triggers a subsequent release of the calcium stored in the sarcoplasmic reticulum (SR) through calcium-release channels termed ryanodine receptors (RyRs).

Consequently, the cytosolic calcium concentration drastically rises, what enables calcium binding to troponin and causes a conformational change in tropomyosin, leading to the exposing of an active site between actin and myosin. Consequently, myosin's head binds to actin and changes conformation, leading to a cross-bridge formation. This permits the myosin head to swing toward the thin filament. The cross-bridge formation and the conformational change of the myosin head result in the hydrolysis of ATP and the binding of a new ATP molecule. Concomitantly, calcium is uptaken by the mitochondria where it enhances the production of the needed ATP. The binding of new ATP causes release of the existing cross-bridge in preparation for the formation of a new one. The cycle of cross-bridge formation will continue until the Ca2+ is removed from the cytoplasm **Fig. 7** [14], [20].

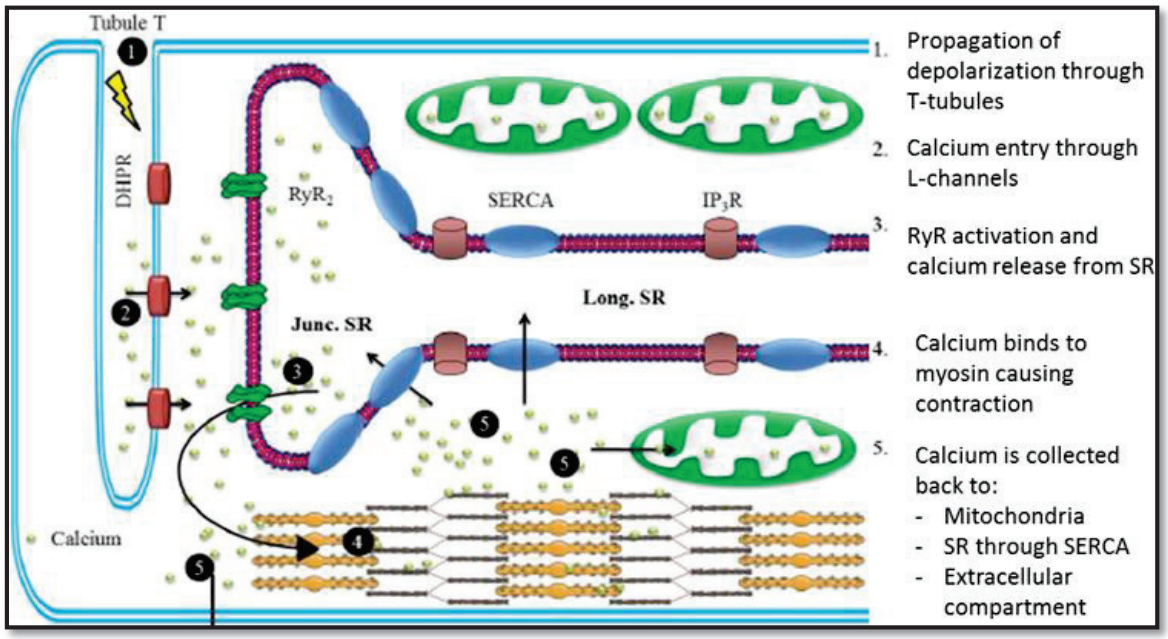

Figure 7. The cardiac excitation-contraction coupling

A representative diagram showing the different steps involved in the cardiomyocyte contraction-excitation coupling, starting from the propagation of the depolarization signal.

3. Cardiovascular diseases

Cardiovascular diseases (CVDs) are the diseases that involve the heart and blood vessels. They are caused by different underlying mechanisms, which vary according to the disease. The majority of the CVDs is associated with a buildup of fatty deposits inside the arteries (atherosclerosis) and with an increased risk of blood clots. As we already stated, these diseases are responsible for over 17.3 million deaths per year, as reported by the WHO. Among the different CVDs is the ischemic heart disease, referred to as myocardial infarction. Myocardial infarction is the pathological model targeted in our current work, whereby we explain its underlying mechanisms along with the cardioprotective approaches applied for diminishing its lesions.

Chapter 2: Myocardial Infarction

The heart is one of the most energy demanding tissues in the body, depending on mitochondrial oxidative phosphorylation for the huge supply of ATP. In order to fuel this ATP production, reducing molecules (NADH and FADH2) and oxygen should be supplied. At the cellular level, ATP is essential for the proper functioning of cardiac cells including membrane transport, chemical compounds synthesis and, most importantly, mechanical functioning (contraction and relaxation). During normal cardiac work, around 2/3 of the ATP is used for the contractile function, while the remaining 1/3 is used for ion pumps. Thus, any deficiency in the production of ATP is accompanied with adverse pathological cardiac effects. Hereby, cardiac ischemia stands as a major cause of many myocardial pathologies, among which myocardial infarction lies [21]–[23].

1. Myocardial Infarction Definition

Myocardial infarction (MI), medically referred to as heart attack, is a major cause of global death. Pathologically, it is defined as a myocardial necrotic cell death due to sustained and significant ischemia in the cardiac muscle. Cardiac ischemia results from an obstruction in the flow of blood to a specific area in the cardiac muscle, leading to a decreased oxygen and nutrients supply [24], [25]. Following the onset of myocardial ischemia, histological cell death does not occur immediately, but it takes a short period of time to develop (starting 20 minutes) in some animal models [26]. It takes several hours before myocardial necrosis can be identified by macroscopic or microscopic examination. The complete necrosis of myocardial cells at risk requires at least 2–4 hours. Overall, the complete process leading to a healed infarction usually takes at least 5–6 weeks [25]. Ischemic cell death during a myocardial infarction leads to a multiphase reparative response in which the damaged tissue is replaced by a fibrotic scar produced by fibroblasts [27] **Fig. 8**.

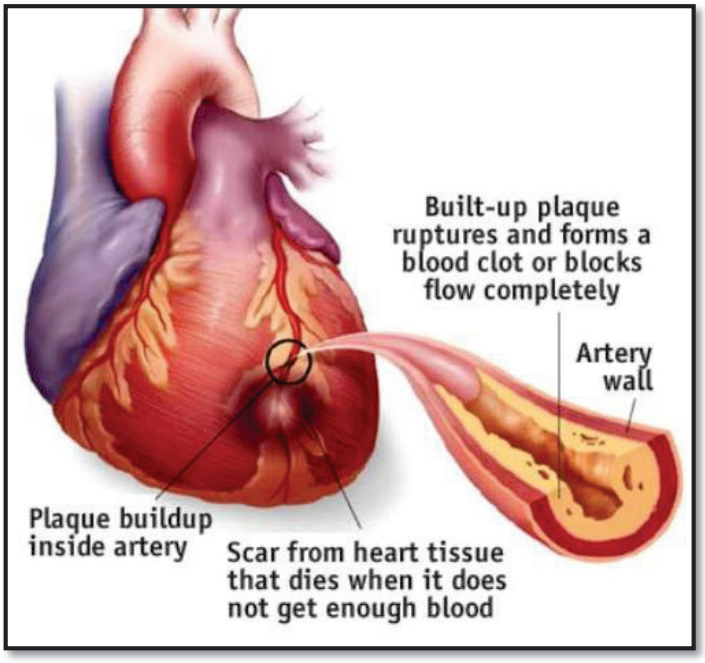

Figure 8. Myocardial infarction

Representative scheme of a heart subjected myocardial infarction resulting from a blockage in one of its arteries, due to the build-up of plaque.

The restoration of the blood flow to the ischemic area, a process termed reperfusion, has become the standard in-hospital treatment due to its ability to salvage the ischemic myocardium. This restoration of blood flow can salvage ischemic myocardium, and it is achieved by various pharmacological or surgical ways. Paradoxically though, the restoration of the blood flow to the ischemic area generates oxidative stress, which presents, on its own, a major cause of myocardial injury [28], [29].

In order to well understand the pathology of MI and reperfused myocardial injury, it is important to understand the pathology and mechanisms of their underlying causes, the ischemia and ischemia/reperfusion injuries.

2. The Ischemic Lesions

Myocardial ischemia is a term used to denote the deficiency in the blood supply to a specific area in the heart due to an obstruction in the coronary arteries. It is characterized by an imbalance between the myocardial oxygen supply and demand, leading to a diminished energy production[30]. This ischemic insult, characterized by low energy production, induces severe structural and functional changes at the level of cardiomyocytes within 30 to 40 minutes of coronary occlusion, leading to irreversible necrotic death. These changes include the depletion of glycogen supplies, abnormal contractility of myofibrils, along with nuclear and mitochondrial changes [26]. The functioning of the cells is affected by the duration and magnitude of ischemia [31].

Studies have shown that not all cells in the ischemic myocardium die simultaneously, whereby ischemic cells in the peripheral epicardial myocardium are available for salvage for a longer period of time, up to hours following the ischemic insult. Due to this fact, the infarcted area (IA) and the area at risk (AAR) are characterized. The AAR represents the whole myocardial perfusion area distal to an occluded coronary artery and is a major determinant of final infarct size. During an acute coronary event, the myocardium in the AAR progresses into necrosis through a 'wavefront' phenomenon, starting at the central subendocardial tissue and moving toward the periphery of the AAR **Fig. 9** [32].

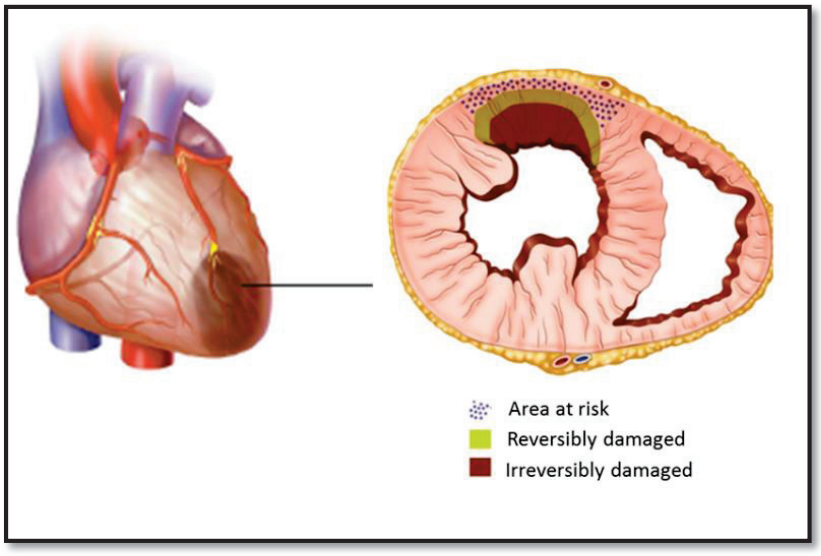

Figure 9. The area at risk representation

A representative scheme showing the area at risk with its reversibly damaged region and the irreversibly damaged one.

Following the deprivation of oxygen and nutrients supply, the mitochondrial oxidative phosphorylation is impaired. This progressively leads to an ATP depletion and mitochondrial membrane depolarization. To maintain the mitochondrial membrane potential, the mitochondrial ATP synthase functions in a reversible manner, where ATP is hydrolyzed leading to an increase in ADP and inorganic phosphate. Meanwhile, the cellular metabolism is shifted to anaerobic respiration, whereby pyruvate is reduced to lactate by lactate dehydrogenase in a process which produces H^+ ions. This reduces the intracellular pH, rendering it an acidic one. The Na+/H+ ion exchanger is then activated, causing H+ to be extruded from the cell and Na+ ions to be uptaken. Consequently, the $2Na+/Ca^{2+}$ ion exchanger is activated, and the cell this time extrudes Na+ while uptaking Ca^{2+}. This results in a Ca^{2+} overload inside the cell [33]. The lack of ATP during ischemia impairs the function of the 3Na+-2K+ ATPase, thereby inducing an intracellular Na+ overload besides the Ca^{2+} overload **Fig. 10** [33]–[35].

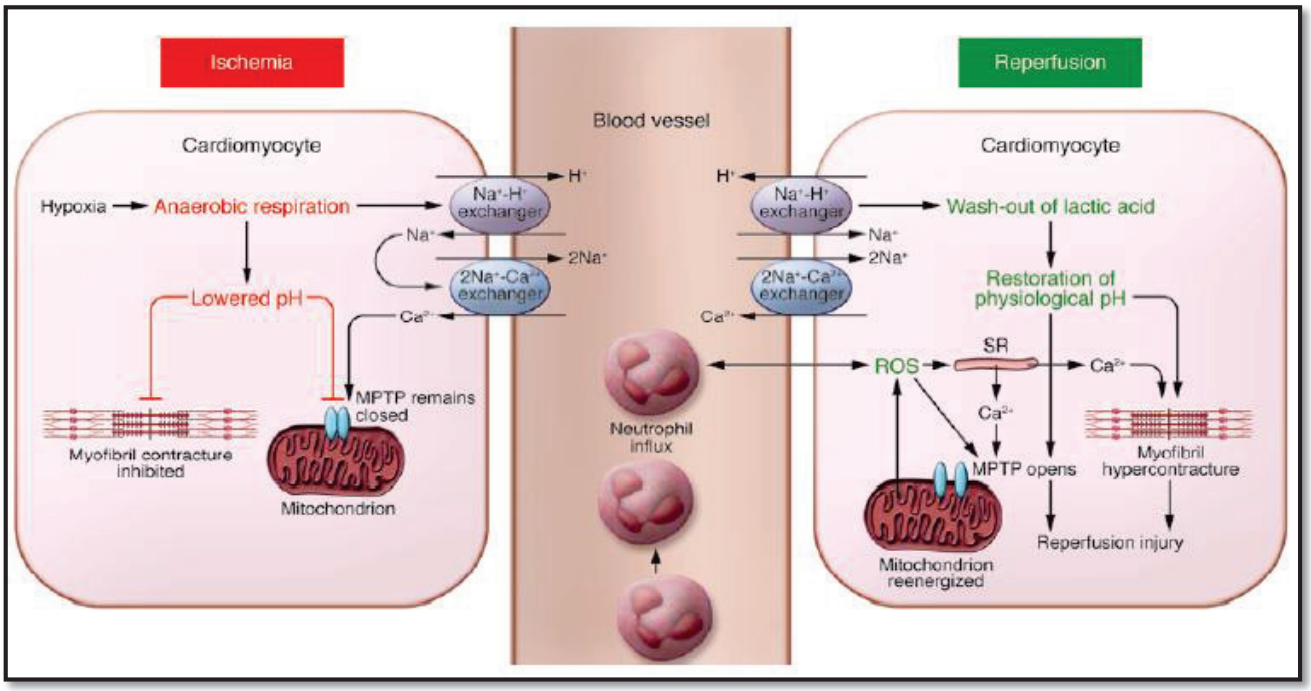

Figure 10.The main proponents of acute myocardial IRI

During acute myocardial ischemia, ischemia switches cell metabolism to anaerobic respiration, resulting in the production of lactate and a drop in intracellular pH. The acidic conditions prevent the opening of the MPTP and cardiomyocyte hypercontraction. During reperfusion, the electron transport chain is reactivated, generating ROS. ROS mediate myocardial reperfusion injury by inducing the opening of the MPTP, acting as a neutrophil chemoattractant, and mediating dysfunction of the sarcoplasmic reticulum (SR). This contributes to intracellular Ca^{2+} overload and damages the cell membrane by lipid peroxidation. The washout of lactic acid then results in the rapid restoration of the physiological pH, which releases the inhibitory effect on MPTP opening and cardiomyocyte contracture. Then calcium is drived into the mitochondria, which can also induce MPTP opening. Several hours after the onset of myocardial reperfusion, neutrophils accumulate in the infarcted myocardial tissue in response to the release of chemoattractant, ROS, cytokines, and activated complement [38].

3. Reperfusion Lesions

Although prompt reperfusion of the ischemic area restores the delivery of oxygen and substrates and normalizes extracellular pH by washing out accumulated H+, reperfusion itself appears to have detrimental consequences, even worse than the ischemic lesions alone **Fig. 11**. This concept originally arose when it was first observed that reperfusion appeared to accelerate the development of necrosis in hearts subjected to coronary ligation in a dog model [36]. It has been termed reperfusion injury to describe causal events associated with re-establishing the blood supply that had not occurred during the preceding ischemic period and can be attenuated or abolished by an intervention given only at the time of reperfusion. Interventions during myocardial reperfusion can reduce infarct size by up to 50%, arguing in the favor of reperfusion phase-specific detrimental events [29], [31].

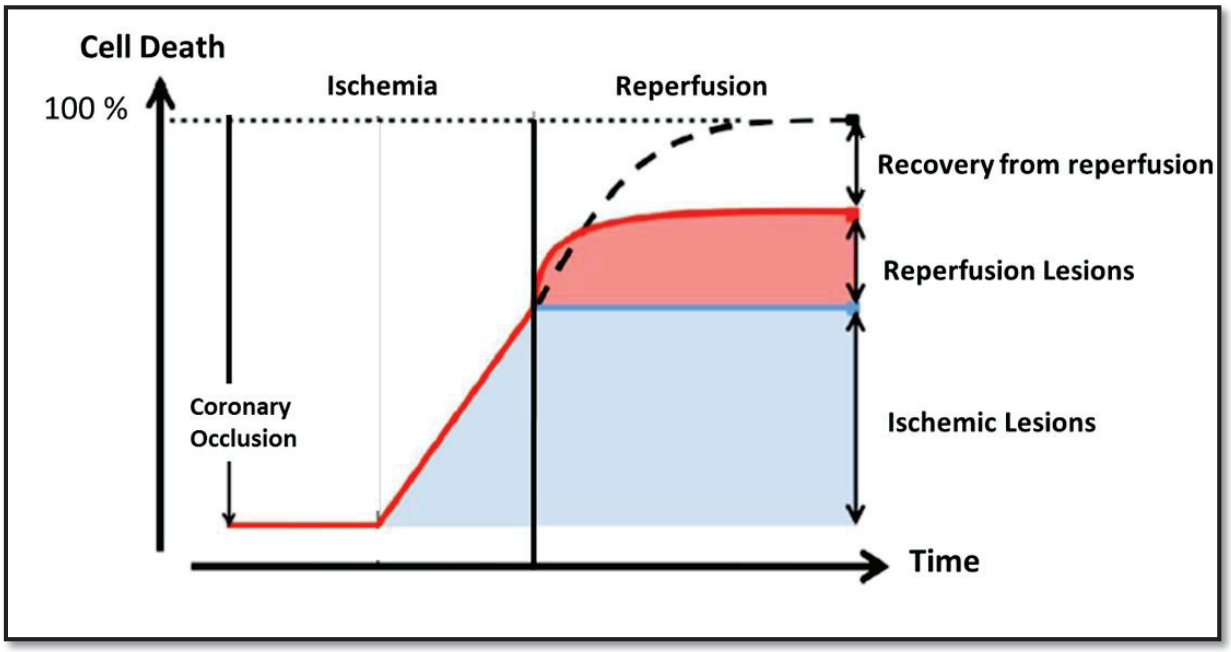

Figure 11. Cell death during ischemia and reperfusion

Few minutes after ischemia, cell death is induced and increases with the increased ischemic period. The restoration of blood flow further increases cellular death. Thus, the lesions of the IR injury are distributed between ischemic and reperfusion lesions. Adapted from [38].

3.1. The Reperfusion Injury Features

The reperfusion injury is characterized by different features, including calcium overload, oxidative stress, rapid pH restoration and mitochondrial transition pore opening **Fig. 11.**

- **Rapid pH Restoration**

Upon reperfusion, the lactic acid accumulated during ischemia is washed out, inducing the activation of NA+/H+ exchangers. The pH is thus rapidly restored, permitting mPTP opening and cardiomyocyte hypercontraction, which aid in contributing to the cellular death during reperfusion. This phenomenon is termed the pH paradox. The reperfusion of ischemic animal hearts with an acidic buffer can reduce MI size. Thus, a potential treatment strategy for the prevention of lethal myocardial reperfusion injury could be to slow the restoration of physiologic pH at the time of myocardial reperfusion [22], [37], [38].

- **Oxidative Stress**

Oxidative stress occurs when there is an imbalance between the generation of reactive oxygen species (ROS) and the antioxidant defense systems in the body so that the latter becomes overwhelmed.

During ischemia, complexes I and III of the mitochondrial electron transport chain are in their reduced state, which favors ROS production.[22], [39]. The increased oxygenation during reperfusion leads to a more exacerbated production of ROS, which generates rapid and severe cell damage. This damage occurs through a number of different mechanisms including direct protein carboxylation, lipid peroxidation and DNA/membrane damages. The most important sources of ROS besides mitochondria are NADPH oxidases (NOX), uncoupled eNOS and xanthine oxidases [22], [39]. .

In addition, oxidative stress during reperfusion reduces the bioavailability of the intracellular signaling molecule nitric oxide, which leads to the loss of its cardioprotective effects [29].

- **Calcium overload**

Upon reperfusion, the washout of accumulated extracellular H+ leads to an increased calcium cellular uptake through transmembrane transport. In addition, Ca2+ transport across the sarcoplasmic reticulum is also affected, where the reuptake is impaired and the release is provoked. These processes lead to a cytosolic calcium overload [22]. The latter activates a variety of systems, contributing to the I/R injury. Excess Ca2+ is taken into the mitochondrial matrix. When intra-mitochondrial Ca2+ levels become excessive, Ca2+ binds and activates the Ca2+ binding domains of the mitochondrial permeability transition pore (mPTP), leading directly to mPTP opening and causing cell death [40].
In addition, high calcium concentration activates calpains. This family of proteases degrades intracellular proteins such as the cytoskeletal, endoplasmic reticulum and mitochondrial ones, which also contributes to cellular damage [22].

- **Mitochondrial permeability transition pore (mPTP) opening**

The mPTP is a large-conductance non-selective channel of the inner mitochondrial membrane (IMM), whose opening leads to detrimental effects causing cell death. This feature is considered a converging end point for the reperfusion injury features stated above. Under normal physiological conditions, with normal physiological mitochondrial calcium concentrations driving adequate ATP production, this pore is closed. During ischemia, the pore remains closed, only to open within the first few minutes following reperfusion in response to mitochondrial calcium over load, inorganic phosphate overload, oxidative stress and pH restoration [23], [29]. Once opened, K+ ions pass back to the matrix, dissipating the mitochondrial membrane potential and causing ATP depletion due to oxidative phosphorylation uncoupling. In addition, the pore opening causes an influx of solutes and water, leading to swelling of the mitochondrial matrix and rupturing of the outer mitochondrial membrane. Consequently, the contents of the intermembrane space (including pro-apoptotic factors, such as cytochrome c and apoptosis-inducing factor) are released into the cytosol, where the process of apoptosis is initiated [22], [41].

3.2. Cell death mechanisms of Reperfusion injury

Ischemia and reperfusion activates various programs of cell death, which can be categorized as necrosis, apoptosis or autophagy-associated cell death. Each of these morphologically unique types of cell death appears to contribute in some way, shape, or form to the pathogenesis of I/R injury. [31]

- **Apoptosis**

Apoptosis is a genetically programmed energy-requiring cell death morphologically featured by cell shrinkage, nuclear condensation, DNA fragmentation and apoptotic bodies formation, with no loss of membrane integrity and no inflammatory response. Apoptotic mechanisms are canonically divided into the "extrinsic" and "intrinsic" pathways, although there is considerable cross talk between the two.

The extrinsic pathway, known as receptor-mediated pathway, involves the activation of cellular receptors like the Fas, TNFα and TRAIL receptors. This activation results in the receptors trimerization, which recruits a number of death domain-containing proteins to the receptor complex. This whole death-inducing signaling complex activates protease caspase-8 that cleaves and activates caspase-3. The latter acts as the cell's executioner by proteolyzing many cellular proteins and inducing cell death.

The intrinsic pathway, known as mitochondria-mediated pathway, occurs following the mitochondrial damage induced by the oxidative stress during I/R. Briefly, oxidative stress induces the translocation and integration of the pro-death members of Bcl2 protein family into the outer mitochondrial membrane. The latter is permeabilized by these proteins, which enables the cytosolic release of pro-apoptotic proteins from the intermembrane space, mainly cytochrome *c* and Smac/DIABLO. Cytochrome *c* binds to the cytosolic protein apaf1 and the resultant "apoptosome" activates the caspase-9 and caspase −3 protease system, while Smac/DIABLO activate caspases by sequestering caspase-inhibitory proteins. These events finally lead the cell toward its fatal end [31], [42], [43].

- **Necrosis**

Necrosis, also called accidental or pathological cell death, is morphologically characterized by organelles/cellular swelling, mitochondrial dysfunction, absence of nuclear fragmentation, plasma membrane rupture and intracellular contents leakage. It is remarkably characterized by inflammation [31].

The mPTP opening serves as a mechanistic link between I/R injury and necrosis. As previously explained, the mPTP opening results in ATP depletion, altered ion homeostasis and mitochondrial swelling [44]. Mitochondrial swelling is by itself a hall mark of necrosis. Besides, the ATP deletion, which results from the mitochondrial dysfunction, inhibits the ionic pumps in the plasma membrane. This causes cell swallowing and eventually induces the rupture of the plasma membrane, the most prominent hallmark of necrosis. This rupture results in the release of the cytosolic components, which causes an inflammatory response during I/R [45].

- **Autophagy**

Autophagy is a physiological mechanism used to remove damaged organelles, such as mitochondria or endoplasmic reticulum. It provides cells with a survival mechanism to withstand stressful conditions such as hypoxia and ROS generation. However, extensive autophagy can cause cell death [45]. Morphologically, autophagy begins with the expansion of an isolation membrane around the targeted damaged compartment/organelle. The membrane then completely envelops the constituents to form the vesicular auto phagosome, which then fuses with a lysosome to degrade the enveloped materials [31]. During ischemia, there is activation of AMPK (5 adenosine monophosphate-activated protein kinase), a negative regulator of mTOR, which is a potent inhibitor of autophagy. Consequently, autophagy is induced [44]. Data suggests that autophagy plays a protective role during ischemia [44], [46]. During reperfusion, autophagy is activated by a different pathway involving increases in Beclin-1 protein. In reperfusion, data suggests a controversial role for autophagy [44], [45].

Overall, death following ischemia-reperfusion injury appears to be a mixture of apoptotic, autophagy, and necrotic cell death and it can have features of all three. The distinction between the modes of death may no longer be an important aspect, since recent data suggests that all three forms of cell death can be regulated and are inter-related [45]. The important issue is that cell death during ischemia-reperfusion appears to be an active process, which can be inhibited with appropriate interventions.

After understanding the pathology of MI through the explanation of the ischemia/reperfusion injury features and mechanisms, it is important to understand the responses which come along with this injury. Among these responses is the inflammatory response, which will be explained in the following chapter. Understanding such responses is the first step toward developing cardioprotective tools and protocols.

Chapter 3: Post-myocardial Infarction Inflammatory Response

Inflammation and inflammatory cell infiltration are hall marks of the myocardial infarction and the reperfusion injury. The activated inflammatory response acts as a doubled-edge sword, whereby it is implicated in the pathogenesis of the reperfusion injury on one hand and is essential for cardiac repair on the other hand. Two phases of inflammatory response follow the reperfusion injury. First comes the pro-inflammatory response, which lead to the removal of necrotic cell debris from the infarcted zone. Following the pro-inflammatory response is the anti-inflammatory one, which allows wound healing and scar formation after several days of the injury [47]. To understand these responses, it's important to understand how are they initiated and which cells are involved in their mediation.

1. Activation of Inflammatory Response

As we previously described, necrosis is a major cell death mechanism induced by the ischemia-reperfusion injury. Following the necrosis of the different cardiac cells, an inflammatory response is initiated through the activation of a complement cascade, the production of ROS and the release of damage-associated molecular patterns (DAMPs) by the dead cells. The DAMPs, acting as major mediators of danger signals, are considered the key molecular link between cell death and inflammation, where they activate several cellular targets including residential cardiac macrophages and mast cells, vascular endothelial cells, fibroblasts and infiltrating leukocytes. This activation occurs via the engagement of DAMPs with toll-like receptors (TLRs) expressed by inflammatory and cardiac resident cells. The activated cells, in turn, secrete a number of pro-inflammatory chemokines and cytokines, which recruit inflammatory cells to the injured area. The major expressed pro-inflammatory chemokines include the CC and CXC chemokine subfamilies (ex: CCL2 and CXCL2), while the major pro-inflammatory cytokines are TNF, IL-1β and IL-6 [47]–[50]. Having in mind this global sequence of events, it's important to understand the roles of each of the different cells which mediate the inflammatory response **Fig. 12**.

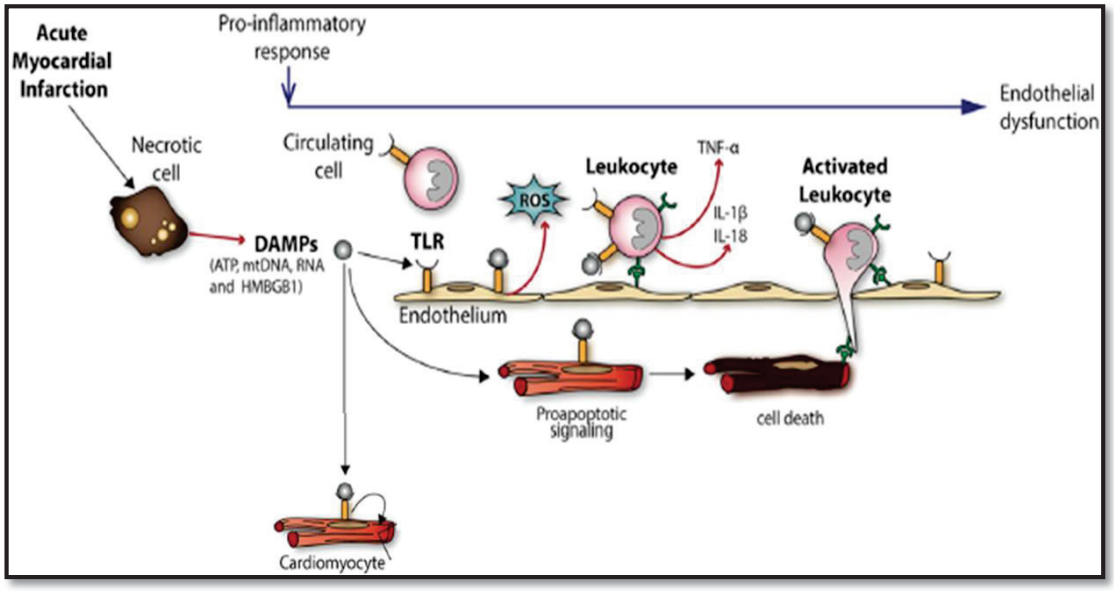

Figure 12. The pro-inflammatory response induced by DAMPs

Following AMI, the release of damage-associated molecular patterns or DAMPs (such as ATP and HMBGB1) induce a pro-inflammatory response which mediates cardiomyocyte death through Toll-like receptors (TLRs) and the recruitment of leukocytes into the infarct zone. Adapted from [52].

2. Mediators of the Inflammatory Response

A wide range of cells, molecules and complexes orchestrate to mediate the IRI-induced inflammatory response. Understanding the roles and involvement of all these mediators in the inflammatory response is critical for the development of new therapeutic strategies **Fig. 13**.

2.1. Endothelial Cells

Endothelial Cells, the most abundant non-cardiomyocytes in adult mouse myocardium, represent a major source of pro-inflammatory chemokines following myocardial infarction[51], [52]. Once activated by DAMPs, endothelial cells increase the expression of intercellular adhesion molecules (ICAMs), which recruit circulating leukocytes [53]. Moreover, the intercellular tight junctions between the endothelial cells become compromised following IRI, resulting in a leaky coronary endothelium and a consequent increased coronary permeability. Overall, endothelial cells thus play prominent role in the recruitment of neutrophils to the damaged area.

2.2. Neutrophils

Following the induction by chemotactic signals (chemokines and complement cascade) or DAMPs released after cardiac injury, neutrophils mobilize from the bone marrow to the blood [54]. They move through the blood and are the first cells to infiltrate the injured zone during the initiated response, being present within few hours of the injury [48], [55]. In order for this infiltration to occur, neutrophils must leave the blood circulation and move across the endothelium of the venules. First, neutrophils are captured by and roll on endothelial cells through cell adhesion receptors called selectins. Second, neutrophils firmly adhere through their chemokine-induced integrins to the endothelial surface receptors ICAMs and VCAMs. Finally, a trans-endothelial migration of neutrophils occurs, leading to infiltration of the injured tissue [56]. Once in the injured area, neutrophils generate high levels of ROS and undergo degranulation, releasing proteases [57]. This represents a main feature of acute inflammation and results in cardiomyocytes apoptosis and degradation of extracellular matrix [58]. Furthermore, neutrophils secrete factors which are chemotactic to monocytes [48]. Subsequently, blood monocyte-derived macrophages infiltrate the injured area to remove cardiac tissue debris and apoptotic neutrophils, which activates reparative pathways necessary for scar formation[57].

Due to their major role in the initiation of the inflammatory response and increasing the extension of myocardial infarction, neutrophils have been a target in studies attempting to reduce the infarct size. Several studies have worked on inhibiting neutrophil adherence to endothelial cells using monoclonal antibodies directed against the neutrophils membrane adhesion molecules, or using anti-inflammatory drugs that inhibit the upregulation of the adhesion molecules on surface of neutrophils [59]–[61]. In this regard, Curtis et al. have used an anti-inflammatory agent that inhibits the up-regulation of the Mac-1 adhesion molecule on surface of neutrophils and consequently decreases their binding to endothelial cells. They have shown that this agent reduced the myocardial infarct size by 51% in a porcine model of ischemia/reperfusion injury [61].

2.3. Monocytes and Macrophages

In the absence of injury, the adult mammalian heart contains small populations of macrophages, called cardiac residential macrophages [62]. Following IRI, inflammatory monocytes are recruited by the marked upregulation of chemokines, basically CCL2[63].
Monocytes are recruited in two phases. The first phase involves predomination of the pro-inflammatory Ly-6c^{high} monocytes, which express high levels of the receptor CCR2 on which CCL2 binds. These cells differentiate into M1 macrophages, which scavenge debris (phagocytosis of dead cells) and secrete inflammatory cytokines and matrix-degrading proteases[64]. After scavenging debris, M1 macrophages decrease the production of pro-inflammatory cytokines and increase the production of anti-inflammatory and pro-fibrotic cytokines, including IL-10. This marks the shift in macrophages toward the M2 anti-inflammatory profile [62]. A second phase of monocytes recruitment is hereby initiated, involving predomination of the anti-inflammatory Ly-6c^{low} monocytes [48]. In this second phase, M2 macrophages facilitate wound healing and regeneration through promoting myofibroblasts accumulation, collagen deposition and angiogenesis [65]. In addition to the strictly M1 or M2 phenotypes, a hybrid M1/M2 phenotype of macrophages was recently reported to be presented in the heart, with co-expressed M1 and M2 markers [66].

2.4. Lymphocytes

In addition to neutrophils and macrophages, T and B lymphocytes infiltrate the infarcted zone through interacting with endothelial cells following chemokines induction[56].
Mature B lymphocytes participate in the augmentation of the pro-inflammatory response through the secretion of CCL7 chemokine, which recruits pro-inflammatory Ly-6C^{high} monocytes, leading to enhanced tissue injury and deterioration of myocardial function [48], [67]. Besides B lymphocytes, T-lymphocytes play their own unique roles. Two types of T-cells participate in the IRI –induced inflammatory response, the effector and the regulatory ones. The effector T-cells participate in the pro-inflammatory response through releasing pro-inflammatory cytokines [56]. On the contrary, the CD4+/CD25+ regulatory T-cells (T-regs) have potent suppressive inflammatory properties [68]. They modulate macrophages phenotype and suppress inflammation by secreting IL-10 and TGF-β. In this context, the mRNA and protein levels of IL10 have been demonstrated to be upregulated in the

myocardium following ischemia/reperfusion, whereby it was first detected at 5 h and peaked at 96–120 h of reperfusion [69]. Moreover, T-regs mediate the anti-inflammatory effects of the CCR5 signaling [56], [70].

2.5. Dendritic Cells (DCs)

Once recruited to the infarcted area, dendritic cells have both detrimental and beneficial effects, with the beneficial ones being more pronounced. DCs secrete anti-inflammatory cytokines, such as IL-10 [71]. They also secrete exosomes which recruit T-cells into the infarcted zone and help prevent left ventricular remodeling [72]. Moreover, they participate in the regulation of post-infarction healing process though controlling monocyte/macrophages homeostasis [71].

2.6. Cardiac Fibroblasts

In addition to their contribution to the scar formation and matrix remodeling, fibroblasts regulate the inflammatory response[73]. They are activated by DAMPs and act as pro-inflammatory mediators during the first 24-72 hours following IRI. They activate their own inflammasomes (defined later) and produce pro-inflammatory cytokines such as IL1β and chemokines. They may also exhibit phagocytic properties, where they engulf dead cells and negatively regulate the inflammatory response [74].

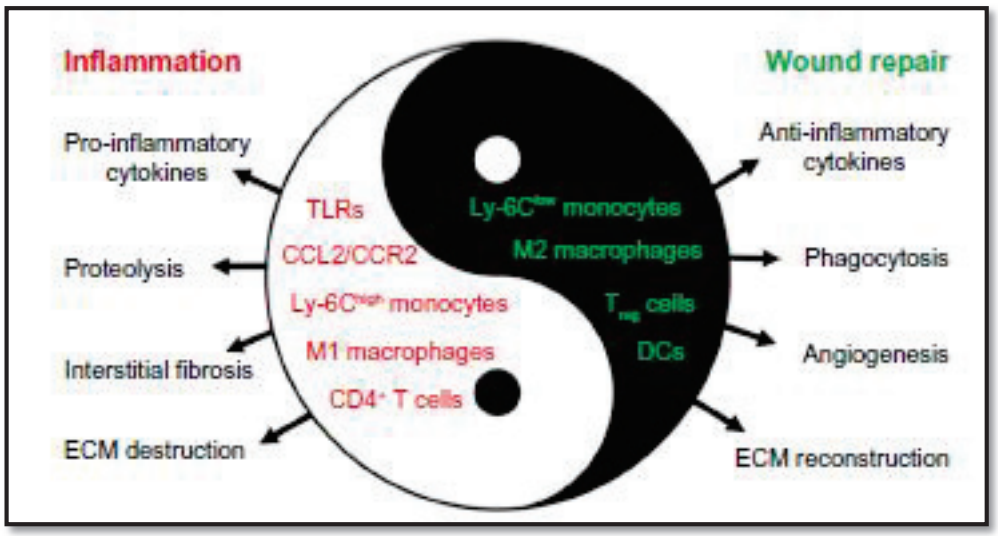

Figure 13. Diverse roles of inflammatory cells in the pathophysiology of MI

The roles of different cells involved in the pro-inflammatory phase and the wound repair phase following inflammation [79].

2.7. Inflammasomes

Inflammasomes are large multiple cytoplasmic protein complexes, forming in the cytosol in response to the DAMPs release. They are composed of three components: a member of NLRP family proteins (most commonly described in IRI is NLRP3); an apoptosis-associated speck-like protein with a caspase recruitment domain (ASC); pro-caspase-1. These complexes mediate the activation of pro-inflammatory cytokines such as IL1β and IL-18, and they also mediate caspase-1 dependent death of cardiomyocytes**.** The common upstream mechanisms implicated in the NLRP3 inflammasome activation include ATP released from injured cells, ROS and potassium efflux **Fig. 14** [48], [75].

Through the activation of caspase-1 and the processing of IL1β, which are prominent mediators of inflammation in MI, the inflammasome is considered an important mediator of the inflammatory response during MI [76]. In this context, experimentations done on a mouse model of myocardial I/R injury showed that ASC was expressed following I/R and that ASC and caspase-1 deficiency reduced inflammatory responses such as inflammatory cell infiltration and cytokine expression [77]. Moreover, in another study conducted on a non-reperfused mouse model of MI, the inhibition of NLRP3 by a small interfering RNA prevented inflammasome activation and cardiac cell death. This resulted in ameliorating myocardial remodeling after MI. These two reports clearly demonstrate that NLRP3 inflammasome plays an important role in the development of MI [78] .

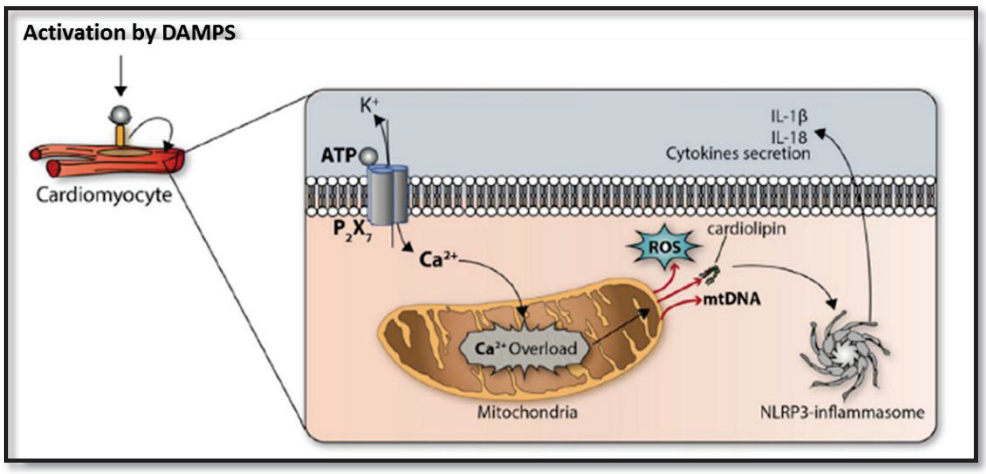

Figure 14. NLRP3 Formation in Cardiomyocytes

The common upstream mechanisms implicated in the NLRP3 inflammasome activation include ATP released from injured cells, ROS and potassium efflux adapted from [52].

Decades of research in the field of myocardial inflammation brought us closer to therapeutic translation, and emerging evidence suggests that modulating inflammation might mediate protective effects of cell therapies [79]. Thus, strategies targeting inflammation were expected to succeed in exerting beneficial actions in patients with myocardial infarction. Such strategies include antibody neutralization of specific inflammatory mediators (including adhesion molecules, cytokines and chemokines) and anti-integrin approaches through the administration of anti-CD11/CD18 antibodies [59], [80]–[83]. Although these strategies reduced infarct size following coronary occlusion and reperfusion in several independent studies in animal models, no similar protective effects were observed in clinical trials. For instance, small clinical trials showed no effects of early anti-integrin approaches in reducing infarct size in human patients with myocardial infarction [84]–[86]. Moreover, a large clinical trial targeting the complement cascade failed to produce beneficial effects in patients undergoing percutaneous interventions for acute myocardial infarction [87].

Considering the highly promising results of experimental studies, the basis for failure to translate into the clinical context remains under major investigation. An important aspect in the context of inflammation would thus be the understanding of the gaps that disconnect between animal studies and clinical investigations.

Chapter 4: The Mitochondria in Ischemia Reperfusion

As the central sites for energy metabolism and lipid metabolism, mitochondria compromise 30-40% [23] of the cardiomyocytes volume. They contribute to the production of ATP, which is highly demanded in the heart. Besides energy production, they store calcium, generate ROS and initiate cell death. Through these roles and other ones, mitochondria are key players in mediating IRI and are thus considered important cellular targets in cardioprotection. Understanding the contributions of mitochondria to IRI requires an understanding of their structure and function.

1. Mitochondrial Structure

Mitochondria are double-membraned organisms. Their outer membrane is selectively permeable, allowing small molecules to freely pass through channels called porins. The inner membrane, which has a large surface area, is markedly folded into structures called cristae. It contains the four complexes of the electron transport chain (ETC), ATP synthase and specific metabolites carriers. In between the two membranes is the inner membrane space. Enclosed within the inner membrane is the mitochondrial matrix, which contains a variety of enzymes and proteins important for energy production. In addition, the mitochondrial matrix contains the mitochondrial genome, which contains 37 genes that encode for some subunits of the ETC complexes. The mitochondria are physically connected with the endoplasmic reticulum through specific microdomains called the mitochondrial associated membranes (MAMs). This connection is important for exchanging messages and molecules in order to maintain intracellular homeostasis [88]–[90].

2. Mitochondrial Function

The strong evolution of scientific research gave us a better understanding of the different functions of the mitochondria, along with providing us strong tools for measuring and assessing each of these functions under various conditions. Through this, we gained a better understanding of the global cellular functioning under physiological and pathological conditions, since mitochondria determine the global cellular fate.

2.1. Oxidative Phosphorylation (OxPhos)

Oxidative phosphorylation is the process by which the mitochondria produce ATP, in the presence of oxygen, via the electron transport chain (ETC). The ETC is a series of protein complexes through which electrons are passed in successive redox reactions from electron donors to electron acceptors, with O2 being the final acceptor. As electrons flow from one complex to another, protons are pumped from the mitochondrial matrix to the inter membrane space. This pumping establishes an electrochemical gradient used to produce ATP. The two initial reduced electron donners are NADH and FADH2.

To start with, NADH transfers two electrons to complex I (NADH dehydrogenase), which passes them to the coenzyme Q (also called ubiquinone). In parallel, FADH2 transfers electrons to complex II (succinate dehydrogenase), which also passes them to coenzyme Q (ubiquinone). Once reduced, ubiquinone delivers its electrons, received from complexes I and II, to complex III (Cytochrome b-C1). The latter passes them to cytochrome C, which transfers them to the fourth complex (cytochrome C oxidase). At this stage, an oxygen molecule is reduced and picks up two hydrogen ions to produce water. The electrochemical gradient, established by the proton pumping coupled to the electron transfer, is finally consummed by F0F1 ATP synthase (complex V) to produce ATP. ATP synthase fluxes back protons to the mitochondrial matrix **Fig. 15** [91].

In the context of IRI, complexes I and III activities are reported to be disturbed mainly during ischemia, leading to ROS generation. During ischemia, in the absence or at low levels of oxygen, complex I undergoes conformational changes toward a deactive form that mainly produces superoxide due to its low ability to accept electrons [92]. This low ability of accepting electrons leads to electron leakage from complex I, where electrons are used by complexes II and III for further ROS production. Thus, blocking electron transport chain immediately before and during ischemia protects against ischemic damage and preserves mitochondrial respiration [92].

During reperfusion, ROS generation by the previously damaged complexes is still observed [92].

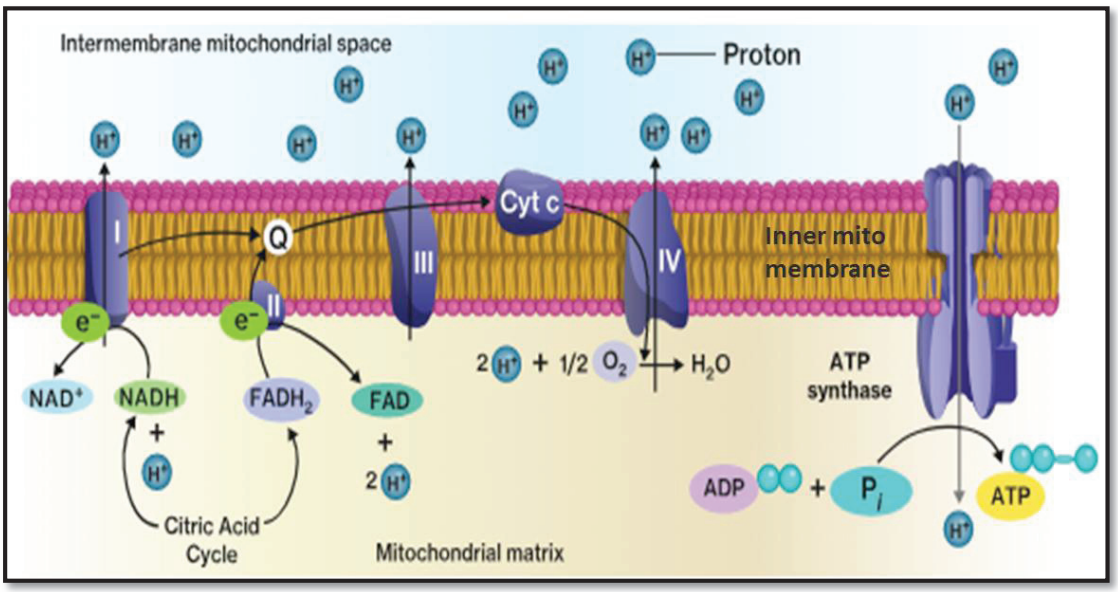

Figure 15. The Electron transport chain
Adapted from [98]

2.2. The Membrane Potential (ΔΨm)

The mitochondrial membrane potential is an electrical potential across the inner mitochondrial membrane [93]. The pumping of protons by Complexes I, III and IV of the ETC participates in maintaining this potential. Together with the proton gradient of concentration (ΔpH), ΔΨm forms the electrochemical gradient of hydrogen ions used to make ATP. In addition, ΔΨm is involved in the mitochondrial calcium sequestration and ROS generation. It also plays a key role in mitochondrial homeostasis through the selective elimination of dysfunctional mitochondria [94], [95]. As we already stated, the dissipation of the membrane potential is one of the manifestations of the IRI, whereby it causes ATP depletion and a final cell death follows.

2.3. ROS Generation

The mitochondria present a major source for ROS generation in the cardiovascular system [23]. Under normal physiologic conditions, the electron transport is coupled to ATP synthesis. Regardless this, a small amount of ROS (estimated to 2% of ETC activity), such as superoxide and hydrogen peroxide, is generated due to the leakage of electrons. Under stress conditions of IRI, complexes I/III are regarded as the key contributors of ROS generation, whereby the rush of oxygen induced by reperfusion markedly enhances

electron leakage from the impaired ETC. This results in an over-production of superoxide and its derived oxidants.

Although mitochondrial ROS production has been considered a non-specific consequence of the interaction of the dysfunctional respiratory chain with the oxygen rushing during reperfusion (as explained in the previous paragraph), an alternative theory linking mitochondrial IR ROS to a specific metabolic process was presented by Chouchani et al. They showed that during ischemia, a fumarate overflow induces succinate accumulation through driving the reversal activity of succinate dehydrogenase. They proved that the selective accumulation of succinate can be considered a universal metabolic signature of ischemia and is responsible for extensive ROS generation by reverse electron transport at mitochondrial complex I [96].

2.4. Calcium Handling and mPTP opening

Among the major functions of the mitochondria is the accumulation of calcium, and the mitochondrial calcium retention capacity (CRC) represents a key parameter to assess the mitochondrial function and global cellular homeostasis. Under normal physiologic conditions, mitochondrial calcium is essential for the activation of the metabolic enzymes, generation of ATP and regulation of cytosolic/cellular calcium homeostasis and signaling [97]. The mitochondrial calcium uptake is mainly mediated by the mitochondrial calcium uniporter (MCU), although other uptake mechanisms exist [98]. As for the calcium efflux, two major systems exist: the mitochondrial Na+/Ca2+ exchanger (mNCX) and the mitochondrial H+/Ca2+ exchanger (mHCX). Besides from its crucial physiological roles, an increased mitochondrial calcium influx is a potent cause of cell death through the triggering of the mPTP opening [98]. This is prominently observed following IRI, where the excessive calcium taken to the mitochondria binds and activates the Ca2+ binding domains of the mitochondrial permeability transition pore (mPTP), leading to the opening of the mPTP and causing cell death [40]. The mPTP opening stands as a final end point for various mechanisms in the IRI.

3. Mitochondria in IRI

Having understood the different mitochondrial functions and the effect of IRI on each of these functions, it's important to gather all the dysfunctions together to understand the global mitochondrial dysfunction in IRI. During ischemia, when ATP is depleted, Ca2+ pumps cannot function. They include SERCA and PMCA, the pumps through which calcium is respectively uptaken by sarcoplasmic reticulum and exchanged across sarcolemma. This results in a calcium rise, which further accelerates ATP depletion. This Ca2+ rise during ischemia and reperfusion leads to mitochondrial Ca2+ accumulation, particularly during reperfusion with the reintroduction of oxygen. The high mitochondrial calcium concentration activates calpains, which degrade intracellular proteins and contribute to cellular damage [22]. Moreover, the mitochondrial Ca2+ overload triggers the mPTP opening, which consequently leads to cell death by apoptosis [99]. In addition to Ca2+ overload, mitochondria are also characterized by the dysfunction of complexes I and III of the ETC during IRI, which leads to ROS accumulation. The accumulation of ROS induces direct protein carboxylation, lipid peroxidation and DNA/membrane damages [22], [39].

In conclusion, mitochondria have long been proposed as central players in cell death, as they are central to synthesis of both ATP and ROS, and since mitochondrial and cytosolic Ca2+ overload are key components of cell death. Many cardioprotective mechanisms converge on the mitochondria to reduce cell death, whereby reducing Ca2+ overload and ROS generation have both been prominent targets to reduce ischemic injury. In the upcoming chapter, we'll be discussing the cardioprotective strategies used to decrease the lesions of the IRI.

Chapter 5: Cardioprotection against Myocardial infarction

The building block of cardioprotection is the well-understanding of the pathophysiology of the ischemia/reperfusion lesions, and this is well accomplished in the cardiovascular research. As we've seen in a previous chapter, the sudden restoration of blood flow to the ischemic area stands as a "double-edged sword", since reperfusion is associated with an exacerbation of tissue injury. Thus, a main goal of research in cardioprotection is the development of effective techniques and strategies to avoid the ischemia-reperfusion lesions. In this regard, myocardial conditioning has aroused as a powerful cardioprotective phenomenon.

Myocardial conditioning refers to the activation of endogenous mechanisms which render the myocardium more tolerant to the reperfusion injury [100]. This phenomenon can be pharmacologically or mechanically applied. The latter is referred to as 'ischemic conditioning'. Ischemic conditioning is achieved by the application of intermittent short episodes of ischemia before the induction of the prolonged ischemia, during ischemia or immediately before reperfusion. It is respectively referred to as ischemic pre-, per- or post-conditioning **Fig. 16** [101].

Although the underlying mechanisms of ischemic conditioning have been extensively studied in experimental animal models, the greatest challenge lies in the translation of these findings to clinical settings to reduce the detrimental effects of myocardial infarction in humans.

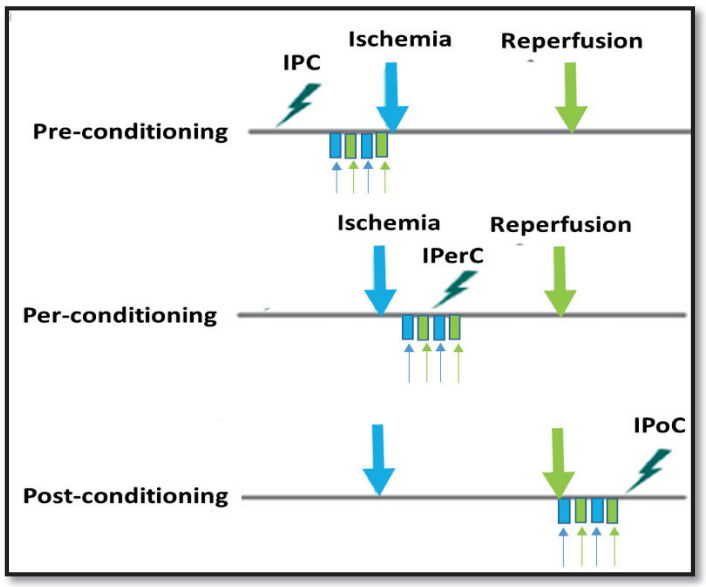

Figure 16. The three types of Ischemic Conditioning

Ischemic conditioning is achieved by the application of intermittent short episodes of ischemia before the induction of the prolonged ischemia, during ischemia or immediately before reperfusion. It is respectively referred to as ischemic pre-, per- or post- conditioning

1. Ischemic Preconditioning (IPC)

In 1986, the cutting edge protocol of ischemic preconditioning has been discovered, where it was shown that the exposition of the heart to brief episodes of ischemia/reperfusion lead to a 75% reduction in the infarct size caused by 40 mins occlusion of coronary artery in dogs [102]. Thereafter, this cardioprotective phenomenon was applied and tested on different species including rats [103], rabbits [104], mice [105], pigs [106] and most importantly humans[107].

The protective effect of IPC is biphasic. The first phase (first window), known as the early classical phase, starts immediately after the preconditioning stimulus and lasts for 2-4 hours [102], [108]. Protection in this phase is conferred through the modification of existing pro-survival proteins in the heart. It has a strong protective effect against necrosis, but does not affect cardiac contractility [109]. The second delayed phase (second window), known as the second window of protection, starts after 12-24 hours and lasts up to 2-3 days [110]–[112]. Protection in this phase is achieved through the synthesis of new proteins. It is less effective against necrosis, but important for the recovery of cardiac contractility [109]. In both phases of IPC, ischemia provokes the release of trigger substances such as adenosine[113],

bradykinin[114] and opioids[103]. These substances, via direct interaction with G-protein coupled receptors, initiate the activation of protective signals.

Although IPC has been reported to be effective in experimental and clinical studies, the need to apply it before prolonged myocardial ischemia (acute myocardial infarction) makes it unfeasible in clinical situations, because myocardial ischemia is usually unpredictable. Thus, ischemic postconditioning has been developed and studied for application in interventional cardiology.

2. Ischemic Postconditioning (IPoC)

In 2003, the discovery of IPoC has revitalized the field of cardiovascular research. As stated before, the term of IPoC refers to the ischemic stimulus applied after the lethal ischemic period rather than before it as in IPC. It was first demonstrated, in a rabbit model, that three repeated cycles of [30secs reperfusion/ 30 secs occlusion] following a 60 mins of coronary artery occlusion, markedly reduced post-ischemic myocardial infarct size and improved cardiac functional recovery [115]. Following this key study, several other studies have investigated the efficacy of IPoC in several *in vivo* animal models including rats [116], [117], rabbits [118], [119], pigs [120], [121] and mice [122], [123], *in vitro* cellular models [124], [125] and most importantly *clinical* human models [126], [127].

The protective effect of IPoC has been mainly and initially assessed through the infarct size reduction, the hallmark of IPoC physiological effects [119]–[121], [128]. Thereafter, studies have gone toward understanding the underlying mechanisms and reported IPoC roles in decreasing apoptosis [119], [129], reducing endothelial dysfunction[115], reducing neutrophils adhesion on the post-conditioned coronary artery endothelium [115], preserving cardiomyocytes function, in addition to anti-arrhythmic roles [130], [131]. The efficacy of the observed protection seems to be variable, depending on the applied protocol itself (the duration, timing and number of the ischemia/reperfusion cycles)[122], [128], [132] and on the used model (species, gender, age) [122], [128], [133] **Fig. 17.**

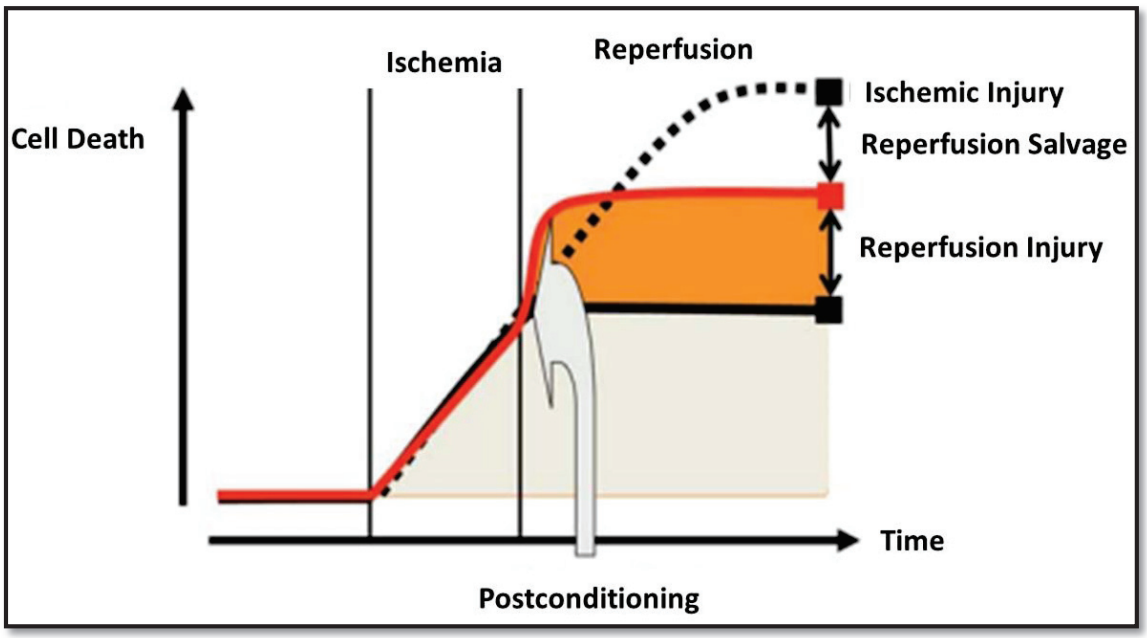

Figure 17. Ischemic post conditioning decreases the reperfusion injury lesions

The application of ischemic postconditioning at the set of reperfusion decreases the cell death due to the reperfusion injury [140].

3. Cardioprotective Signaling pathways

In order to understand how ischemic conditioning confers cardioprotection, it's important to understand the main global sequences of events happening at the cellular level, along with the main components of these sequences. Overall, ischemic conditioning involves several factors, which are divided into three main groups: The triggers, mediators and effectors. The triggers, which are agonists produced during conditioning, bind to their receptors and activate downstream mediating signaling pathways.

The latter, composed of different cascades, transduce the protective signals toward the end effectors. The main final effector and integration point, where most signals converge, is the mitochondria[134]. The signaling pathways through which IPC and IPoC transduce the protective messages from sarcolemma to mitochondria are different, but they overlap. In the following part, we will precisely focus on the IPoC pathways.

Two main intracellular pathways have been characterized in IPoC: the RISK (Reperfusion Injury Salvage Kinase) pathway, which involves the activation of MEK1/2-ERK1/2 and PI3K-Akt signaling cascades [118], [132], [135]; and the SAFE (Survivor Activator Factor Enhancement) pathway, which involves the activation of JAK-STAT3 signaling cascade **Fig. 18** [136], [137].

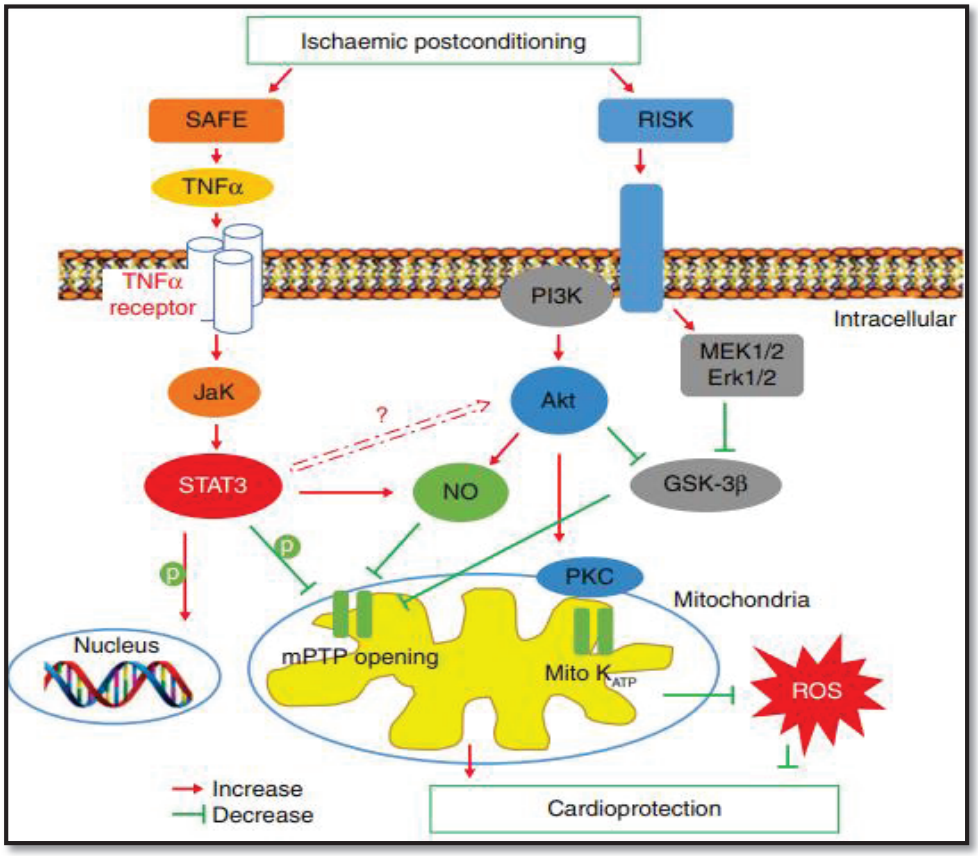

Figure 18. Schematic mechanisms of cardioprotection by ischemic postconditioning

Ischemic postconditioning confers cardioprotection through the SAFE and RISK pathways. These involve the activation of Jak/STAT3, PI3K/Akt and MEK/ERK1/2, which subsequently decreases mitochondrial permeability transition pore (mPTP) opening and increases mitochondrial KATP (Mito KATP) channel opening, which attenuates myocardial ischemia reperfusion injury [107] .

3.1. The RISK pathway

3.1.1. The signaling cascades

The actual term of RISK pathway was first coined by Yellon and co-authors in 2002[138], while the first studies to link the RISK pathway to the IPoC protocol were conducted in 2004. During this year, Tsang et al. showed, for the first time, that IPoC protects the myocardium by activating the pro-survival kinases cascade PI3K-Akt [139]. On their side and for the first time also, Yang et al. linked IPoC with the MEK1/2-ERK1/2 kinases cascade of the RISK pathway [118]. A number of subsequent studies have then confirmed the involvement of RISK pathway, through both cascades, in the IPoC signaling. These studies involved variable applied IPoC protocols (number and duration of cycles) along with different models including rabbits[140], [141] , rats[142] , canines[143], murine[144] and even humans [127]. The involvement of MEK-ERK and PI3K-Akt cascades in the protective effects of IPoC was basically assessed by two approaches. The first approach implicated only the study of kinases activation through their phosphorylation, whereby several papers showed that IPoC induced the phosphorylation of ERK1/2 and Akt within minutes of reperfusion, in parallel with the infarct size reduction [139]–[142], [144]. The second approach implicated the use of pharmacological inhibitors to validate the true link between activation and protection, where by PD98059 was widely used for MEK-ERK pathway inhibition [118], [145], while LY-294002 and/or Wortmannin were used for the PI3K/Akt pathway inhibition[127], [145], [146].

In addition to the above kinases, IPoC signaling involves other kinases which are considered as members of the RISK pathway [147]. They include protein kinase C (PKC)[148], protein kinase G (PKG)[149], p38 kinase and c-Jun N-terminal kinase (c-JNK) [150]. The ERK1/2, p38 and c-JNK belong to the same family of kinases named mitogen-activated protein kinase (MAPK) family. Although there are conflicting reports on the role of MAPKs in death or survival after stress, it is commonly agreed that p38 and JNK MAPKs are pro-apoptotic, while ERKs are modulators of cell survival signaling[151]–[153]. In this regards, IPoC was shown to attenuate cardiomyocyte apoptosis via the inhibition of JNK and P38 MAPKs [153], [154].

3.1.2. Activation and downstream signal

In order for the components of the RISK pathway to be activated, upstream pharmacologic activators must be presented. In this context, studies have shown that following the IPoC stimulus, initiating factors are released. These factors basically include autacoids (adenosine, bradykinin and opioids) and cytokines. They act through binding to their specific receptors, including G-protein coupled receptors, cytokine receptors, tyrosine receptors and serine threonine receptors [155], [156].

Once activated by receptor ligands, the two main cascades of the RISK pathway transduce the signal via phosphorylating downstream substrates. These substrates mainly include glycogen synthetase kinase 3β (GSK3β) [134], [146] and nitric oxide synthase (NOS). PKC and PKG are also considered among the downstream effectors of the MEK-ERK and PI3-Akt [101], [157].

3.1.3. Mechanisms of cardioprotection

The mechanisms underlying the cardioprotection mediated by ERK1/2 and Akt mainly involve the mitochondria as a final effector. The first mechanism involves inhibiting the opening of the mPTP, a critical determinant of cellular death. This is maintained through the generation of nitric oxide by eNOS [158]; the phosphorylation and consequent inhibition of GSK3β [134]; the Akt-dependent induction of sarcoplasmic reticulum calcium uptake, which decreases the mitochondrial calcium load [159]; Akt-dependent modification of mitochondrial morphology, rendering it more resistant to mPTP opening. [160]. The second mechanism involves the recruitment of anti-apoptotic signaling pathways [147]. These anti-apoptotic pathways include the phosphorylation and inhibition of pro-apoptotic proteins (such as Bcl-2 associated death factor)[161] , along with the activation of anti-apoptotic ones (such as PIM-1 kinase)[162].

3.1.4. Controversial Issues of RISK pathway

The involvement of RISK pathway in IPoC signaling has sparked various controversial issues. The first study to highlight such issues has reported the failure of PI3K-Akt implication in ex vivo conditioned rabbit hearts[141]. Thereafter, other reports showed an absence of link between RISK components activation and infarct size limitation[132], or infarct size limitation in absence of the RISK pathway activation [163]. Moreover, the involvement of GSK3β in the cardioprotective effect of IPoC has also been doubted [164]. These controversial issues surrounding the RISK pathway activation in IPoC signaling opened the door toward arguing for the existence of RISK-independent pathways in IPoC. Thus, the SAFE pathway concept has evolved in parallel

3.2. The SAFE pathway

The SAFE pathway was first discovered in IPC [165], but its roles where later on confirmed in IPoC [117], [122]. This pathway involves the activation of the tumor necrosis factor alpha (TNFα) and the transcription factor STAT3 as key players.

3.2.1. Signaling cascades

Unlike the RISK pathway, the SAFE pathway includes only one major signaling cascade, the JAK-STAT3 one. The Janus kinase-signal transducer and activator of transcription 3 (JAK-STAT3) cascade represents a major mechanism used to transmit signals from extracellular receptors to the nucleus. It is a principal signaling mechanism for a wide array of growth factors and cytokines [166]. JAK proteins are tyrosine kinases associated with the cytoplasmic domain of cytokine and growth factors receptors. Upon binding of activating ligands to these receptors, JAKs are phosphorylated and subsequently phosphorylate STAT3 molecules, which form dimers and translocate to the nucleus to function as a transcription factor [167]. Through its role as a transcription factor, STAT3 regulates expression of genes involved in cardioprotection (explained later).

Similar to the approaches used in the RISK pathway, the involvement of JAK-STAT3 signaling cascade in IPoC was confirmed by measuring the phosphorylation of JAK or STAT3 during IPoC, or by studying the effect of JAK/STAT3 pharmacological inhibition on cardioprotection. In this context, several studies have reported that IPoC induces an increase in STAT3 phosphorylation, within minutes up to several hours of reperfusion [117], [119],

[122], [168], [169]. This was accompanied to a reduction in the infarct size, indicating cardioprotection. This protective effect was abolished by the use of the JAK2 inhibitor, AG490 [119], [169]. Similarly, the pharmacological inhibition or genetic ablation of STAT3, respectively using Stattic (STAT3 inhibitor) [169] or STAT3 KO models [122], [170], lead to a loss of the cardioprotective effect of IPoC.

3.2.2. Activation and downstream signal

The upstream activators of SAFE pathway have been poorly studied. Nevertheless, several agents produced during IPoC have been shown to confer their protective effects via the SAFE pathway. In this regard, Angiotensin II[171], bradykinin[172], [173], adenosine and opioids [147] were shown to activate TNFα and STAT3.

TNFα, on its own, is an activator of the JAK/STAT3 signaling cascade through its TNFR2 receptor. TNFα plays roles in the myocardial inflammatory response during reperfusion, acting as pro-inflammatory cytokine. Paradoxically, it's considered an important endogenous cardio-protectant [174]. The observed contradicting roles depend on the amount of TNFα presented and the receptor on which TNFα binds, whereby TNFR1 may be considered cardio-toxic, while TNFR2 is cardioprotective through JAK/STAT3 activation[136]. In this regard, IPoC applied in TNFR2-KO mice was reported to be non-protective, and this effect was associated with an absence of STAT3 phosphorylation. Furthermore, the inhibition of STAT3 in mice post-conditioned with TNF was also been shown to be non-protective [137]. Noteworthy, TNF has been reported to strongly activate JNK and moderately evoke response of the p38-MAPK [175].

In addition to TNFα, JAK/STAT3 can be activated by sphingosine-1-phosphate [176], IL6 family cytokines and growth factors.

3.2.3. Mechanisms of cardioprotection

As a transcription factor activated downstream JAK, STAT3 translocates to the nucleus and mediates cardioprotection through increasing the expression of the anti-apoptotic bcl2 gene [117], [119] and the anti-oxidative (MnSOD and Metallothionein MT1/MT2) ones [177], [178], along with decreasing the expression of the pro-apoptotic gene bax [179]. The transcriptional activity of STAT3 during IPoC is only studied in the context of apoptotic and anti-oxidative genes, but it is not investigated in other contexts. Moreover, STAT3 can phosphorylate and

inactivate GSK3β, a common downstream target with RISK pathway [180]. Aside from this ascribed transcriptional activity, a non-genomic mitochondrial activity of STAT3 has emerged. In this context, a study conducted on isolated pigs mitochondria reported that IPoC preserved complex I activity and increased the mitochondrial calcium retention capacity in comparison to IR alone [121]. The *in vivo* administration of the JAK/STAT inhibitor AG490 or the *in vitro* treatment of mitochondria by the STAT3 inhibitor Stattic lead to the loss of the induced IPoC effect on complex I respiration and CRC. Noteworthy, this group reported that the *in vivo* use of Stattic was toxic in their model.

3.2.4. Controversial Issues of SAFE pathway

Although many studies have reported the activation and involvement of the SAFE pathway in IPoC, some studies failed to confirm this concept. For instance, in a study conducted on a rat model, Barsukevich et al. have reported that RISK rather than SAFE pathway is involved in the protective effect of IPoC, whereby the blockade of SAFE pathway using AG490 had no effect on cardioprotection [181]. Although AG490 is able to inhibit STAT3, it may also inhibit other STAT family members since it's a JAK2 inhibitor. Thus, it's important to keep in mind that the use of AG490 could induce effects which are not strictly related to STAT3. This points out the importance of using STAT3-specific inhibitors, among which Stattic is well known. Unfortunately, controversial results were reported for the *in vivo* use of Stattic. In this regard, Heusch et al have abandoned the *in vivo* use of Stattic in their pigs model due to toxicity [182]. On the contrary, another study has used Stattic in mice, in the context of I/R, without reporting toxicity [183]. In this study, Stattic was injected intraperitoneally in order to investigate the involvement of STAT3 in the cardioprotective effects of rapamycin against IR. However, no previous studies have assessed the *in vivo* effects of Stattic in the context of IPoC.

The contradicting results on the involvement of RISK or SAFE pathway, observed in different papers, could be due to the variation in the applied protocol, species, age and gender. A prominent demonstration of this notion is highlighted in the study tangled by Boengler et al., who showed that cardioprotection by the IPoC through applying 3 cycles of (10 secs ischemia- 10 secs reperfusion) was impaired in aged mice, but not in young mice. Modifying this IPoC protocol into 5 cycles of (5 secs ischemia- 5 secs reperfusion), has surprisingly protected aged mice[122]

3.3. Interlink RISK-SAFE

It is now clear to us that IPoC can protect against the detrimental effects of the ischemia reperfusion injury through either the RISK or the SAFE pathway. However, the inhibition of either pathways appears to completely abolish the cardioprotective effects of IPoC. This suggests that there's either an interaction between the two pathways or that the used models are failing to distinguish between partial or complete inhibition of cardioprotection. This issue provoked the investigation of the interplay between the two pathways. Interestingly, Goodman et al. found, using an ex vivo Langendorff perfused mice heart model, that the pharmacological inhibition of STAT3 by Stattic abrogated the IPoC-induced phosphorylation of STAT3 and Akt, which suggests that STAT3 is upstream Akt[169]. Similarly, another study conducted in Wistar rats reported that JAK2 inhibition by AG490 decreased the levels of both phosphorylated Stat3 and Akt, which was accompanied to the loss of the cardioprotection induced by IPoC [117]. This cardioprotective effect of IPoC was characterized by a decrease in apoptosis and a reduction in infarct size, which were loss by AG490 treatment. However, the use of the PI3K inhibitor Wortmannin decreased Akt but not STAT3 phosphorylation, again highlighting that STAT3 might post probably be upstream Akt.

Having relatively low amount of reports targeting the interplay between the SAFE and RISK pathways, precisely between STAT3 and the components of RISK other than Akt, this field of research constitutes an interesting and important target for researchers in the cardiovascular research. Among the different mentioned proteins and kinases in the cardioprotective pathways, STAT3 has been of a major focus for a lot of cardioprotective studies. In the upcoming chapter, we'll be focusing on STAT3.

Chapter 6: STAT3

As a prominent key player in cardioprotection and in the maintenance of cardiac function, STAT3 has been thoroughly studied in the field of cardiovascular research. Its cardiac functions are ascribed to its genomic actions as a transcription factor and to its non-genomic actions targeting mitochondrial functions and autophagy. In the following chapter, we'll have an overview of STAT3, along with its involvement in IRI and IPoC.

1. Definition and Structure

The signal transducer and activator of transcription 3, STAT3, is an 89 KDa protein composed of 770 amino acids. It's both a signaling molecule and a transcription factor with five main domains. First comes the N-terminal domain, with roles in nuclear translocation and protein interactions, followed by coiled-coil, DNA-binding, SH2 and variable TAD domains **Fig. 19**. The coiled-coil domain is involved in nuclear export and regulation of tyrosine phosphorylation, while the DNA-binding domain mediates recognition of sequences in the promoters of responsive genes. As for the SH2 domain, it is the domain through which STAT3 forms dimers. Finally comes the divergent C-terminal TAD which mediates transactivation [166],[184].

Figure 19. The different STAT3 domains.
Adapted from [173]

2. Post-translational modifications and Activation

STAT3 is modified at several residues by a number of post translational modifications with functional consequences, mainly phosphorylation and acetylation. In addition, methylation, ubiquitination, s-nitrosylation and gluta-thionylation also occur [185].

2.1. Phosphorylation

STAT3 phosphorylation is the addition of a phosphate molecule (PO_4^{3-}) to a residue on STAT3. It's a crucial post-translational modification for STAT3 activation in response to various stimulations. STAT3 is phosphorylated on two residues: Tyrosine 705 (Y705) and Serine 727 (S727).

2.1.1. Tyrosine Phosphorylation

STAT3 is activated by Y705 phosphorylation. This phosphorylation is mediated by non-receptor and receptor tyrosine kinases, primarily JAKs (JAK1 and JAK2), in response to stimulation by a variety of ligands including cytokines, growth factors and onco-proteins. Once the ligand binds to JAK-associated receptor subunits, dimerization of two receptor subunits occurs. This ligand-mediated receptor dimerization brings two JAK molecules into close proximity, allowing a trans-phosphorylation and activation. The activated JAKs subsequently phosphorylate the receptors themselves and STATs, including STAT3 at its Y705 residue. Two Tyrosine phosphorylated STAT3 (PY705-STAT3) molecules dimerize through an -SH2 interaction, and they consequently enter the nucleus to regulate transcription of targeted genes through binding to DNA **Fig. 20** [167].

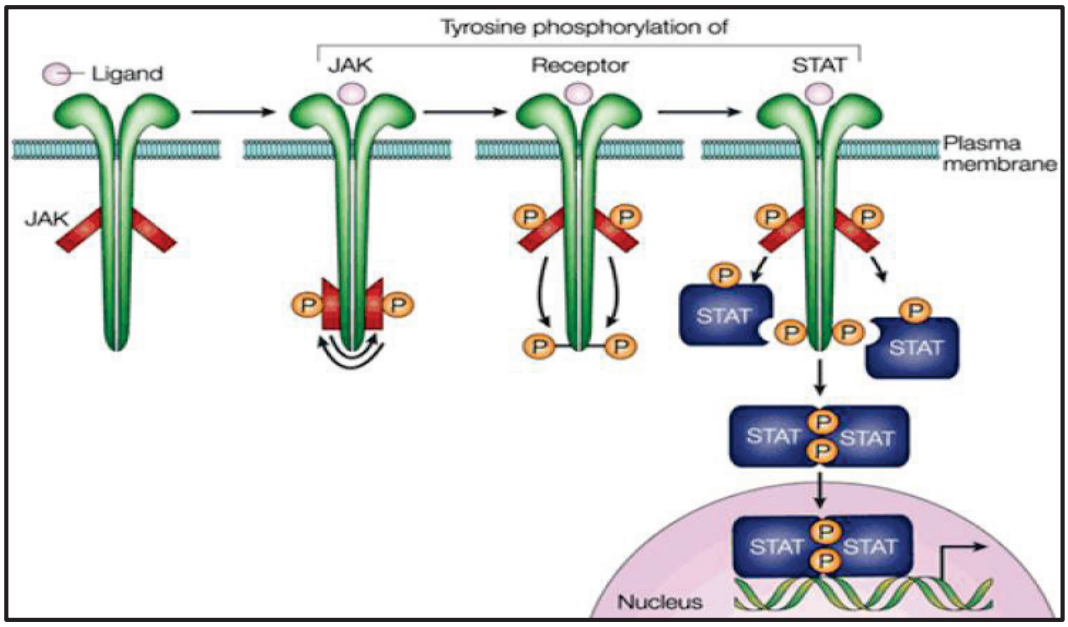

Figure 20. The JAK-STAT pathway activation

Following the ligand binding, the receptor subunits dimerize and bring two JAK molecules into close proximity, allowing a trans-phosphorylation and activation. The activated JAKs subsequently phosphorylate the receptors themselves and STATs, including STAT3 at its Y705 residue. Two Tyrosine phosphorylated STAT3 (PY705-STAT3) molecules dimerize and enter the nucleus to regulate transcription of targeted genes through binding to DNA.

2.1.2. Serine Phosphorylation

STAT3 is phosphorylated on its S727 residue by serine/threonine kinases such as MAPKS, PKC, m-TOR and CDK5. Among them, MAPKs are the main involved kinases, with ERK1/2 being characterized as the best serine kinase involved in S727-STAT3 phosphorylation [185]–[189].

S727 STAT3 phosphorylation is considered a secondary event following Y705-STAT3 phosphorylation, whereby it's required for the maximal transcriptional activity of STAT3 but not for DNA binding. It seems to boost STAT3 transcriptional activity by recruiting transcriptional co-factors [190]–[193]. Interestingly, S727 phosphorylation was suggested to negatively modulate Y705 phosphorylation [194], [195], but this idea is not well elaborated in literature.

In addition to the stated roles, S727 STAT3 phosphorylation has been suggested to be involved in directing the translocation of STAT3 to the mitochondria, where it regulates mitochondrial functioning (discussed later) [121], [196].

2.2. Acetylation

In addition to phosphorylation, the function of STAT3 is also regulated by p300-mediated acetylation of several lysine residues. STAT3 acetylation is important for its transcriptional activity since it provokes the retention of STAT3 in the nucleus. In addition, acetylated STAT3 positively enhances the accessibility of other transcription factors to specific genes promoters [197]–[199].

3. Pharmacological inhibition

The pharmacological inhibition of STAT3 has been thoroughly used as a tool to study STAT3 signaling and its respective downstream functions. The approaches used for specifically inhibiting STAT3 have targeted the -SH2 domain, which is used by STAT3 for homo-dimerization. In this regard, Stattic has been widely used as a STAT3 inhibitor, with an IC50 against STAT3 phosphorylation of 20 μM for 1 h incubation at 30°C [200]. It inhibits the activation, dimerization, and nuclear translocation of STAT3. Before Stattic, STA-21 has been used for inhibiting the DNA binding of phosphorylated STAT3 [201]. However, the effectiveness of this inhibitor against non-phosphorylated STAT3 was not proven. Following Stattic, the S3I-201 inhibitor was identified by the National Cancer Institute chemical libraries [202]. Like Stattic, it inhibits STAT3 homo-dimerization, DNA-binding and transcriptional activities

4. Cellular STAT3 pools

STAT3 is predominately cytoplasmic in resting cells, but it has the ability to translocate to the nucleus in order to transduce signals from the receptors. In addition to its nuclear translocation, mitochondrial STAT3 translocation and roles have evolved later on **Fig. 21**.

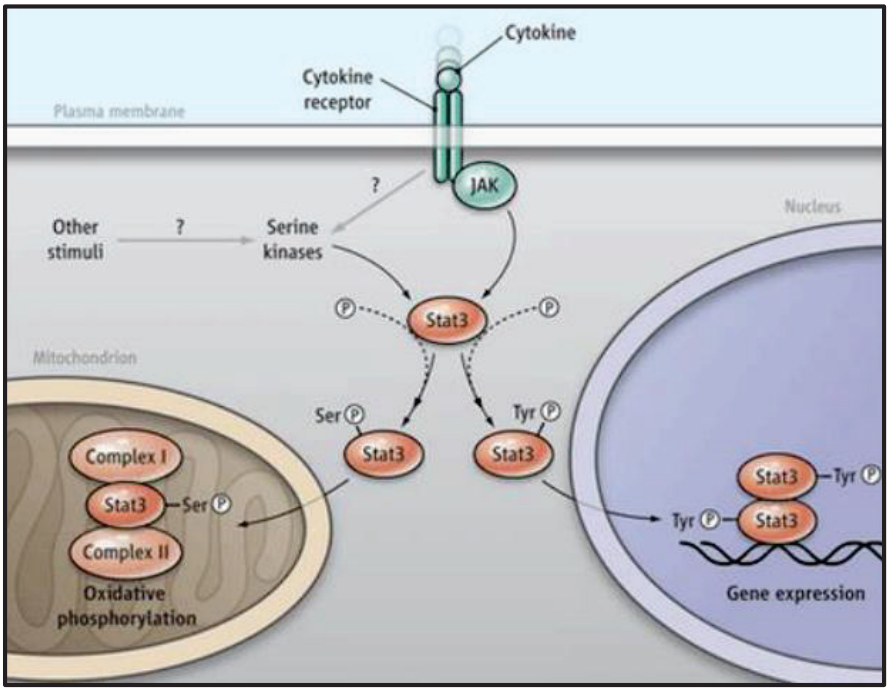

Figure 21. STAT3 nuclear and mitochondrial pools

The phosphorylation of STAT3 on the serine residue provokes its mitochondrial translocation, while the phosphorylation on the tyrosine residue provokes the nuclear translocation. [211]

4.1. Nuclear STAT3

As a transcription factor, steady-state STAT3 plays important roles in the heart. It positively regulates the expression of anti-apoptotic (Bcl2 and Bcl-xl) [186] and anti-oxidative (MnSOD and Metallothionein MT1/MT2) genes [178]. It also reduces the expression of the pro-apoptotic factor BAD and regulates the expression of several growth factors such as the vascular endothelial growth factor (VEGF) [136]. Moreover, it increases the expression of COX-2 and HO-1 proteins, which are involved in cardioprotection [203].

STAT3 is not only important for transcription, but it is also crucial for the development, whereby the embryonic knock out of STAT3 gene leads to embryonic lethality [204]. Thus, attempts to assess the role of STAT3 in adult tissues utilized other techniques such the Cre-loxP recombination systems or cell-specific knocking out of STAT3 [205]. Focusing on the heart, the specific deletion of STAT3 in mice cardiac cells increased the susceptibility to cardiac injury and increased cardiac fibrosis, as shown by histologic examination [206]. Moreover, these STAT3-deficient mice developed heart dysfunction with advancing ages. Taking into consideration the physiological importance of STAT3 in the heart and having in mind that STAT3 regulates genes involved in metabolism and mitochondrial activity [207], [208], any attempt to use STAT3 KO models shall be carefully handled to avoid any mis-interpretations of the observed effects.

4.2. Mitochondrial STAT3

Although STAT3-dependent biological effects are due to its potency as a transcription factor, controversial non-canonical and non-genomic activities have emerged. Several studies have detected mitochondrial STAT3 in various types of cells and tissues including cardiac myocytes and the heart tissue, which opened up new perspectives on the importance of STAT3 in controlling cellular homeostasis [121], [178], [187], [209]. The mitochondrial translocation and activity of STAT3 have been linked to its S727 phosphorylation [210], [211].

In the mitochondria, STAT3 participates in controlling cellular respiration and ATP production through controlling the activities of complexes I and II of the electron transport chain. In this context, the CM-specific deletion of STAT3 or its pharmacologic inhibition have been shown to decrease mitochondrial respiration and complexes I/II activities[178], [210]. Moreover, STAT3 might also be involved controlling the mPTP opening [212].

5. STAT3 in Cardioprotection

STAT3 has been implicated in protecting the heart from acute ischemic injury under basal conditions and as a crucial component of the ischemic conditioning protocols. Moreover, evidence indicates that STAT3 in protective to the heart under chronic stress conditions including hypertension, pregnancy and aging [185].

5.1. STAT3 in IRI

During ischemia, STAT3 is mainly phosphorylated on its Y705 residue, with a further increase during early reperfusion [170], [213]–[217]. However, the phosphorylation of STAT3 following prolonged reperfusion is not well established in literature. This phosphorylation is activated by the ligands which are released during the IRI and bind to JAK-coupled receptors. These ligands include IL-6 cytokines [188], [216], [218]–[220], angiotensin II [217], TNF [221] and insulin [170].

The activated STAT3 contributes to the protection against IRI through decreasing ROS generation and increasing their scavengers, decreasing apoptosis, delaying mPTP opening and increasing angiogenesis. This is achieved by regulating gene expression and interfering in the mitochondrial functions [177], [222]–[224].

5.2. STAT3 in Ischemic Conditioning

As the main key player in the SAFE pathway, STAT3 is involved in mediating the protective effect of ischemic conditioning. This role was already elaborated in the previous chapter. Briefly, this involvement was assessed in different studies using STAT3 KO models or JAK-STAT pathway inhibitors. The majority of studies have focused on measuring the Y705-STAT3 phosphorylation, with very few ones targeting S727 phosphorylation. However, due to its evolving prominent roles, studying S727 STAT3 phosphorylation during ischemic conditioning remains of important interest.

As in IRI, STAT3 participates in the conditioning-induced cardioprotection by reducing apoptosis, reducing ROS generation increasing the expression of cardioprotective proteins, preserving mitochondrial respiration and delaying the mPTP opening [117], [119], [179], [203], [225]. Focusing on the mitochondrial STAT3 functions in cardioprotection, the exact phosphorylation site that is important for the improvement of mitochondrial activity by STAT3 is not clear and varies with species. In mouse cardiomyocytes mitochondria it was S727 site[210], [226], but it was both Y705 and S727 in rats cardiomyocytes mitochondria[212]. In pigs, Y705 site has been linked to the mitochondrial STAT3 activity[182].

6. STAT3 in Cardiac Inflammation

Based on what we've mentioned in the previous parts and chapters, it's now clear to us that STAT3 plays cardioprotective roles against IRI, which reflects its physiological importance in the protection against myocardial infarction (MI). In addition to what was stated before about STAT3 in this context, STAT3 was also shown to play important roles in regulating cardiac remodeling following MI [227]. When speaking about myocardial infarction, inflammation stands out as a prominent feature, since the inflammatory response is a prominent hallmark of IRI. In the context of inflammation, STAT3 has been linked to cytokine signaling, neutrophils trafficking and macrophages polarization, which is elaborated in the following sections.

6.1. STAT3 in Inflammatory Cytokine Signaling

STAT3 is a central signaling molecule downstream several cytokine receptors, including pro- and anti- inflammatory cytokines.

As a pro-inflammatory signaling molecule, STAT3 is acutely activated downstream IL-6 via the gp130 receptor. This activation is known to be suppressed by the suppressor of cytokine signaling (SOCS3), which binds to gp-130 receptor subunit and prevents receptor dimerization. The expression of SOCS3 is by itself regulated by STAT3 [215], [228]. Thus, a negative feedback loop is initiated by STAT3 in the pro-inflammatory response to regulate its own activation.

In this pro-inflammatory context, Kleiner et al have shown that a mutation in mice gp130 receptor subunit enhanced STAT3 activation and increased IL-6 expression, which was associated with an increased inflammation during myocardial infarction[229]. The cardiomyocytes-specific deletion of STAT3 in the mutated mice enhanced survival rates and lowered the degree of post-MI inflammation, assessed by the amount of CD45-positive cells (leukocytes and macrophages). This shows the IL-6 dependent activation of STAT3 downstream gp130 increases the inflammatory response.

On the other hand, STAT3 is activated downstream IL-10 as an anti-inflammatory response mediator. STAT3 activity, by itself, does not result in an activated anti-immune response. Instead, STAT3 activates expression of one or more effector genes that selectively repress sets of inflammatory genes such as TNFα, IL-12p40, IL-1α, IL-1β, IL-6 [230], [231]. In this context, Jacoby et al have reported that the cardiomyocytes-specific knockout of STAT3 resulted in a higher sensitivity to inflammation, whereby STAT3 KO cardiomyocytes secreted more TNF in response to LPS treatment in comparison to WT cardiomyocytes [206].

6.2. STAT3 in neutrophils/macrophages recruitment

IL-6 represents an important regulator of neutrophil trafficking during the inflammatory response through orchestrating the chemokine production and leukocyte apoptosis. This process has been suggested to be dependent on STAT3 signaling, whereby the hyper activation of STAT3 induced a more rapid clearance of neutrophils in mice with LPS-induced inflammation [232]. This coincided with a pronounced down-modulation in production of the neutrophil-attracting chemokine CXCL1/KC [232]. This points toward the possibility that STAT3 might regulate neutrophils clearance via modulating cxcl-1 production. In addition, STAT3 was linked to the regulation of monocytes and macrophages recruitment following MI through regulating the production of Reg3β, which is secreted by cardiomyocytes in response to OSM stimulation, and plays prominent roles in monocytes and macrophages recruitment to the infarcted area [64]. In this study, the KO of STAT3 in cardiomyocytes abolished Reg3β secretion, which lead to the loss of paracrine effects of cardiomyocytes on inflammatory cells in mice models of MI.

6.3.STAT3 in macrophages Polarization

As we already stated, two types of macrophages exist: The M1 and the M2. M1 macrophages are pro-inflammatory and express inflammatory genes, including iNOS. In contrast, M2 macrophages are involved in the resolution of inflammation and secrete arginase-1 and IL-10 [233]. In this regard, a role for STAT3 in polarizing macrophages to the M2 phenotype, following MI, has been highlighted [234], [233], [235]. The polarization was suggested to be mediated by STAT3 downstream the IL-10 activation [235].

Cardioprotective strategies against MI have previously targeted inflammation. Although STAT3 has been linked to the inflammatory and non-inflammatory responses during MI, no previous reports have investigated its involvement in the regulation of the inflammatory response during the cardioprotective IPoC. Having in mind that STAT3 is a mediator of cardioprotection, an important aspect would be to investigate its involvement in the inflammatory response during IPoC.

AIMS

Having introduced the IRI and IPoC, it is now clear to us that the co-involvement of both the SAFE and RISK pathways in the protective effects of IPoC is controversial. In addition, the mechanisms of involvement of the different effectors of these pathways in cardioprotection are not well understood and elaborated. As previously explained, the SAFE pathway involves the JAK-STAT3 cascade, while the RISK pathway mainly involves MEK-ERK and PI3K-Akt cascades, in addition to the MAPKs P38 and JNK.

STAT3, the key player in the SAFE pathway, is suggested to contribute to cardioprotection against IRI through regulating the mitochondrial functions and gene transcription. In an attempt to study the mitochondrial evolving cardioprotective activity of STAT3, **we aimed to investigate the mitochondrial roles of STAT3 under IR and IPoC conditions**. However, the obtained results pointed toward absence of such activity. This shifted our work toward targeting the signaling and genomic STAT3 activities.

Taking into consideration the complexity and connection of the biological processes in the body from the systemic down to the cellular level, studying STAT3 and the SAFE pathway, independently of RISK, might be highly misleading. Interestingly, the SAFE and RISK pathways are suggested to interlink, but the interlink between them is not well defined and is still under investigation in this field of research. **Hereby, we aimed to study the kinetics of phosphorylation of STAT3, Akt, and the MAPKs (ERK, P38 and JNK) following IR and IPoC up to prolonged reperfusion in one single study and model, in addition to deciphering the interlink between them under both conditions.**

The role of STAT3 as a transcription factor is not well defined during IPoC. In this context, very few are the reports which have targeted its transcriptional function. Thus, as a holistic approach, we moved from investigating the activation of STAT3 as a signaling molecule to studying its transcriptional activity at the genomic level**. At this level, we aimed to study the biological functions of selected STAT3-regulated genes, during IR and IPoC.**

Overall, our work represents a holistic approach for STAT3, involving both canonical and non-canonical functions, at the proteomic and genomic levels.

MATERIALS and METHODS

As we have already mentioned, our work was divided between several aims. The general flow of the work, showing the used materials and methods, is presented in the following schemes. The detailed methods are then explained.

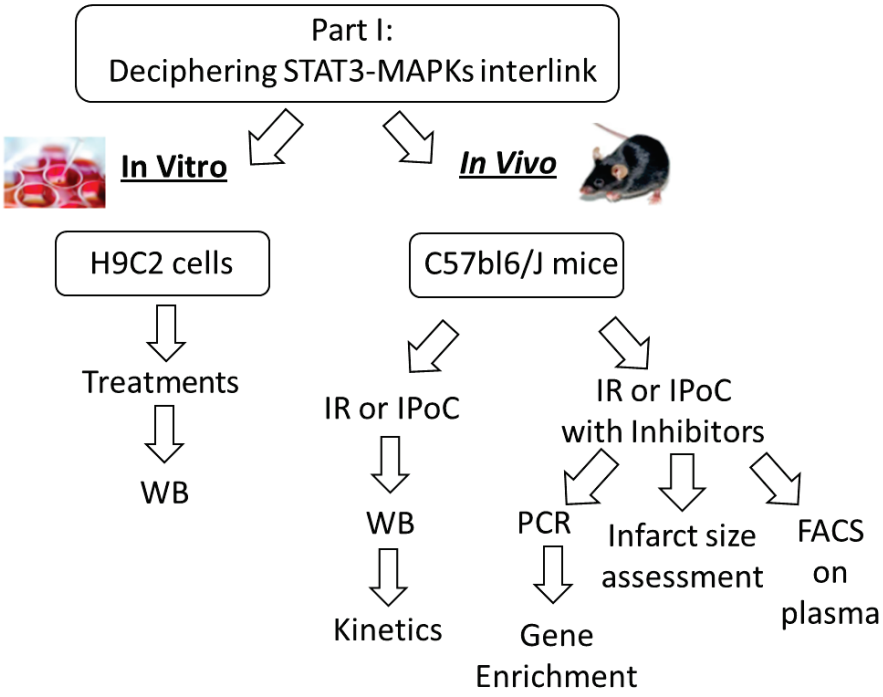

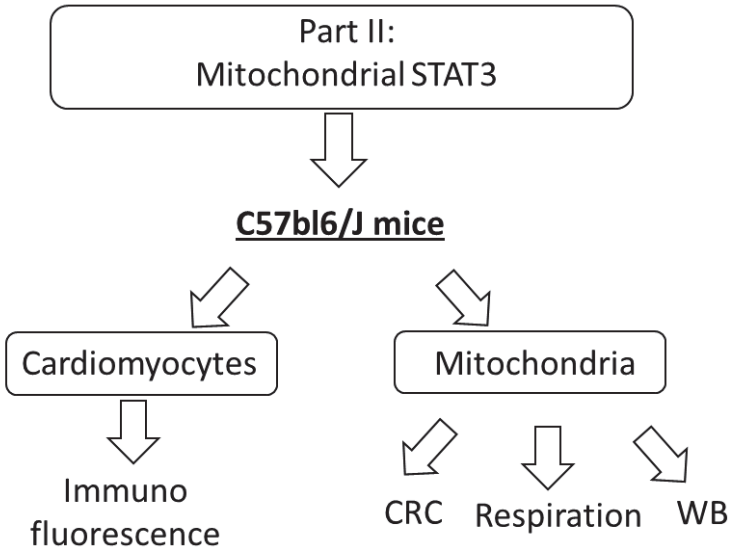

1. Biological Models

1.1. In Vivo Models

1.1.1. Animals

The experiments were carried out on young C57bl/6J male mice aged between 8-12 weeks, obtained from Charles River Laboratories. The mice were chosen at a young age to ensure their ability of responding to the applied IPoC protocol, since the use of old mice showed resistance to cardioprotection[122]. Once characterizing the molecular mechanisms in this IPoC-responding model, it'll be interesting to move toward finding out the mechanism leading to a resistance to cardioprotection (IPoC) in old animals. These mice were housed in the animal facility of the laboratory in controlled-temperature (24°C) conditions, with a 12-h light/12-h dark cycle and had free access to water and standard rodent diet. They received human care according to the NIH Guide on the Use of Laboratory Animals (NIH Publication No. 85-23, revised 1996). All the procedures were approved by the local institutional animal research committee (N°BH2012-65 for the surgical procedure and N°BH2012-64 for heart collect).

1.1.2. Acute Myocardial Ischemia-Reperfusion (IR) Injury

The mice received an intra-peritoneal (IP) premedication of 0.075 mg/kg Buprenorphine and 2 mg/kg Lidocaine (Vetergesic ®) as analgesics. After calming down, they were anesthetized by another IP injection of 80 mg/kg Alfaxan and 0.3 mg/kg Medetomideine mixture. They were then placed on a blanket at 38°C for 10-15 minutes until they were fully asleep. Electrocradiogram (ECG) and heart rate were monitored using EGC electrodes, and an oximeter was attached to the left hind leg of the animal for SpO2 monitoring. A tracheotomy was performed and mice were mechanically ventilated. For the induction of local myocardial infarction, the tissues that hold the muscles protecting the rib cage together were delicately dissected and were then removed without damage, releasing access to the rib cage. The pericardium was then opened and an 8-0 polypropylene suture was placed around the left anterior descending aretery (LAD). 45 minutes ischemia were then achieved by tightening these sutures. After ischemia was over, the suture was loosened to allow cardiac reperfusion for various durations of time (15 minutes, 3 hours and 24 hours)

(n=8/group). The mice were finally euthanized by cervical dislocation, after which the areas at risk were collected.

1.1.3. Ischemic Post-Conditioning (IPoC)

Following the 45 minutes ischemia described above, ischemic postcondiitoning was mechanically performed, within one minute of reperfusion, by applying 3 cycles of 1 minute ischemia/1 minute reperfusion. These cycles were followed by 15mins, 3 hours or 24 hours of non-stopped reperfusion (n=8/group) . At the end of reperfusion, the mice were euthanized by cervical dislocation, after which the areas at risk were collected.

1.1.4. In Vivo Inhibitors

In a seperate series of experiments, mice were subjected to 40 minutes of ischemia. They then received an intraveneous injection of DMSO (vehicle), the STAT3 inhibitor Stattic (9 mg/kg) and the MEK-ERK inhibitor PD98059 (2.5 mg/kg). The inhibitors and the DMSO vehicle were prepared in 70% cremophor EL (Sigma C5135) castor oil and diluted six times in NaCl to ensure their solubility and dispersion once injected *in vivo*. Our attempts to use the inhibitors without cremophor oil failed to show any effects, which might most probably be due to the lack of absorbance of these products. Five minutes following the injection (when the 45 minutes ischemia were completed), the infacted areas were reperfused for three hours. This reperfusion was applied in the presence or absence of IPoC. At the end of reperfusion, the areas at risk were collected for RNA extraction and PCR analysis. Moreover, blood samples were also collected for ELISA analysis of extracted plasma. A control sham group, subjected to the surgery protocol with no LAD occlusion, was also presented to eliminate the surgery effect.

Mice were distributed among ischemia, ischemia-reperfusion (IR) or ischemic post conditioning (IPoC) [with and without inhibitors] groups, as shown in **Fig. 22.**

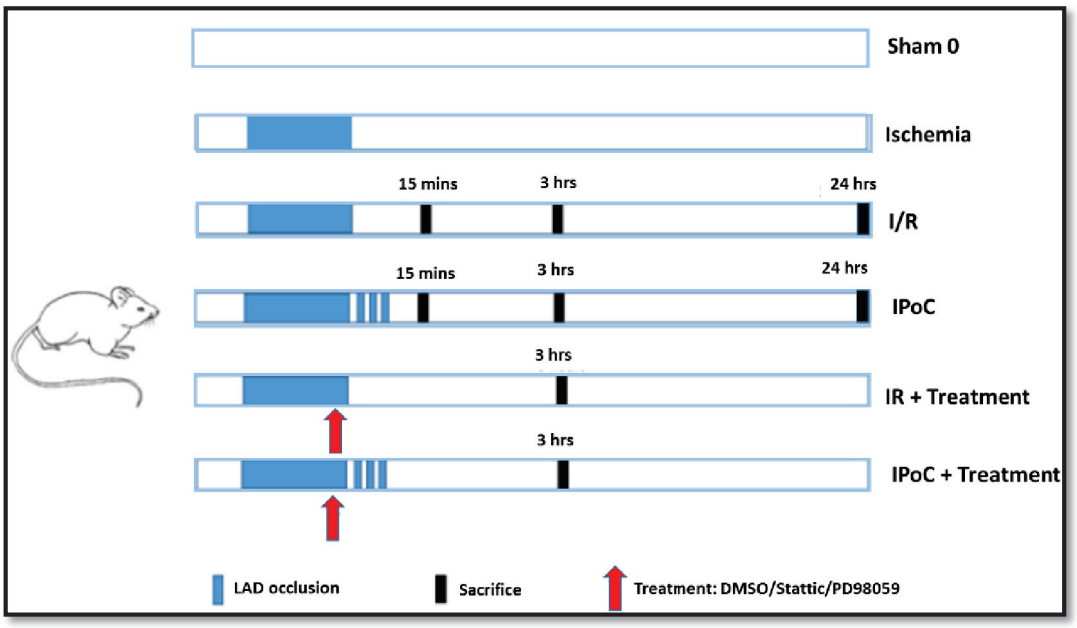

Figure 22. The different used in vivo animal groups

The C57bl6/J mice were subjected to 45 minutes ischemia followed by 15 minutes, 3 hours or 24 hours of reperfusion. This was performed with and without ischemic postconditioning (n=8).
Another series of experiments was done, whereby mice were subjected to 45 minutes ischemia followed by 3 hours of reperfusion. The mice were treated with DMSO, Stattic and PD98059 10 minutes before reperfusion. This was done with and without ischemic postconditioning.

1.1.5. Infarct Size Measurement

The infarct sizes were measured in 4 groups of mice (n=5/group). The 4 groups were IR+DMSO, IPoC+DMSO, IPoC+Stattic, IPoC+PD98059. Following 40 mins ischemia, inhibitors/vehicle were injected (5 mins before reperfusion). Once the 45 mins of ischemia were over, the ischemic areas were reperfused for 24 hours. At the end of the 24-hour reperfusion, the mice were deeply anesthetized to allow re- occlusion of the artery (the suture material was still in place from the previous surgery), and Unisperse blue pigment (0.5 mg/kg i.v.; Ciba-Geigy) was injected in the inferior vena cava. With this technique, the non-ischemic myocardium appears blue, whereas the ischemic myocardium (area at risk (AAR)) remains unstained. The hearts were then excised and the atrial and right ventricular tissues were removed. The left ventricles were then cut into four 1mm-thick transverse slices. The basal surface of each slice was photographed for later measurement of the AAR. Slices were then incubated for 15 minutes in a 1% solution of 2,3,5-triphenyltetrazolium chloride (TTC) at 37°C. With this technique, the viable myocardial tissues appear brick red, whereas the infarcted tissues remain pale. The slices were then photographed for later

measurement of the necrotic area. The extent of the area at risk and the infarcted area were quantified by computerized planimetry using SigmaScanPro software and corrected for the weight of the tissue slices.

1.2. *In vitro* Models

1.2.1. Culture of H9C2

The rat derived H9C2 cell line of cardiomyoblasts was cultured in Dulbecco's Modified Eagle's Medium (DMEM) (41965-039 Gipco), supplemented with 10% Fetal Bovine Serum (FBS) and 100 U/ml penicillin/streptomycin (Sigma Chemical Co., St. Louis, MO) under a humidified incubator aerated with 5% CO_2 at 37℃.

1.2.2. Experimental groups of H9C2

In order to study the interlink between STAT3 and other kinases, H9C2 cells were divided into different experimental sets. In each set, cells were treated by DMSO vehicle or by a specific inhibitor of kinases **(table 1).** The effect of the kinase inhibiton on its downstream phosphorylation or on STAT3 phosphorylation was then studied by western blotting **Fig. 23**.

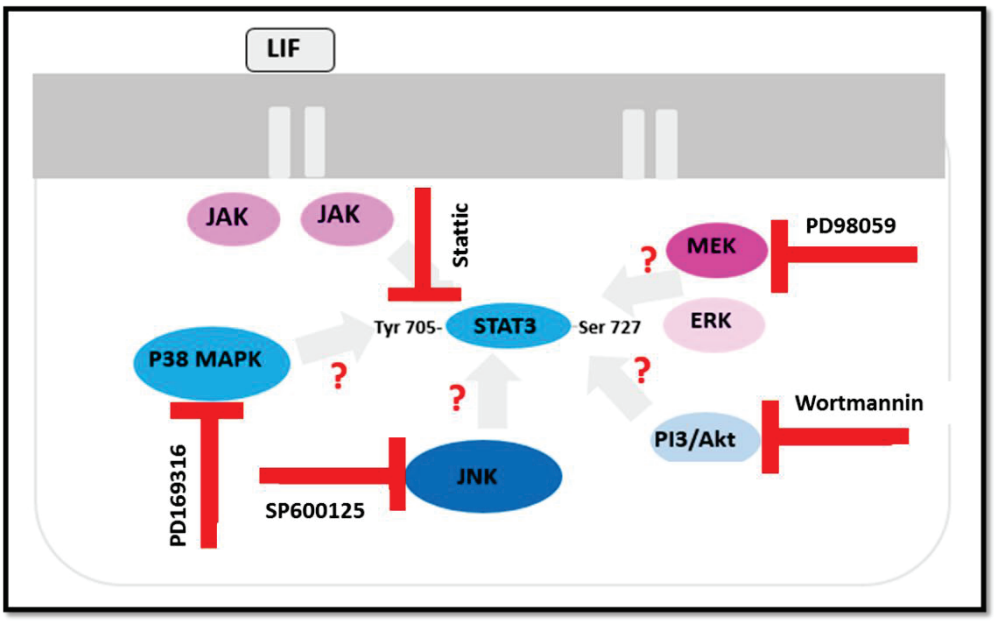

Figure 23. The scheme of the different inhibitors used in vitro

To decipher the *in vitro* interlink between STAT3, Akt and the MAPKs, H9C2 cells were treated with different inhibitors, including PD98059 (MEK-ERK), Wortmannin (Akt), SP600125 (JNK), PD98059 (P38 MAPK).

Reagent	Target	Function	Dose	Time	supplier	Reference
DMSO	-	vehicle	variable	variable	Sigma	D2650
LIF	STAT3	Activator	2 ng/mL	15 mins	Sigma	L5158
PD98059	MEK-ERK	Inhibitor	30 µM	1 hour	Sigma	P215
SP600125	JNK	Inhibitor	100 µM	1 hour	Sigma	S5567
PD169316	P38	Inhibitor	50µM	30 mins	Sigma	P9248
wortmannin	PI3K-Akt	Inhibitor	4µM	1 hour	Cell signaling	9951
Stattic	STAT3	Inhibitor	50 µM	1 hour	sigma	S7946

Table 1. The list of the used reagents for the in vitro studies

1.3. Ex vivo Model of Cardiomyocytes

1.3.1. Cardiomyocytes Isolation

As previously described [236], mice received an intraperitoneal injection of 50UI/kg heparin sodium for 10 mins. The mice were euthanized and the heart was harvested and cannulated through the aorta in a langendorf isolation system. The heart was firstly perfused for three minutes with perfusion buffer (NaCl 120.4 mM, KCl 14.7 mM, KH2PO4 0.6 mM, Na2HPO4 0.6 mM, MgSO4-7H2O 1.5 mL, Na-HEPES 10 mM, NaHCO3 4.6 mM, Taurine 30 mM, 2,3-butanedione monoxime (BDM) 10 mM, and Glucose 5.5 mM, pH 7.0). The latter was then replaced by digestion buffer (50 mL of perfusion buffer and Collagenase II 2.4 mg/mL) for 2 minutes 30 seconds and 100 mM CaCl2 (final concentration 40 µM) were added. Perfusion was continued for 6 minutes and 30 seconds. During all the procedure, the heart was perfused at 4mL/min rate and the solutions were maintained at 37°C to mimic physiological conditions. After 12 minutes, the heart was placed in a dish and cut into small pieces that were placed in a tube containing 2.5 mL of myocyte digestion buffer. Small pieces were gently pipetted several times to ensure complete digestion. Digestion stop buffer (45 mL of perfusion buffer, 5 mL of fetal bovine serum (10 %), and 6.25 µM of 100 mM CaCl2 (12.5 µM)) was then added up to a final volume of 10 mL. The tube was then centrifuged for 3 mins at 20g at room temperature (Eppendorf 5810R). The pellet was resuspended in 10 mL of myocyte stop buffer containing 200 mM of ATP prior to calcium reintroduction. The suspension was again centrifuged 3 minutes at 20g. Calcium lifts were realized by successive centrifugations (3 minutes, 20g), each with a higher calcium concentration until reaching a final calcium concentration of 0.9 mM.

1.3.2. Hypoxia-Reoxygenation of cardiomyocytes

The isolated cardiomyocytes were deposited in 8-well plates and were subjected to 90 min hypoxia (0.5 % oxygen) in glucose-free medium (mM: 140 NaCl, 5 KCl, 1 $MgCl_2$, 10 HEPES [pH 7.4], 10 $CaCl_2$) in a hypoxic incubator (Eppendorf; galaxy 48R-CO48EN200259), followed by 1 h of reoxygenation (glucose-containing medium). Cells were then immuno-labeled and visualized by microscopy.

1.3.3. Stattic treatment of cardiomyocytes

In order to choose a suitable Stattic does for the inhibition of PY705-STAT3 phosphorylation, isolated adult cardiomyocytes were treated, in suspension, with either Stattic (10-100µM) or DMSO vehicle for 1 or 2 hours at 37°C. The proteins were then extracted and analyzed by Western blotting.

2. Biochemical Analysis

2.1. Western Blotting

2.1.1. Principle

This analytical technique allows us to identify the proteins of interest according to their molecular weights in a midst of a complex protein mixture. It is a semi-quantitative method which permits us to determine the quantity of a specific protein relative to other reference proteins. It is majorly divided into five main steps: migration, transfer, blockage, immunodetection and revelation. Prior to these five steps, protein extracts are prepared and the total protein content is quantified.

2.1.2. Protocol

A- Protein Extraction

- **Complete lysis Buffer preparation:**

The lysis of heart samples was induced by complete lysis buffer of RIPA (NaCl 150mM, Triton X100 1%, Sodium deoxycholate 0.5%, and Tris 50mM) supplemented with 5mM EDTA, 1mM DTT, 1mM anti-protease cocktail (sigma), and 1mM of anti-phosphatase.

- **Tissues homoginization and protein extraction**

300 µL of the lysis buffer were added to the heart samples in special homogenization tubes (precellys P000933-LYSK0-A, Ozyme). The tubes were then placed in tissue homogenizer (Precellys 24, Bertin technologies) set at 6000 agitations/min 3 times 10 secs. After homogenization, the samples were transferred to Eppendorf tubes and centrifuged for 10 minutes at 13000 RPM (Hilac CT15RE). The supernatants were then collected in new Eppendorf tubes for protein quantification.

- **Protein Extraction from cells**

50 µL of the lysis buffer were added per a plate of cells (9 cm^2). The cells were collected in Eppendorf tubes and kept on ice for 30 minutes, with a 1-minute vortexing every 10 minutes. After the 30 minutes were over, the cells were centrifuged for 10 minutes at 13000 RPM (Hilac CT15RE). The supernatants were then collected in new Eppendorf tubes for protein quantification.

B- Protein Dosage by BC Assay

A standard curve of BSA (Bovine Serum Albumin) was prepared in RIPA buffer (0µg/µL, 0.125µg/µL, 0.250µg/µL, 0.500 µg/µL, 1µg/µL, 2µg/µL). Then, in 96-wells plates, 10µL of each preparation of the standard curve were added per well, in duplicates. In addition, the samples were diluted at a suitable dilution factor in RIPA, and 10 µL of each diluted sample were added per well (in duplicates also). Following that, 200µL of BCA reagent (UP 40840A-Interchim) were added per well, and the samples were incubated for 30 minutes at 37°C. The optical densities were finally measured at 526 nm.

C- Preparation of migration gels

The migration gels were composed of two parts: the stacking and running gels. The running gel, whose acrylamide percentage depends on the size of studied protein, was prepared first (Tris 1.5M pH 8.8, acrylamide 30%, SDS 10%, and H2O) and finally, TEMED 0.1% and APS 0.075% were co-added directly before pouring the composition in the corresponding glass for polymerization. Once the running gel dried up, the stacking gel, whose concentration of composition is fixed, was prepared and poured over it (Tris 0.5M pH 6.8, acrylamide 5%, SDS 0.1%, and H2O). The TEMED (0.1%) and APS (0.075%) were similarly co-added at the last moment.

D- Sample Preparation

Samples were prepared with a total quantity of proteins enough to detect the proteins of interest (30 or 50 µg of proteins). In addition to the proteins, the necessary water and lamelli (which contains β-mercapto-ethanol) amounts were added. The samples were heated for 5 minutes at 95 °C and were loaded on the gels. A protein marker (ProSieve™ QuadColor™) was loaded on the same gel for the determination of proteins sizes.

E- Migration and transfer

The migration of samples by electrophoresis was performed in a Transfer system of migration (Biorad) in which a migration buffer (Euromedex) was used following a 10-times dilution with distilled water. The system was run at 100V until full migration of the proteins. Once the migration was terminated, the proteins were transferred to nitrocellulose membranes using a Trans-Blot Turbo Transfer apparatus (Biorad).

F- Immuno detection of Proteins

After blocking the membranes for one hour with 5% BSA (04-100-812-E, Euromedex) prepared in TBS-Tween 0.5%, the membranes were incubated at 4°C over night with primary antibodies prepared in 5% BSA as well **(Table 2)** with gentle agitation. The membranes were then washed three times (10 minutes each) with washing buffer (TBS-Tween 0.5%) and were then incubated for 1 hour at room temperature with corresponding HRP (horse raddish peroxidase) conjugated secondary antibodies **(Table 3**). Following this incubation, the same three washes were again applied.

Antibody	Dilution	Source	company	Reference
Total STAT3	1:2000	Rabbit	Cell signaling	4904
PY705-STAT3	1:1000	Rabbit	Cell signaling	9145
PS727-STAT3	1:1000	Mouse	Santa Cruz	sc-136193
P-JNK	1:200	Mouse	Santa Cruz	Sc-6254
Total JNK	1:200	Mouse	Santa Cruz	Sc-7345
p-P38 MAPK	1:1000	Rabbit	Cell Signaling	4092
Total P38	1:1000	Rabbit	Cell Signaling	8690
pS472-Akt	1:500	Mouse	Cell Signaling	4051
Total Akt	1:200	Rabbit	Sigma	sab4500797
p-ERK 1/2	1:2000	Mouse	Cell Signaling	9106
Total ERK	1:1000	Rabbit	Cell Signaling	9102
GRIM19	1:200	Mouse	Santa Cruz	sc-514111
Tom 20	1:200	Mouse	Santa Cruz	sc-17764
Anti-UQCRC2 (complex 3)	1:1000	Mouse	Abcam-MitoSciences	MS-304
Anti-NDUFB6 (complex 1)	1:1000	Mouse	Abcam-MitoSciences	MS-104
Tubulin	1:2000	Mouse	Santa Cruz	Sc-5286
GAPDH	1:500	Rabbit	Santa Cruz	Sc-25778

Table 2: The list of primary antibodies used in Western blotting

Antibody	Dilution	Source	company	Reference
Anti-mouse IgG-HRP	1:10000	Sheep	GE Healthcare	NA934V
Anti-rabbit IgG-HRP	1:10000	Donkey	GE Healthcare	NA934V

Table 3: The list of secondary antibodies used in Western blotting

G- Revelation

Proteins were finally detected using a chemiluminescence kit (ECL™ Prime Western blotting Reagent, RPN2236, GE Healthcare). The ECL reagents were mixed and added on the membranes for 5 minutes. In the presence of hydrogen peroxide, the HRP catalyzes the oxidation of luminol. Following oxidation, the luminol is in an excited state (intermediate reaction product), which quickly decays to the ground state by emitting light**.** The the light being emitted is finally visualized by Bio-Rad Molecular Imager Gel Doc XR+ (BioRad). The results were represented in the form of intensity bands which were later quantified and analyzed.

H- Quantification and Results Analysis

The intensities of the bands were quantified by densitometry using ImageLab™ software (BioRad).They were then normalized to the house keeping genes or to the total form of the phosphorylated proteins.

2.2. Immunofluorescence (IF):

2.2.1. Principle

This method was used to localize proteins of interest in H9C2 cells and adult cardiomyocytes isolated from C57bl6J mice. Its principle is similar to WB, but the secondary anti-bodies used here are coupled to fluorophores with specific wavelengths to permit the detection and localization of proteins by confocal microscopy.

2.2.2. Protocol of immuno-labeling

CMs and H9C2 cells, deposited in glass Labtech plates (PEZGS0816, Merck Millipore), were fixed for 15 minutes with 2% paraformaldehyde (Diapath-P0016) prepared in phosphate buffered saline (PBS-Gibco® by life technologies). They were washed four times with PBS for 5 minutes and were then permeabilized with 0.1% Triton-PBS (T9284- Sigma Aldrich) for 10mins at room temperature. Four similar washes were again applied, and the nonspecific binding was then blocked with 5% BSA-PBS for 45 minutes. The cells were incubated for 1^{h}30 at room temperature with primary antibodies prepared in 5% BSA-PBS **(Table 4).**

Following four new washes with PBS, secondary antibodies **(Table 5),** diluted in the blocking buffer also, were applied for another 1h at RT in darkness. The cells were washed again, and the nuclei were stained through a 10-minutes incubation with Bis-benzimide (5µg/mL). Once finished, the Labtech system was unlocked and slides were left to dry. After drying up, they were mounted with Fluoromount™ Aqueous Mounting Medium (Sigma-F4680) and were gently covered by glass cover slips . The slides were stored in darkness at 4°C for later examination using a NIKON eclipse Ti confocal microscope, and the images were processed with Nis software (Nikon).

Antibody	Dilution	Source	company	Reference
Total STAT3	1:200	Rabbit	Cell signaling	4904
PS727-STAT3	1:200	Mouse	Santa Cruz	sc-136193
Tom 20	1:200	Rabbit	Cell signaling	42406
GRIM 19	1:200	Mouse	Santa Cruz	sc- 514111
Ryanodine Receptor	1:500	Mouse	Abcam	Ab-2827

Table 4 : The list of primary Antibodies used in immunofluorescence

Antibody	Dilution	source	company	Reference
Anti IgG Rabbit coupled to Alexa Fluor 488	1:2000	Goat	ThermoFisher Scientific	A-11034
Anti IgG Mouse coupled to Alexa Fluor 647	1:2000	Goat	ThermoFisher Scientific	A21235

Table 5: The list of secondary antibodies used in immuno fluorescence

2.3. Mass spectrometry

To validate the specificity of the used STAT3 antibodies, mass spectrometry analysis was performed to ensure the presence of STAT3 at its corresponding size, in the band detected by these antibodies. For achieving this, 30 µg of cardiomyocytes lysate were loaded on 7.5% acrylamide gels. The gels were then stained by EZ blue™ gel staining reagent (Sigma G1041) according to the manufacturer's protocol. The band corresponding to around 90 KDa (expected STAT3 size) was then cut and sent for MS analysis.

The sample was analyzed in the Protein Science Facility of the "Institut de biologie et Chimie des Protéines-Lyon", using an Ultimate 3000 nano-RSLC (Thermo Scientific, San Jose California) coupled on line with a Q Exactive HF mass spectrometer via a nano-electrospray ionization source (Thermo Scientific, San Jose California). Proteins were finally identified by database searching using SequestHT with Proteome Discoverer 2.2 software (Thermo Scientific) against the swissprot Mus musculus database. Proteins were filtered with a 1% false discovery rate.

3. Mitochondrial Activity

In order to assess the mitochondrial functioning, their calcium retention capacities and aerobic respiration (oxidative phosphorylation) were studied. For studying these functions, crude mitochondrial fractions were used. In addition, pure mirochondrial fractions were also extracted and were used for western blot analysis

3.1. Mitochondrial Extraction

3.1.1. Crude Mitochondrial Extraction

The mouse was euthanized by cervical dislocation, and the chest was immediately opened to remove the heart very quickly. The extracted heart was then rinsed and cleaned on ice in buffer A (Tris 50mM, EDTA 1mM, saccharose 70mM, mannitol 210 mM, pH 7.4). It was then weighed, and buffer A was renewed (1 ml/100 mg of core mass).The heart was then cut roughly and crushed in a glass-glass potter on ice. The ground material was then transferred to a hemolysis tube for the purpose of performing differential centrifugations at 4 ° C. The first centrifugation was carried out at 3000-rpm for 3 minutes, allowing the cellular debris to be pushed. The supernatant was then recovered and centrifuged at 8000 rpm for 10

minutes, causing the sedimentation of the mitochondria. The pellet thus obtained was then resuspended in buffer B (same composition as buffer A without EDTA). A final centrifugation was carried out at 8000 rpm for 10 minutes, making it possible to purify mitochondria as much as possible while eliminating EDTA from buffer A. The final pellet was then resuspended in 100 µL of buffer B. Mitochondrial proteins were finally quantified by Bradford assay. The mitochondrial pellet was diluted 1/30 and deposited in parallel with a BSA standard range, with 50 µL of pure Bradford reagent and 150 µL of distilled water. After 10 minutes incubation in darkness at room temperature, absorbance was measured at an emission of 550 nm.

3.1.2. Pure Mitochondrial Extraction

The mice were euthanized by cervical dislocation, and the chests were immediately opened to remove the hearts very quickly. The extracted hearts were then rinsed and cleaned on ice in IB1 buffer (225mM mannitol, 75mM sucrose, 0,5% BSA, 0,5mM EGTA and 30mM Tris HCl ph7,4). The hearts were dried, weighed and cut into small pieces. The pieces were then homogenized by applying 10-20 strokes in a 1mL glass tissue grinder in 5mL of buffer IB1. The homogenates were then transferred to falcon tubes and centrifuged at 740g for 5 min at 4°C. The supernatants were then taken and also centrifuged at 740g for 5 min at 4°C. Again, the supernatants were collected and centrifuged at 9000g for 10mins at 4°C. The pellets were gently resuspended in 10 mL of buffer SB (225mM mannitol, 75mM sucrose, 30mM Tris-HCl pH7,4) and centrifuged at 10000g for 10 min at 4°C. The pellets of crude mitochondria was resuspended in 2mL of Mitochondria Resuspending Buffer, MRB (250mM mannitol, 5mM HEPES (pH7,4) and 0,5mM EGTA). For obtaining pure mitochondria, the 2 ml suspensions of crude mitochondrial fraction were layered on top of 8 ml Percoll medium (225mM mannitol, 25mM HEPES, 1mM EGTA and 30% Percoll (vol/vol)) in 14 ml thin-wall ultracentrifuge tubes. About 3.5 ml of MRB were finally layered on top of the mitochondrial suspension to fill up the tubes. The latter were centrifuged at 95000g for 30 min at 4°C.

Purified mitochondria are usually localized at the bottom of the tube as a dense band. They were collected with a Pasteur pipette in a falcon, diluted ten times with MRB and centrifuged at 6300g for 10 min at 4°C. The final pure mitochondrial pellets are diluted in a small volume of MRB (50µL) and stored at -20°C.

3.2. Mitochondrial Functioning

3.2.1. Aerobic Respiration (Oxidative phosphorylation)

A- Principle

Oxidative phosphorylation is used to determine the general state of the isolated mitochondria, and more precisely to estimate the amount of O2 used during the activation and the inhibition of each complex of the respiratory chain, thus reflecting the activity of these different complexes.

B- Protocol

350 µg of mitochondrial proteins are required.The measurement is carried out using a Clark oxygen electrode (Oroboros® oxygraph, Austria). The crude mitochondria (350µg) are incubated with 2mL of respiration buffer (100mM KCl, 50mM MOPS, 1mM EGTA, 5mM KH2PO4 and 1mg / mL BSA without fatty acid at pH 7.4) with GMP (Glutamate, Malate, Pyruvate 5mM each) of complex I of the respiratory chain. This basal state is named state 2. After stabilization, the addition of ADP (200 µM) makes it possible to determine the maximum activity of complex I, called state 3. Once the complex V has consumed the ADP, complex I activity returns to a basal state, here called state 4. In a second step, the complex I is inhibited by the addition of its specific inhibitor, rotenone (6.25 µM). The complex II is then activated by the addition of its specific substrate, succinate (5 mM) making it possible to determine the specific activity of complex II (state 3 of complex II). When the succinate is completely consumed, complex III is inhibited by the addition of antimycin A (12.5 µM). The state 3 of complex IV is estimated by adding TMPD (tetramethylphenylenediamine 0.125 mM) and ascorbate (1.25 mM). The TMPD is an artificial electron transporter capable of transferring the electrons to the IV complex, oxidized by cytochrome c and reduced by ascorbate. Finally, the respiratory chain is decoupled in order to estimate the maximum state of complex IV. For this, the FCCP (carbonyl cyanide-p-trifluoromethoxyphenylhydrazone, etc.) is added to the medium. The oxygen consumption by the mitochondria is expressed in nmole O2 / min / mg proteins. The respiratory coupling index (RCI) is defined as the ratio of state 3 / state 4.

3.2.2. Calcium Retention Capacity (CRC)

A- Principle

CRC is a measure of mitochondrial function. It is defined as the amount of calcium required to trigger mPTP opening in vitro. In this assay, the mitochondria are triggered by spikes of calcium ions until the amount of inos uptaken by the them exceeds their capacity to retain it, thus triggering the opening of the mPTP. Upon mPTP opening, Ca^{+2} leaks into the assay buffer and binds to a low-affinity membrane impermeable dye and increases its fluorescence emission.

B- Protocol

Measurement of CRC was performed at 25 °C using a spectrofluorophotometer F-2500 digi lab Hitachi® equipped with magnetic stirring and thermostatic control. Extra-mitochondrial free Ca2+ was measured in the presence of the calcium sensitive probe Calcium Green®-5N (1 µM) (Life technologies C3737) with excitation and emission wavelengths set at 500 and 530 nm respectively. 250 µg of crude mitochondria (were resuspended in 2mL of buffer C (50 mM KCl, 2 mM KH2PO4, 20 mM Tris, 150 mM sucrose, 5 mM succinate pH 7.4) in a spectrophotometer cuvette at 25 °C. Calcium green was then added to the cuvette which was then placed in the spectrophotometer. Following a 2 minutes preincubation period, 10 nmol of CaCl2 were added every 2 minutes. After sufficient CaCl2 loading, a rapid increase of fluorescence indicates a massive release of Ca2+ by mitochondria due to mPTP opening.

4. Molecular Biology Techniques

4.1. RNA Extraction

In order to study the expression of selected STAT3-regulated genes by polymerase chain reaction (PCR), RNA was extracted from areas at risk collected from hearts of mice subjected to I/R or IPoC and treated with DMSO, Stattic or PD98059 (as previously described) and stored in RNAlater. RNA was extracted from myocardial tissue pieces (10µg) using RNAzol ® RT column kit (Molecular Research Center #Rc 290) according to the manufacturer's protocol. The myocardial tissues were removed from RNAlater solution and homogenized in 1 mL RNAzol ® RT using a Precellys homogenizer associated with a Cryolys cooling system to ensure homogenization at 4 C°. A volume of 0.4 mL water was then added per 1mL of RNAzol. The resulting mixture was vigorously shaked for 15 seconds, stored for 5 minutes at room temperature and then centrifuged for 15 minutes at 12,000 g. The supernatant was then transferred into a clean tube, and an equal volume of isopropanol was added. The latter mixture was then transferred into a column and stored 5 minutes at room temperature. Following that, the column was centrifuged for 20 secs at 12,000 g, which retained the large RNA on the column. The latter was then inserted into a clean wash tube, and 250 µL of pure ethanol was added prior to a 20 secs centrifugation at 12,000 g. Finally, the column was inserted into an elution tube, where 30 µL of RNase-free water was applied for hydration. Following a one minute hydration, the RNA was eluted from the column by a 12,000 g centrifugation for 20 secs. RNA purity and quantity were assessed by spectrophotometry (NanoDrop ND-1000, NanoDrop Technologies).

4.2. cDNA Synthesis

This step is applied for the reverse transcription of RNA to obtain the cDNA required for real-time PCR (RT-PCR). It uses PrimeScript reverse transcriptase for extendibility. Before synthesizing the cDNA, 1 µg of RNA was treated with DNaseI (Sigma AMPD1-1KT). Following DNase treatment, cDNA was synthesized using PrimeScript™ RT Reagent kit (TaKaRa-PR037A) according to the manufacturer's protocol. Briefly, a 10µL master mix was prepared. It contained: PrimeScript buffer, PrimeScript RT enzyme, hexamers and RNase Free dH2O. This mix was added to the 1µg of DNase-treated RNA. The whole mixture was then placed in an Eppendorf Mastercycler programmed at 85°C for 15 seconds then 37°C for 15 minutes. The obtained cDNA was finally stored at -20°C.

4.3. Polymerase Chain Reaction (PCR)

Primers shown in (**tables 6, 7, 8, 9)** were designed using Primer-blast software (https://www.ncbi.nlm.nih.gov/tools/primer-blast/) and tested for efficiency. Primers with 95-105% efficiency were used. All PCR reactions were run in CFX96 C1000 system supplied by Bio-Rad. Genes amplification was performed using TB Green™ Premix Ex Taq™ (Tli RNaseH Plus) (Takara- Cat# RR420L) under the following thermal cycling conditions: initial 95 °C for 5 minutes then a 42 times repeated cycle of 95 °C for 10 seconds, 60 °C for 30 seconds and 72 °C for 30 seconds. A melt curve was constructed in the temperature interval 65-95 °C with an increment of 0.5 °C for 5 seconds. PCR results were analyzed using the relative quantification method $2^{-\Delta Cq}$, where a normalization factor (Cq_{ref}) was used as a control to which all genes were normalized. This Cq_{ref} was calculated as a geometric mean of three selected reference genes (choice explained below). The attempt to use GAPDH didn't work because we found that GAPDH is significantly varying at the gene level.

- Normalization factor

In experiments of tissue analysis and multiple biological variables, proper selection of reference genes cannot be achieved randomly. Thus, we selected three genes which have no significant variation at the transcriptomic level between the different time points. These genes are Senp2, Malat1 and Fem1c. GAPDH and HPRT were not used due to the significance variation in their expression levels between our selected time points. Because we detected minor variations, we concluded that the 3 reference genes should be used for normalization instead of randomly selecting 1 or 2 of them. Therefore, a normalization factor (Cq_{ref}) was calculated by geometric averaging of the Ct of the 3 reference genes [237]. Scatterplots of Senp2, Malat1 and Fem1c Ct values in function of (Cq_{ref}) showed a better correction of gene expression **Fig. 24**.

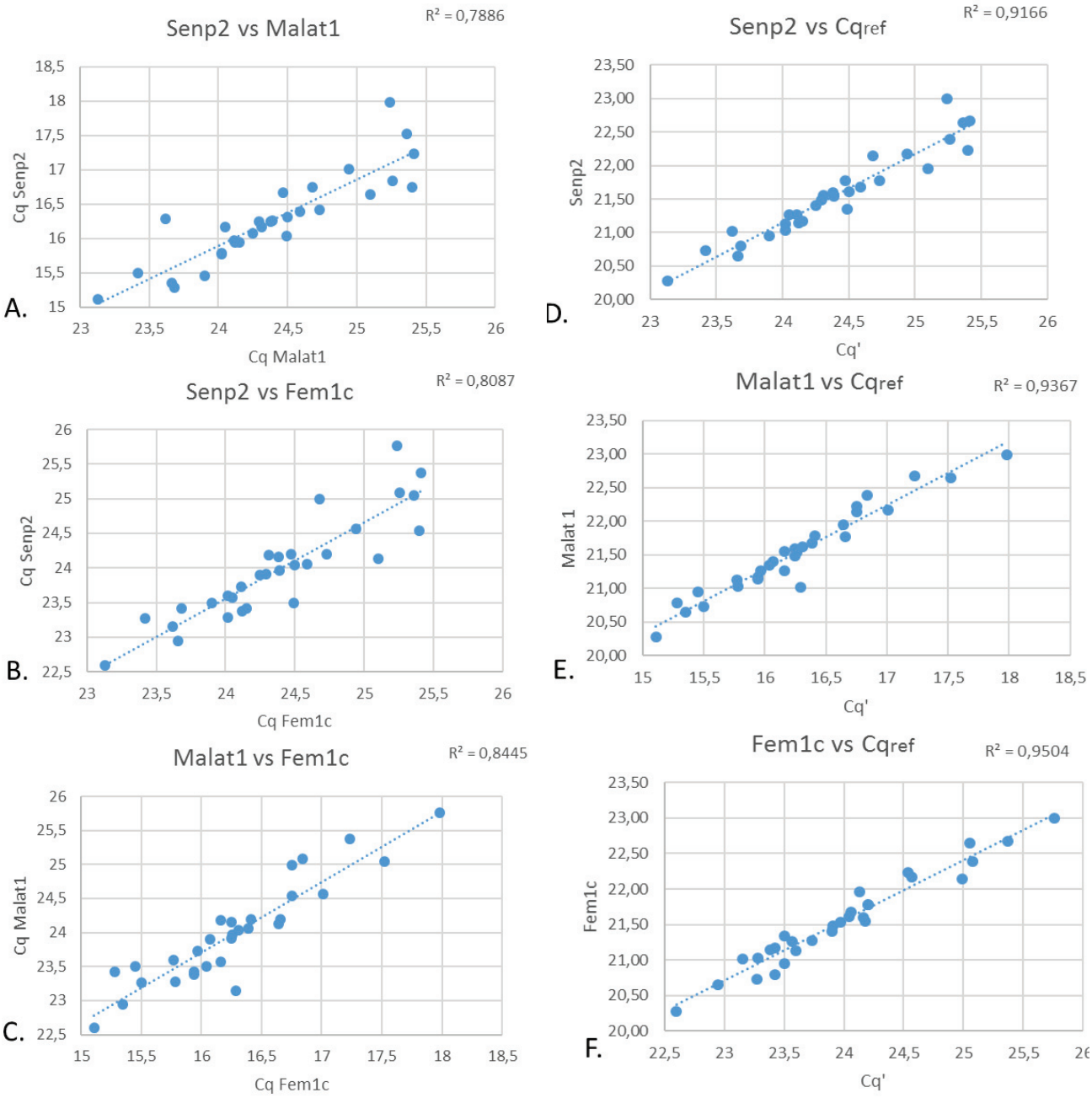

Figure 24: Scatter plots of the three used reference genes

(A)(B)(C) Scatter plots for the Cq of each reference gene (Senp2, Fem1c and malat1) plotted against another reference gene.

(D)(E)(F) Scatter plots for the Cq of each reference gene (Senp2, Fem1c and malat1) plotted $Cq_{ref.}$

4.4. Gene Ontology (GO) Enrichment Analysis

- **Principle**

When performing high through-put experiments that yield sets of genes significantly varying under certain conditions, we aim to retrieve a functional profile for these genes sets. This helps us understand the biological processes in which these genes are involved. To achieve this, our gene set is given as an input in specific database, and consequently, gene ontology enrichement analysis is performed. The output of the analysis is a ranked list of GO terms, each associated with a p-value or FDR (false discovery rate). The GO terms, under a specific threshold, are then retrieved and grouped into larger biological families or functions.

- **Performed Analysis**

A- Short Time-series Expression Miner (STEM) analysis:

For checking the profiles of genes variation over time, STEM analysis was used. STEM version 1.3.11. (Ernst and Bar-Joseph 2006), a Java clustering algorithm, was used to visualize expression profiles from short time series experiments (fewer than 8 time points). STEM algorithm defines a set of model temporal profiles which correspond to possible profiles of the genes' behavior over time. All these model profiles start at 0 and then they are either increased, decreased or remained steady between different time points. Input data are transformed so that expression profiles can start at 0. Genes are assigned to profiles based on a correlation coefficient.

B- STRING Analysis (Search Tool for the Retrieval of Interacting Genes/Proteins)

After screening the expression of the targeted genes by PCR, GO analysis was performed on the significantly varying genes in order to determine and classify the biological functions of the proteins encoded by these genes. For this analysis, the biological database STRING was used [238]. A threshold of flase discovery rate (FDR) <0.005 was set to select the GO terms used for further analysis. In STRING software, the input is the significant genes, while the output is the proteins encoded by these genes. These proteins are given in a form of network showing any existing interactions between them. In addition, the GO terms of the encoded proteins are given. **Fig. 25** shows an example.

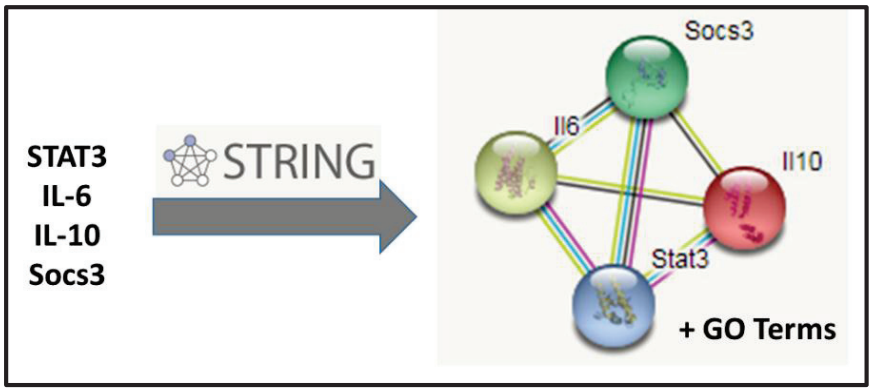

Figure 25: **Illustration of STRING function**

The genes entry to STRING database gives the interactions occurring between the proteins encoded by the entered genes.

In addition to determining the biological functions and the networks formed between the encoded proteins, STRING also predicts further interactions with other proteins based on curated data from literature. The first network formed with the main encoded proteins is the core network, referred to as core "shell". The addition of the first predicted interactive proteins yields a new network called "shell 1". In the same sense, every new predicted shell is given an increasing number **Fig. 26.**

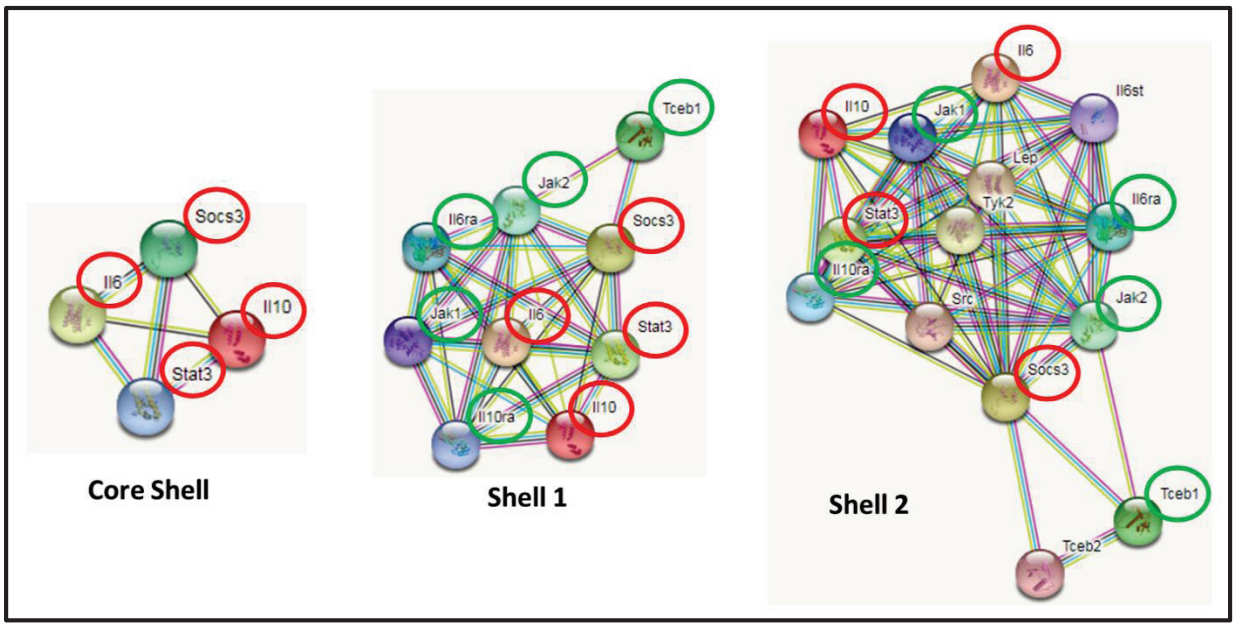

Figure 26: Illustration of the predictive networks in STRING

An illustration showing the prediction of new networks, with increasing sizes, upon adding new protein interactions.

5. Statistical Analysis

The data were analyzed with GraphPad Prism 6.0 using one or two-way ANOVA followed by multiple comparisons tests, or using *t*-test depending on the experiments. $P < 0.05$ was considered indicative of a significant difference.

Primer's Name	Sequence
mSerpine1/F	TCTTTCCGACCAAGAGCAGC
mSerpine1/B	TGTGCCGAACCACAAAGAGA
mFgl2/F	GTCACAGCCGGTTCAACATC
mFgl2/B	AGTTGGTGCTGCCATCAAGG
mLmcd1/F	GCCTCACTCGTGGAGGAAAA
mLmcd1/B	GCGGTGAGAGTGGCATACTT
mThbs1/F	CAGCTCAGCTACCAACGTCC
mThbs1/B	GTTCTCTTCCGTCACTTTTCGG
mMt2/F	TACTTCCTGCAAGAAAAGCTGC
mMt2/B	GTGGAGAACGAGTCAGGGTTG
megfr/F	GCCATCTGGGCCAAAGATAC
megfr/B	GGTGTGAGAGGTTCCACGAG
mCasp1/F	GGACCCTCAAGTTTTGCCCT
mCasp1/B	AACTTGAGCTCCAACCCTCG
mMet/F	GGACAAGACCACCGAGGATG
mMet/B	CGTGAAGTTGGGGAGCTGAT
mFgf2/F	GGCTGCTGGCTTCTAAGTGT
mFgf2/B	GTCCCGTTTTGGATCCGAGT
mHspa1a/F	CACCATCGAGGAGGTGGATT
mHspa1a/B	AGCCCACGTGCAATACACAA
mCop1/F	GCCACAGCTTTTGCTACAAGT
mCop1/B	ACCTATGCCCATTGGTGCTAC
mKlf4/F	GACTAACCGTTGGCGTGAGG
mKlf4/B	GTCTAGGTCCAGGAGGTCGT
mId3/F	CATCTCCCGATCCAGACAGC
mId3/B	GAAGCTCATCCATGCCCTCA

Table 6: List 1 of PCR Primers

Primer's Name	Sequence
mSod2/F	ACAACAGGCCTTATTCCGCT
mSod2/B	CCCCAGTCATAGTGCTGCAA
mRbbp6/F	AGGAAGAGGAAAAGAAAAAGTCCA
mRbbp6/B	AGGACCGAGAGTAAGAGCGT
mBcl2/F	GATAACGGAGGCTGGGATGC
mBcl2/B	CTCACTTGTGGCCCAGGTAT
mHopx/F	AGGTCAGGCGACTTTCAGTG
mHopx/B	TGCGCGTGTGGAAGTCTG
mBirc6/F	CTGCTCTCAAGCGCCACA
mBirc6/B	TCGAAGCCTTTGTGTCTACGA
mPdk4/F	GTCCGAACCCTTCACCCAGG
mPdk4/B	GAGAACAGCTCGACCTCCCT
mTnfrsf25/F	TGTTTTGGGTCCAGGTGCTT
mTnfrsf25/B	GAGAGATGGGCAGTCTGTGG
mPhlda1/F	CCGGGCCACTCAAGGTTTTG
mPhlda1/B	CGACGCAAAATCTGCTTCCT
mDusp5/F	CCCGGTTGAAATCCTTCCCT
mDusp5/B	CCTTCTTCCCTGACACAGTCAATA
mPtgs2/F	CGTAGCAGATGACTGCCCAA
mPtgs2/B	TTTAAGTCCACTCCATGGCCC
mFads2/F	TCGACCGCAAGGTCTACAAC
mFads2/B	TCTGAGAGCTTTTGCCACGG
mFasn/F	ACCCAGAGGGATCTGGTGAA
mFasn/B	CTGTCGTGTCAGTAGCCGAG
mEif2ak2/F	CCGGGAAAACGAAACAGAAGAG
mEif2ak2/B	TCCCAGTGGCCAAAGTTTCTG

Table 7: List 2 of PCR Primers

Primer's Name	Sequence
mFoxo1/F	GCTAAGAGTTAGTGAGCAGGCTA
mFoxo1/B	CATCCTGCACAGGAAAGTGC
Ccl2/F	GATGCAGTTAACGCCCCACT
Ccl2/B	TGGCCTTGGTTTCCCCATTG
MT1/F	TCCACCGGCGGCTCC
MT1/B	ACAATACAATGGCCTCCGGG
mSumo1/F	TCTGACCAGGAGGCAAAACC
mSumo1/B	TCCATTCCCAGTTCTTTCGGA
mCyr61/F	AGGCTTCCTGTCTTTGGCAC
mCyr61/B	ACAAGGACGCACTTCACAGA
mPalld/F	TACCACAGACCAAGCAGTCC
mPalld/B	CCTGTGTCCTTGCTTTCGGT
mVldlr/F	TGACGCAGACTGTTCAGACC
mVldlr/B	GGTTCGAGAAGGGCAGTTGA
mEpas1/F	CACCCCAGGGAACACTACAC
mEpas1/B	GAAGTCCGTCTGGGTACTGC
mMmp2/F	ACAAGTGGTCCGCGTAAAGT
mMmp2/B	AGGCCATGGGTTGGATCTTC
mFlt1/F	GTGTCTATAGGTGCCGAGCC
mFlt1/B	CGGAAGAAGACCGCTTCAGT
mVim/F	GCAGTATGAAAGCGTGGCTG
mVim/B	CAGGGACTCGTTAGTGCCTTT

Table 8: List 3 of PCR Primers

Primer's Name	Sequence
mCD80/F	TTCTGTAAGCACAGAAGCTGTT
mCD80/B	AGAGCCAGGGTAGTGCTAGG
mSTAT3/F	TCCTGGTGTCTCCACTTGTCT
mSTAT3/B	TATTGCTGCAGGTCGTTGGTGT
mIL6/F	CAAAGCCAGAGTCCTTCAGAG
mIL6/B	GTCCTTAGCCACTCCTTCTG
mLy6g/F	CAGAGAGGAAGTTTTATCTGTGC
mLy6g/B	TCAGGTGGGACCCCAATACA
mDusp1/F	TCTCCAAGGAGGATATGAAGCG
mDusp1/B	CGAGAAGCGTGATAGGCACT
mHmox1/F	TGACACCTGAGGTCAAGCAC
mHmox1/B	GGCAGTATCTTGCACCAGGC
mGadd45b/F	GCTCTTGGGGATCTTCCGTG
mGadd45b/B	CTGTCGGGGTCCACATTCAT
mMRC1/F	GGCTGATTACGAGCAGTGGA
mMRC1/B	ATGCCAGGGTCACCTTTCAG
CxCl1/F	CAGACCATGGCTGGGATTCA
CxCl1/B	TGGGGACACCTTTTAGCATCT
Socs3/F	CGGGGAGCTAGTCCCGAA
Socs3/B	CCCTTCCCGGCCCAG
Bcl3/F	AGCCGCAGGGTCATTGATA
Bcl3/B	AAGCCAGGAGCATCTTTCGG

Tnip3/F	GGATGCCTTGACCATTGGGA
Tnip3/B	CTGAGGAGAAACCATGTGCCT
Etv3/F	GGGAGGGTGACCGAGCG
ETV3/B	TTCATTTTCGCCCTCCCTGC
Tpl2/F	TTTGCTGAGCCTGGACTCCC
Tpl2/B	ACTCCTGGCTCTTCACTTGC
CD68/F	GGAAGAAAGGCTTGGGGCAT
CD68/B	ATTCCACCGCCATGTAGTCC
CD86/F	TGGACCCCAGATGCACCAT
CD86/B	ACTACCAGCTCACTCAGGCT
Lcn2/F	ACGGACTACAACCAGTTCGC
Lcn2/B	AATGCATTGGTCGGTGGGG
TNF/F	CTTCTGTCTACTGAACTTCGGG
TNF/B	CAGGCTTGTCACTCGAATTTTG
IL1b/F	ACGGACCCCAAAAGATGAAG
IL1b/B	TTCTCCACAGCCACAATGAG

Table 9: List 4 of PCR Primers

RESULTS

Section I: Mitochondrial STAT3

In an attempt to study the cardioprotective roles of STAT3, which are linked to the regulation of the mitochondrial activity during IR and IPoC, we first questioned its mitochondrial translocation and localization. Surprisingly, we were unable to detect STAT3 in pure mitochondrial fractions of adult cardiomyocytes. In addition, no involvement for STAT3 in the mitochondrial activity was observed. Thereafter, the aspect of this aim has shifted toward studying the pattern of localization of STAT3 in adult cardiac myocytes under various conditions. The detailed work and results, in the context of mitochondrial STAT3, are presented in our following published paper.

Contents lists available at ScienceDirect

Journal of Molecular and Cellular Cardiology

journal homepage: www.elsevier.com

Critical appraisal of STAT3 pattern in adult cardiomyocytes

Zeina Harhous [a, b, c], Sally Badawi [a, b, c], Noelle Gallo Bona [a, b], Bruno Pillot [a, b], Lionel Augeul [a, b], Melanie Paillard [a, b], George W. Booz [d], Emmanuelle Canet-Soulas [a, b], Michel Ovize [a, b], Mazen Kurdi [c, **], Gabriel Bidaux [a, b, *]

[a] Univ-Lyon, CarMeN Laboratory, INSERM 1060, INRA 1397, University Claude Bernard Lyon1, INSA Lyon, Oullins, France
[b] IHU OPeRa, Groupement Hospitalier EST, Bâtiment B13, 59 boulevard Pinel, F-69500 Bron, France
[c] Lebanese University, Faculty of Sciences, Doctoral School of Sciences and Techlogy, Laboratory of Experimental and Clinical Pharmacology, Hadat, Lebanon
[d] Department of Pharmacology and Toxicology, School of Medicine, The University of Mississippi Medical Center, Jackson, MS, USA

ARTICLE INFO

Keywords:
Mitochondria
Cardiomyocytes
Ischemia-reperfusion
T-tubules
Subcellular distribution
Mitochondria associated membranes

ABSTRACT

The signal transducer and activator of transcription 3, STAT3, transfers cellular signals from the plasma membrane to the nucleus, acting as a signaling molecule and a transcription factor. Reports proposed an additional non-canonical role of STAT3 that could regulate the activity of complexes I and II of the electron transport chain and the opening of the mitochondrial permeability transition pore (PTP) after ischemia-reperfusion in various cell types. The native expression of STAT3 in heart mitochondria, together with a direct versus an indirect transcriptional role in mitochondrial functions, have been recently questioned.

The objective of the present study was to investigate the cellular distribution of STAT3 in mouse adult cardiomyocytes under basal and stress conditions, along with assessing its presence and activity in cardiac mitochondria using structural and functional approaches. The analysis of the spatial distribution of STAT3 signal in the cardiomyocytes interestingly showed that it is transversely distributed along the T-tubules and in the nucleus. This distribution was neither affected by hypoxia nor by hypoxia/re-oxygenation conditions. Focusing on the mitochondrial STAT3 localization, our results suggest that serine-phosphorylated STAT3 (PS727-STAT3) and total STAT3 are detected in crude but not in pure mitochondria of mouse adult cardiomyocytes, under basal and ischemia-reperfusion conditions. The inhibition of STAT3, with a pre-validated non-toxic Stattic dose, had no significant effects on mitochondrial respiration, but a weak effect on the calcium retention capacity. Overall, our results exclusively reveal a unique cellular distribution of STAT3 in mouse adult cardiomyocytes, along the T-tubules and in nucleus, under different conditions. They also challenge the expression and activity of STAT3 in mitochondria of these cells under basal conditions and following ischemia-reperfusion. In addition, our results underline technical methods, complemental to cell fractionation, to evaluate STAT3 roles during hypoxia-reoxygenation and at the interface between nucleus and endoplasmic reticulum.

Critical Appraisal of STAT3 Pattern in Adult Cardiomyocytes

Zeina Harhous[1,2,3], Sally Badawi[1,2,3], Noelle Gallo Bona[1,2], Bruno Pillot[1,2], Lionel Augeul[1,2], Melanie Paillard[1,2], George W Booz[4], Emmanuelle Canet-Soulas[1,2], Michel Ovize[1,2], Mazen Kurdi[3]*, Gabriel Bidaux[1,2]*,

Abstract

The signal transducer and activator of transcription 3, STAT3, transfers cellular signals from the plasma membrane to the nucleus, acting as a signalling molecule and a transcription factor. Reports proposed an additional non-canonical role of STAT3 that could regulate the activity of complexes I and II of the electron transport chain and the opening of the mitochondrial permeability transition pore (PTP) after ischemia-reperfusion in various cell types. The native expression of STAT3 in heart mitochondria, together with a direct versus an indirect transcriptional role in mitochondrial functions, have been recently questioned.

The objective of the present study was to investigate the cellular distribution of STAT3 in mouse adult cardiomyocytes under basal and stress conditions, along with assessing its presence and activity in cardiac mitochondria using structural and functional approaches. The analysis of the spatial distribution of STAT3 signal in the cardiomyocytes interestingly showed that it is transversely distributed in along the T-tubules and in nucleus. This distribution was neither affected by hypoxia nor by hypoxia/re-oxygenation conditions. Focusing on the mitochondrial STAT3 localization, our results suggest that serine-phosphorylated STAT3 (PS727-STAT3) and total STAT3 are detected in crude but not in pure mitochondria of mouse adult cardiomyocytes, under basal and ischemia-reperfusion conditions. The inhibition of STAT3, with a pre-validated non-toxic Stattic dose, had no significant effects on mitochondrial respiration, but a weak effect on the calcium retention capacity. Overall, our results exclusively reveal a unique cellular distribution of STAT3 in mouse adult cardiomyocytes, along the T-tubules and in nucleus, under different conditions. They also challenge the expression and activity of STAT3 in mitochondria of these cells under basal conditions and following ischemia-reperfusion. In addition, our results underline technical methods, complemental to cell fractionation, to evaluate STAT3 roles during hypoxia-reoxygenation and at the interface between nucleus and endoplasmic reticulum.

1. INTRODUCTION

The signal transducer and activator of transcription 3 (STAT3) is a member of the STAT family of proteins. It transfers information from the plasma membrane to the nucleus, acting as a signaling molecule and a transcription factor [188]. It is activated by growth factors, cytokines, inflammation, stress conditions and oncogenic kinases [239]. The activation of STAT3 occurs through phosphorylation of its tyrosine 705 (Y705) residue. PY705-STAT3 molecules form dimers which translocate to the nucleus, bind to certain targeted DNA sequences and regulate expression of various genes [240]. STAT3 is also phosphorylated at its serine 727 (S727) residue. Phosphorylation of S727 has been described to be required and self-sufficient for STAT3 transcriptional activity [3], [241], [242]. Alternatively, a non-canonical role of STAT3 has been reported in the mitochondria [240], [243]. Mitochondria are major players in ischemia-reperfusion-induced cell death, including through opening of the mitochondrial permeability transition pore [244]–[246]. STAT3 has been suggested to enhance the activity of the electron transport chain, to increase ATP production and to decrease ROS generation by interacting with mitochondria complexes I and II [243], [224]. Recent reports using pharmacological or genetic modulation of STAT3 activity and expression in adult cardiomyocytes and various cell lines propose that mitochondrial STAT3 could contribute to protection against ischemia-reperfusion injury by ischemic conditioning [243], [196], [212], [247], [248]. Alternatively, several attempts and approaches to detect STAT3 in the mitochondria have been unsuccessful, and the specificity of its pharmacological inhibitor, Stattic, raises questions. Besides from the controversial mitochondrial STAT3 localization and roles, an evolving role for STAT3 in the endoplasmic reticulum have been recently discovered, where STAT3 was suggested to contribute to the regulation of calcium homeostasis and apoptosis [249], [250].

Therefore, the aim of the present study was to investigate the cellular distribution of STAT3 in mouse adult cardiomyocytes under basal and stress conditions, in addition to the examination of its expression and activity in mitochondria of these cells under different conditions. Our results mainly show a unique pattern of STAT3 distribution along the T-tubules and in the nucleus, under basal and stress conditions. Besides, using several independent methods, we could confirm neither total nor phosphorylated STAT3 expression in cardiac mouse mitochondria under both baseline and ischemia-reperfusion conditions. Moreover, we were unable to confirm that STAT3 inhibition, by a non-toxic concentration of Stattic, could impair mitochondrial respiration. We finally discuss how STAT3 might, however, play a role in ischemia-reperfusion injury and possible important methodological drawbacks in this field of research.

2. MATERIALS AND METHODS

2.1 Animals

The present study was performed following the approval by the local institutional animal research committee (N°DR2018-35v2). It conforms to the NIH Guide on the Use of Laboratory Animals (NIH Publication No. 85-23, revised 1996). C57bl/6J male mice aged between 8-12 weeks were obtained from Charles River Laboratories.

2.2 In vivo Myocardial Ischemia-Reperfusion Injury

As previously described [251], mice received a sub-cutaneous injection of the anesthetics mix (buprenorphine 0.075mg/kg + medetomidine 0.3mg/kg) and the analgesics mix (lidocaine 2mg/kg + Alfaxan 80mg/kg). They were then placed on a blanket at 37°C until fully asleep. ECG and heart rate were monitored using EGC electrodes, and an oximeter was used for SpO2 monitoring. A tracheotomy was performed and mice were mechanically ventilated. The hearts was exposed via a left thoracotomy, and myocardial infarction was induced by placing an 8-0 suture around the left anterior descending (LAD) artery. Following 45 min ischemia, the infarcted area was reperfused for 15 min through the loosening of the suture. The area at risk were identified by the absence of blue staining and was collected for pure mitochondrial isolation prior to western blot analysis.

2.3 Cell Culture

The rat derived H9C2 cell line of cardiomyoblasts and mouse embryonic fibroblasts (MEFs), wild type (WT) and STAT3 knockout (KO), were cultured in Dulbecco's Modified Eagle's Medium (DMEM) (41965-039 Gibco), supplemented with 10% Fetal Bovine Serum and 100 U/ml penicillin/streptomycin under a humidified incubator aerated with 5% CO_2 at 37℃. WT and KO MEFs were generated by Valeria Poli (University of Torino, Torino, Italy).

2.4 Mitochondrial Isolation

To optimize the yield of intact mitochondria, all procedures were carried out on ice, with the centrifugations performed at 4°C. Crude mitochondria were used for the assessment of mitochondrial functions, while pure mitochondria were used for the qualitative detection of STAT3 under various conditions.

2.4.1 Crude Mitochondrial isolation

As previously described [252], after euthanizing the mice by cervical dislocation, the hearts were extracted while still beating and immediately placed in cold buffer A [70mM sucrose, 210 mM mannitol, 1 mM EDTA and 50 mM Tris HCl (pH 7.4)]. Atria were then removed, and ventricular tissues thoroughly minced with scissors. A Potter-Elvehjem (glass-glass) tissue grinder was used for homogenization. The homogenates were centrifuged at 1,300g for 3 min and the supernatants then collected and centrifuged at 10,000g for 10 min. The mitochondrial pellets were suspended in isolation buffer B (same as buffer A except for EDTA 0.1 mM). The suspensions were centrifuged at 10,000g for 10 min and homogenized in 100µL of buffer B. Protein contents were assessed using Bradford reagent with bovine serum albumin as standard.

2.4.2 Pure Mitochondrial isolation

As previously described [253], after euthanizing the mice by cervical dislocation, the hearts were extracted and immediately placed in Isolation Buffer, IB1, (225 mM mannitol, 75 mM sucrose, 0.5% BSA, 0.5 mM EGTA and 30 mM Tris HCl pH7.4). Atria were then removed, and the tissues finely minced with scissors. The pieces were then homogenized by applying 10-20 strokes in a glass-teflon tissue grinder. The homogenates were centrifuged at 740g for 5 min, and the supernatants were then taken and similarly centrifuged. The new supernatants were collected and centrifuged at 9,000g for 10 min at 4°C. The pellets were gently resuspended in a Stop Buffer, SB, (225 mM mannitol, 75 mM sucrose, 30 mM Tris-HCl pH7.4) and centrifuged at 10,000g for 10 min. The pellets of crude mitochondria were resuspended in Mitochondria Resuspending Buffer, MRB, (250 mM mannitol, 5 mM HEPES (pH7.4) and 0.5 mM EGTA). For obtaining pure mitochondria, suspensions of crude mitochondrial fractions were layered on top of Percoll medium (225 mM mannitol, 25 mM HEPES, 1 mM EGTA and 30% Percoll (vol/vol) in 14 ml thin-wall ultracentrifuge tubes. MRB was finally layered on top of the mitochondrial suspensions to fill up the tubes. The latter were centrifuged at 95,000g for 30 min. Purified mitochondria, localized at the bottom of the tube as a dense band, were collected and washed twice by centrifugation at 6,300g for 10 min.

2.5 Mitochondrial Oxidative Phosphorylation

Oxidative phosphorylation of 350 µg crude mitochondria was measured at 25°C using a Clark-type electrode (Oroboros oxygraph, Austria) in 2 mL of respiration buffer (pH 7.4) [100 mM KCl, 50 mM MOPS, 1 mM EGTA, 5 mM KH_2PO_4 and 1 mg/mL fatty acid-free BSA], as previously described [254]. Glutamate/Malate/Pyruvate (5 mM each), succinate (5 mM) and TMPD-ascorbate (0.125-1.25 mM respectively) were used as substrates for complexes I, II, and IV respectively. Rotenone (1 µM) and Antimicyn A (12.5 µM) were respectively added as specific inhibitors of complexes I and III. The maximal oxygen uptake after uncoupling of respiratory chain with FCCP (2.8µM) was also determined. The ADP (200µM)-stimulated respiration was measured. The oxygen consumption of the complexes is expressed in nmol O_2/min/mg of proteins.

2.6 Mitochondrial Calcium Retention Capacity (CRC)

The calcium retention capacity of 250 µg of crude mitochondrial proteins was determined in 2 mL of incubation buffer C (150 mM sucrose, 50 mM KCl, 2 mM KH_2PO_4, 20 mM tris/HCl) at 25°C using 5 mM (Glutamate/Malate/Succinate), with ADP-stimulated respiration in the presence of $MgCl_2$ (1.2 mM), as previously described [252]. The extra-mitochondrial Ca^{2+} concentration was estimated with a spectrofluorometer using 1 µM of the calcium sensitive probe calcium green 5N (Life technology) (excitation wavelength: 500nm; emission: 530nm). Mitochondria were gently stirred, and 40 nmol $CaCl_2$ pulses were applied every 2 min until a rapid calcium release occurred indicating PTP opening. CRCs were expressed in nmoles of Ca^{2+}/mg of proteins.

2.7 Pharmacologic inhibition of STAT3

A dose-effect assessment of the STAT3 inhibitor, Stattic (sigma-S7946), was tested on isolated mouse cardiomyocytes as follows: cells were treated for 1 or 2 hours, at 37°C, with either Stattic (10-100µM) or DMSO vehicle. Crude mitochondria were incubated with 50 µM Stattic, a concentration which induced a significant decrease in Y705-STAT3 phosphorylation, or with DMSO vehicle for 1 hour at 4°C. The mitochondrial calcium retention capacities and oxygen consumption were consequently measured.

2.8 Western blotting

Proteins were extracted from cells and mitochondria (pure and crude) using complete RIPA lysis buffer with anti-proteases (Sigma; P8340) and anti-phosphatases (Sigma; p5726). The collected proteins were then quantified, and SDS-PAGE Western blotting was performed. Membranes were cut in strips in order to detect several proteins (STAT3 and markers of compartments) at the same time. Reblotting was performed in order to assess the detection of the different forms of STAT3 and different markers of the same size. Membrane strips were blocked for 1 hour with 5% bovine serum albumin (BSA)-PBS. Immunoblotting was performed by incubating the membranes, overnight at 4°C, with primary antibodies: Rabbit anti-PY705-STAT3 (dil: 1/1,000; Cell Signaling; 9145), rabbit anti-total STAT3 (dil: 1/1,000; Cell Signaling; 4904), mouse anti-PS727-STAT3 (dil: 1/1,000; Santa Cruz; sc-136193) batch 1 (May 2016) and batch 2 (March 2018), mouse anti-GRIM19 (1/200; Santa Cruz; sc- 514111), mouse anti-TOM20 (dil: 1/200; Santa Cruz; sc- 17764), mouse anti-tubulin (dil: 1/2,000; Santa Cruz; sc-5286), rabbit anti-GAPDH (dil: 1/500; Santa Cruz; sc-25778), mouse anti-cytochrome C (dil: 1/500; Santa Cruz; sc-13156) or anti-NDUFB6 (dil: 1/1,000; Abcam; ms108) prepared in 5% BSA-PBS. Corresponding horseradish-peroxidase conjugated anti-mouse and anti-rabbit secondary antibodies (dil: 1/10,000) were added and followed by 1h incubation at room temperature. Revelation was done using the reaction substrate ECL prime reagent (GE healthcare), and the acquisition was performed with Bio-Rad Molecular Imager Gel Doc XR+ (Bio-Rad). Image Lab software was used for quantification.

2.9 Hypoxia-Reoxygenation of cardiomyocytes

Cardiomyocytes were isolated from hearts of C57bl/6J mice using Langendorff system, as previously described [236]. They were deposited in 8-well plates and were subjected to 90 min hypoxia (0.5 % oxygen) in glucose-free medium (mM: 140 NaCl, 5 KCl, 1 $MgCl_2$, 10 HEPES [pH 7.4], 10 $CaCl_2$) in a hypoxic incubator (Eppendorf; galaxy 48R-CO48EN200259), followed by 1 h of reoxygenation (glucose-containing medium). Cells were then immuno-labeled and visualized by microscopy.

2.10 Immunofluorescence

Cardiomyocytes, plated in glass Labtech plates (PEZGS0816, Merck Millipore), were fixed for 15 min with 2% paraformaldehyde-PBS prior to 4 washes with PBS. They were then permeabilized with 0.1% Triton-PBS for 10 min. Following 4 times PBS washes, the nonspecific binding was blocked using 5% BSA-PBS for 1h at room temperature (RT). The cells were then incubated for 1 h at room temperature with primary antibodies prepared in the blocking buffer. Following the primary antibody incubation, the wells were washed 4 times with PBS and corresponding secondary antibodies (Alexa Fluor 488 rabbit and/or Alexa Fluor 647 mouse - 1/2,000 - Jackson Immunoresearch) were applied for another 1h at room temperature in darkness. The nuclei were stained through a 10 min incubation with Bis-benzimide (5µg/mL). After washing 3 times with PBS, the cells were mounted with Fluoromount™ Aqueous Mounting Medium (Sigma-F4680) and were gently covered by glass coverslips.

The primary antibodies were: mouse anti-ryanodine receptor (RyR) (Abcam; ab2827) (1/500), mouse anti-PS727-STAT3 (batch 1) (Santa Cruz; sc-136193), rabbit anti-PS727-STAT3 (Cell Signaling; 9134), rabbit anti-total STAT3 (Cell Signaling; 4904), mouse anti-total STAT3 (Santa Cruz; sc-8019), rabbit anti-TOM22 (Santa Cruz, sc-14896) and mouse anti-GRIM19 (Santa Cruz; sc- 514111) all diluted at 1/200.

2.11 Cloning of STAT3-eYFP

Mouse STAT3 coding sequence was amplified by PCR with High Fidelity Phusion DNA polymerase (Finnzymes; Thermo Fisher Scientific, Waltham, MA). After a 0.8% (w/vol) agarose-gel extraction of specific DNA bands (Wizard SV gel and PCR Clean-Up System; Promega, Madison, WI), PCR products and recipient vector pVLL-42-mEYFP [255] were digested with High Fidelity NheI and AgeI (New England Biolabs, Ipswich, MA) at 37°C overnight, cleaned-up on column prior to be ligated with T4 ligase (New England Biolabs) at 16°C overnight. Products were transformed in JM109 chemo-competent bacteria (New England Biolabs). Plasmid clones were extracted and sequenced before experiments.

2.12 Mass Spectrometry

The sample was analyzed using an Ultimate 3000 nano-RSLC (Thermo Scientific, San Jose California) coupled on line with a Q Exactive HF mass spectrometer via a nano-electrospray ionization source (Thermo Scientific, San Jose California). Proteins were finally identified by database searching using SequestHT with Proteome Discoverer 2.2 software (Thermo Scientific) against the swissprot Mus musculus database. Precursor mass tolerance was set at 10 ppm and fragment mass tolerance was set at 0.02 Da, and up to 2 missed cleavages were allowed. Oxidation (M), acetylation (Protein N-terminus) were set as variable modification, and Carbamidomethylation (C) as fixed modification. Proteins were filtered with a 1% false discovery rate.

2.13 Confocal Imaging

Confocal imaging was performed using a confocal microscope (Nikon Eclipse Ti, A1R confocal microscope) with a 40x oil immersion objective (N.A. 1.3), equipped with thermos-controlled chamber. The laser lines 405, 488, 514 and 633 nm were used for excitation. The emission wavelengths were acquired sequentially to prevent spectral overlapping. The depth of the focal plan was 0.5 µm, pixel size was chosen between 60 nm to 90 nm in order to respect the Shannon criterion and images were acquired by averaging 4 scanning-lines. Images were further processed with NIS software (Nikon) to adjust brightness and contrast and to calculate the spatial cross-correlation of the two fluorescent signals.

2.14 Statistics

All values are expressed as mean ± standard error of the mean (SEM) for n number of independent observations. Data were analyzed with GraphPad Prism 5.0 using one way ANOVA followed by Dunnett's multiple comparison test or using *t*-test. $P < 0.05$ was considered indicative of a significant difference.

3.RESULTS

3.1. STAT3 is detected in crude but not pure heart, liver and brain mitochondria

We focused on crude and pure mitochondrial protein extracts by western blotting. In crude cardiac mitochondrial fraction, phosphorylated (PY705 and PS727) and total STAT3 forms were detected, along with the mitochondrial proteins GRIM-19 and Tom20. However, the cytoplasmic protein tubulin was also strongly detected, which indicates fraction contamination with cytosolic proteins (n=3) **(Fig. 1A)**. Specificity of anti PS727-STAT3 for phosphate group was assessed by a serine phosphatase treatment that gradually removed the signal **(Fig. S1)**. Since the crude mitochondrial fraction is not reliable for true assessment of exact STAT3 localization, we proceeded toward enriched mitochondrial investigation. Under baseline aerobic conditions, the western blot analysis of cytosolic and enriched, usually defined as "pure", mitochondrial fractions extracted from heart, liver, and brains (n=3) of C57bl6J mice showed that PS727-STAT3 and total STAT3 were exclusively expressed in the cytosolic fraction, along with the cytosolic proteins tubulin and GAPDH **(Fig. 1B).** On the pure mitochondrial level, the mitochondrial protein markers NDUFB6 (complex I subunit) and GRIM-19 were detected, ensuring the validity of this fraction.

During ischemia, STAT3 is activated by phosphorylation, and a further increase in STAT3 phosphorylation occurs during reperfusion[256]. A key pathologic event in cardiac ischemia reperfusion injury is mitochondrial energetic dysfunction, and several studies have attributed this to complex I (CxI) inhibition [257]. A previous study have reported that ischemia stimulates the de novo import of mitochondrial STAT3, where it regulates complexes I and II activities [178]. However, this team used STAT3 with a mitochondrial localized sequence (MLS). Moving from these finding reported by other teams, we aimed to determine if ischemia-reperfusion might induce the mitochondrial translocation of STAT3. C57bl6J mice were subjected to 45 min of ischemia followed by 15 min of reperfusion (n=5). Samples were harvested from the area at risk, proteins were extracted and analyzed by western blotting. PS727-STAT3 and total STAT3 were checked along with the cytosolic proteins GAPDH and tubulin. The mitochondrial proteins NDUFB6 (complex I subunit), GRIM-19 andcytochrome C were also detected. A strong total STAT3 signal was detected in the cytosolic fraction and faint bands could be seen in pure mitochondrial fractions **(Fig. 1C).** However, faint bands could also be detected for the cytosolic freely diffusing GAPDH, while no signal could be found for the cytosolic and polymeric tubulin. Altogether, these results suggested that the faint total STAT3 and GAPDH signals most probably came from contamination of mitochondrial fractions by leakage of cytosolic proteins. Surprisingly, by means of a second batch of anti PS727-STAT3 (b2), we detected a strong band for PS727-STAT3 in the pure mitochondrial fractions exclusively, under both stress and control conditions **(Fig. S2).** Since the presence of PS727-STAT3 in control mitochondria contradicts what was previously observed in the three different organs experiment, and since PS727-STAT3 is part of the total STAT3 (i.e. total STAT3 must be detected where PS727-STAT3 is detected), we headed toward investigating the presence of such a band through validating the specificity of the antibodies used in these experiments. For this validation, STAT3-KO MEFs were used. The second batch of PS727-STAT3 antibody (PS727(b2)-STAT3) detected a dimer in control and a single band in KO cells. This showed that this batch was STAT3 unspecific. The first batch of PS727-STAT3 antibody (PS727-STAT3 b1), PY705-STAT3, and total STAT3 all detected a single band in control cells only (n=3) **(Fig.1 D)**. Moreover, in order to ensure the specificity of our antibody beyond just the molecular weight, the complete gel analysis on the

whole cardiac cell proteome was performed. The results showed that the total STAT3 antibody had one prominent band at the appropriate STAT3 size, ensuring specificity. However, the complete gel analysis using PS727(b2)-STAT3 antibody showed several non-specific bands, which ensures non-specificity **(Fig. S2 B and C).** Furthermore, the mass spectrometry analysis of the band representing the appropriate STAT3 size showed that STAT3 was identified with 20 unique peptides representing 38% of sequence coverage. In all the following experiments, only the specific PS727(b1)-STAT3 antibody, which was also validated on serine phosphatase-treated protein extracts **(Fig.S1)**, was used.

3.2. STAT3 is transversely distributed in cardiomyocytes according to the architecture of T-tubules

Following the detection of STAT3 by western blotting, we sought to study its localization and distribution pattern in cardiomyocytes (CMs) under various experimental conditions. Our results show that total STAT3 (t-STAT3) is arranged according to a transversal pattern similar to that of ryanodine receptors (RyRs), which lie within regularly spaced transverse striations corresponding to the positions of the T-tubules **(Fig. 2A)**. In addition to the co-labeling of RyR and total STAT3 in CMs, we co-labeled total STAT3 and PS727-STAT3 with the mitochondrial proteins GRIM-19 and TOM22, respectively **(Fig. 2 B and C)**. Our results suggest that STAT3 follows a pattern perpendicular to that of the mitochondrial proteins patterns, with the former being transversely dispersed in the cell, while the latter two are longitudinally dispersed following the normal cellular mitochondrial distribution pattern. The spatial cross-correlation of the fluorescent signals pattern was analyzed **(Fig. 3A and 3D)** and no cross-correlation could be found between STAT3 signal and mitochondrial signals.

We then studied if hypoxia-reoxygenation stress conditions could modulate the distribution of STAT3 and induce its mitochondrial translocation. CM underwent 90 minutes of hypoxia followed by 60 minutes of reoxygenation. Neither hypoxia **(Fig. 3B)** nor hypoxia-reoxygenation **(Fig. 3C)** induced a visible mitochondrial translocation of STAT3. Total STAT3 continued to follow a transversal distribution pattern in the cell and no cross-correlation patterns could be detected between STAT3 and GRIM19 **(Fig 3 B and C).** 3D images, collected following a Z-stacking, ensured the absence of co-localization of the two proteins **(Fig. 3E)** although STAT3 signal resided in structures close to mitochondria under such stress conditions**.** The specificity of antibodies used in the immuno-fluorescence experiments was also pre-validated on STAT3-EYFP-transfected cells **(Fig. S3)**.

Finally, we assessed whether STAT3 overexpression could reveal the existence of a mitochondrial transportation mechanism. We thus overexpressed STAT3-EYFP and GRIM19 in H9C2 cardiomyoblasts, and we analyzed the localization of both proteins. A low intensity co-localization could be assumed as reported by the faint yellow color displayed by some of the mitochondria, as depicted in the supplementary material (**Fig. S4)**. To validate this eye-viewed co-localization, we used the classical line-intensity profile analysis of STAT3 and GRIM19 signals. At the first glance, a strong over-lap between the two fluorescent signals could be observed at the level of four different mitochondria (four peaks). With a more careful analysis, we observed that, first, the peaks of fluorescence intensity of the 2 wavelengths were slightly shifted for profiles 2 and 3. Taken into account the diffraction limit of optical systems, this suggested that STAT3 signal could have been outside the mitochondria. Second, the 4^{th} and 5^{th} peaks of green fluorescence reporting STAT3 signal showed a similar shape and peak intensity, whereas the 4^{th} peak co-localized with a mitochondria

while the 5th was not. This could have been explained by a random co-localization between STAT3 hotspots and mitochondria. Since this line profile analysis does not report a 2D spatial co-localization, we performed the spatial cross-correlation of the fluorescent signals **(Fig. S4B)**. Strikingly, clear and vivid donut-shaped cross-correlation patterns, around the mitochondria, were observed. This what reports that the highest cross-correlation of the two fluorescent signals was found at the mitochondrial circumference rather than inside them. This presents a tipping point toward the probability that STAT3, even when over-expressed, might most-probably be located outside or around the mitochondrial rather than inside the mitochondria themselves.

The fact that we could not detect any clear STAT3 signal in mitochondria, whatever methods we used, does not guarantee that no STAT3 is expressed in mitochondria, but rather that its concentration is below the sensitivity of both Western-blot and immunofluorescence. Our results are in line with those of Phillips et al. who detected very small amount of STAT3 by mass-spectrometry in cardiac cells, at a concentration unlikely to be involved in a biological function in mitochondria[258].

3.3. **The inhibition of STAT3 does not modify mitochondrial function**

The mitochondrial oxygen consumption and calcium retention capacity were measured following pharmacological inhibition of STAT3 by Stattic. Boengler et al[224] originally demonstrated a strong inhibition of complex I and II activities following administration of 100 µM Stattic. Literature reports indicate that Stattic can be toxic as previously observed in cancer cells [259]. A dose-dependent assessment of this inhibitor (10-100 µM) showed that a 1 h treatment with 50 and 100 µM of Stattic significantly decreased PY705-STAT3 level (>50%), without any significant effect on PS727-STAT3 level **(Fig.4 A and B)**. However, a 2 h Stattic treatment induced protein degradation at a 100µM dose (Fig. 4C). Subsequently, a dose of 50 µM Stattic, with a 1 h treatment, was used for further mitochondrial experiments.

The ADP-stimulated oxygen consumption of complexes I, II and IV was recorded following the incubation of crude mitochondria with DMSO (vehicle) or Stattic (50µM) for 1 h at 4°C (with agitation). Our results showed no significant effect for Stattic on complex activities under ADP-stimulated conditions (n=3) **(Fig.4 D)**. The oxygen consumption of complexes I, II, and IV were 35.2 $\pm$ 4.20, 25.2 $\pm$ 3.41 and 80.63 $\pm$ 12.3 nmole O_2/min/mg protein, respectively, following DMSO treatment. These levels slightly and non-significantly shifted toward 34.2 $\pm$ 5.24, 23.9 $\pm$ 2.57 and 73.9 $\pm$ 7 nmole O_2/min/mg protein, respectively, following Stattic treatment (n=3).

Under the same treatment conditions, the calcium retention capacity (CRC) was measured in the presence of glutamate/malate and succinate as substrates for complexes I and II, respectively. ADP and $MgCl_2$ were added for mimicking normal physiological conditions and ensuring optimal mitochondrial respiration. The results show that the CRC was, unexpectedly, increased from 666 $\pm$ 68 nmole calcium/mg protein to 760 $\pm$ 86 nmole calcium/mg protein (13%) in the presence of Stattic (n=3) **(Fig.4 E)**.

4. DISCUSSION

In the present study, taking into account both sensitivity and specificity of the methods used, we could not detect significant levels of STAT3 proteins in mouse heart mitochondria under both baseline conditions and after prolonged ischemia-reperfusion. However, we report a novel prominent distribution of STAT3 along the architecture of T-tubules. We discuss the potential role of STAT3 in the regulation of mitochondrial permeability transition and more largely in cardioprotection

4.1 STAT3 in heart mitochondria

In the original study revealing the localization of STAT3 in heart mitochondria, Wegrzyn al. [243] proposed that about 10% of STAT3 proteins were expressed within mouse heart mitochondria. In the same study, they reported a high concentration of PS727-STAT3 in heart mitochondria. Unfortunately, we could not exactly compare our experiments since the original antibodies which were used are no longer provided by the manufacturers and have been substituted with "more specific" ones as it is indicated on the manufacturer website (Santa Cruz). In the present study, we could not detect 10% of STAT3 being expressed in mitochondria whatever the anti-STAT3 antibody used (3 different validated antibodies). In a more recent study performed on mouse heart mitochondria as well, the authors also failed to detect PS727-STAT3 in mitochondria [247]. Rainer et al. showed that STAT3 was expressed in wild type heart mitochondria; however, a faint pair of bands was also detected in the mitochondria fraction of STAT3-KO [212]. Although a decrease in intensity can be seen, the fact that bands unrelated to STAT3 can be detected in extract of KO STAT3 cells question the specificity of the antibody. In our experiments with the unspecific S727(b2)-STAT3, we detected bands of low intensity of the expected size for STAT3 in STAT3 KO MEFs cells. This result was correlated with an opposite detection of signal in mitochondria *vs.* cytosolic fractions. Since we used 3 different antibodies validated against KO STAT3 extracts and showing a similar detection in cytosolic but not in mitochondrial fractions, we concluded the non-specificity of the antibody S727(b2)-STAT3. Our results indicate that one should avoid using antibodies that detect bands at the expected size of the candidate protein in its KO models. Following cell fractionation, one cannot guarantee the absolute purity of the fractions, hence only strong signals should be considered as acceptable. Noteworthy, the reference to "pure" mitochondrial fraction instead of enriched mitochondria fraction has maybe become misleading. This technical limitation strongly applies to proteins known to be expressed in ER or mitochondria associated membranes (MAMs), like STAT3 [249], since there is no guarantee that 100% of these membranes have been retrieved from the "pure" mitochondrial fraction. This might explain why we detected a strong STAT3 signal in crude mitochondrial extracts and virtually no or a non-consistent signal in pure mitochondria. This pattern is indeed the one often observed in several published studies.

The specificity of such detection is usually addressed by labeling compartment-specific proteins in order to show the clear cell compartment discrimination between the different fractions, taking into account a comparable (long enough for weak signals) exposure time of the membrane for all protein markers, together with an appropriate choice of these markers. STAT3 is a soluble protein which is freely diffusing by Brownian motion in its media, whether it is cytoplasm, nucleoplasm or mitochondrial matrix. Authors historically used tubulin, a polymer anchored to membrane, as marker of cytosol; VDAC, a transmembrane protein, as marker of the outer mitochondrial membrane; and the sub-unit of the complex I, like GRIM19, as marker of the mitochondrial matrix. Although these markers are good to assess the contamination of fractions by membranes of other

compartments, they are not suitable to assess contamination by protein diffusion that would occur when membranes are damaged. Since GRIM19 is a soluble protein, and because only a fraction of GRIM19 proteins is bound to the holoenzyme of complex I, we can consider it as a good marker for mitochondrial matrix. However, we claim here that tubulin is not the best marker to assess for contamination by cytosolic proteins, in such kind of experiments, and should be substituted by another protein such as GAPDH. As shown in **(Fig. 1C)**, tubulin was not detected in the mitochondrial fraction while GAPDH showed a weak band. Accordingly, although we indeed detected a weak STAT3 signal in the mitochondrial fraction, we could not conclude whether it was contamination or a specific localization. In this context too, the weak STAT3 band observed in the pure brain mitochondrial fraction **(Fig. 1B)** could be due to contamination since a similar signal is observed for both GAPDH and tubulin.

While western blots do not conserve the original spatial information and assesses a cell population, immunofluorescence can be analyzed at the single cell level and provides information as to spatial localization by cross-correlation of signals labelling the proteins of interest and the compartments of interest. However, similar to western blotting, immunofluorescence relies on specificity and sensitivity of the antibodies. Using immuno fluorescence we showed a good spatial cross-correlation between STAT3 signal and the ryanodine receptor localized in the junctional SR but no strong cross-correlation between STAT3 and mitochondria. Assuming that near 10% of STAT3 is expressed in mitochondria, we would have expected to detect a strong spatial cross-correlation between STAT3 and a marker of mitochondria.

We questioned the localization of STAT3 in the mitochondria of cell lines. An extensive literature supports the fact that STAT3 can be translocated to the mitochondria in different cell lines, particularly upon a strong expression in cytosol. According to the literature, experiments targeting STAT3 to the mitochondria by means of a mitochondria-localization site [247] or incubating mitochondria in the presence of a high concentration of STAT3 [196] induced a strong translocation of STAT3 into the mitochondria. An import mechanism of STAT3 to the mitochondria does exist, even though it likely requires either STAT3 overexpression or dysregulation, which could occur in cancer cells. In this study, we reported that the overexpression of STAT3-EYFP in H9C2 cardiomyoblasts-derived cell line was correlated with a significant level of fluorescence in the mitochondria, what supports the fact that a fraction of STAT3 may translocate into the mitochondria under specific conditions. However, our cross-correlation analysis also clearly demonstrated that the major STAT3 signal was actually observed all around the mitochondria not inside them. Given the dotted pattern of STAT3 signal, it is likely that a proportion of STAT3 proteins are bound to structures like membranes rather than freely diffusing in the cytosol. This suggests that a high proportion of STAT3 may be bound to ER membrane surroundings the mitochondria. This hypothesis is supported by a recent study [249] and could explain why a strong STAT3 signal is detected in the crude mitochondrial fraction which includes a large proportion of ER membranes. It could also explain why a STAT3 contamination could be observed in "pure" mitochondrial fraction, since it is difficult to guarantee 100% removal of ER membranes.

Several studies reported that upon induction (including ischemia-reperfusion), STAT3 translocates from cytosol to nucleus or to mitochondria. On our side, we failed to detect STAT3 in mitochondria after ischemia-reperfusion, with both Western-blot and immunofluorescence, in both *in vivo* and *in vitro* models while, conversely, a strong signal was observed in cells nuclei.

Altogether, our results do not support a role for STAT3 in mouse cardiac mitochondria [247].

4.2 Specificity, sensitivity, and toxicity of *Stattic*

Stattic is a specific inhibitor of STAT3 [200] and has been used in numerous studies. We observed that in some studies [212], high concentration of Stattic (>100μM) were used regardless its IC50 for STAT3 phosphorylation (20 μM for 1hr incubation at 30°C) and for cell death induction (20 μM) [200]. Noteworthy, in the original article showing Stattic specificity, Stattic inhibited STAT1 at 40% with an IC50 of 10 μM at 30°C. In a recent study, authors confirmed that 10 μM Stattic inhibited both STAT1 and STAT3 phosphorylation activity [259]. In this latter study, a prolonged 20 μM Stattic treatment was found to be toxic and induced cell death. In our hands, a 100 μM Stattic treatment for 2 h induced STAT3 and tubulin degradation confirming that high Stattic concentration could trigger toxic effects non-related to its effect on STAT3 **(Fig. 4C)**. We could not detect any inhibition of mitochondrial respiration when we treated isolated mitochondria with 50 μM for 1 h at 4°C (this temperature was used to preserve mitochondria during incubation). Boengler et al found a 50% decrease in complex I activity when incubating heart mitochondria with 200 μM Stattic for 1 h at 4°C [212]. Although the temperature of incubation is slowing down the reaction, Stattic can be considered as being in saturating condition since majority of cellular STAT3 is absent in crude mitochondrial fraction. Therefore, it is very unlikely that we could not observe an inhibitory effect of 50 μM Stattic if STAT3 is expressed in mitochondria and is regulating complex I activity. Conversely, the use of 200 μM Stattic could have induced: i) protein degradation and subsequent toxic effect down-regulating complex I activity, and ii) inhibition of STAT1 as it was detected in heart mitochondria [212]. Besides, it should be kept in mind that respiration and CRC experiments are usually carried on crude mitochondrial fractions, which incorporates a lot of STAT3 protein outside of the mitochondria. In case a direct effect on STAT3 inhibition would be observed, such as the small increase in CRC we observed, it should not be claimed that it is more likely related to an effect on STAT3 from the inside of mitochondria rather than from the outside of the mitochondria. In conclusion, both data of the literature and our results suggest a careful control of the non-specific effect of Stattic, particularly in experiments with cell fractions which may include no or low STAT3 levels.

4.3 The STAT3 KO phenotype

Previous reports suggest that mitochondrial respiration is down-regulated in cardiomyocytes of STAT3 KO mice and in STAT3 KO cell lines [243] [260]. Since STAT3 is primarily a transcription factor and is known to regulate genes involved in metabolism and mitochondrial activity :[207], [208], one should not exclude a canonical genomic explanation to the down-regulation of respiration in heart mitochondria of STAT3 KO mice. In addition, sharing an apparent similar phenotype between *in vivo* cardiomyocytes and *in vitro* cell lines could not mandatorily be recapitulated by a common mechanism. Indeed, since we could not detect STAT3 in heart mitochondria but could see STAT3-EYFP around mitochondria of H9C2, it is unlikely that the effect of STAT3 on respiration would be caused by a common mechanism.

In conclusion, our results show a novel vivid distribution for STAT3 along the T-tubules of cardiomyocytes and in the nucleus, under different conditions. Moreover, we neither find a significant amount of STAT3 in mouse heart mitochondria, nor detect a direct involvement for it in the regulation of mitochondrial activities under physiologic conditions. Although we agree that under non-physiological conditions, such as STAT3 overexpression or MLS-tagged STAT3, STAT3 could be translocated to mitochondria, we speculate that this mechanism could mainly be relevant to cell lines already showing a strong expression of STAT3. Alternatively, our localization and functional experiments support the fact that STAT3 is localized around the mitochondria in a cardiomyoblasts cell line, and it may indeed support an indirect effect on their activity.

AUTHOR CONTRIBUTIONS

Conceived experiments: ZH, SB, MK, GB.

Performed experiments: ZH, SB, NGB, MP, BP, LA.

Wrote the manuscript: ZH, MO and GB.

Supervised the study: MK, GB.

Review the manuscript: MP, GWB, ECS, MO.

AKNOWLEGDMENTS

This study benefits from grants offered by INSERM, the Lebanese University, and The Cedar program of Campus France (#37303QA 2017-2018).

This work was supported by the IHU OPeRa (ANR-10-IBHU-004) within the program "Investissements d'Avenir" operated by the French National Research Agency (ANR).

Zeina Harhous was supported by the "Association de Specialisation et d'orientation Scientifique".

Sally Badawi was supported by the Council for Scientific Research and Lebanese University fellowship (CNRS-L) program and the Eiffel scholarship program of excellence of Campus France.

We acknowledge the financial support from ITMO Cancer AVIESAN (Alliance Nationale pour les Sciences de la Vie et de la Santé, National Alliance for Life Sciences and Health) within the framework of the cancer plan for Orbitrap mass spectrometer founding.

We also thank Adeline Page for performing the mass spectrometry analysis (Protein Science Facility, SFR BioSciences CNRS UMS3444, Inserm US8, UCBL, ENS de Lyon, 50 Avenue Tony Garnier, 69007 Lyon, France).

FIGURES

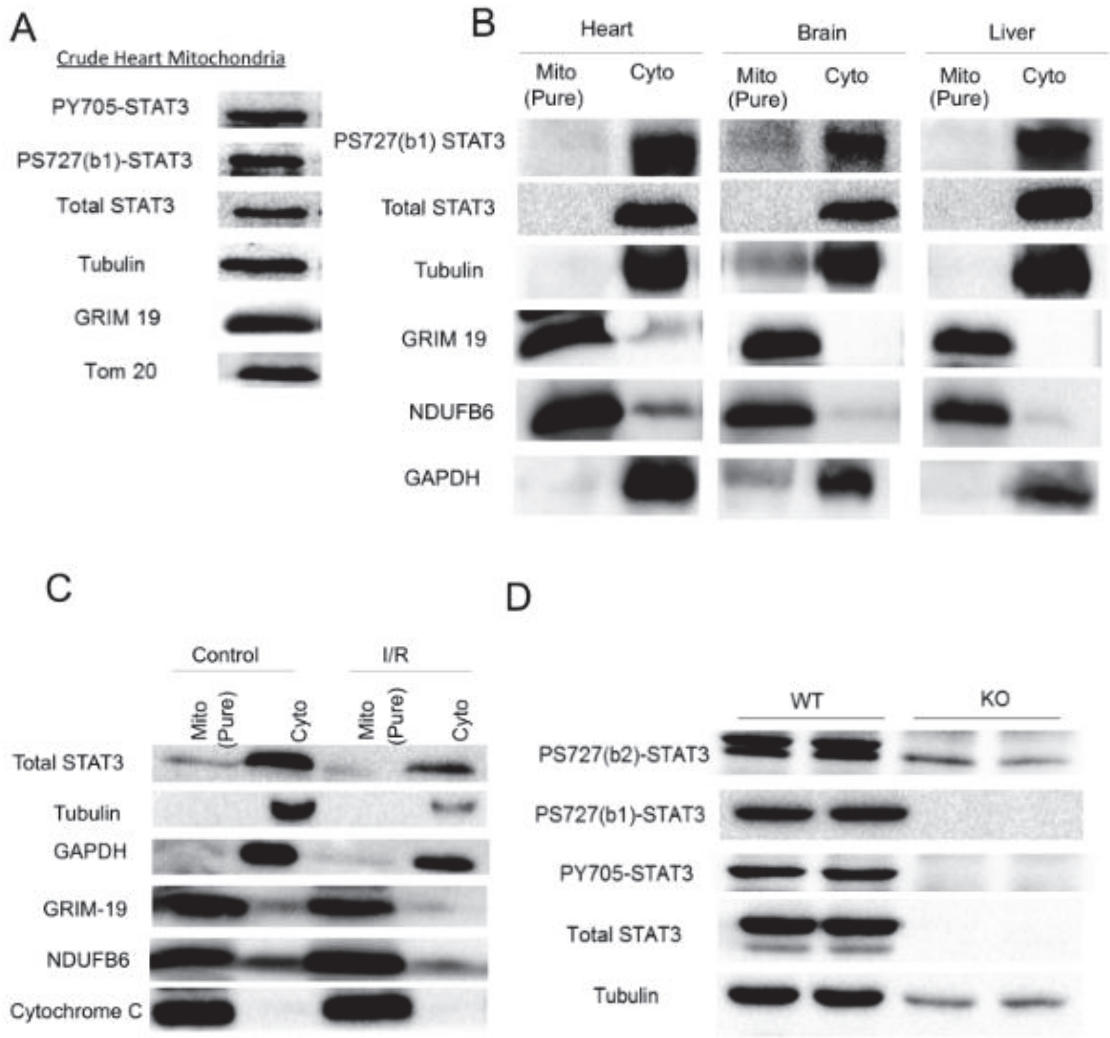

Figure 1. Cytosolic and mitochondrial fractions show the absence of STAT3 in pure mitochondria of different organs.

Western blots showing the detection of Y705- and S727-phosphorylated and total STAT3 forms; the cytosolic proteins tubulin and GAPDH; and the mitochondrial proteins Tom20, GRIM19, cytochrome C and NDUFB6 (complex I subunit) in (A) protein extract of crude mitochondria fraction (40µg) (n=3), (B) pure mitochondrial and cytosolic extracts from hearts, brains, and livers of control C57bl/6J mice (90 µg of protein extract per well) (n=3), (C) pure mitochondrial extracts from the area-at-risk of mouse heart subjected to 45 minutes of ischemia followed by 15 minutes of reperfusion (30 µg of protein extract per well) (n=5), (D) verification of the specificity of several STAT3 antibodies in 40 µg of total protein extract of wild type (*wt*) and STAT3-KO MEFs: PS727-STAT3 (batches one and two: b1 and b2), PY705-STAT3 and total STAT3 (n=3).

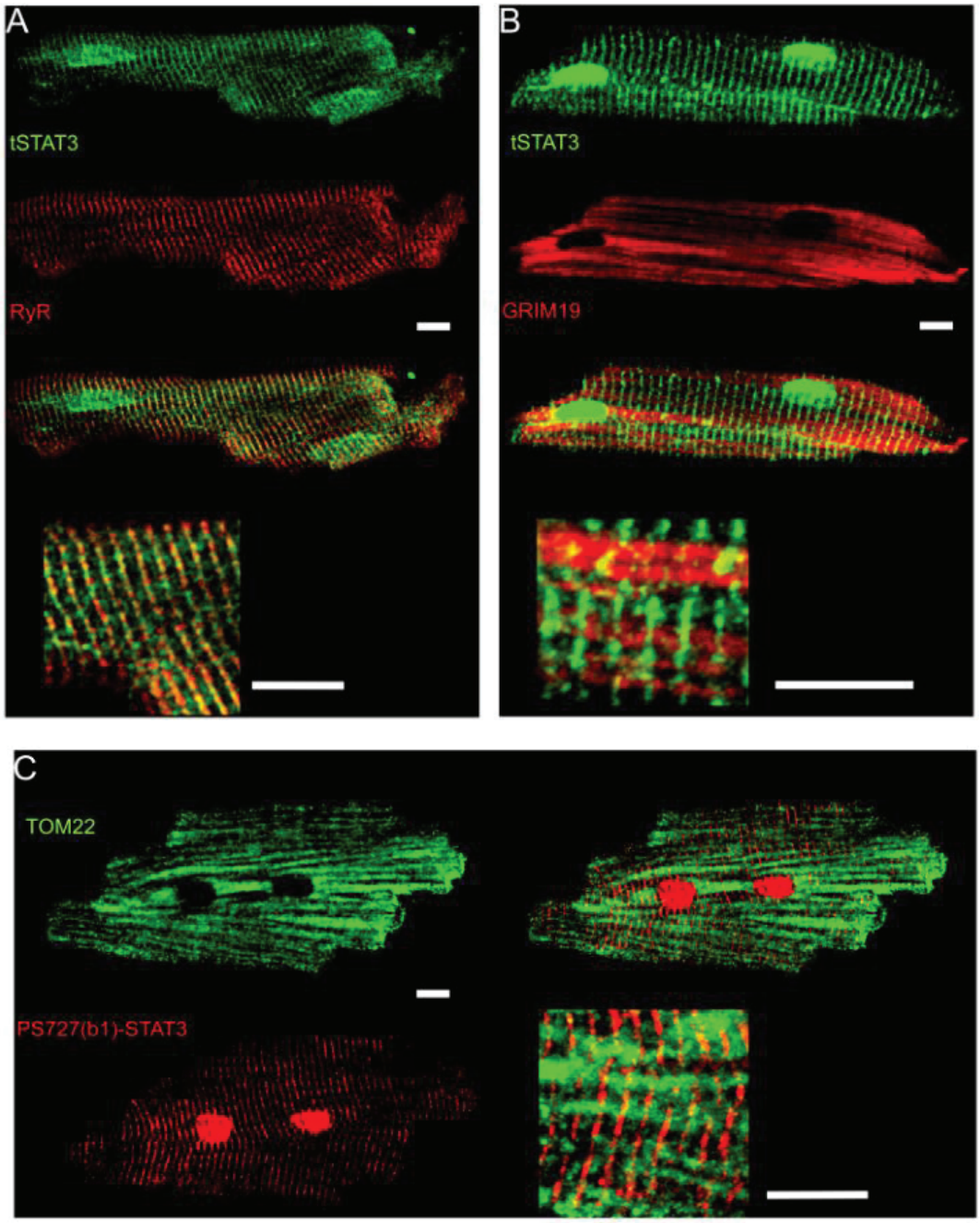

Figure 2. STAT3 is distributed in nucleus and along t-tubules of cardiomyocytes.

Confocal images of mouse isolated cardiomyocytes immuno-labelled with antibodies against **(A)** a marker of junctional sarcoplasmic reticulum, the ryanodine receptor type II (RyR2) in red and total STAT3 (green), **(B)** a mitochondrial marker, GRIM-19 (Red), and total STAT3 (Green) or the mitochondrial marker Tom20 (green) and **(C)** PS727(b1)-STAT3 (Red). Depth of the focal plane: 1 µm. Three independent experiments were carried out on different mouse hearts. Scale bars: 10 µm.

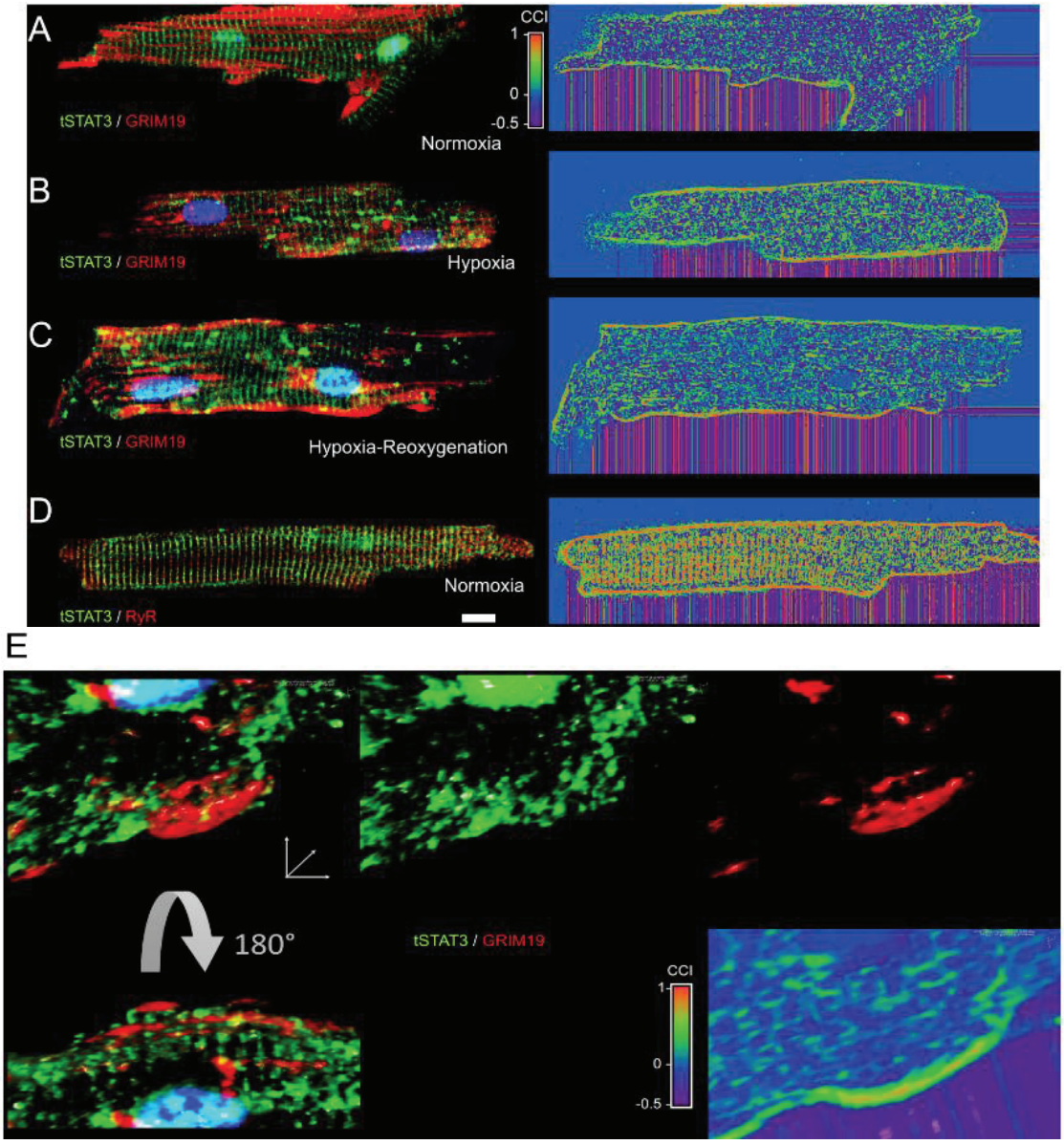

Figure 3. Hypoxia and hypoxia-reoxygenation do not induce the mitochondrial translocation of STAT3 in mouse-isolated cardiomyocytes.

Confocal images showing the merging of fluorescence image of total STAT3 (green) and GRIM-19 (red) in mouse isolated cardiomyocytes incubated under **(A)** normoxia, **(B)** hypoxia for 90 min or **(C)** hypoxia as in (B) followed by reoxygenation for 1 h (HR). Right images are quantifying the spatial cross-correlation intensity (CCI) of the 2 fluorescent signals. **(D)** The confocal image and co-localization pattern of total STAT3 (green) and RyR2 (red) in cardiomyocytes under normoxia conditions. **(E)** A 3D reconstructed projection showing the localization pattern of total STAT3 (green) and GRIM-19 (Red) in cardiomyocytes subjected to HR. Top row of image is showing the 3D rendering from above for merged fluorescence (left), STAT3 fluorescence alone (middle) and GRIM-19 fluorescence alone (right). Bottom row showing the 3D rendering from below (left) and the 3D spatial cross-correlation image. Three independent experiments were carried out on different mouse hearts. Scale bar: 10 µm.

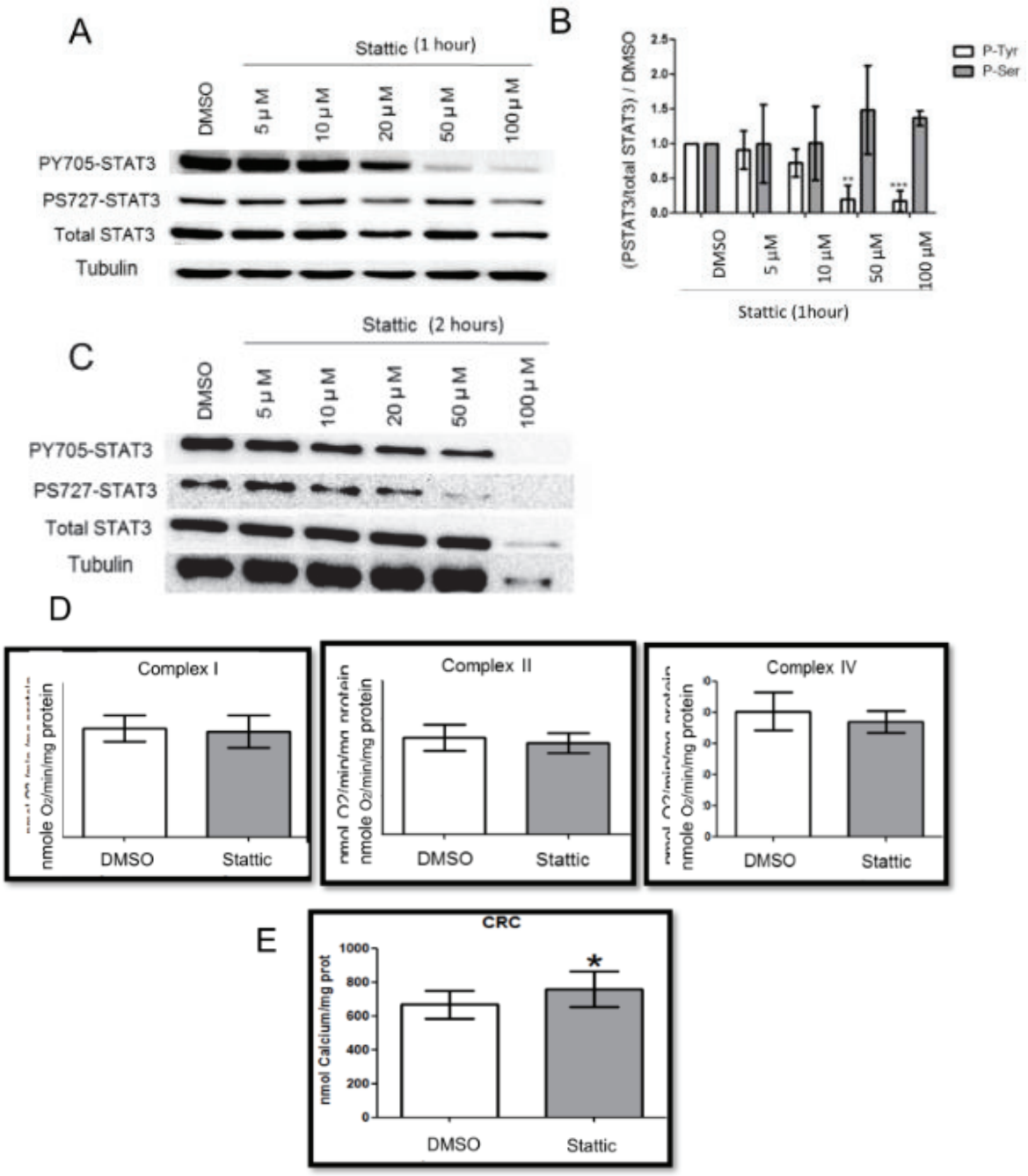

Figure 4: Pharmacological inhibition of STAT3 by Stattic has no effect on ADP-stimulated mitochondrial oxygen consumption but slightly increases calcium retention capacity.

Western-blots showing the dose-effect of a one hour- or **(C)** two hours- treatment with the STAT3 inhibitor, Stattic, on the phosphorylation of STAT3 in mouse isolated adult cardiomyocytes. **(B)** Phosphorylation of Y705 and S727 residues of STAT3 was quantified and divided by the amount of total STAT3 protein. STAT3 ratios for one hour Stattic-treated cells were normalized by DMSO treated condition. **(D)** Oxygen consumption rate by complexes I, II and IV (state 3) measured in isolated mitochondria of mouse cardiomyocytes, incubated with either DMSO or 50 µM Stattic for 1 h at 4°C. **(E)** Calcium retention capacity measurement for mitochondria treated with DMSO or 50 µM Stattic for 1 h at 4°C. Three independent experiments were carried out on different mouse hearts.

Supplementary Data

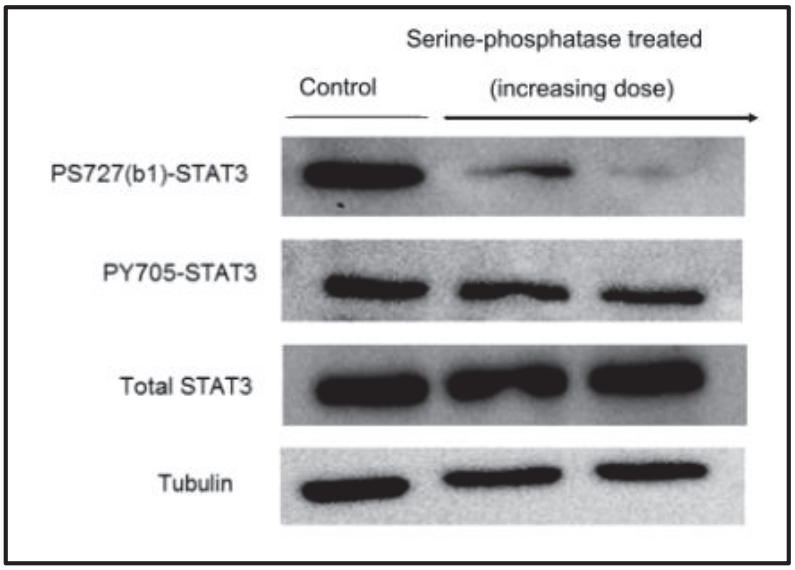

Figure S1: Specificity of the PS727(b1)-STAT3 antibody

Western blot analysis showing the effect of a serine-phosphatase treatment on the level of phosphorylation of Y705 and S727 STAT3. Tubulin reports the protein loads in each well. Three independent experiments were carried out on different mouse hearts.

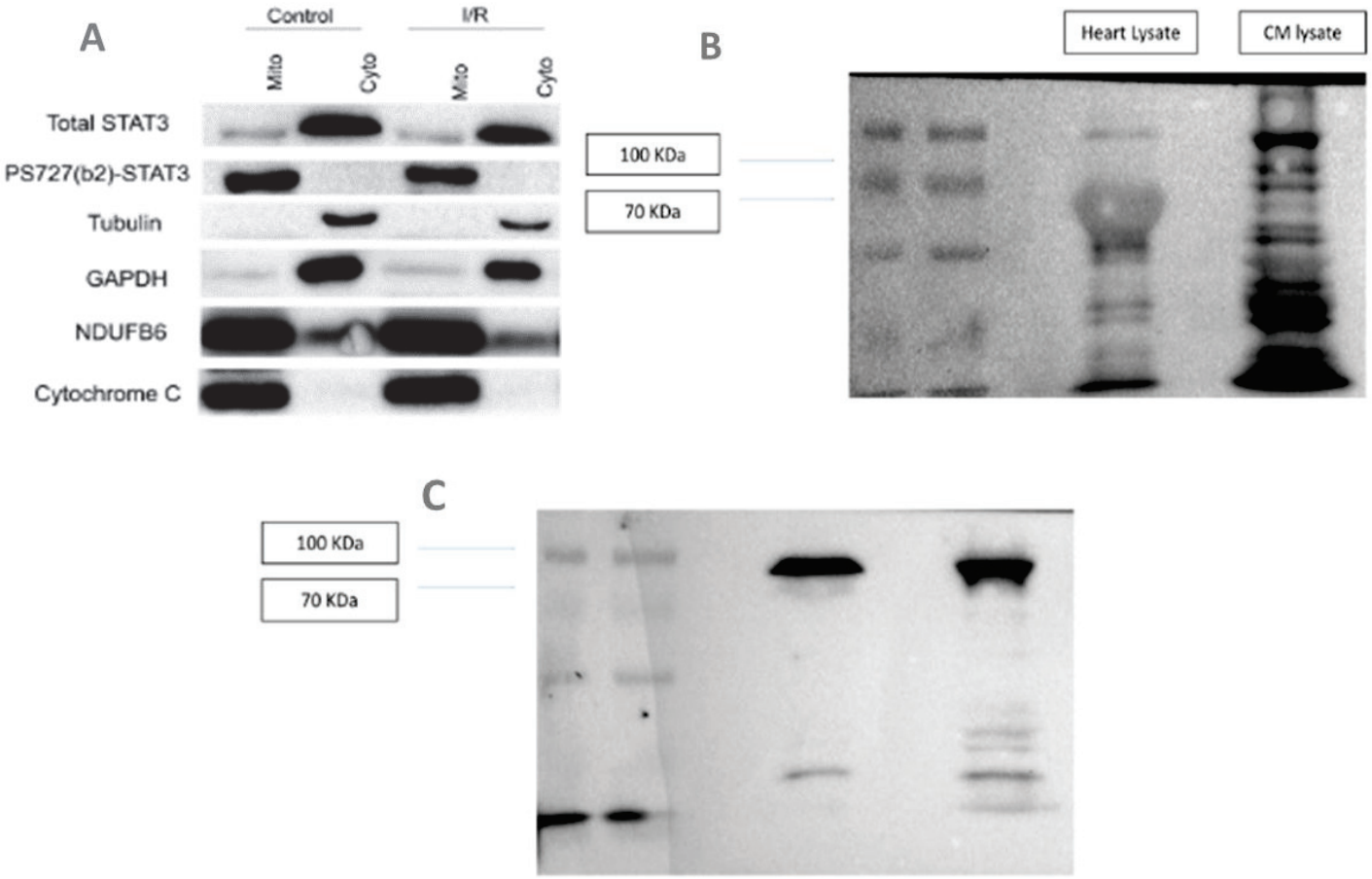

Figure S2: Lack of specificity of PS727(b2)-STAT3 antibody in mitochondrial and complete cardiac cell proteomic fractions

(A) Western blot analysis of PS727(b2)-STAT3, total STAT3, tubulin, GAPDH, Cytochrome C and GRIM-19 in pure mitochondrial extracts from the areas at risk of mice hearts subjected to 45 minutes of ischemia followed by 15 minutes of reperfusion or from control mice. Note that while PS727(b2)-STAT3 detects a band in the mitochondrial fraction, no total STAT3 can be detected, which is unfathomable. Six independent experiments were carried out on different mouse hearts.

(B) Western blot analysis of PS727(b2)-STAT3 in total cardiomyocyte proteomic sample.

(C) Western blot analysis of Total STAT3 in total cardiomyocyte proteomic sample

I. Specific and used Antibodies

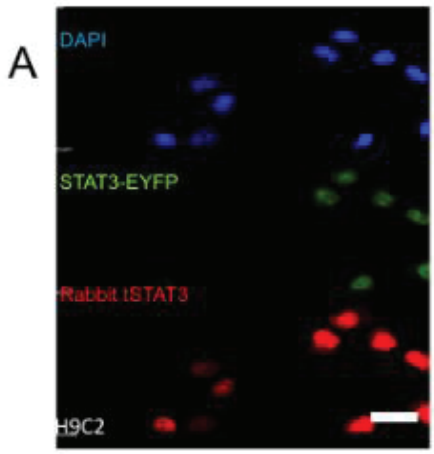

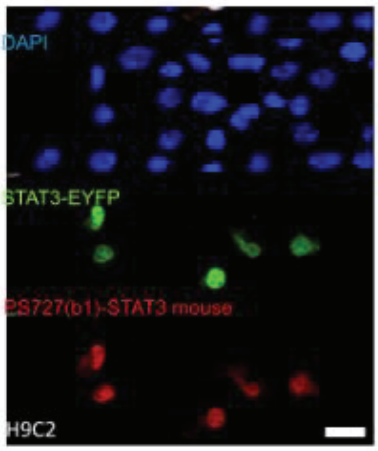

II. Non-specific Antibodies (unused)

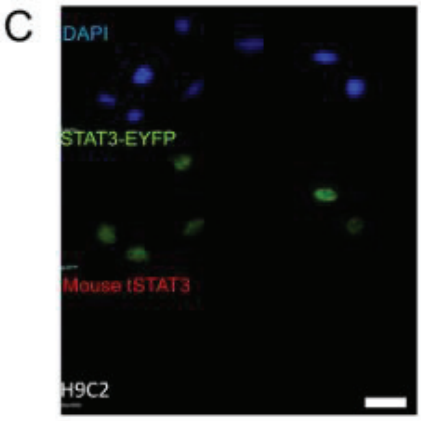

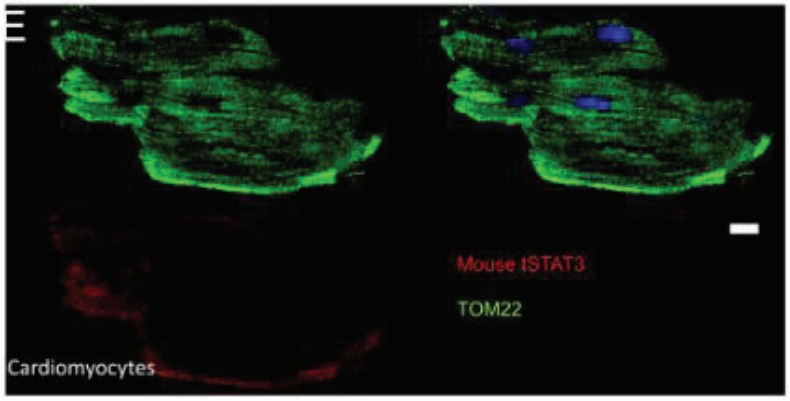

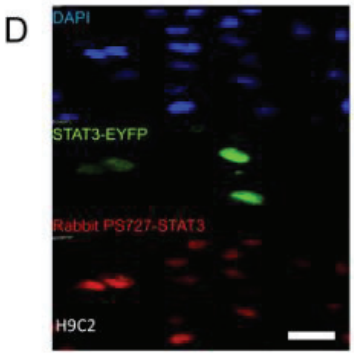

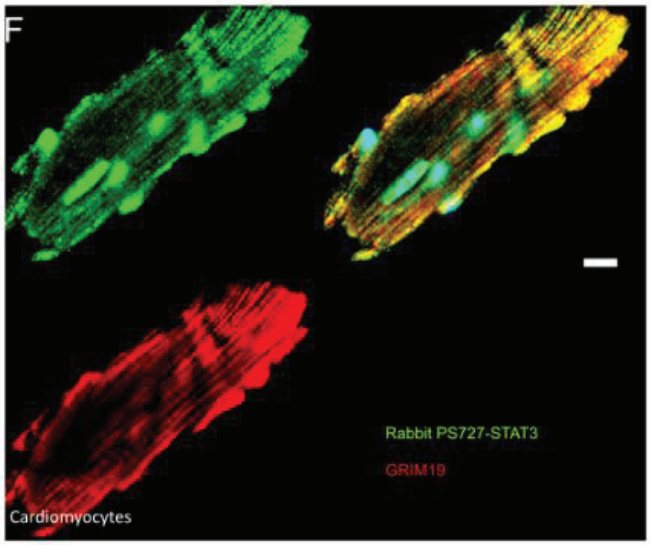

Figure S3: Specificity of the STAT3 antibodies in immunofluorescence experiments.

Confocal images of H9C2 cells transfected with STAT3-EYFP plasmids for 48h and then labeled with different antibodies:

I- Specific used antibodies **(A)** rabbit IgG anti-total STAT3 (tSTAT3), **(B)** mouse IgG anti- S727 phosphorylation of STAT3 (PS727(b1)-STAT3);

II- Non-specific unused antibodies **(C)** mouse IgG anti-total STAT3 (mouse tSTAT3**)** and **(D)** rabbit IgG anti- S727 phosphorylation of STAT3 (rabbit PS727-STAT3). **(E) and (F),** Immunofluorescence experiments on mouse isolated cardiomyocytes show the detection of TOM22 and GRIM19 proteins, respectively, in mitochondria and concomitantly to the non-specific fluorescent signal given by mouse IgG anti-total STAT3 (mouse tSTAT3) and rabbit IgG anti- S727 phosphorylation of STAT3 (rabbit PS727-STAT3), respectively. Three independent experiments were carried out on different mouse hearts.

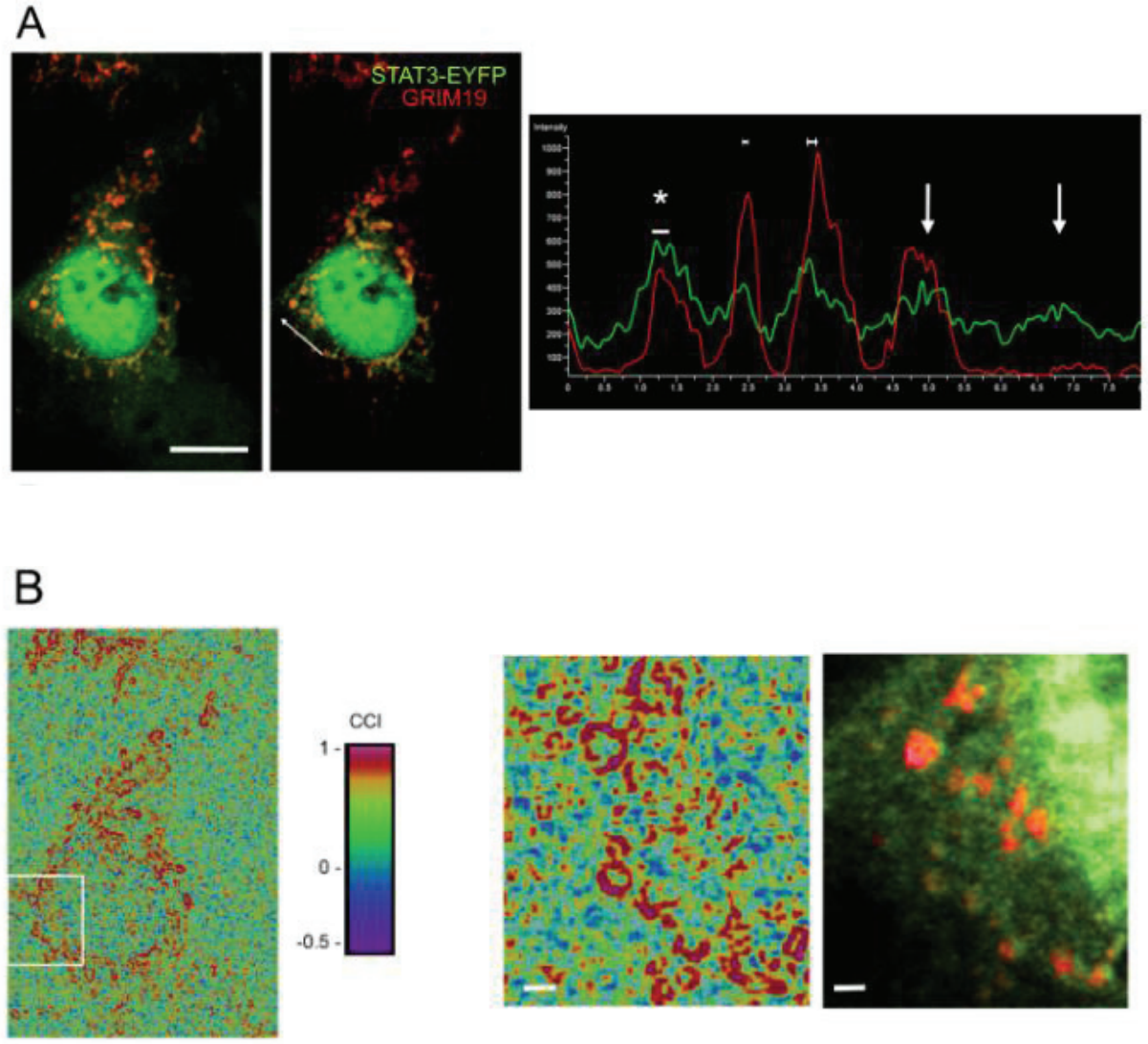

Figure S4: STAT3 and GRIM19 co-localize at the mitochondrial circumference in H9C2 cardiomyoblasts.

(A) Confocal images of H9C2 cardiomyoblasts co-transfected with STAT3-EYFP (green signal) and mCherry GRIM19 (red signal) plasmids for 48h (left panel), along with the line intensity profiler (middle right panel) and plot showing intensity profiles of both signals in four different randomly chosen mitochondria (right panel). Scale bar 10µm

(B) Map of the spatial cross-correlation intensity (CCI) of the two fluorescent signals (left panel) and a representation of the correlation pattern of distribution (red pattern) in a randomly chosen zoomed-in area (right panel), showing a donut-shaped co-localization pattern around mitochondria rather than inside them. Scale bar 1µm

Section II: STAT3 in signaling and transcription

After investigating the involvement of STAT3 in the regulation of mitochondrial functioning during IRI and reporting the absence of such roles along with the absence of STAT3 in mitochondria, we reoriented our project toward investigating the functioning of STAT3 in IR and IPoC in a mitochondria-independent manner. In this regard, we aimed to study the temporal variation in the phosphorylation of STAT3 and the kinases of the cardioprotective RISK pathway (ERK1/2, Akt, p38 and JNK) along with deciphering the interlink between STAT3 and these kinases. In addition to this signaling approach, we used a genomics approach, whereby we aimed to study the transcriptional activity of STAT3 during IR and IPoC. Thus, this section is divided into signaling and genomics parts.

Part I. Signaling

1. The in vitro Interlink

In order to decipher the *in vitro* interlink between STAT3, Akt and the MAPKs (ERK, P38 and JNK), the H9C2 cell line was used as a preliminary model. PD98059 (30 µM), Wortmannin (4 µM), SB600125 (50 µM) and PD169316 (50 µM) were respectively used for inhibiting MEK/ERK, PI3K/Akt, JNK and P38.

1.1. The MEK/ERK – STAT3 Interlink

The treatment of H9C2 cells with PD98059 significantly inhibited ERK ($p<0.05$) and S727-STAT3 phosphorylation ($p<0.001$) (n=3). A non-significant increase in Y705-STAT3 phosphorylation was observed **Fig. 27.**

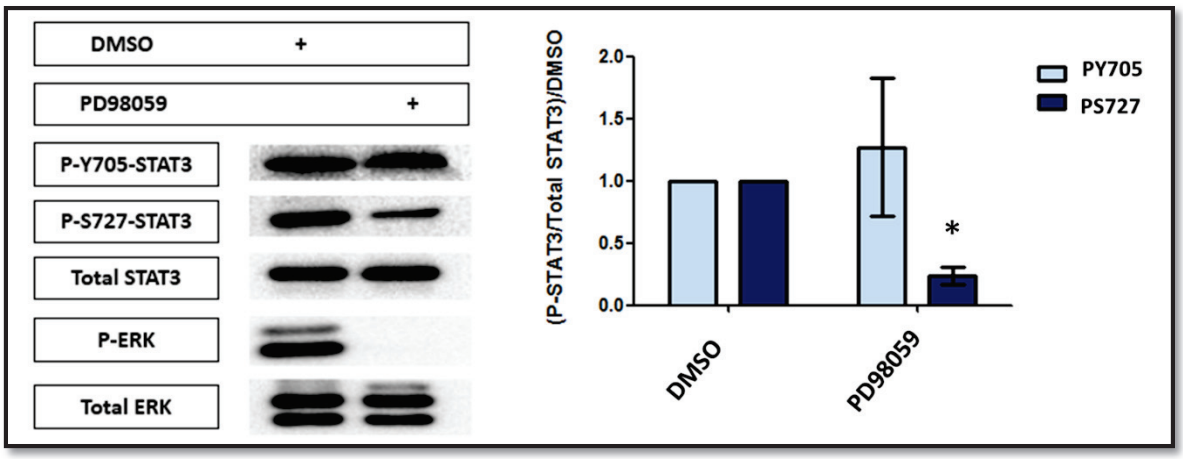

Figure 27*:* The effect of MEK/ERK inhibition on STAT3 phosphorylation

Western Blot analysis of phosphorylated STAT3 and ERK1/2 levels in H9C2 cells following ERK1/2 inhibition by PD98059 (30µM) (n=3). ** P<0.05*

1.2. The PI3/Akt - STAT3 Interlink

The treatment of H9C2 cells with Wortmannin had no significant effect on STAT3 phosphorylation **Fig. 28**.

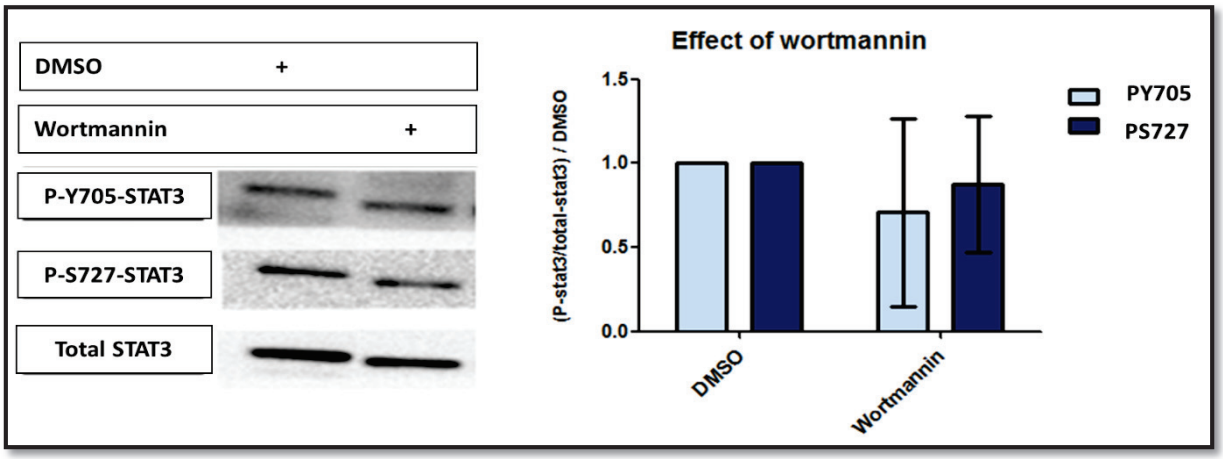

Figure 28. The effect of PI3K inhibition on STAT3 phosphorylation

Western Blot analysis of phosphorylated STAT3 levels in H9C2 cells following PI3K inhibition by Wortmannin (4μM) (n=3).

1.3.The JNK – STAT3 Interlink

Similar to Wortmannin, the treatment of H9C2 cells with SB600125 had no significant effect on STAT3 phosphorylation **Fig. 29.**

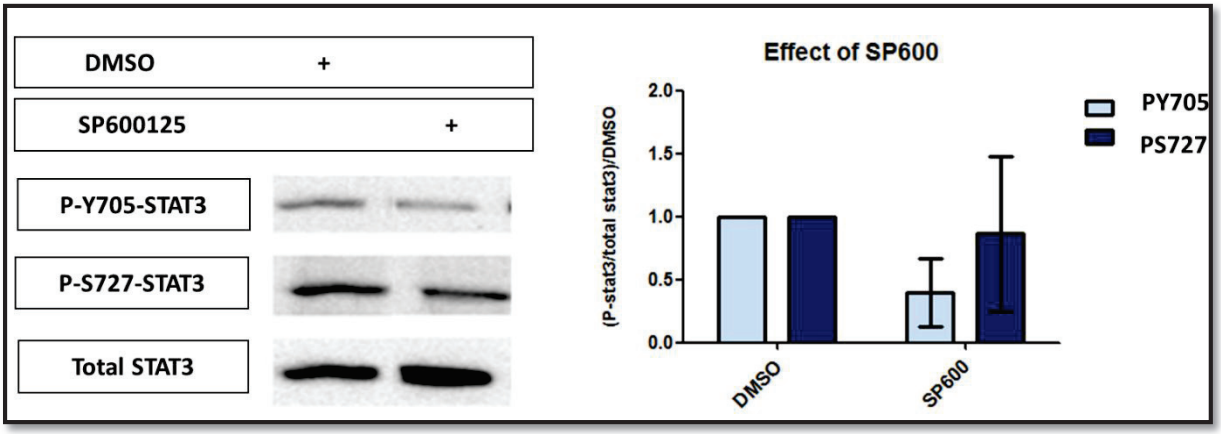

Figure 29. The effect of JNK inhibition on STAT3 phosphorylation

Western Blot analysis of phosphorylated STAT3 in H9C2 cells following JNK inhibition by SP600125 (100μM) (n=3).

1.4.The P38 – STAT3 Interlink

The treatment of H9C2 cells with PD169316 induced a significant decrease in both Y705 and S727 STAT3 phosphorylation **Fig. 30.**

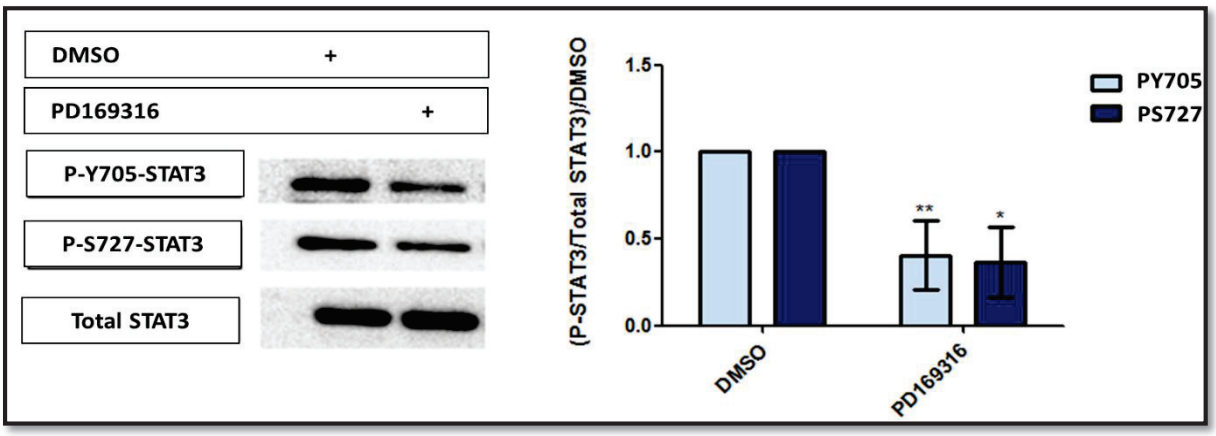

Figure 30. The effect of P38 inhibition on STAT3 phosphorylation

Western Blot analysis of phosphorylated STAT3 in H9C2 cells following P38 inhibition by PD169316 (50μM). ** P<0.05 **P<0.01*

Overall, the above results show that a possible interlink exists between STAT3 and ERK1/2 and P38 but not Akt and JNK kinases. Moreover, the increase in Y705-STAT3 phosphorylation which accompanied the decrease in YS727-STAT3 phosphorylation under PD98059 treatment, although non-significant, provoked us to question the relationship between Y705 and S727 STAT3 phosphorylation.

1.5. A Competitive Relationship Exists between PY705 and PS727 STAT3 phosphorylation

For investigating the relationship between Y705 and S727 STAT3 phosphorylation, H9C2 cells were treated for 15 minutes with the IL-6 cytokine, LIF (2ng/mL), which is known as an activator of STAT3. Our results show that LIF significantly ($p<0.001$) induced Y705-STAT3 phosphorylation. Interestingly, the co-treatment of cells with LIF and PD98059, whereby the latter decreases S727 phosphorylation (according to the results of section 1.1), induced a further significant increase in Y705-STAT3 phosphorylation compared to the treatment with LIF alone **Fig. 31.**

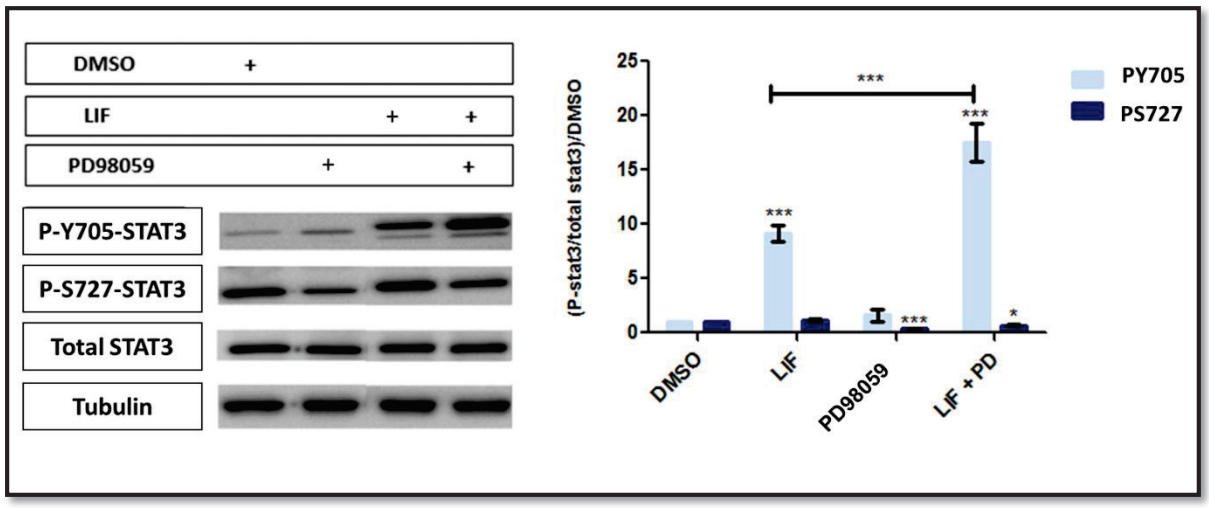

Figure 31. The competitive relationship between PY705 and PS727 STAT3

Western Blot analysis of PY705- and PS727- STAT3 levels in H9C2 cells following LIF (2ng/mL), and/or PD98059 (30µM) treatment. * P<0.05 *** P<0.005

In conclusion, our *in vitro* results report two major interlinking kinases with STAT3: the ERK1/2 and p38 MAPKs. ERK 1/2 regulates S727 STAT3 phosphorylation, while p38 MAPK regulates phosphorylation of both residues. The IL-6 family member, LIF, activates STAT3 through stimulating its Y705 phosphorylation. Moreover, a competitive relationship seems to exist between Y705 and S727 STAT3 phosphorylation **Fig. 32**.

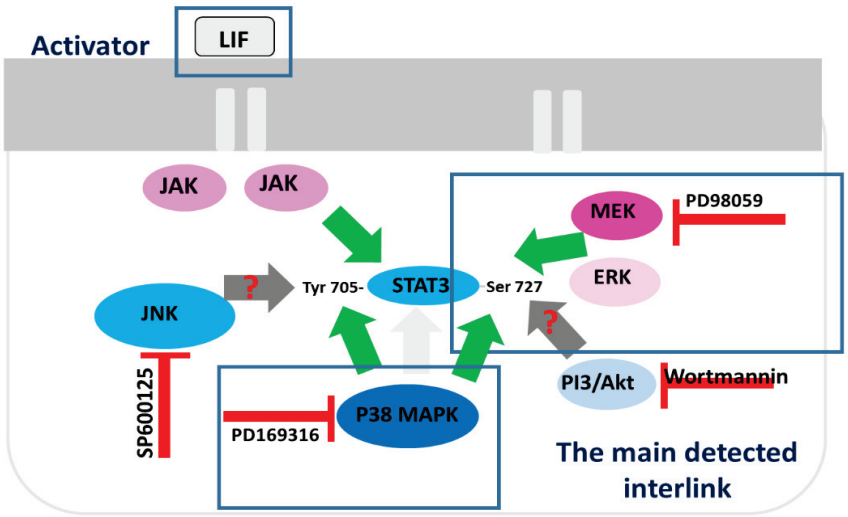

Figure 32. The in vitro interlink between STAT3 and MAPKS
A representative scheme of the in vitro results showing the main interlink between STAT3 and MAPKS in H9C2 cells.

2. The in vivo Kinetics and Correlation during I/R and IPoC

In order to study the kinetics of phosphorylation of STAT3, Akt and the MAPKs, C57bl/6J mice were subjected to 45 mins of ischemia followed by 15mins, 3hours and 24 hours of reperfusion. This was applied in the presence or absence of IPoC **Fig. 33**. The Sham operated mice were used as a control for the ischemic surgery effect. The areas at risk were collected and analyzed by western blotting and the following results were obtained (n=8/condition). In addition, the samples from areas remote to the AARs were also collected.

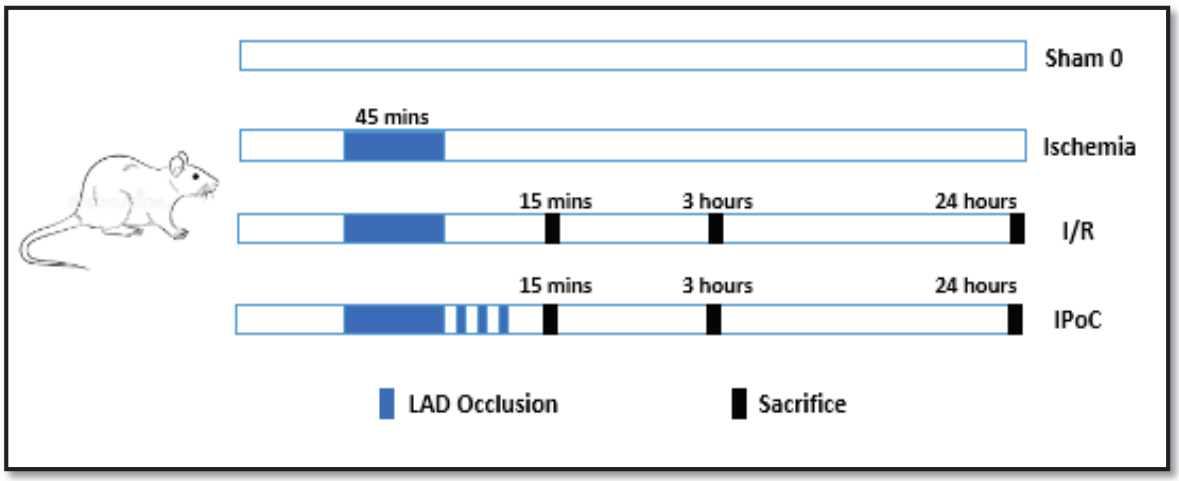

Figure 33. Representative scheme of the different in vivo conditions

2.1. Kinetics of Phosphorylation of STAT3 following I/R and IPoC

Applying ischemia, solely, had no significant effect on STAT3 phosphorylation in comparison to the sham group. However, the early (15 minutes) reperfusion of the ischemic area induced a significant increase in PY705-STAT3 ($P<0.05$) and PS727-STAT3 ($P<0.001$). The application of IPoC had no additional effect on PS727-STAT3, but it induced a significant ($P<0.05$) increase in PY705-STAT3 which lasted up to 3hours of reperfusion **Fig. 34**. The prolonged reperfusion up to 24 hours had no significant effect on the phosphorylation of both residues even when IPoC was applied. Thus, a short period of reperfusion is required to activate STAT3, and IPoC only targets Y705-STAT3 phosphorylation.

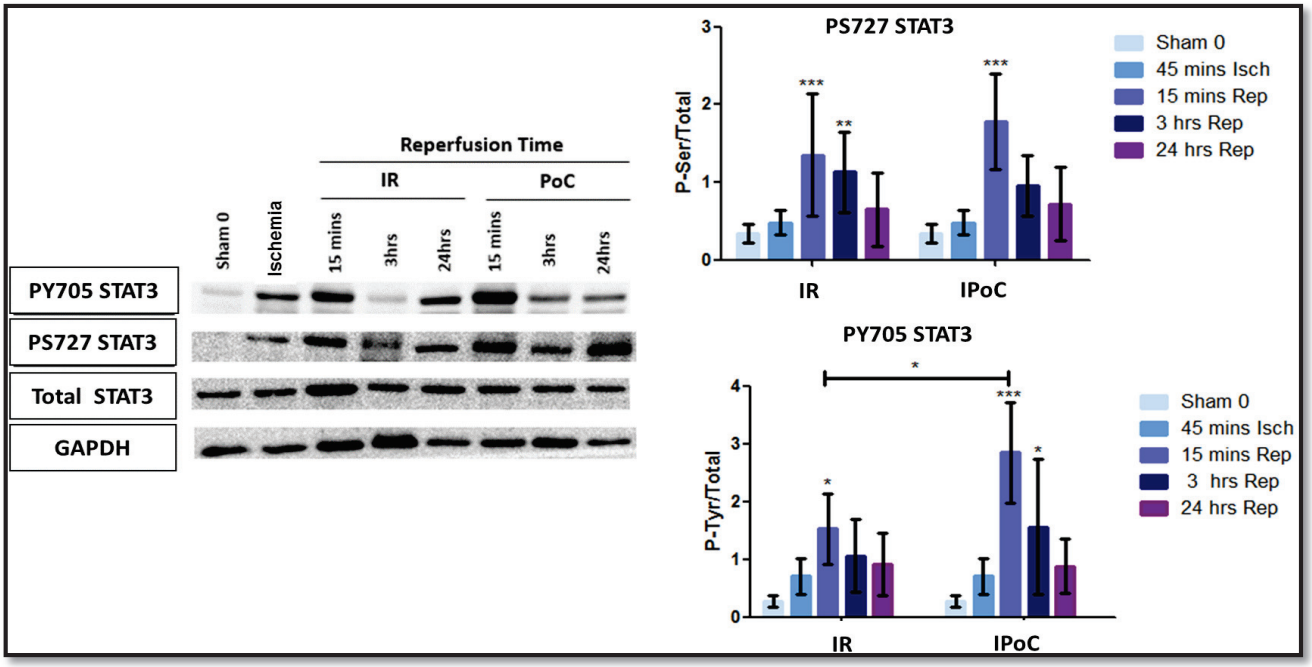

Figure 34. Kinetics of variation in STAT3 phosphorylation level following I/R and IPoC

Western Blot analysis of the phosphorylation levels of Y705 and S727 STAT3 in C57bl/6J mice following 15mins, 3hrs and 24 hrs of reperfusion under I/R and IPoC conditions (n=8).
* P<0.05 **P<0.01 *** P<0.005

2.2. Kinetics of Phosphorylation of ERK1/2 MAPK following IR and IPoC

Applying ischemia, solely, had no significant effect on ERK1/2 phosphorylation in comparison to sham hearts. However, ERK1/2 phosphorylation was significantly induced ($p<0.001$) within 15 minutes of reperfusion following ischemia. The application of IPoC had no additional effect on ERK phosphorylation in comparison to I/R alone. As for the prolonged reperfusion up to 24 hours, no pronounced effect on the ERK1/2 phosphorylation was observed **Fig. 35**. Thus, similarly to STAT3 activation, a short period of reperfusion activates ERK, and IPoC doesn't have an additive effect on ERK activation.

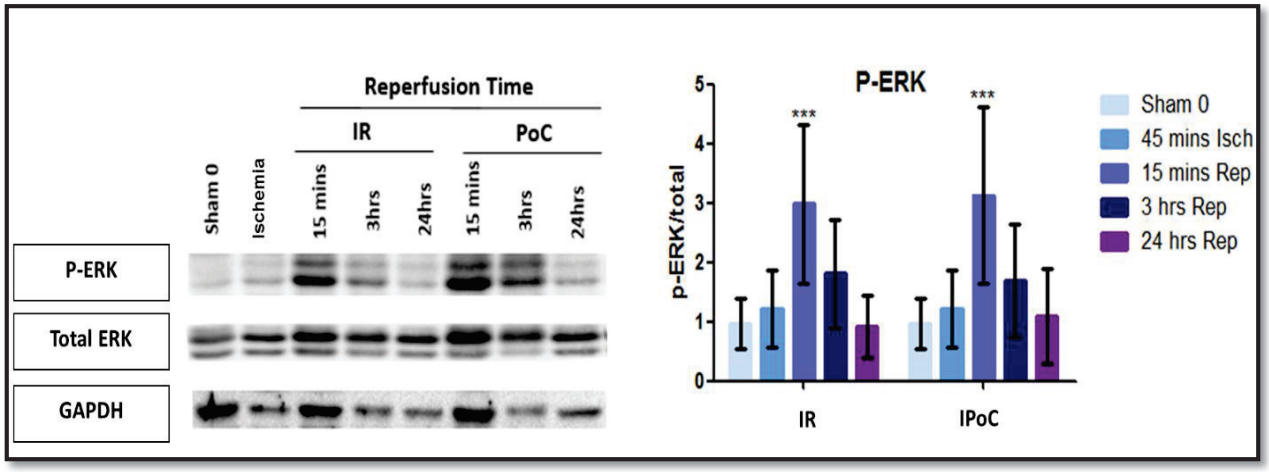

Figure 35. Kinetics of variation in ERK1/2 phosphorylation levels following I/R and IPoC

Western Blot analysis of the phosphorylation levels of ERK1/2 in C57bl/6J mice following 15mins, 3hrs and 24 hrs of reperfusion under I/R and IPoC conditions (n=8). *** P<0.005

2.3.Kinetics of Phosphorylation of the MAPKs JNK and P38 during IR and IPoC

Following ischemia, the phosphorylation levels of JNK and p38 MAPKs had no significant variation following short or prolonged reperfusion, in the presence or absence of IPoC. However, ischemia on its own induced a significant increase in p38 MAPK phosphorylation **Fig. 36.**

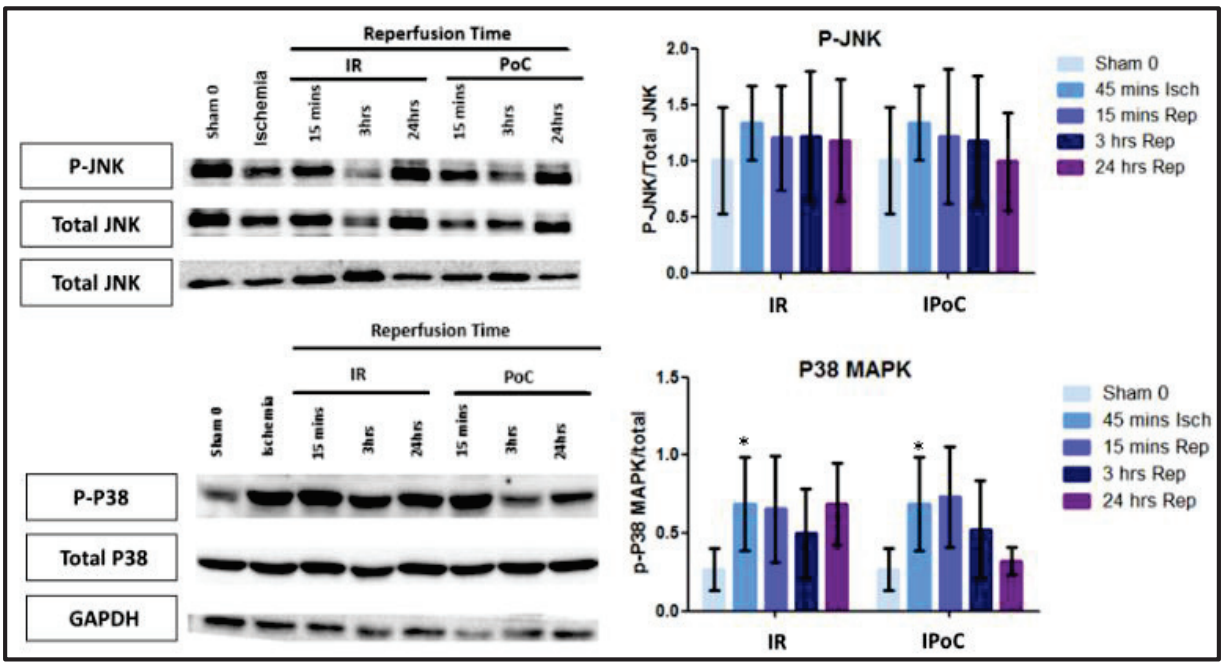

Figure 36. Kinetics of variation in JNK and P38 phosphorylation levels following I/R and IPoC

Western Blot analysis of the phosphorylation levels of JNK and P38 in C57bl/6J mice following 15mins, 3hrs and 24 hrs of reperfusion under I/R and IPoC conditions (n=8).

2.4. Kinetics of Phosphorylation of Akt during IR and IPoC

Applying Ischemia alone had no significant effect on S437-Akt phosphorylation in comparison to sham hearts. The reperfusion of the ischemic area for 15 minutes induced a significant ($p<0.05$) increase in the level of P-S437-Akt. This level, however, was not affected by reperfusion for 3 or 24 hours. The application of IPoC induced a shift in the phosphorylation timing of S437-Akt, whereby a significant ($p<0.001$) increase in PS437-Akt level was observed after 24 hours of reperfusion following IPoC **Fig. 37**.

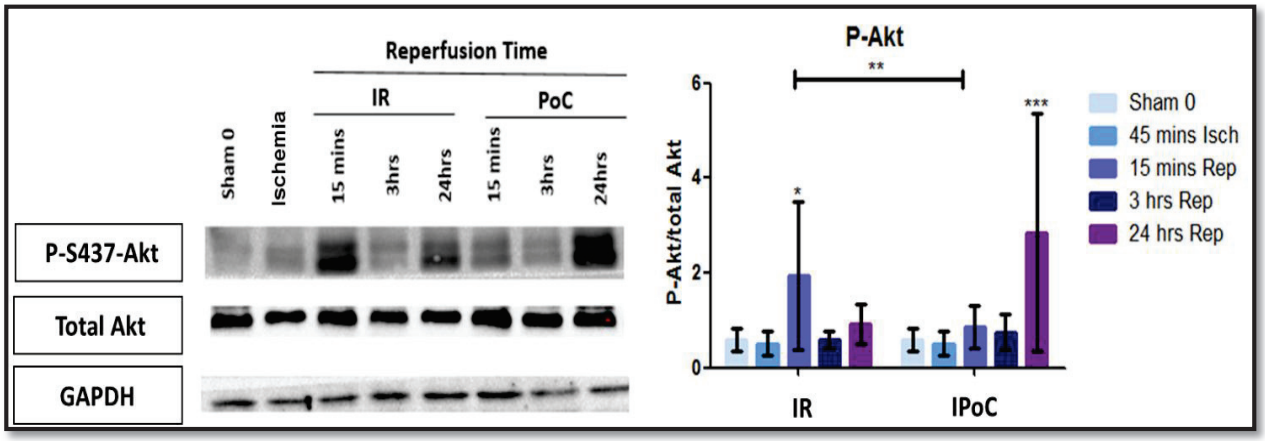

Figure 37. Kinetics of variation in Akt phosphorylation levels following I/R and IPoC

Western Blot analysis of the phosphorylation levels of Akt in C57bl/6J mice following 15mins, 3hrs and 24 hrs of reperfusion under I/R and IPoC conditions (n=8). * P<0.05 **P<0.01 *** P<0.005

2.5. The *in vivo* ratios of PS727/PY705 following IR and IPoC

The *in vitro* results suggested a competitive relationship between S727 and Y705 STAT3 phosphorylation, where a decrease of one phosphorylation level was accompanied with an increase of the other.

Moving to the *in vivo* results, we have seen that the phosphorylation levels of both residues increased within 15 minutes of reperfusion following ischemia. The application of IPoC induced a further increase in Y705 phosphorylation, with no pronounceable effect on S727 phosphorylation. This might indicate that the observed increase in S727 phosphorylation during IR, which is higher and more significant than the Y705 phosphorylation, prevented the higher increase in Y705 phosphorylation level. To investigate this pattern, the ratios of PS727/PY705-STAT3 were calculated following IR and IPoC **Fig. 38**. Our results show a significant decrease in the PS727/PY705-STAT3 ratios at 15 minutes and at 3 hours of reperfusion following IPoC, which indicates that IPoC is favoring the Y705 phosphorylation of STAT3.

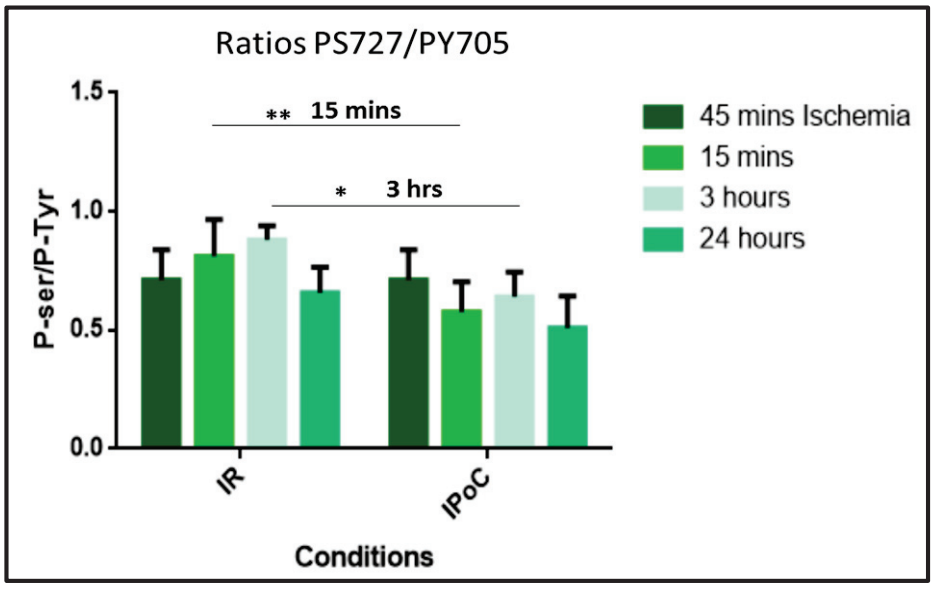

Figure 38. The ratios of phosphorylation levels of S727-STAT3 to Y705-STAT3

The ratios of the phosphorylation levels of S727 and Y705 STAT3 residues following IR and IPoC. *p<0.05 **p <0.01.

In conclusion, the *in vivo* results show that the early reperfusion of the ischemic area following a 45 mins ischemia activates STAT3, ERK and Akt phosphorylation, but it has no significant effect on JNK and p38 MAPKs phosphorylation. The application of the IPoC protocol induces a significant increase in STAT3 phosphorylation at its Y705 residue, but it provoked no additive increase in S727-STAT3 or ERK1/2 phosphorylation levels.

Following up the kinetics of variation of STAT3, Akt and the three MAPKs shows that the phosphorylation levels of STAT3 and ERK1/2 time-dependently correlate during I/R and IPoC, whereby p-ERK and p-STAT3 levels slightly increase following the ischemic insult, highly and significantly increase to peak at 15 minutes of reperfusion and finally decrease back to the initial levels following 3 and 24 hours of reperfusion **Fig 39**.

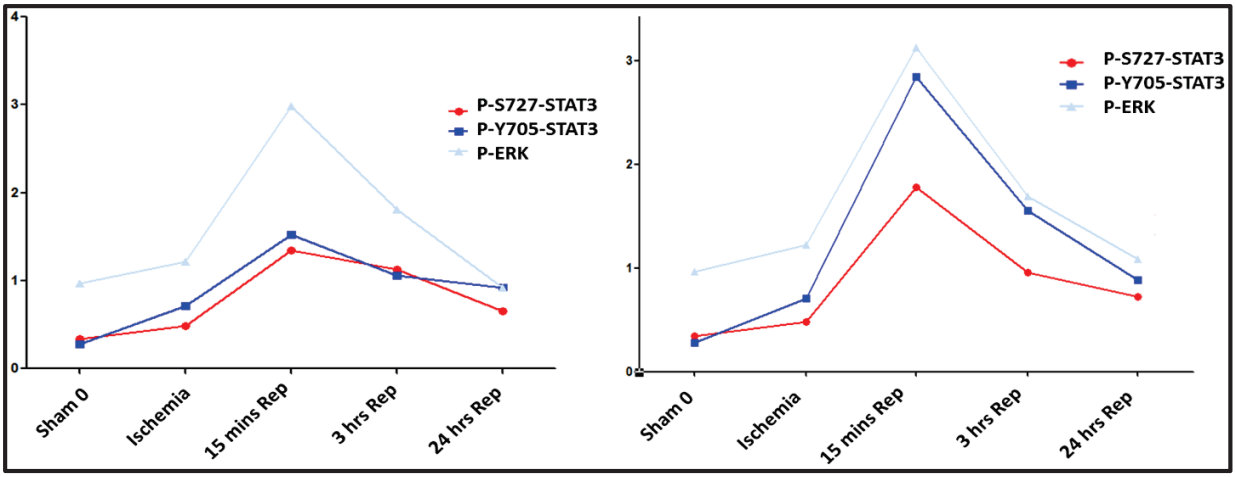

Figure 39. Representative plots for the kinetics of phosphorylation of STAT3 and ERK1/2 under I/R and IPoC

The representative plots for the kinetics of phosphorylation of STAT3 and ERK1/2 following I/R and IPoC showing that STAT3 and ERK1/2 follow common phosphorylation profile, whereby they peak at 15 mins at decrease back to around the basal level within 24 hours.

Overall, the results presented above, on both the *in vitro* and the *in vivo* levels, point toward an interlink and a correlation between the MEK-ERK pathway and STAT3, precisely PS727-STAT3. The *in vitro* results suggest a competitive relationship between S727 and Y705 STAT3 phosphorylation, while the *in vivo* results clearly show that IPoC is favoring Y705 phosphorylation of STAT3 but not S727 phosphorylation. This suggests that Y705 phosphorylation is necessary for the IPoC-mediated STAT3-dependent cardioprotective effects, which was then validated through modulating the phosphorylation of STAT3 at Y705 residue during IPoC.

As a transcription factor, STAT3 is activated through the Y705 phosphorylation. However, few reports have highlighted the involvement of S727 phosphorylation in its transcriptional activity. Keeping in mind that ERK inhibition decreases S727 STAT3 phosphorylation and that IPoC induces Y705-STAT3 phosphorylation, and having in our hands validated inhibitors for Y705-STAT3 and ERK1/2 phosphorylation, we moved to question how the inhibition of Y705-STAT3 or ERK1/2 phosphorylation modifies the transcriptional activity of STAT3 following I/R and IPoC. We hereby move, in the upcoming part of the results, from the signaling level to the genomics one **Fig. 40.**

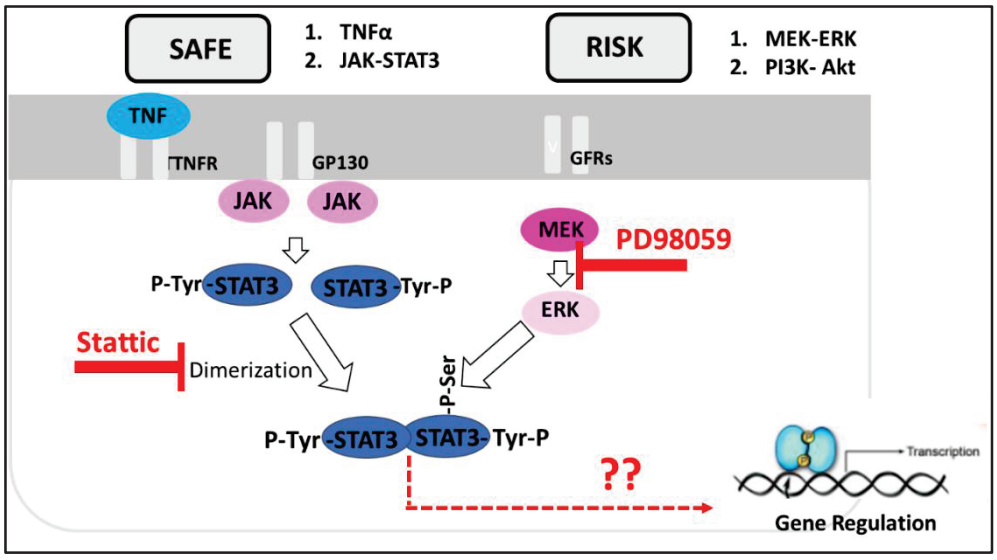

Figure 40. The investigation of STAT3's transcriptional activity under inhibitory conditions.

An illustration showing the use of the STAT3 inhibitor Stattic and the MEK/ERK inhibitor PD98059 for the investigation of STAT3's transcriptional activity.

Part II. Genomics

In an attempt to study the transcriptional activity of STAT3 during I/R and IPoC following the inhibition of ERK1/2 or Y705-STAT3 phosphorylation, C57bl/6J mice were treated with PD98059 (ERK 1/2 inhibitor), Stattic (Y705-STAT3 inhibitor) or DMSO (Vehicle) during I/R or IPoC. In the upcoming paragraphs, PD98059 will be sometimes referred to as PD only.

In these experiments, different samples were collected for different assessments **Fig. 41**:

- Following 15 minutes of reperfusion, AARs were collected and analyzed by WB to validate the inhibitory effect of the used doses (n=3/condition).
- Following 3 hours of reperfusion (choice of this duration is explained below), AARs were collected for the analysis of gene expression by PCR (n=5/condition). Moreover, plasma was also collected for ELISA analysis.
- Following 24 hours of reperfusion, AARs were collected for the determination of the necrotic areas (n=5/condition).

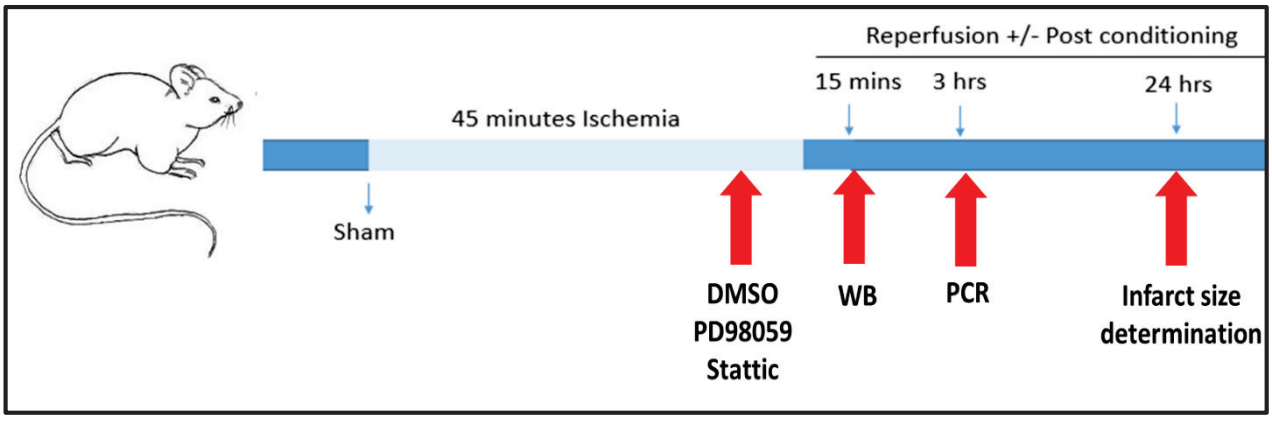

Figure 41. Representative scheme of the in vivo experiments of the genomics section

The *in vivo* experiments of the genomics section, described above, were performed in parallel with a transcriptomic study conducted to perform a dynamic transcriptomic analysis following IR (another study in our team). This study aimed to determine the gene expression profiles following different durations of ischemia and reperfusion and thus determines which genes are significantly induced by ischemia or reperfusion and at which time point. In our current work, the choice of the time point at which gene expression was studied by PCR (3 hours) was based on this study (choice of time point explained in the coming parts) **Fig.42**.

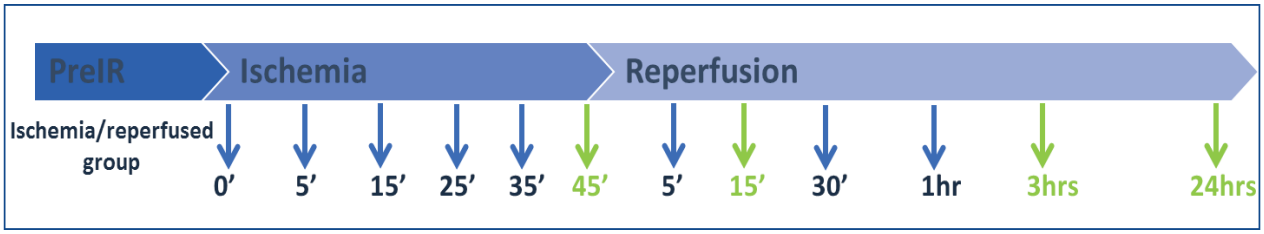

Figure 42. The time points of the dynamic transcriptomic analysis

The different time points at which the samples were collected for studying the gene expression profiles. The green arrows indicate the common time points with our current study.

1. In vivo Drug Efficiency

In order to validate the used inhibitors' doses and investigate if ERK1/2 inhibition modifies STAT3 phosphorylation, mice were subjected to ischemia followed by 15 minutes of reperfusion in the presence of DMSO, Stattic and PD98059. Western blot analysis was then performed on the collected AARs to determine the phosphorylation level of Y705-STAT3 and ERK ½. Although non-significant (n will be increased to ensure significance), our results show that the approximate inhibition of ERK1/2 phosphorylation by PD98059 was 50%, while that of Y705-STAT3 phosphorylation by Stattic was 40% **Fig. 43.** Interestingly, the *in vivo* ERK1/2 inhibition also inhibited both Y705-STAT3 and S727-STAT3 phosphorylation. This indicates that, unlike to what was observed on the *in vitro* level, ERK1/2 also regulates the *in vivo* Y705 STAT3 phosphorylation. Thus, an ERK1/2-dependent STAT3 transcriptional activity is expected to exist.

Noteworthy, this 40% inhibition in the phosphorylation levels detected in the AAR lysates is not assumed to be the same in the different cellular populations of the heart. In this regard, endothelial cells are expected to receive the highest amount of the injected drug due to their presence at the lining of the blood vessels. Thus, the observed inhibitory effects could more likely be due to the regulation of STAT3 and ERK1/2 majorly in endothelial cells.

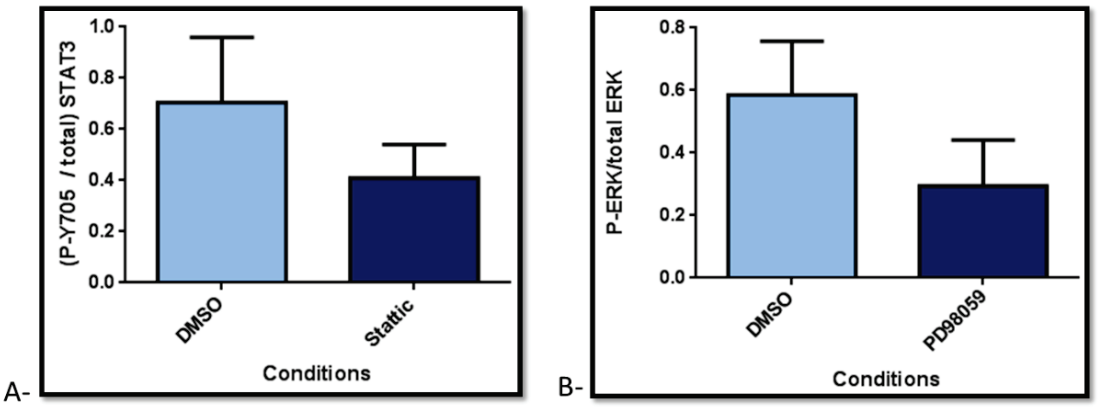

Figure 43. The in vivo validation of the inhibitors doses

Bar graphs representing the normalized ratios of PY705-STAT3 (A) and P-ERK (B) under DMSO, Stattic or PD98059 treatment in C57bl/6J mice subjected to Ischemia followed by 15 mins of reperfusion.

2. Necrotic Area Determination

In order to determine if the inhibitors can diminish the protective effect of IPoC, mice were injected with DMSO, Stattic and PD98059 before the application of IPoC. As a control for the IPoC with DMSO vehicle, a group of mice was injected with DMSO and subjected to I/R. Although very weak, a tendency of decrease in the infarct size upon applying IPoC in the presence of DMSO vehicle is observed. This tendency of decrease was lost in the presence of Stattic and PD98059. The experiment will be further repeated up to n=10 per condition to ensure reproducibility and significance **Fig. 44**.

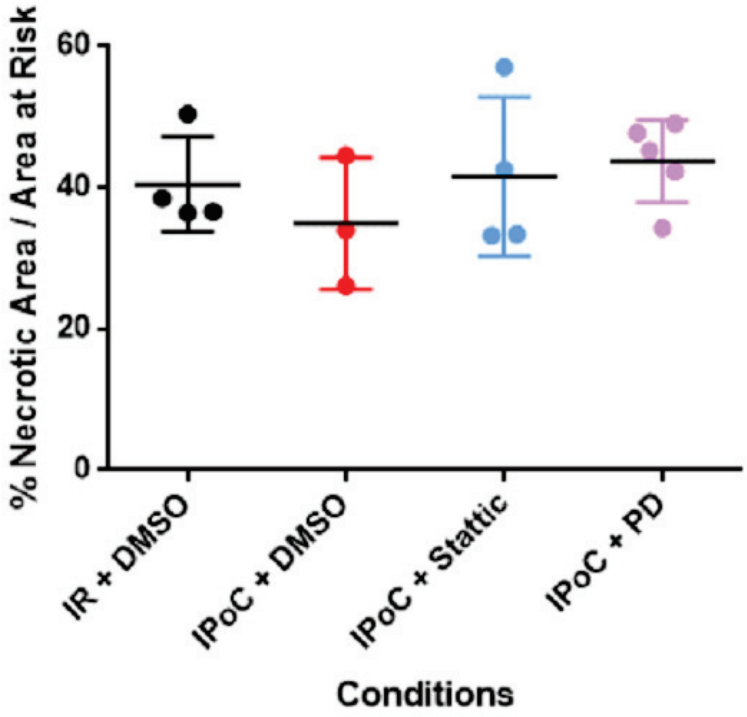

Figure 44. Percentages of necrotic areas to healthy areas under different conditions

The percentage on necrotic area to the total areas at risk following 24 hours of reperfusion in C57bl/6J mice subjected to I/R and injected with DMSO, or subjected to IPoC and injected with DMSO, Stattic or PD98059.

3. Gene Analysis

In order to investigate the transcriptional activity of STAT3 by PCR, a literature screening was done and 479 STAT3-regulated genes were selected. These genes were then screened in the gene data base built from of the transcriptomic study described above. This data base retrieved the group of genes, out of the total mouse genome, that significantly varied following different durations of reperfusion.

Out of the 479 selected genes, 142 were found to be significantly varying at different time points following reperfusion in our MI mouse model. The next step was to choose the time point at which gene expression should be measured, along with selecting a group of genes whose expression is to be measured at this selected time point.

3.1. Selection of time point

Having retrieved 142 significant genes, we aimed to select the time point (15mins, 3hrs or 24 hrs) at which the majority of the selected genes vary. DESeq2 statistical package was therefore used, whereby LRT test was performed and a principal component analysis (PCA) plot was obtained **Fig. 45**. The PCA plot, which clusters together the genes varying with a common feature, showed that the genes were clustered by their temporal variation. In this variation, the 3 hours of reperfusion corresponded to the highest significant variation in the data. Thus, 3 hours was the chosen time point for PCR analysis.

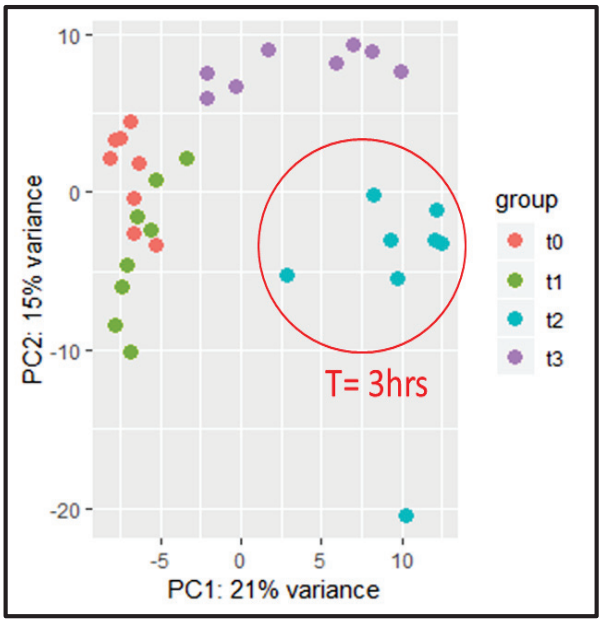

Figure 45. PCA plot of STAT3-induced genes clustered over time

The PCA plotting showing the clustering of genes at different time points. The t0 corresponds to 45 minutes ischemia, while t1, t2, t3 respectively correspond to 15 minutes, 3hours and 24 hours of reperfusion.

3.2. Selection of genes

Having chosen 3 hours as the best time point, we moved to select the genes that vary at 3 hours out of the total 142 genes. To achieve this, we used an algorithm that enables us to cluster and visualize the genes based on their similar behavior over time (based on the similarity of their expression profiles). Thus, STEM analysis was used and yielded different temporal profiles **Fig. 46**. Interestingly, many profiles had a significant variation at 3 hours following reperfusion. Thereafter, we selected 50 genes from the profiles containing the highest number of significant genes and varying at 3 hours.

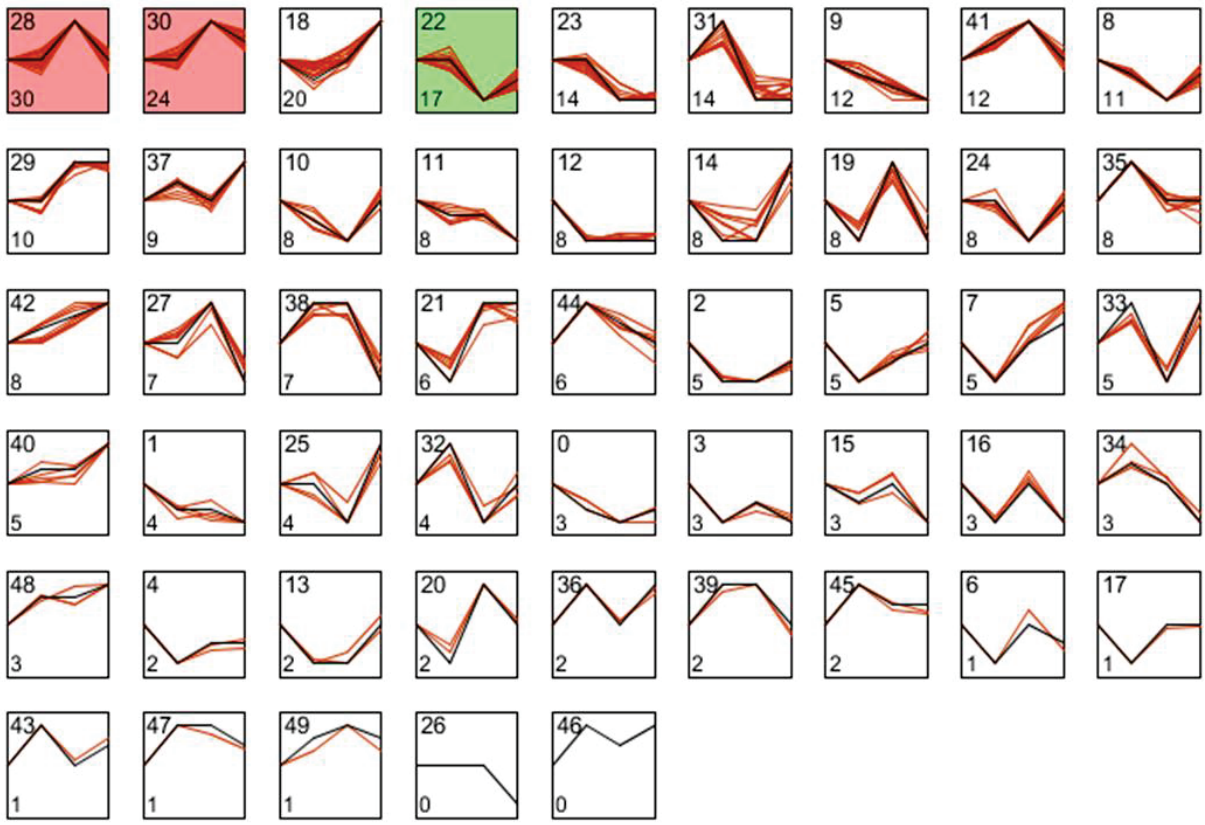

Figure 46. STEM analysis clustering profiles at the different time points

The different profiles showing the variation in genes expression at different time points (45mins isch, 15mins rep, 3 hrs reperfusion, 24 hrs reperfusion). The numbers on the top and bottom left of the clusters respectively correspond to the clusters name/ID and number of genes assigned to each cluster.

3.3. Significant STAT3-dependent genes

Out of the 50 selected genes, 42 were screened by PCR to determine their expression levels following I/R and IPoC, in the presence of DMSO, Stattic and PD98059. Following the statistical analysis of the normalized expression levels, we obtained different groups of significant genes. We targeted the genes that varied upon applying IPoC in comparison to IR, since we were interested in studying the transcriptional activity of STAT3 activated by IPoC. A total of 21 significant genes was retrieved, among which 12 genes were varying under Stattic treatment, while 8 genes were varying under PD treatment (one common gene with the stattic-dependent genes). The next step was the gene enrichment analysis to check biological functions in which these genes are involved.

3.4. Significant STAT3-dependent genes

In order to determine the biological functions which could be regulated by the retrieved genes, STRING data base was used. As mentioned before, the input for this data base is the Stattic-varying genes or the PD-varying genes, while the output is the GO terms assigned to the given genes. In addition, STRING also gives us the connections (interactions) between the proteins encoded by these genes and predicts further interactions and networks. Every new predicted network is referred to as a "shell".

In our data, we had two lists of input: The Stattic-varying genes and the PD98059-varying genes. After entering our gene lists in STRING, we collected the list of GO terms (with FDR < 0.005) from the first 4 predicted shells (networks) in order to cover a wide range of predicted interactions that might be affected by the injected inhibitors. Following the collection of the significant GO terms from 4 shells, we had to choose the first shell covering the widest range of GO terms but marking saturation in the number of added GO terms. For achieving this, we calculated the percentage homology between the GO terms of every two successive shells and finally chose the shell with the highest percentage homology (this shell marks the shell after which

fewer GO terms are added). Shell 3 (290 GO terms) was chosen for the Stattic-dependent genes, while shell 4 (492 GO terms) was chosen for PD-dependent genes. Following the shell selection, we retrieved the two lists of GO terms and compared them to retrieve the common ones. By retrieving the common GO terms (190 GO terms) separately, we obtained a strictly Stattic-dependent list of GO terms (100 GO terms independent of PD98059) and a strictly PD98059-dependent list of GO terms (302 GO terms independent of Stattic). The high number of common GO terms (190) interestingly highlights the prominent co-regulation of biological processes by STAT3 and the ERK1/2 pathway, which is a consequence for the regulation of Y705 STAT3 phosphorylation downstream ERK1/2 (which we reported above).

These lists of GO terms were finally sorted and categorized into families of biological functions, expressed as percentage of the total GO terms. Our results show that besides signaling, Stattic-dependent GO terms were categorized into development (29%), inflammation (15%), metabolism (12%) and other minor processes **Fig. 47**.

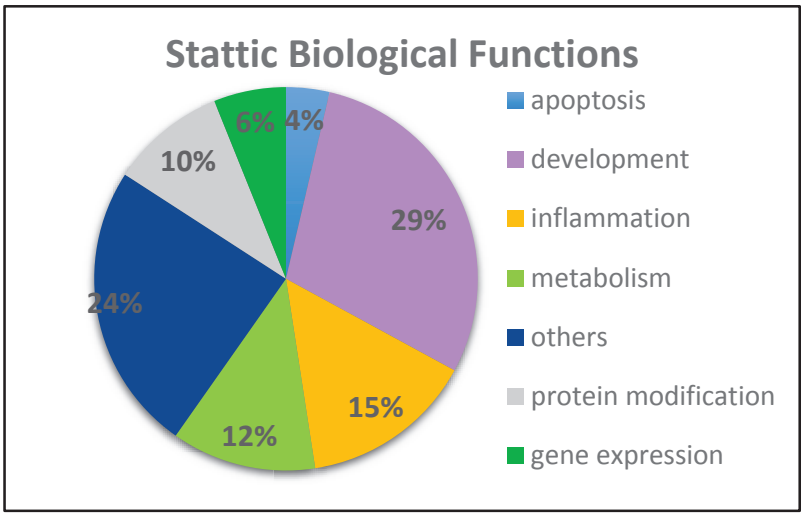

Figure 47. The families of biological functions for Stattic-dependent genes.

Pie chart showing the percentages of biological functions in which the retrieved Stattic -dependent genes are involved.

As for the PD98059-dependent GO terms, they were categorized into development (25%), inflammation (22%), metabolism (13%) and other functions **Fig. 48**.

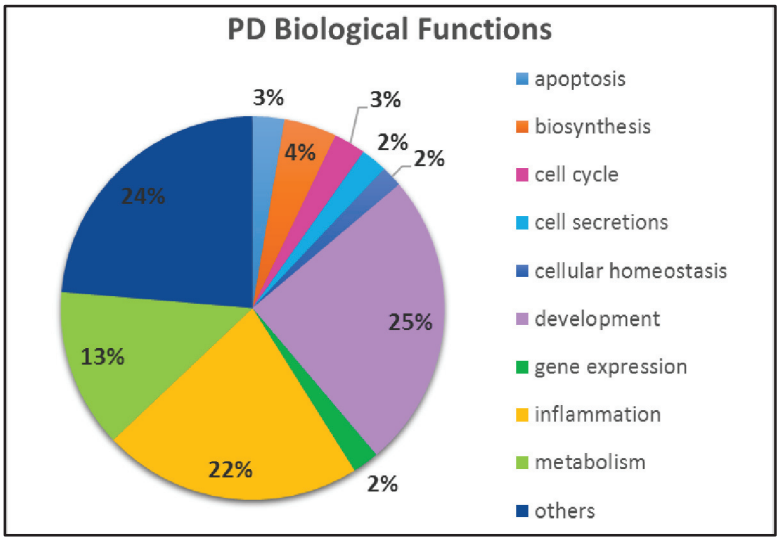

Figure 48. The families of biological functions for PD-dependent genes

Pie chart showing the percentages of biological functions in which the retrieved PD-dependent genes are involved

Moving to the co-dependent GO terms, they were categorized into development (28%), metabolism (22%), inflammation (11%) and other functions **Fig. 49**

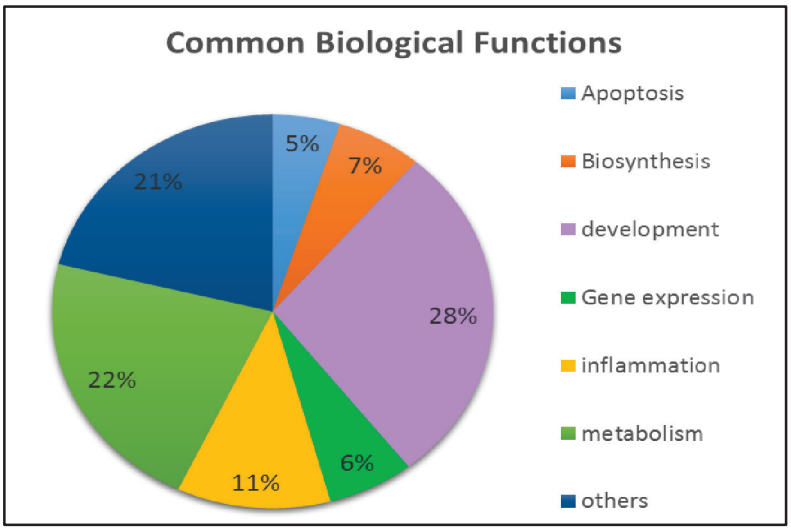

Figure 49. The families of biological functions of the common GO terms

Pie chart showing the percentages of biological functions of the GO terms which are commonly shared between Stattic- and PD- dependent genes.

3.5. Inflammatory approach

After obtaining several major biological families through the analysis shown above, we moved to choose a biological family and validate how STAT3 is involved in its regulation. Among the different major biological families, inflammation grasped our attention and focus. The choice of inflammation relied on two major reasons. First, as mentioned in the introduction, inflammation is a prominent hallmark of the IRI and is thus a target for protection. In this context, it is unknown if IPoC can regulate the inflammatory response in a STAT3-dependent manner. Second, STAT3 is considered an important key player in inflammation through mediating the inflammatory cytokine signaling, regulating neutrophils/macrophages recruitment and participating in macrophages polarization. However, no previous reports have studied the inflammatory roles of STAT3 from a cardioprotective approach (during IPoC).

Interestingly, taking a closer look at the Stattic-dependent GO terms grouped in the inflammation family of biological functions, we found that they are linked to the positive regulation of chemokine production and chemotaxis, in addition to a positive link with cellular migration and endothelial adhesion. However, the PD-dependent inflammatory GO terms were mostly linked to the proliferation, activation and differentiation of immune cells, in addition to the negative regulation of chemokine production and adhesion. This suggests that the Y705-STAT3 phosphorylation, activated by IPoC, is involved in the regulation of inflammation through regulating chemotaxis and inflammatory cells migration, while ERK1/2 activation is involved in regulating the activation and proliferation of the inflammatory cells, in addition to cytokine synthesis. As for the common GO terms, they were linked to cytokine signaling and cell migration. This indicates that each of STAT3 and ERK1/2 regulates its own inflammatory processes, but they have synergic roles in the regulation of cytokine signaling and cellular migration during inflammation.

Interestingly too, the shell of Stattic-dependent genes shows that STAT3 interacts with inflammatory-linked proteins such as IL-6, IL-10 and socs3 **Fig. 50**.

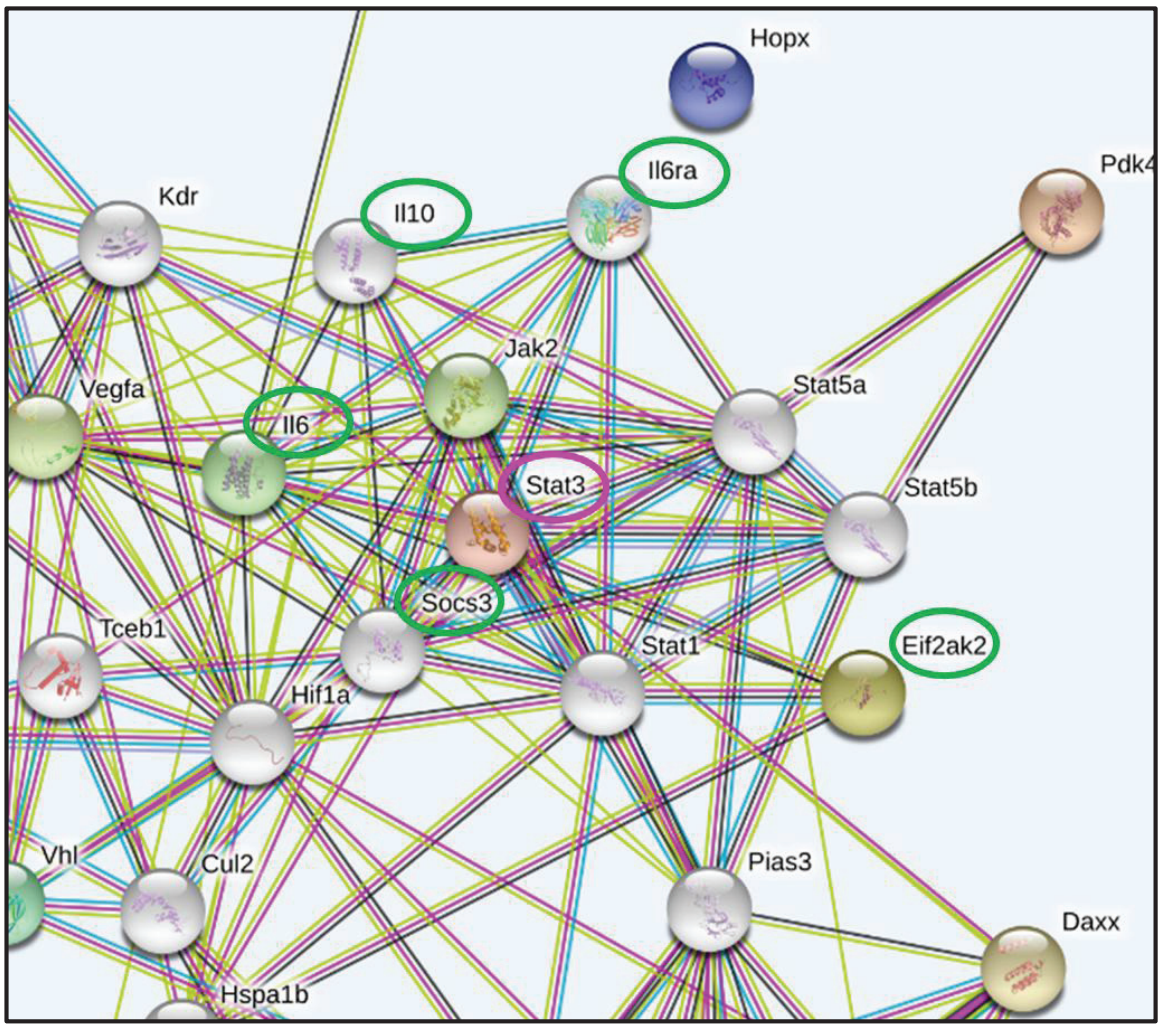

Figure 50. The Shell of interacting proteins obtained from Stattic-dependent genes.

The shell obtained from the entry of Stattic-dependent genes into STRING data base showing that STAT3 interacts with the inflammation-linked proteins IL6, IL-10, SOCS3 and Eif2ak2.

Having in mind that IPoC activates STAT3 through the Y705 phosphorylation, that Stattic-dependent genes are biologically involved in inflammation and that STAT3 is linked with various inflammatory molecules, we moved to investigate the STAT3-dependent gene expression of several pro- and anti- inflammatory cell markers/genes. This gene expression was studied under IR and IPoC, in the presence and absence of Stattic, which permits us to determine how does STAT3 regulate the inflammatory response during IPoC. Moreover, the expression was also studied under PD98059 treatment to detect any interference for ERK in the regulation of the selected genes.

These genes included:

A. STAT3-regulated genes induced by IL10.

They were collected from articles, which targeted the IL10-STAT3 axis during inflammation. They include socs3, bcl3, tnip3, etv3, hmox1, dusp1, gadd45b, tpl2.

B. Markers of macrophages: CD68 and F4
C. Markers of M1 macrophages: CD86 and CD80
D. Markers of M2 macrophages: CD206 (MRC1)
E. Markers of neutrophils: Ly6g and Lcn2
F. Neutrophils-recruiting chemokine cxcl-1
G. Inflammatory cytokines: IL6, IL1b and TNF

Our results show that under basal conditions (vehicle treatment), IPoC decreased the expression of the neutrophils marker ly6g, but it increased the expression of the M1 macrophages marker CD80, the pro-inflammatory cytokine IL-6 and STAT3 **Fig. 51**.

The inhibition of STAT3 by Stattic during IPoC induced a tendency of decrease in the expression of STAT3, but it increased the expression of the neutrophils-binding chemokine cxcl-1 (in comparison to vehicle) **Fig. 52**. In addition, the treatment with Stattic decreased the expression of M2 macrophages marker MRC1 during IPoC and also decreased and the expression levels of the two selected genes known to be regulated by the IL10-STAT3 axis (dusp1 and gadd45b).

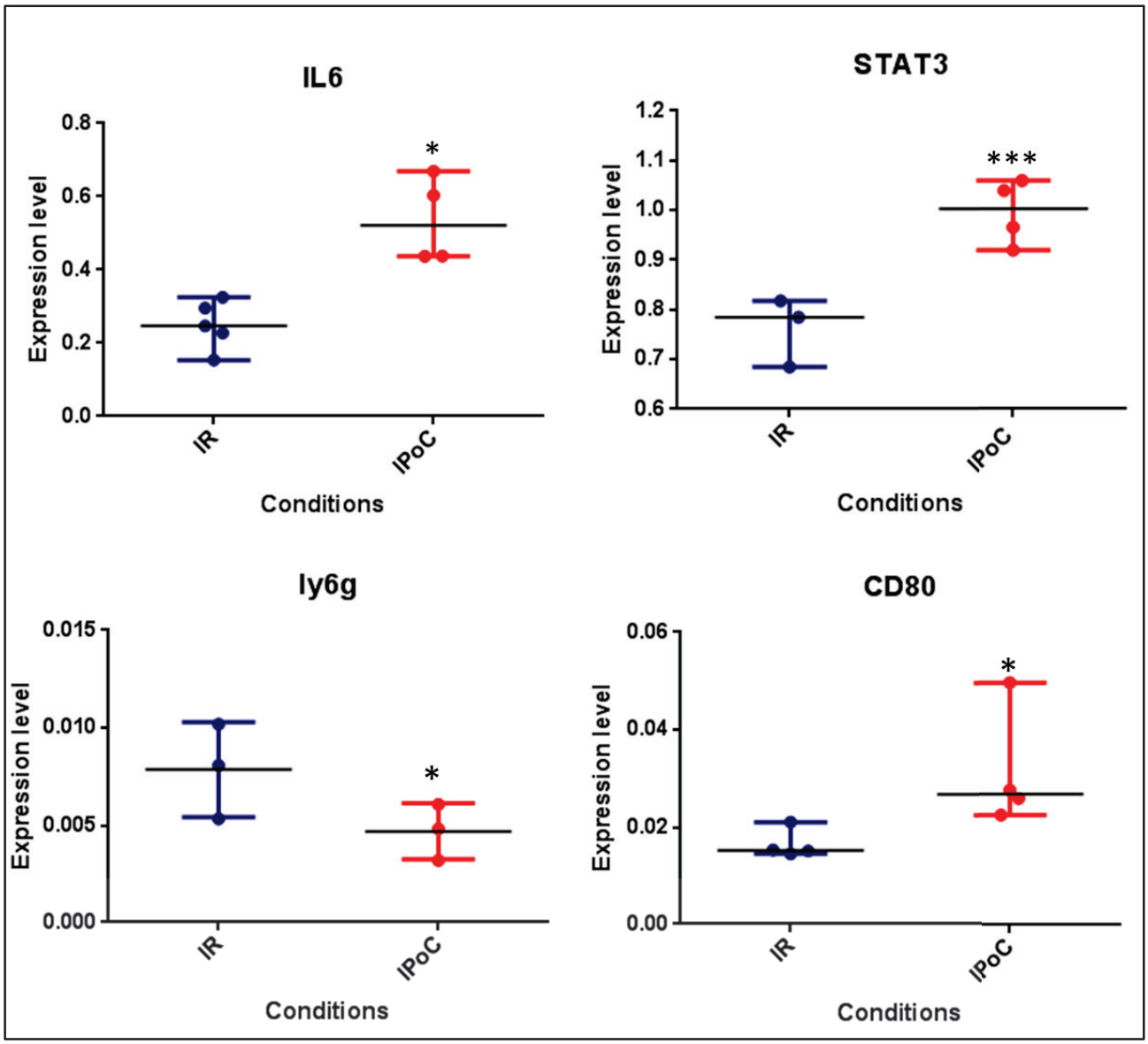

Figure 51. The expression levels of some inflammatory markers under DMSO treatment during IR and IPoC

The normalized expression levels of the inflammatory markers IL6, CD80 and Ly6g in addition to STAT3, measured by PCR following IR and IPoC under DMSO treatment.

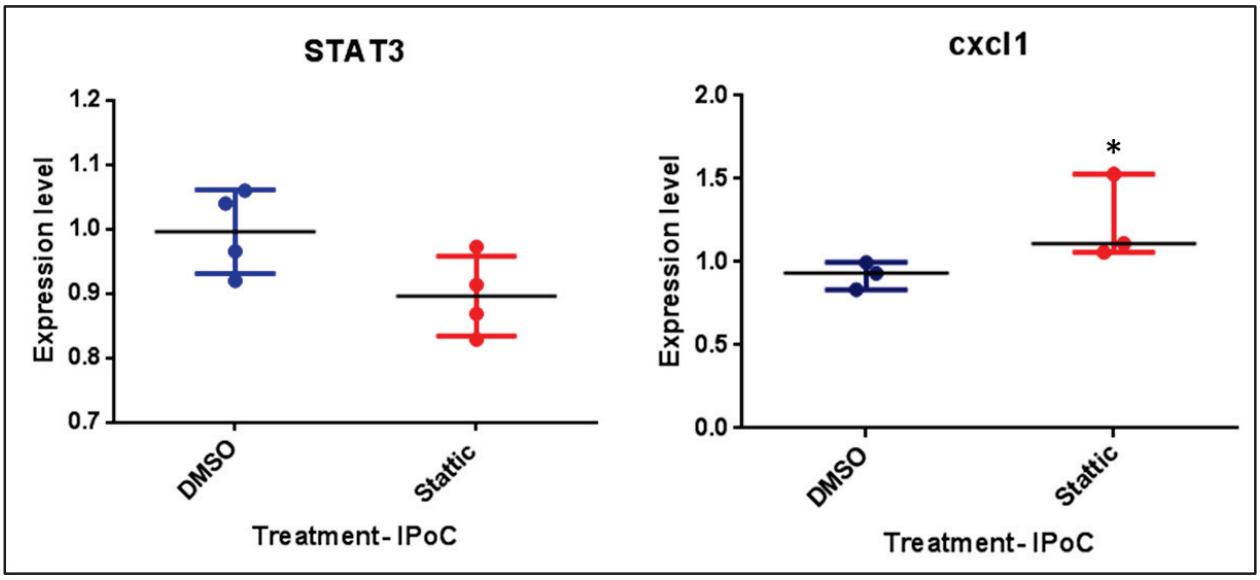

Figure 52. The expression levels of STAT3 and Cxcl-1 during IPoC, under DMSO and Stattic treatment

The normalized expression levels of STAT3 and cxcl-1, measured by PCR following IR and IPoC under DMSO treatment.

Moving to ERK1/2 inhibition, our results show that the treatment with PD98059 during IPoC decreased the expression levels of the STAT3 gene itself and the STAT3-regulated gene hmox-1. This regulation of STAT3 expression level by ERK1/2 emphasizes the interlink at the genomic level, in parallel to that seen at the signaling level .

In conclusion, our genomics results show that the selected STAT3-dependent genes significantly vary at 3 hours of reperfusion. The inhibition of Y705 STAT3 and ERK1/2 phosphorylation, respectively by Stattic and PD98059, induced a significant variation in the expression levels of several STAT3-dependent genes. The gene ontology analysis of these genes, followed by the retrieval of GO terms, pointed toward major biological families, among which inflammation lies. The study of the expression levels of the selected inflammatory markers showed that IPoC interferes in regulating inflammation through regulating the expression of IL-6, the polarization of macrophages and the recruitment of neutrophils. In addition, the results suggest that STAT3 interferes in regulating the inflammatory response during IPoC through regulating macrophages polarization and through regulating neutrophils recruitment in a cxcl-1 dependent manner.

In order to verify the above deductions, heart cells will be collected from hearts subjected to IR or IPoC (basal or treated with PD/stattic). The cellular populations will be screened for neutrophils and macrophages (M1 and M2) markers by flow cytometry. This will enable us to validate if IPoC indeed regulates neutrophils recruitment and macrophages polarization or not, and if STAT3 is interfering in these processes. Moreover, the plasma levels of IL6 and cxcl-1 will be measured at 3 and 24 hours of reperfusion following IR and IPoC, in the presence and absence of inhibitors. The troponin plasma levels will also be measured to validate the protective effect of IPoC.

In addition, since IPoC was previously shown to decrease neutrophils adherence to endothelial cells, we aim to measure the plasma levels of *v-cams* to investigate if IPoC might provoke a decrease in the expression of *v-cams* by endothelial cells leading to less neutrophils adherence. In the same context, since the inflammatory stattic-dependent GO terms pointed toward regulation of endothelial adhesion, we aim to investigate if STAT3 is involved in the expression of *v-cams* and *i-cams* by endothelial cells. To achieve this, endothelial cells will be treated with both an activator or an inhibitor of STAT3, after which the cells will be analyzed by flow cytometry for measuring the expression levels of *v-cams* and *i-cams*.

Section III: Collaborative work

In the cardiovascular field of research, different animal models have been used for different cardiac surgeries. Unfortunately, the surgery itself has been reported to trigger an important inflammatory response that might exacerbate the observed effect. Thus, a thorough characterization of the sham effect in the myocardium was performed, aiming to identify the interfering inflammatory reaction in order to avoid misinterpretation of the data via systems biology approaches. In this work, a comprehensive analytical pipeline of mRNA seq dataset and systems biology analysis were used to characterize the acute phase response of mouse myocardium at 0, 45 minutes and 24 hours after surgery in order to better characterize the molecular processes inadvertently induced in sham animals.

Statistically, this work showed that the surgical intervention, on its own, induced 1209 differentially expressed transcripts (DETs). In addition, the activation of signalization pathways was fingerprinted at 45 mins and the recruitment of neutrophils and the differentiation of macrophages was identified at 24 hrs (Data not shown). Moreover, a major role of the IL-6 pathway, the major upstream activator of STAT3, was revealed. In this regard, the retrieval of the transcription factors network by STRING showed that IL6 is a major central hub in this network **Fig. 53.**

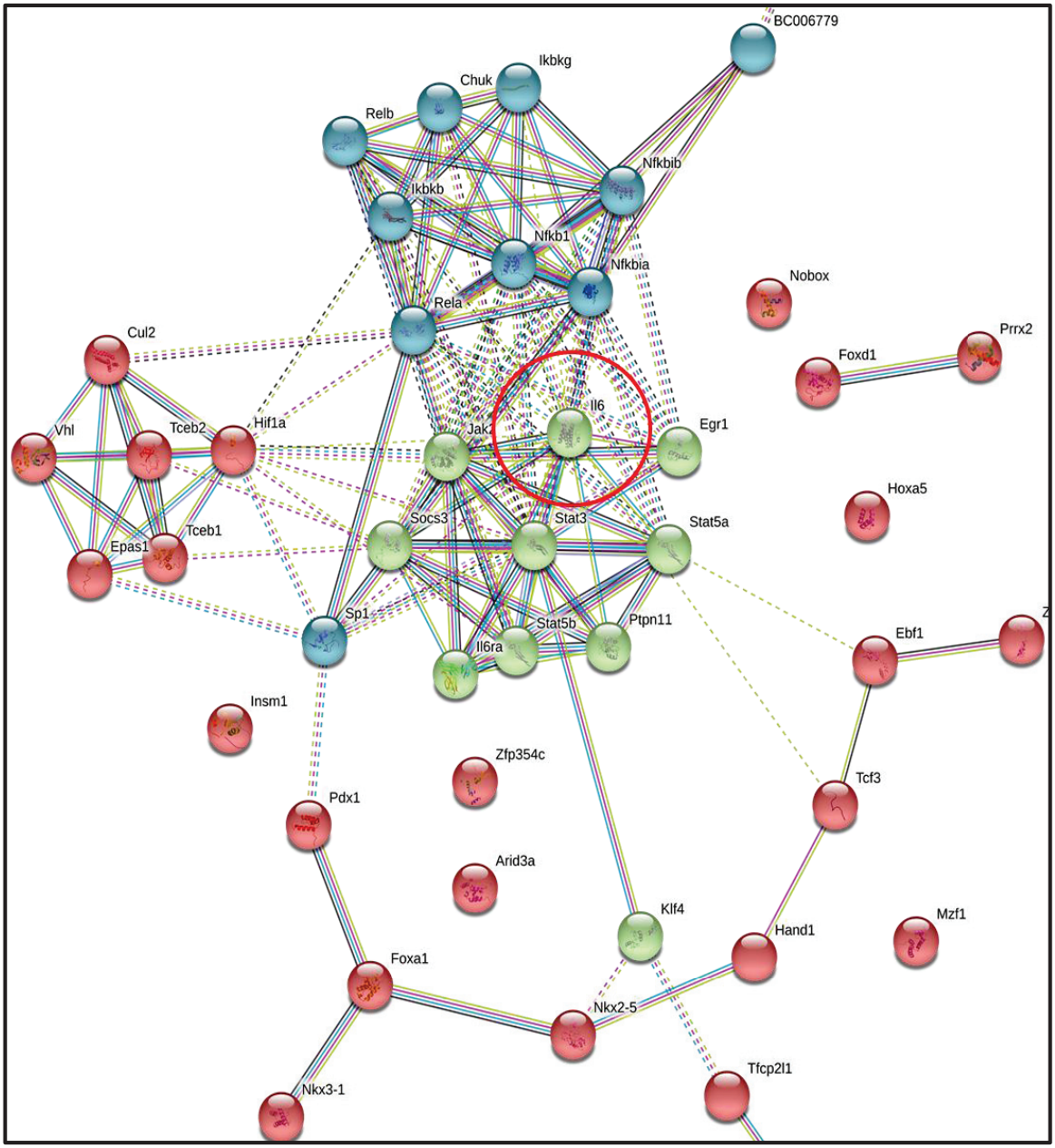

Figure 53. The network of transcription factors retrieved from the enrichment analysis of DEGs in the sham model

The network obtained from the input of the transcription factors, obtained from enrichment analysis of DETs in sham mice, into STRING. IL-6 can be observed as a central molecule in this network.

In order to biologically validate the observed IL-6 intervention, the levels of IL-6 were measured in the plasma collected 45 mins or 24 hours after the surgery. The results show that a significant increase is observed in circulating IL-6 at 45min after surgery **Fig. 54**.

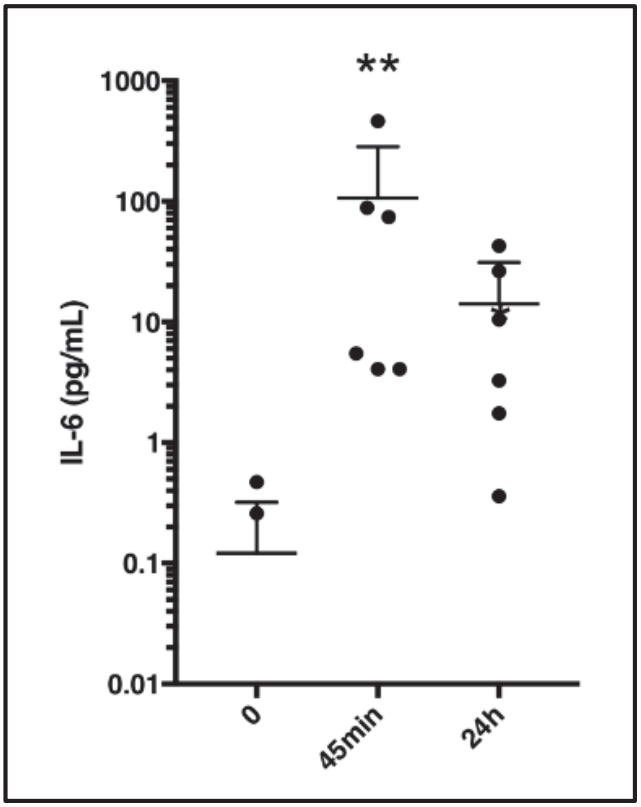

Figure 54. IL-6 increases in plasma of sham mice following 45 mins of surgery

The measurement of IL-6 levels in c57bl/6J mice following 45 mins and 24 hours of sham surgery shows a peaking in this level after 45 minutes of surgery.

The increase of IL6 level in plasma, observed following 45 minutes of surgery application, suggests that the surgery itself is inducing a systematic IL6-dependent effect. Having this observation in mind, we further investigated if the I/R injury similarly induces an IL6 augmentation in plasma. Interestingly, a rise in the IL6 level was observed within 5 minutes of reperfusion following I/R.

Since STAT3 is a major signaling molecule activated by Y705 phosphorylation downstream IL6, we questioned a systematic STAT3 activation by the circulating IL6. In other words, we investigated if STAT3 is not only locally activated in the AAR at 15 minutes of reperfusion (as we've shown in the kinetics part), but if it's also systematically activated in the remote area due to the release and the circulation of IL6.

The proposed investigation was realized through measuring STAT3 phosphorylation levels in the remote area following ischemia and 15 minutes of reperfusion. The results show that PY705-STAT3 levels are significantly increased in the remote area after 15 minutes of reperfusion following ischemia. The application of IPoC didn't induce a further increase in the phosphorylation level of STAT3 in comparison to IR. On the contrary, no variations in PS727-STAT3 and P-ERK1/2 levels were remotely observed **Fig. 55**. This indicates a systemic activation of STAT3 solely through Y705 phosphorylation. The application of IPoC did not induce a further significant increase in Y705 STAT3 phosphorylation in the remote area, indicating that IPoC does not provoke the systematic IL6 effect following early reperfusion.

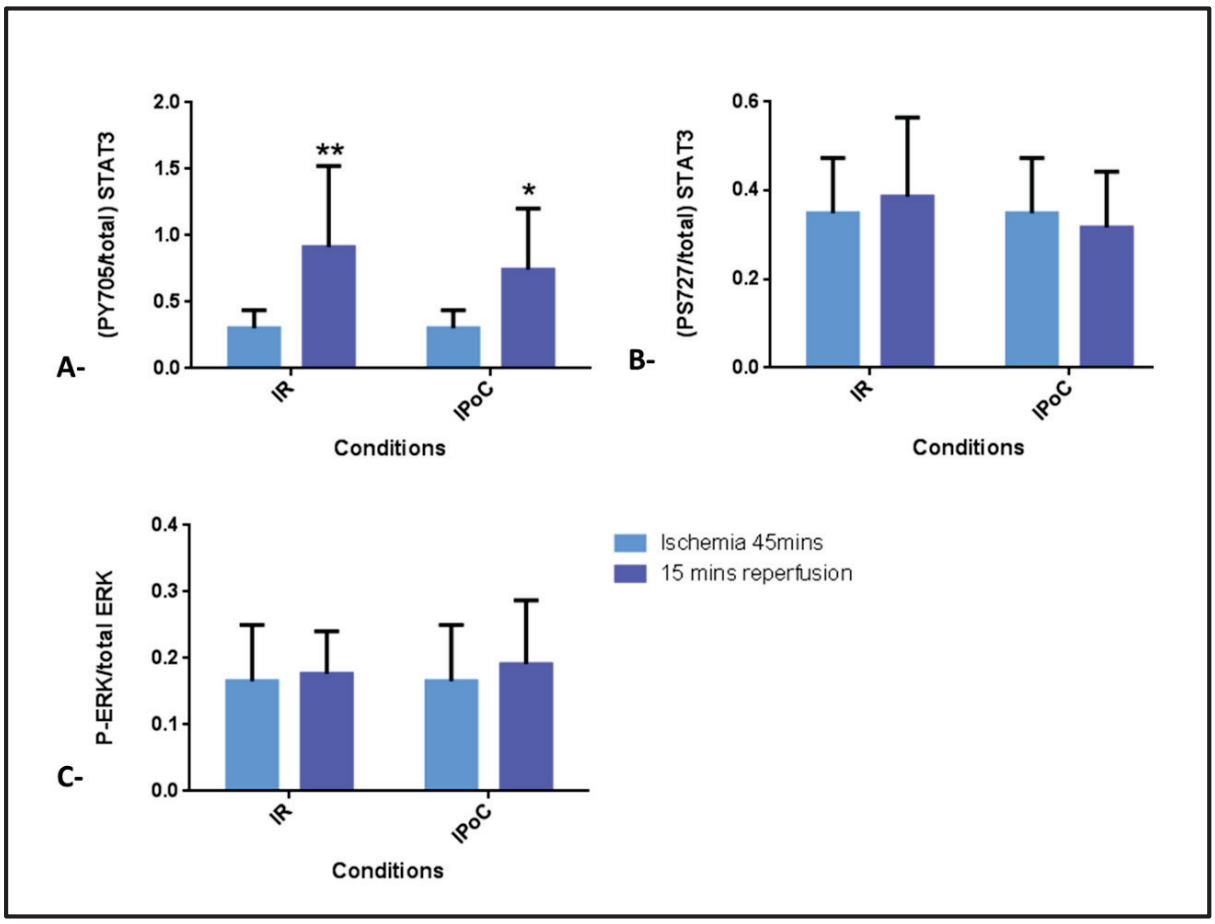

Figure 55. The phosphorylation levels in the remote areas

Bar graphs for the phosphorylation levels of Y705 and S727-STAT3, in addition to ERK1/2 in the remote areas following 45 minutes ischemia or 45 minutes ischemia+ 15 minutes of reperfusion, detected by WB. (n=8). * P<0.05 **P<0.01

Throughout the above data, we've seen that STAT3 is locally and systematically activated following early but not prolonged reperfusion. This provoked us to investigate how STAT3 phosphorylation might be inhibited at 3 hours. Having in mind that IL6 locally and systematically activates STAT3 within 15 minutes of reperfusion, we questioned if STAT3 inhibition at 3 hours is linked to the suppression of IL6 signaling. Therefore, we checked if STAT3 regulates the expression level of the suppressor of cytokine signaling 3 (socs3), which binds to the gp-130 receptor subunit and prevents IL6 receptor dimerization leading to the inhibition of the IL6 signal propagation. Our results show that in the presence of Stattic, socs3 expression level was decreased at 3 hours following I/R.

This indicates that STAT3 induces the expression of socs3 at 3 hours of reperfusion, which shall be accompanied to a suppression of cytokine signaling leading to regulation of STAT3 activation **Fig. 56**.

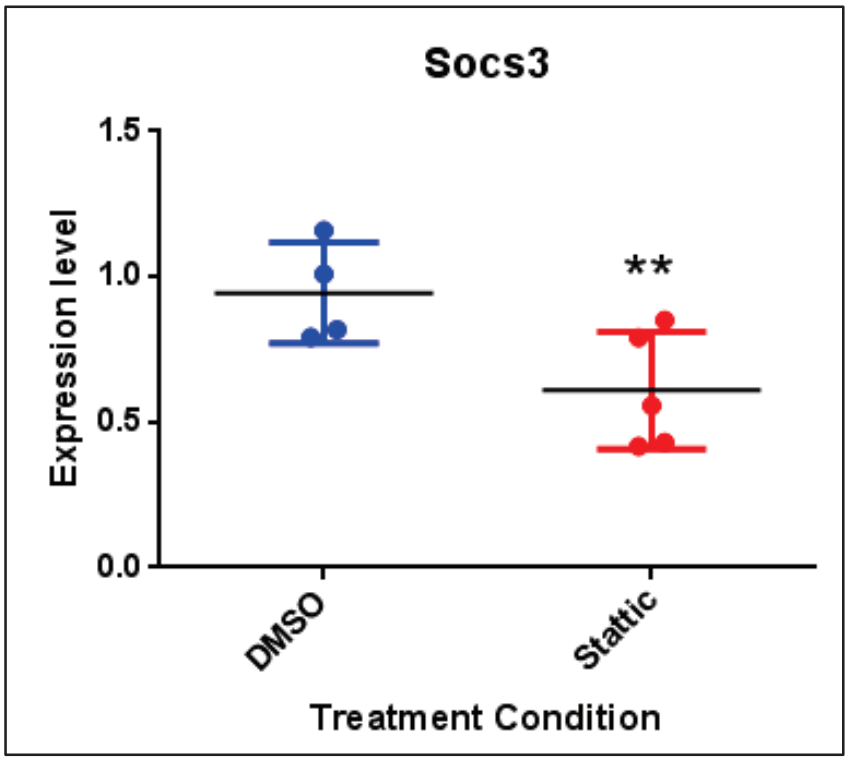

Figure 56. The expression levels of Socs3 during IR, under DMSO and Stattic treatment

The normalized expression levels of Socs3, measured by PCR following 3 hours of reperfusion under DMSO and Stattic treatment.

Overall, this collaborative study highlights the neglected surgery effects. It shows that a strong induction of the IL-6 axis occurs in sham animals over the first 24hrs and leads to the induction of inflammation and tissues' homeostasis processes. Interestingly, the network of IL-6 shows that STAT3 is among the main interactors, which again reflects that the activation of IL-6 could consequently lead to the activation of STAT3 signaling. This rise in the plasma levels of IL6 is expected to induce a systematic STAT3 response, which was validated by the activation of STAT3 in the remote area following IR.

DISCUSSION

The signal transducer and activator of transcription 3, STAT3, continues to excite much interest in heart research. As a signaling molecule, STAT3 is a downstream activator for various biological stimulators, including growth factors and cytokines. Thus, it stands out as a prominent key player in variable cellular responses induced during both I/R and IPoC. With such involvement in different signaling responses, STAT3 represents a point of convergence for different signals, which renders it at the core of signaling complexity in the cell. Once activated, STAT3 translocates to the nucleus, whereby it regulates the transcription of a wide array of genes involved in different cellular functions. Being such a central signaling molecule and transcription factor, the focus on STAT3's activation regardless investigating other interlinking modulators might lead to an incomplete vision of the real image of biological events. Thus, the common approaches used for interpreting STAT3's activities through solely measuring its phosphorylation levels under conditions of interest, regardless investigating interfering regulators of this phosphorylation, are quite incomplete. Moreover, targeting STAT3 solely at the signaling level, without correlating the activated signal with the specific-induced transcriptional activity in parallel, could also lead to an incomplete understanding of the real events.

In our current work, we targeted STAT3's cardioprotective roles in IPoC using a holistic approach. We started by investigating its cardioprotective roles that are attributed to the mitochondrial activity regulation and then shifted our work toward investigating its roles as a signaling molecule and a transcription factor activated during IPoC.

STAT3: An active mediator of IPoC through the Y705 residue

In the present study, we have first demonstrated that I/R alone is able to induce STAT3 phosphorylation at its Y705 and S727 residues. This re-emphasizes that STAT3 is among the proteins which are involved in regulating the response to the reperfusion injury through a dual phosphorylation of its residues. In this regard, the majority of previous studies have mainly focused on the Y705 STAT3 phosphorylation. They have reported that ischemia alone stimulates Y705 STAT3 phosphorylation with a further increase in its level during reperfusion, which our results agree with [213], [214], [261]. Focusing on the S727 residue in IR, a study has reported that its phosphorylation is suppressed in the mitochondria and nucleus during reperfusion [261]. This doesn't go along with the increase that we have seen, which may be due to the fact that we were assessing the global cellular PS727-STAT3 and not specifically the nuclear or the putative "mitochondrial" ones.

Moving to IPoC, the prominent protective roles of STAT3 were previously confirmed through the genetic ablation/modification [122], [169], [212] or pharmacological inhibition [117], [169]. In the context of genetic ablation, it is important to emphasize that the use of KO models to validate the involvement of STAT3 in IPoC might be misleading, since STAT3 has a steady-state activation under basal conditions for regulating different processes in the cell. Thus, it won't be clear if the protection observed in WT models (in comparison to KO) is due to the basal activated STAT3 or to the STAT3 which is over-activated by IPoC. As for the pharmacological inhibition of STAT3, many reports have previously used the JAK2 inhibitor AG490. Although AG490 is able to inhibit STAT3, it may also inhibit some other STAT family members since it's a JAK2 inhibitor. Thus, the use of AG490 could induce effects which are not strictly related to STAT3. This points out the importance of using STAT3-specific inhibitors, among which Stattic is well known. Unfortunately, controversial results were reported for the *in vivo* use of Stattic. In this regard, Heusch et al have abandoned the *in vivo* use of Stattic in their pigs model due to its toxicity [182]. On the contrary, another study has used Stattic in mice, in the context of I/R, without reporting toxicity [183]. In this study, Stattic was injected intraperitoneally in order to investigate the

involvement of STAT3 in the cardioprotective effects of rapamycin against IR. However, no previous studies have assessed the *in vivo* effects of Stattic in the context of IPoC. Thus, we are the first to validate and use a non-toxic Stattic dose, through an intravenous injection, and investigate its effect on IPoC. In this regard, it's important to note that the Stattic dose we used induced bradycardia once injected, but the heart rate was stable after that with absence of mortality.

Focusing on STAT3 activation in IPoC, we have confirmed that Y705 STAT3 phosphorylation was over-activated within 15 minutes of reperfusion. This gets along with what was reported by Heusch et al, who have reported that the IPoC significantly induced an increase in Y705 phosphorylation in a pigs model within 5 minutes of reperfusion [121]. In the same line of evidence, Goodman et al. have also reported that IPoC significantly induced Y705 STAT3 phosphorylation within 40 minutes of reperfusion in a Langendorff C57bl6/J mice hearts [169]. However, we exclusively went forward toward 24 hours of reperfusion, in a C57bl6/J *in vivo* model, but have seen no significant effect for the prolonged reperfusion, although prolonged reperfusion following IPoC has been suggested to reduce myocardial apoptosis via a JAK-STAT3 dependent pathway [117]. This indicates that STAT3 is over-activated early and acutely during reperfusion following IPoC, but its transcriptional activity-dependent effects are still observed up till prolonged time following reperfusion.

Directing the attention toward S727 residue, it has been reported that IPoC (3 cycles of 10 secs.) induced an increase in PS727-STAT3 within 10 minutes of reperfusion [122]. However, we could not confirm this fact since we have detected no significant additive effect for IPoC on P-S727 STAT3 level in comparison to IR alone. This variation in the results could be due to the variation in the used IPoC protocol since the same mentioned paper have stated that upon modifying the protocol, the S727 STAT3 phosphorylation was lost [122]. We thus ensure that our IPoC protocol, applied on C57Bl6J mice, induces activation of STAT3 solely through Y705 phosphorylation and more precisely by unbalancing the Y705/S727 ratio.

SAFE and RISK: Two sides of the same coin

The investigation of the mechanisms underlying IPoC has initially led to the discovery of the RISK pathway components. However, controversial issues surrounding the RISK pathway activation in IPoC signaling opened the door toward arguing for the existence of RISK-independent pathways in IPoC. Thus, the SAFE pathway concept has evolved thereafter as another independent pathway. However, since almost nothing is linear in biology, the complexity of the biological processes is established through the connection and the interlink of multiple pathways which variably orchestrate following any stimulation. Thus, the interlink between STAT3 and the kinases of RISK pathway has been questioned and examined by various teams. This point was investigated through inhibiting a pathway followed by studying the effect of this inhibition on the phosphorylation level of another activated protein [117]. A previous study showed that the inhibition of Akt and ERK 1/2 lead to the inhibition of STAT3 activation by sphingosine-1-phosphate, while the knockdown of STAT3 inhibited Akt and ERK activation [176]. This indicates that each pathway might be important for the activation of the other. However, the PI3K inhibition in another study conducted on C57Bl6 mice showed no effect on STAT3 phosphorylation and activity, although IPoC-induced cardioprotection was lost [169]. Similarly, Barsukevich et al reported that only the inhibition of RISK inhibited cardioprotection, while the inhibition of SAFE had no effect on the RISK activation or cardioprotection in Wistar rats [181]. Meanwhile, other studies have solely focused on the JAK-STAT3 signaling cascade, reporting its activation and direct involvement in the cardioprotective roles of IPoC regardless the RISK pathway activation [119], [121]. This variety in the published data again shows that the variability of the used models and protocols can strictly affect the outcome and points toward the importance of validating the activation of all the signaling cascades, along with questioning the interlink down-stream the signaling level.

In the current study, the *in vitro* results in the H9C2 cellular model showed that S727-STAT3 phosphorylation is regulated by the MEK-ERK pathway, whereby the use of the MEK-ERK pathway inhibitor PD98059 significantly decreased the PS727-STAT3

levels. This indicates that ERK1/2 regulates the *in vitro* STAT3 phosphorylation on its S727 residue, which clearly agrees with Chung et al who provided *in vitro* and *in vivo* evidences about the involvement of ERK1/2 in S727-STAT3 phosphorylation [194].

Moving to the *in vivo* model, we found that the STAT3 and ERK1/2 phosphorylation kinetics are positively cross-correlated, but not the other kinases. Interestingly, the *in vivo* inhibition of ERK1/2 induced an inhibition of Y705 STAT3 phosphorylation also. This shows that, unlike to the *in vitro* results, ERK1/2 is involved in the regulation of Y705 STAT3 phosphorylation, which is expected to be accompanied to a regulation of its transcriptional activity. Thus, the ERK1/2 pathway strongly supports the SAFE pathway in the cardioprotective effects of IPoC.

This observed regulation of STAT3 by ERK1/2 and the controversial previously published results concerning the dual activation of PI3K-Akt and MEK-ERK1/2 cascades as part of the same pathway in IPoC, in addition to the presence of common upstream activators of SAFE and RISK (sphingosine-1-P and autacoids), provoked us to question the validity of categorizing the signaling pathways into SAFE and RISK pathways. Such categorization might indeed be misleading, as it discriminates the signaling cascades as independent cascades rather than provoking the investigation of their complexity and co-regulation. Therefore, based on our data, we no longer view the SAFE and RISK pathways as two independent pathways, but rather as two sides of the same coin. Hereby, a better approach toward understanding IPoC would be through an objective targeting of the different cascades as interconnected cascades of IPoC rather than independent cascades categorized between SAFE and RISK.

Genetic expression in IPoC – A dual ERK/STAT3 signature

The transcriptional activity of STAT3 has been previously thought to be basically dependent on its activation by Y705 phosphorylation. Nevertheless, S727 phosphorylation has been shown to be important for the transcription of a set of unique genes, whereby mutating this residue induced a loss of their regulation [262]. This shows that, not only the transcriptional activity of STAT3 is dependent on both the Y705 and S727 residues, but also that a specific gene signature could be associated with variation in the p-Y705/p-S727 ratio. Interestingly, we have seen that the *in vivo* STAT3 phosphorylation is regulated by ERK1/2. The activation of STAT3 in IPoC on one hand, and the involvement of ERK1/2 in the support of this activation on the other hand, provoked us to investigate the transcriptional activity of STAT3 in IPoC and to study the involvement of ERK1/2 in regulating this activity. This was achieved by inhibiting the phosphorylation of Y705 STAT3 and ERK1/2 respectively by Stattic and PD98059.

After performing GO analysis on the Stattic and PD-dependent genes, we collected the GO terms and compared them. This permitted us to obtain three lists of GO terms: strictly Stattic-dependent, strictly PD-dependent and common ones. The common GO terms highlight the commonly regulated processes by STAT3 and ERK1/2, and most likely represent the functions that are modified by STAT3 in an ERK1/2-dependent manner. Thus, these GO terms are at the point of convergence between STAT3 and ERK1/2 and represent a dual signature of both proteins. Grouping the three lists of GO terms into biological families showed that development, metabolism and inflammation are the top families. In the context of development, STAT3 has been previously reported to be involved in the embryonic development, cell proliferation, angiogenesis, growth and differentiation [184], [186], [263], [264]. In the context of metabolism, STAT3 has been linked to the regulation of the glycolysis-dependent energy metabolism in tumor cells, where the Warburg effect is favored [207], [265]. Moving to inflammation, we've already mentioned in our introduction the prominent roles of STAT3 in IL-6 and IL-10 signaling, neutrophils/macrophages recruitment and macrophages polarization toward the M2 profile. In addition, independently from

STAT3, PoC has been already reported to participate in cardioprotection through decreasing the inflammatory response [266]–[268]. This effect was mainly proved through the measurement of the cytokines' levels in plasma rather than measuring genes expression, whereby many previous studies have reported a decrease in the levels of IL-6 and TNF in the serum of post conditioned animals, within 1 to 3 hours of reperfusion [267], [269], [270]. On the genomics level, the mRNA levels of IL-6 and TNF in renal and cerebral ischemia have reported to be decreased by conditioning but following at least 24 hours of reperfusion [268], [271].

In our results, taking a closer look at the Stattic-dependent GO terms grouped in the inflammation family of biological functions, we found them to be linked to the positive regulation of chemokine production and chemotaxis, in addition to a positive link with cellular migration and endothelial adhesion. However, the PD-dependent inflammatory GO terms were mostly linked to the proliferation, activation and differentiation of immune cells, in addition to the negative regulation of chemokine production and adhesion. This suggests that the Y705-STAT3 phosphorylation, activated by IPoC, is involved in the regulation of inflammation through regulating chemotaxis and inflammatory cells migration, while ERK1/2 activation is involved in regulating the activation and proliferation of the inflammatory cells, in addition to cytokine synthesis. As for the common GO terms, they were linked to both cytokine signaling and cell migration. This indicates that each of STAT3 and ERK1/2 regulates its own inflammatory processes, but the ERK1/2-dependent regulation of STAT3 induces a regulation of cytokine signaling and cellular migration during inflammation **Fig. 57**.

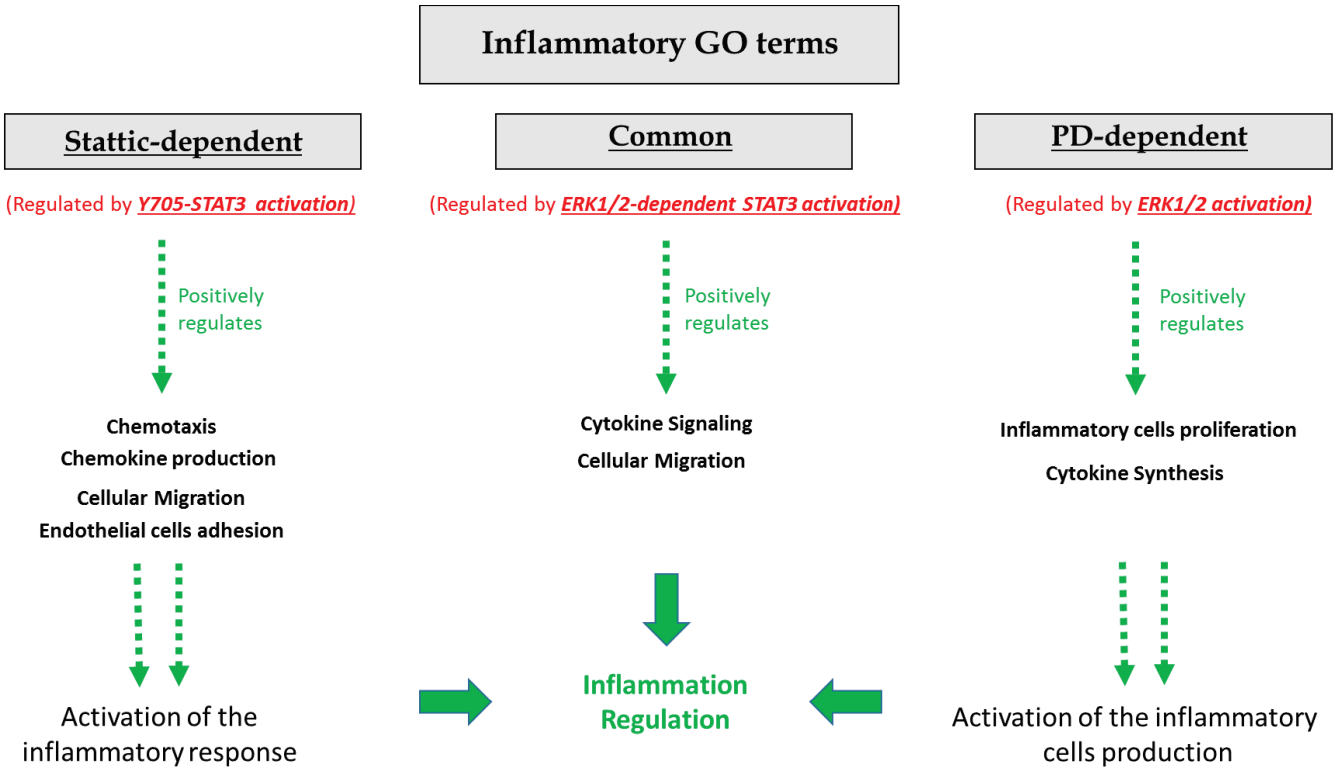

Figure 57. The Inflammatory GO Terms regulated by Stattic and PD98059

A representative scheme showing the inflammatory GO terms which are regulated by Stattic, PD and both. The Stattic-dependent GO terms regulate inflammation through regulating inflammatory processes including chemotaxis, cell migration and cell adhesion. Moving to the PD-dependent GO terms, they regulate the immune cells proliferation and inflammatory cytokine synthesis.

From these observations, we moved to measure the gene expression of several selected inflammatory markers and genes at 3 hours of reperfusion. Although 3 hours is relatively considered a very short duration of time to detect a modification in the inflammatory response at the genes level, it could still give us hints about the involvement of IPoC in the regulation of the early phase of response. Our results show that IPoC decreased the expression of the neutrophils marker ly6g, but increased the expression of the M1 macrophages marker CD80 and the expression of IL-6 as well. Neutrophils are the first leukocytes to be detected in the necrotic area for the initiation of the inflammatory response, through producing proteases and pro-inflammatory mediators [272]. They usually peak at 1 day following acute myocardial infarction [48]. The successful resolution of inflammation is dependent upon the coordinated transition from the initial recruitment of neutrophils to a more sustained population of mononuclear cells, which consequently differentiate to macrophages. The decrease which we observed in the neutrophils marker during IPoC reflects less abundancy of neutrophils in the infarcted area. This indicates that IPoC may induce less necrosis leading to less neutrophils recruitment and abundancy, or that it may regulate the duration of neutrophils peaking and clearance. Moving to macrophages, the increased level of M1 macrophages induced by IPoC could be due to the fact IPoC is inducing a quicker recruitment of monocytes in comparison to IR, which differentiate to M1, leading to a quicker resolution of the pro-inflammatory phase. Moreover, IPoC induced an increase in both the IL-6 and STAT3 levels. The increased STAT3 level is considered a normal consequence of the increased STAT3 activation during IPoC, since STAT3 regulates its own expression in an IL-6 dependent manner [273]. As for the increase in the IL6 gene expression levels, which seems contradicting to the previously reported anti-inflammatory roles of IPoC, it might be a preliminary increase at the gene level preceding an observed decrease at 24 hours. To validate this hypothesis, a further measurement of IL6 gene expression level shall be done at 24 hours of reperfusion following IPoC. This will permit a tracing of the temporal kinetics of expression of the IL6 gene following reperfusion. Besides, the serum levels of IL6 will also be measured at 3 and 24 hours of reperfusion following IPoC and compared

with the gene expression levels for evaluating any correlation, which will be done later in our current work.

Aside from the observed effect of IPoC under basal conditions, the effect of Stattic treatment on inflammatory gene expression showed an expected decrease in STAT3 expression level, likely due to the autoregulation by the activated STAT3. In addition, a decrease in the M2 macrophages marker, MRC1, was observed during IPoC. This indicates that the activated STAT3 during IPoC participates in the polarization of macrophages toward the M2 phenotype. This gets along with what was recently reported by Lee al [233], who showed that STAT3 favors the M2 polarization of macrophages *in vitro*. In addition to these results, Stattic treatment increased the expression of the chemokine cxcl-1, which points toward STAT3's participation in the regulation of neutrophils recruitment during IPoC. In this regard, Fielding et al. have previously reported that IL-6-driven signaling via STAT3 limited the inflammatory recruitment of neutrophils, which represents a critical event for the termination of the innate immune response [232]. They have shown that the hyper activation of STAT3 led to a pronounced down-modulation in the production the neutrophils-attracting chemokine cxcl-1, which led to a more rapid neutrophils clearance.

Moreover, our results also show that among the genes known to be regulated by the anti-inflammatory IL10-STAT3 axis, two genes were inhibited by Stattic treatment during IPoC. This highlights the role of STAT3 in regulating the expression of anti-inflammatory proteins during IPoC. Interestingly, the decrease in the expression levels of two STAT3-regulated genes was stronger and more significant following PD98059 treatment than following Stattic, and the expression level of STAT3 was lower under PD98059 inhibition than under Stattic inhibition. This is due to the fact that ERK1/2 inhibition by PD98059 had a higher inhibitory effect on Y705 STAT3 phosphorylation than Stattic and again points toward the involvement of ERK1/2 in the regulation of the transcriptional activity of STAT3 through regulating its phosphorylation.

The STAT3-IL6 Axis – A unique multiplayer

The relation between STAT3 and IL-6 is a loop-like relationship, whereby IL-6 activates STAT3 signaling, which in turn regulates the activation of IL-6. In this regard, we have shown in our own study that STAT3 inhibition decreased the IL-6 expression, pointing toward the regulation of IL-6 by STAT3. In another collaborative study done in the lab, in which the effect of the surgery on gene transcription was assessed, IL-6 appeared as the major hub and a key player in the network of the transcription factors which were shown to be activated by the surgery. This pointed toward a prominent role of IL6 in the activation of the retrieved transcriptional factors. This predicted role of IL-6 was then biologically assessed and validated, where the level of IL6 was found to be indeed significantly elevated 45 minutes after the surgery. This increase was also detected following I/R injury, whereby our results showed a rise in the IL6 level at 5 minutes of reperfusion and a peak at 3 hours. These elevated plasma levels we observed get along with what was previously reported by Miyao *et al*, who showed an elevated IL6 plasma levels in myocardial infarction patients [274]. We found that the released IL-6 in the plasma was correlated with the phosphorylation of Y705-STAT3 in the remote area of the heart following I/R. However, no induction of ERK1/2 or S727 STAT3 phosphorylation was observed. This shows that a remote effect is initiated within 15 minutes of reperfusion, leading to the activation of Y705 STAT3 phosphorylation. This effect is most probably due to the released IL6, because the measurement of gene expression levels of STAT3 in the remote area shows no significant variation of STAT3 gene expression. In addition, when we followed the temporal kinetics of IL6 in the plasma, we saw that IL6 peaks at 3 hours and decreases back to the basal level at 24 hours following I/R. Interestingly, we observed that the gene expression of the suppressor of cytokine signaling (socs3) was decreased at 3 hours of reperfusion by Stattic treatment. This suggests that the activated STAT3 during I/R upregulates the expression of socs3, which in turn suppresses IL6 signaling. The inhibition of IL6 signaling consequently leads to the loss of the increase in STAT3 phosphorylation (as observed at 3 and 24 hours of reperfusion), which in turn ceases its over-activated transcriptional activity at these time points and leads to

the loss of induction of IL6 starting 3 hours. As a result, IL6 levels decrease back to the basal level at 24 hours of reperfusion. Thus, a loop effect is initiated within the IL6-STAT3-socs3 axis **Fig. 58.**

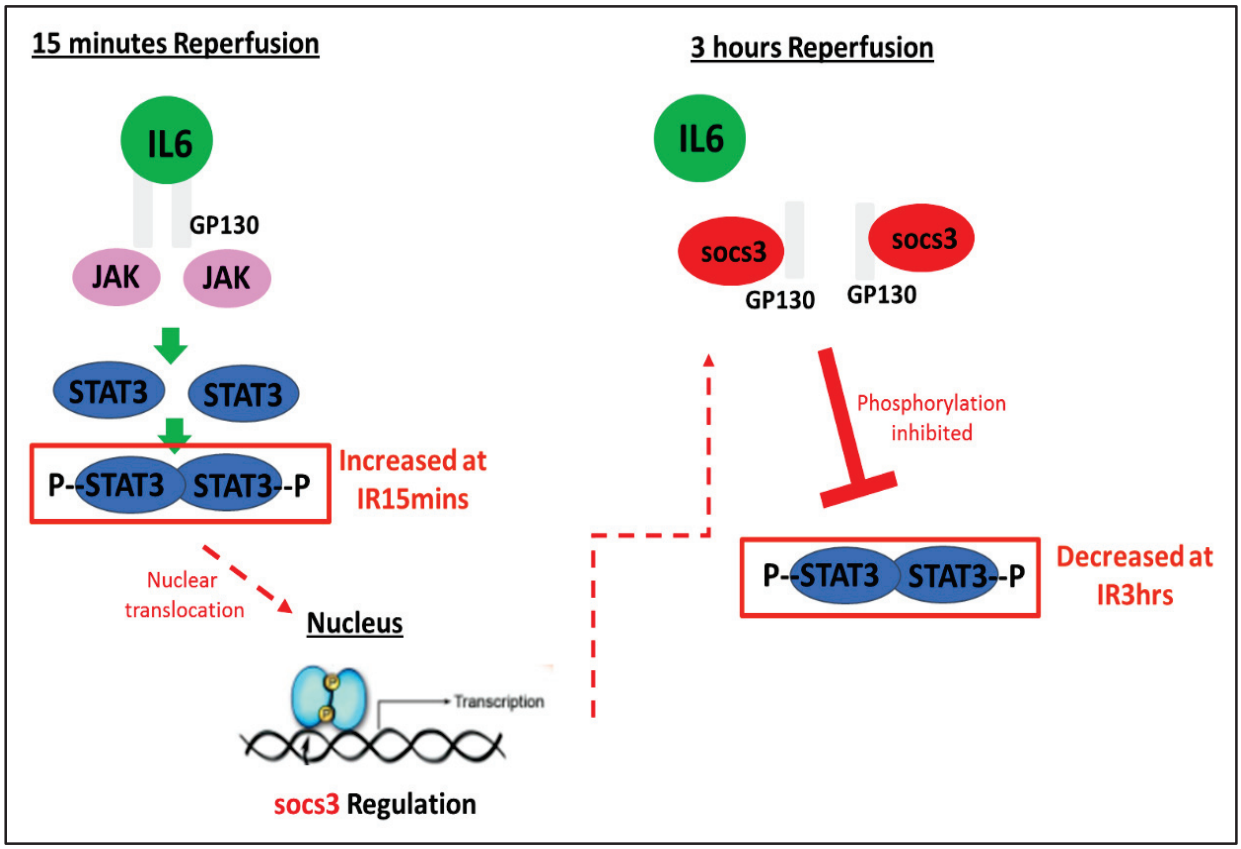

Figure 58. The IL6-STAT3-Socs3 loop effect during I/R

An illustration of the negative loop which is initiated during I/R for the regulation of STAT3 phosphorylation.

To sum it all up, the importance and interest of research lies in its ability to conquer the unknown and the unexpected, leading toward new approaches and acquaintances. In our current work, we initially aimed to investigate and target the mitochondrial functioning of STAT3. Our inability to detect STAT3 in the mitochondria lead us toward an exclusive interesting STAT3 pattern in adult cardiomyocytes. This, in parallel, shifted our work toward investigating the cardioprotective roles of STAT3 as a signaling molecule in IPoC and its interlinks, in a mitochondrial-independent manner, at the signaling level. Based on the results obtained at the signaling level, we directed our work toward the genomic one, whereby we used curative data bases and gene ontology analysis to reach our final end point. This work, overall, represents a systemic holistic approach integrating genomics, transcriptomics and proteomics in one single study.

CONCLUSION and PERSPECTIVES

This thesis work is the first to combine in a single study and decipher the interlinks between 1) the phosphorylation kinetics for SAFE and RISK pathways during I/R and IPoC, up to prolonged reperfusion, 2) STAT3 transcription activation and targets, and 3) the biological functions these processes regulate. It pointed toward the involvement of STAT3 in development, metabolism and inflammation and more precisely towards the modulation of immune cell recruitment in the injured myocardium.

Standing as a hall mark of the IR injury and as a cardioprotective therapeutic target, inflammation represents an important approach in our work. In this regard, we have shown that it's among the top biological functions in which STAT3-regulated genes are involved during IPoC and investigated these findings on the gene expression level. However, to have a good understanding of the overall image and validate the observed variation on the gene expression level, the plasma levels of selected pro- and anti- inflammatory interleukins shall be measured. This will be done in our upcoming work. In addition, neutrophils and macrophages (M1 and M2) markers will be analyzed by flow cytometry in cardiac cells isolated from hearts treated with Stattic and subjected to IPoC. This will enable us to validate the involvement of STAT3 in neutrophils recruitment/clearance and macrophages polarization.

Aside from the canonical activities of STAT3, this work targeted the mitochondrial non-canonical activity. We showed, using structural and functional approaches, that STAT3 is not presented in mitochondria of adult cardiac myocytes but are rather distributed in a unique pattern along the T-tubules and nucleus.

As a general future perspective for our current work, development and metabolism are still on our list of targets, having in mind that STAT3 is previously reported to interfere in both processes. Moreover, we also aim to investigate the involvement of STAT3 in the cardioprotective effect of hypothermia.

REFERENCES

[1] myVMC, « Anatomy of the human heart and cardiovascular system », *myVMC*, 25-juin-2006. [En ligne]. Disponible sur: https://www.myvmc.com/anatomy/cardiovascular-system-heart/. [Consulté le: 06-mars-2019].

[2] « Anatomy of the Heart and Cardiovascular System », *Texas Heart Institute*. [En ligne]. Disponible sur: https://www.texasheart.org/heart-health/heart-information-center/topics/anatomy-of-the-heart-and-cardiovascular-system/. [Consulté le: 06-mars-2019].

[3] I. Hazan-Halevy *et al.*, « STAT3 is constitutively phosphorylated on serine 727 residues, binds DNA, and activates transcription in CLL cells », *Blood*, vol. 115, nº 14, p. 2852‑2863, avr. 2010.

[4] « The Cardiovascular System (Heart and blood) | Medical Terminology for Cancer ». [En ligne]. Disponible sur: http://www.cancerindex.org/medterm/medtm8.htm. [Consulté le: 06-mars-2019].

[5] « Heart (Human Anatomy): Overview, Function, Structure », *Biology Dictionary*, 27-juill-2017. .

[6] J. Paton, « Anatomy of the Heart », *Queensland Cardiovascular Group*, 03-oct-2018. [En ligne]. Disponible sur: https://qcg.com.au/patients/anatomy-heart. [Consulté le: 06-mars-2019].

[7] « Layers of the Heart », *Kenhub*. [En ligne]. Disponible sur: https://www.kenhub.com/en/library/anatomy/layers-of-the-heart. [Consulté le: 06-mars-2019].

[8] « Human Heart – Diagram and Anatomy of the Heart », *InnerBody*. [En ligne]. Disponible sur: https://www.innerbody.com/image/card01.html. [Consulté le: 06-mars-2019].

[9] « Myocardium: Definition & Function - Video & Lesson Transcript », *Study.com*. [En ligne]. Disponible sur: http://study.com/academy/lesson/myocardium-definition-function.html. [Consulté le: 06-mars-2019].

[10] J. Pinnell, S. Turner, et S. Howell, « Cardiac muscle physiology », *Contin. Educ. Anaesth. Crit. Care Pain*, vol. 7, nº 3, p. 85‑88, juin 2007.

[11] « Human Physiology/The cardiovascular system - Wikibooks, open books for an open world ». [En ligne]. Disponible sur: https://en.wikibooks.org/wiki/Human_Physiology/The_cardiovascular_system#Myocardium. [Consulté le: 06-mars-2019].

[12] G. Gray, I. Toor, R. Castellan, M. Crisan, et M. Meloni, « Resident cells of the myocardium: more than spectators in cardiac injury, repair and regeneration », *Curr. Opin. Physiol.*, vol. 1, p. 46‑51, févr. 2018.

[13] P. Zhou et W. T. Pu, « Recounting cardiac cellular composition », *Circ. Res.*, vol. 118, nº 3, p. 368‑370, févr. 2016.

[14] C. A. Walker et F. G. Spinale, « The structure and function of the cardiac myocyte: A review of fundamental concepts », *J. Thorac. Cardiovasc. Surg.*, vol. 118, nº 2, p. 375‑382, août 1999.

[15] E. A. Woodcock et S. J. Matkovich, « Cardiomyocytes structure, function and associated pathologies », *Int. J. Biochem. Cell Biol.*, vol. 37, nº 9, p. 1746‑1751, sept. 2005.

[16] G. Olivetti, « Aging, Cardiac Hypertrophy and Ischemic Cardiomyopathy Do Not Affect the Proportion of Mononucleated and Multinucleated Myocytes in the Human Heart », *J. Mol. Cell. Cardiol.*, vol. 28, nº 7, p. 1463‑1477, juill. 1996.
[17] P. Camelliti, T. K. Borg, et P. Kohl, « Structural and functional characterisation of cardiac fibroblasts », *Cardiovasc. Res.*, vol. 65, nº 1, p. 40‑51, janv. 2005.
[18] « Physiology of the Heart | Boundless Anatomy and Physiology ». [En ligne]. Disponible sur: https://courses.lumenlearning.com/boundless-ap/chapter/physiology-of-the-heart/. [Consulté le: 07-mars-2019].
[19] « Cardiac Cycle | Anatomy and Physiology II ». [En ligne]. Disponible sur: https://courses.lumenlearning.com/suny-ap2/chapter/cardiac-cycle/. [Consulté le: 07-mars-2019].
[20] D. M. Bers, « Cardiac excitation–contraction coupling », vol. 415, p. 8, 2002.
[21] W. C. Stanley et M. P. Chandler, « Energy Metabolism in the Normal and Failing Heart: Potential for Therapeutic Interventions », p. 16.
[22] A. Lejay *et al.*, « Ischemia reperfusion injury, ischemic conditioning and diabetes mellitus », *J. Mol. Cell. Cardiol.*, vol. 91, p. 11‑22, févr. 2016.
[23] E. Murphy et C. Steenbergen, « Preconditioning: The Mitochondrial Connection », *Annu. Rev. Physiol.*, vol. 69, nº 1, p. 51‑67, 2007.
[24] Task Force Members *et al.*, « Universal definition of myocardial infarction: Kristian Thygesen, Joseph S. Alpert and Harvey D. White on behalf of the Joint ESC/ACCF/AHA/WHF Task Force for the Redefinition of Myocardial Infarction », *Eur. Heart J.*, vol. 28, nº 20, p. 2525‑2538, sept. 2007.
[25] « Expert Consensus Document. Third Universal Definition of Myocardial Infarction », *Rev. Esp. Cardiol. Engl. Ed.*, vol. 66, nº 2, p. 132, févr. 2013.
[26] « Structural Changes in Myocardium During Acute Ischemia | Circulation Research ». [En ligne]. Disponible sur: https://www.ahajournals.org/doi/10.1161/res.35.3_supplement.iii-156. [Consulté le: 11-mars-2019].
[27] V. Talman et H. Ruskoaho, « Cardiac fibrosis in myocardial infarction—from repair and remodeling to regeneration », *Cell Tissue Res.*, vol. 365, nº 3, p. 563‑581, 2016.
[28] R. Bolli, L. Becker, G. Gross, R. Mentzer, D. Balshaw, et D. A. Lathrop, « Myocardial Protection at a Crossroads: The Need for Translation Into Clinical Therapy », *Circ. Res.*, vol. 95, nº 2, p. 125‑134, juill. 2004.
[29] D. M. Yellon et D. J. Hausenloy, « Myocardial Reperfusion Injury », *N. Engl. J. Med.*, p. 15, 2007.
[30] H. Shimokawa et S. Yasuda, « Myocardial ischemia: Current concepts and future perspectives », *J. Cardiol.*, vol. 52, nº 2, p. 67‑78, oct. 2008.
[31] T. Kalogeris, C. P. Baines, M. Krenz, et R. J. Korthuis, « Cell biology of ischemia/reperfusion injury », *Int. Rev. Cell Mol. Biol.*, vol. 298, p. 229‑317, 2012.
[32] B. Redfors, Y. Shao, et E. Omerovic, « Myocardial infarct size and area at risk assessment in mice », *Exp. Clin. Cardiol.*, vol. 17, nº 4, p. 268‑272, 2012.
[33] E. Marban, Y. Koretsune, et H. Kusuoka, « Disruption of Intracellular Ca2+Homeostasis in Hearts Reperfused after Prolonged Episodes of Ischemia a », *Ann. N. Y. Acad. Sci.*, vol. 723, nº 1, p. 38‑50, 1994.
[34] D. J. Hausenloy et D. M. Yellon, « Myocardial ischemia-reperfusion injury: a neglected therapeutic target », *J. Clin. Invest.*, vol. 123, nº 1, p. 92‑100, janv. 2013.
[35] M. M. Pike *et al.*, « NMR measurements of Na+ and cellular energy in ischemic rat heart: role of Na(+)-H+ exchange », *Am. J. Physiol.-Heart Circ. Physiol.*, déc. 1993.

[36] R. B. Jennings, H. M. Sommers, G. A. Smyth, H. A. Flack, et H. Linn, « Myocardial necrosis induced by temporary occlusion of a coronary artery in the dog », *Arch. Pathol.*, vol. 70, p. 68‑78, juill. 1960.
[37] J. J. Lemasters *et al.*, « The pH paradox in ischemia-reperfusion injury to cardiac myocytes », *EXS*, vol. 76, p. 99‑114, 1996.
[38] T. Qian, A. L. Nieminen, B. Herman, et J. J. Lemasters, « Mitochondrial permeability transition in pH-dependent reperfusion injury to rat hepatocytes », *Am. J. Physiol.*, vol. 273, nº 6 Pt 1, p. C1783-1792, déc. 1997.
[39] J. González-Montero, R. Brito, A. I. Gajardo, et R. Rodrigo, « Myocardial reperfusion injury and oxidative stress: Therapeutic opportunities », *World J. Cardiol.*, vol. 10, nº 9, p. 74‑86, sept. 2018.
[40] A. P. Halestrap, « Calcium, mitochondria and reperfusion injury: a pore way to die », *Biochem. Soc. Trans.*, vol. 34, nº Pt 2, p. 232‑237, avr. 2006.
[41] D. Hausenloy, « The mitochondrial permeability transition pore: its fundamental role in mediating cell death during ischaemia and reperfusion », *J. Mol. Cell. Cardiol.*, vol. 35, nº 4, p. 339‑341, avr. 2003.
[42] Z.-Q. Zhao *et al.*, « Reperfusion induces myocardial apoptotic cell death », *Cardiovasc. Res.*, vol. 45, nº 3, p. 651‑660, févr. 2000.
[43] G. Takemura, M. Kanoh, S. Minatoguchi, et H. Fujiwara, « Cardiomyocyte apoptosis in the failing heart — A critical review from definition and classification of cell death », *Int. J. Cardiol.*, vol. 167, nº 6, p. 2373‑2386, sept. 2013.
[44] R. S. Whelan, V. Kaplinskiy, et R. N. Kitsis, « Cell Death in the Pathogenesis of Heart Disease: Mechanisms and Significance », *Annu. Rev. Physiol.*, vol. 72, nº 1, p. 19‑44, 2010.
[45] E. Murphy et C. Steenbergen, « Mechanisms Underlying Acute Protection from Cardiac Ischemia-Reperfusion Injury », *Physiol. Rev.*, vol. 88, nº 2, p. 581‑609, avr. 2008.
[46] M. Chiong *et al.*, « Cardiomyocyte death: mechanisms and translational implications », *Cell Death Dis.*, vol. 2, nº 12, p. e244, déc. 2011.
[47] N. G. Frangogiannis, « The inflammatory response in myocardial injury, repair, and remodelling », *Nat. Rev. Cardiol.*, vol. 11, nº 5, p. 255‑265, mai 2014.
[48] S.-B. Ong *et al.*, « Inflammation following acute myocardial infarction: Multiple players, dynamic roles, and novel therapeutic opportunities », *Pharmacol. Ther.*, vol. 186, p. 73‑87, 2018.
[49] Marchant David J. *et al.*, « Inflammation in Myocardial Diseases », *Circ. Res.*, vol. 110, nº 1, p. 126‑144, janv. 2012.
[50] A. Herskowitz, S. Choi, A. A. Ansari, et S. Wesselingh, « Cytokine mRNA expression in postischemic/reperfused myocardium », *Am. J. Pathol.*, vol. 146, nº 2, p. 419‑428, févr. 1995.
[51] A. G. Kumar *et al.*, « Induction of monocyte chemoattractant protein-1 in the small veins of the ischemic and reperfused canine myocardium », *Circulation*, vol. 95, nº 3, p. 693‑700, févr. 1997.
[52] N. G. Frangogiannis, « Cell biological mechanisms in regulation of the post-infarction inflammatory response », *Curr. Opin. Physiol.*, vol. 1, p. 7‑13, févr. 2018.
[53] S. D. Prabhu et N. G. Frangogiannis, « The Biological Basis for Cardiac Repair After Myocardial Infarction: From Inflammation to Fibrosis », *Circ. Res.*, vol. 119, nº 1, p. 91‑112, 24 2016.
[54] M. L. Entman *et al.*, « Neutrophil induced oxidative injury of cardiac myocytes. A compartmented system requiring CD11b/CD18-ICAM-1 adherence », *J. Clin. Invest.*, vol. 90, nº 4, p. 1335‑1345, oct. 1992.

[55] B. Petri et M.-J. Sanz, « Neutrophil chemotaxis », *Cell Tissue Res.*, vol. 371, nº 3, p. 425‑436, mars 2018.
[56] N. G. Frangogiannis, « Regulation of the inflammatory response in cardiac repair », *Circ. Res.*, vol. 110, nº 1, p. 159‑173, janv. 2012.
[57] S.-L. Puhl et S. Steffens, « Neutrophils in Post-myocardial Infarction Inflammation: Damage vs. Resolution? », *Front. Cardiovasc. Med.*, vol. 6, 2019.
[58] J. Vinten-Johansen, « Involvement of neutrophils in the pathogenesis of lethal myocardial reperfusion injury », *Cardiovasc. Res.*, vol. 61, nº 3, p. 481‑497, févr. 2004.
[59] P. J. Simpson, R. F. Todd, J. C. Fantone, J. K. Mickelson, J. D. Griffin, et B. R. Lucchesi, « Reduction of experimental canine myocardial reperfusion injury by a monoclonal antibody (anti-Mo1, anti-CD11b) that inhibits leukocyte adhesion », *J. Clin. Invest.*, vol. 81, nº 2, p. 624‑629, févr. 1988.
[60] P. J. Simpson *et al.*, « Sustained limitation of myocardial reperfusion injury by a monoclonal antibody that alters leukocyte function », *Circulation*, vol. 81, nº 1, p. 226‑237, janv. 1990.
[61] W. E. Curtis *et al.*, « Inhibition of neutrophil adhesion reduces myocardial infarct size », *Ann. Thorac. Surg.*, vol. 56, nº 5, p. 1069‑1073, nov. 1993.
[62] H. B. Sager, T. Kessler, et H. Schunkert, « Monocytes and macrophages in cardiac injury and repair », *J. Thorac. Dis.*, vol. 9, nº Suppl 1, p. S30‑S35, mars 2017.
[63] O. Dewald *et al.*, « CCL2/Monocyte Chemoattractant Protein-1 regulates inflammatory responses critical to healing myocardial infarcts », *Circ. Res.*, vol. 96, nº 8, p. 881‑889, avr. 2005.
[64] H. Lörchner *et al.*, « Myocardial healing requires Reg3β-dependent accumulation of macrophages in the ischemic heart », *Nat. Med.*, vol. 21, nº 4, p. 353‑362, avr. 2015.
[65] N. G. Frangogiannis, C. W. Smith, et M. L. Entman, « The inflammatory response in myocardial infarction », *Cardiovasc. Res.*, vol. 53, nº 1, p. 31‑47, janv. 2002.
[66] W. Walter *et al.*, « Deciphering the Dynamic Transcriptional and Post-transcriptional Networks of Macrophages in the Healthy Heart and after Myocardial Injury », *Cell Rep.*, vol. 23, nº 2, p. 622‑636, avr. 2018.
[67] Y. Zouggari *et al.*, « B lymphocytes trigger monocyte mobilization and impair heart function after acute myocardial infarction », *Nat. Med.*, vol. 19, nº 10, p. 1273‑1280, oct. 2013.
[68] D. R. Littman et A. Y. Rudensky, « Th17 and regulatory T cells in mediating and restraining inflammation », *Cell*, vol. 140, nº 6, p. 845‑858, mars 2010.
[69] N. G. Frangogiannis *et al.*, « IL-10 Is Induced in the Reperfused Myocardium and May Modulate the Reaction to Injury », *J. Immunol.*, vol. 165, nº 5, p. 2798‑2808, sept. 2000.
[70] M. Dobaczewski, Y. Xia, M. Bujak, C. Gonzalez-Quesada, et N. G. Frangogiannis, « CCR5 Signaling Suppresses Inflammation and Reduces Adverse Remodeling of the Infarcted Heart, Mediating Recruitment of Regulatory T Cells », *Am. J. Pathol.*, vol. 176, nº 5, p. 2177‑2187, mai 2010.
[71] A. Anzai *et al.*, « Regulatory role of dendritic cells in postinfarction healing and left ventricular remodeling », *Circulation*, vol. 125, nº 10, p. 1234‑1245, mars 2012.
[72] H. Liu *et al.*, « Exosomes derived from dendritic cells improve cardiac function via activation of CD4(+) T lymphocytes after myocardial infarction », *J. Mol. Cell. Cardiol.*, vol. 91, p. 123‑133, févr. 2016.
[73] A. V. Shinde et N. G. Frangogiannis, « Fibroblasts in myocardial infarction: a role in inflammation and repair », *J. Mol. Cell. Cardiol.*, vol. 0, p. 74‑82, mai 2014.

[74] M. Nakaya *et al.*, « Cardiac myofibroblast engulfment of dead cells facilitates recovery after myocardial infarction », *J. Clin. Invest.*, vol. 127, nº 1, p. 383‑401, 03 2017.
[75] Ø. Sandanger *et al.*, « The NLRP3 inflammasome is up-regulated in cardiac fibroblasts and mediates myocardial ischaemia-reperfusion injury », *Cardiovasc. Res.*, vol. 99, nº 1, p. 164‑174, juill. 2013.
[76] M. Takahashi, « Role of NLRP3 Inflammasome in Cardiac Inflammation and Remodeling after Myocardial Infarction », *Biol. Pharm. Bull.*, vol. 42, nº 4, p. 518‑523, avr. 2019.
[77] Kawaguchi Masanori *et al.*, « Inflammasome Activation of Cardiac Fibroblasts Is Essential for Myocardial Ischemia/Reperfusion Injury », *Circulation*, vol. 123, nº 6, p. 594‑604, févr. 2011.
[78] E. Mezzaroma *et al.*, « The inflammasome promotes adverse cardiac remodeling following acute myocardial infarction in the mouse », *Proc. Natl. Acad. Sci.*, vol. 108, nº 49, p. 19725‑19730, déc. 2011.
[79] D. Luger *et al.*, « Intravenously Delivered Mesenchymal Stem Cells: Systemic Anti-Inflammatory Effects Improve Left Ventricular Dysfunction in Acute Myocardial Infarction and Ischemic Cardiomyopathy », *Circ. Res.*, vol. 120, nº 10, p. 1598‑1613, mai 2017.
[80] M. Arai, D. J. Lefer, T. So, A. DiPaula, T. Aversano, et L. C. Becker, « An anti-CD18 antibody limits infarct size and preserves left ventricular function in dogs with ischemia and 48-hour reperfusion », *J. Am. Coll. Cardiol.*, vol. 27, nº 5, p. 1278‑1285, avr. 1996.
[81] T. Aversano, W. Zhou, M. Nedelman, M. Nakada, et H. Weisman, « A chimeric IgG4 monoclonal antibody directed against CD18 reduces infarct size in a primate model of myocardial ischemia and reperfusion », *J. Am. Coll. Cardiol.*, vol. 25, nº 3, p. 781‑788, mars 1995.
[82] D. J. Lefer, S. M. Shandelya, C. V. Serrano, L. C. Becker, P. Kuppusamy, et J. L. Zweier, « Cardioprotective actions of a monoclonal antibody against CD-18 in myocardial ischemia-reperfusion injury », *Circulation*, vol. 88, nº 4 Pt 1, p. 1779‑1787, oct. 1993.
[83] X. L. Ma, P. S. Tsao, et A. M. Lefer, « Antibody to CD-18 exerts endothelial and cardiac protective effects in myocardial ischemia and reperfusion », *J. Clin. Invest.*, vol. 88, nº 4, p. 1237‑1243, oct. 1991.
[84] K. W. Baran *et al.*, « Double-blind, randomized trial of an anti-CD18 antibody in conjunction with recombinant tissue plasminogen activator for acute myocardial infarction: limitation of myocardial infarction following thrombolysis in acute myocardial infarction (LIMIT AMI) study », *Circulation*, vol. 104, nº 23, p. 2778‑2783, déc. 2001.
[85] D. P. Faxon, R. J. Gibbons, N. A. F. Chronos, P. A. Gurbel, F. Sheehan, et HALT-MI Investigators, « The effect of blockade of the CD11/CD18 integrin receptor on infarct size in patients with acute myocardial infarction treated with direct angioplasty: the results of the HALT-MI study », *J. Am. Coll. Cardiol.*, vol. 40, nº 7, p. 1199‑1204, oct. 2002.
[86] J. M. Rusnak *et al.*, « An anti-CD11/CD18 monoclonal antibody in patients with acute myocardial infarction having percutaneous transluminal coronary angioplasty (the FESTIVAL study) », *Am. J. Cardiol.*, vol. 88, nº 5, p. 482‑487, sept. 2001.
[87] APEX AMI Investigators *et al.*, « Pexelizumab for acute ST-elevation myocardial infarction in patients undergoing primary percutaneous coronary intervention: a randomized controlled trial », *JAMA*, vol. 297, nº 1, p. 43‑51, janv. 2007.

[88] H. S. Sherratt, « Mitochondria: structure and function », *Rev. Neurol. (Paris)*, vol. 147, nº 6‑7, p. 417‑430, 1991.
[89] S. Castellana, S. Vicario, et C. Saccone, « Evolutionary patterns of the mitochondrial genome in Metazoa: exploring the role of mutation and selection in mitochondrial protein coding genes », *Genome Biol. Evol.*, vol. 3, p. 1067‑1079, 01 2011.
[90] P. Pinton, « Mitochondria-associated membranes (MAMs) and pathologies », *Cell Death Dis.*, vol. 9, nº 4, p. 413, mars 2018.
[91] « Oxidative Phosphorylation - Biology - OpenStax CNX ». [En ligne]. Disponible sur: https://cnx.org/contents/GFy_h8cu@9.85:7oTVAgrZ@7/Oxidative-Phosphorylation. [Consulté le: 16-avr-2019].
[92] E. J. Lesnefsky, Q. Chen, B. Tandler, et C. L. Hoppel, « Mitochondrial Dysfunction and Myocardial Ischemia-Reperfusion: Implications for Novel Therapies », *Annu. Rev. Pharmacol. Toxicol.*, vol. 57, nº 1, p. 535‑565, 2017.
[93] R. C. Scaduto et L. W. Grotyohann, « Measurement of Mitochondrial Membrane Potential Using Fluorescent Rhodamine Derivatives », *Biophys. J.*, vol. 76, nº 1, p. 469‑477, janv. 1999.
[94] D. G. Nicholls et M. W. Ward, « Mitochondrial membrane potential and neuronal glutamate excitotoxicity: mortality and millivolts », *Trends Neurosci.*, vol. 23, nº 4, p. 166‑174, avr. 2000.
[95] L. D. Zorova *et al.*, « Mitochondrial membrane potential », *Anal. Biochem.*, vol. 552, p. 50, juill. 2018.
[96] E. T. Chouchani *et al.*, « Ischaemic accumulation of succinate controls reperfusion injury through mitochondrial ROS », *Nature*, vol. 515, nº 7527, p. 431‑435, nov. 2014.
[97] K. Bianchi, A. Rimessi, A. Prandini, G. Szabadkai, et R. Rizzuto, « Calcium and mitochondria: mechanisms and functions of a troubled relationship », *Biochim. Biophys. Acta*, vol. 1742, nº 1‑3, p. 119‑131, déc. 2004.
[98] C. Giorgi, S. Marchi, et P. Pinton, « The machineries, regulation and cellular functions of mitochondrial calcium », *Nat. Rev. Mol. Cell Biol.*, vol. 19, nº 11, p. 713‑730, nov. 2018.
[99] T. Briston *et al.*, « Mitochondrial permeability transition pore: sensitivity to opening and mechanistic dependence on substrate availability », *Sci. Rep.*, vol. 7, nº 1, p. 10492, sept. 2017.
[100] E. K. Iliodromitis, I. Andreadou, K. Iliodromitis, et N. Dagres, « Ischemic and Postischemic Conditioning of the Myocardium in Clinical Practice: Challenges, Expectations and Obstacles », *Cardiology*, vol. 129, nº 2, p. 117‑125, 2014.
[101] Z. Xia, H. Li, et M. G. Irwin, « Myocardial ischaemia reperfusion injury: the challenge of translating ischaemic and anaesthetic protection from animal models to humans », *Br. J. Anaesth.*, vol. 117 Suppl 2, p. ii44‑ii62, sept. 2016.
[102] C. E. Murry, R. B. Jennings, et K. A. Reimer, « Preconditioning with ischemia: a delay of lethal cell injury in ischemic myocardium. », *Circulation*, vol. 74, nº 5, p. 1124‑1136, nov. 1986.
[103] J. E. Schultz, E. Rose, Z. Yao, et G. J. Gross, « Evidence for involvement of opioid receptors in ischemic preconditioning in rat hearts », *Am. J. Physiol.*, vol. 268, nº 5 Pt 2, p. H2157-2161, mai 1995.
[104] K. Ytrehus, Y. Liu, et J. M. Downey, « Preconditioning protects ischemic rabbit heart by protein kinase C activation », *Am. J. Physiol.*, vol. 266, nº 3 Pt 2, p. H1145-1152, mars 1994.

[105] D. L. Miller et D. M. Van Winkle, « Ischemic preconditioning limits infarct size following regional ischemia–reperfusion in in situ mouse hearts », *Cardiovasc. Res.*, vol. 42, nº 3, p. 680‑684, juin 1999.
[106] R. Schulz, H. Post, C. Vahlhaus, et G. Heusch, « Ischemic Preconditioning in Pigs: A Graded Phenomenon: Its Relation to Adenosine and Bradykinin », *Circulation*, vol. 98, nº 10, p. 1022‑1029, sept. 1998.
[107] D. M. Yellon, A. M. Alkhulaifi, et W. B. Pugsley, « Preconditioning the human myocardium », *The Lancet*, vol. 342, nº 8866, p. 276‑277, juill. 1993.
[108] P. Pagliaro, D. Gattullo, R. Rastaldo, et G. Losano, « Ischemic preconditioning: from the first to the second window of protection », *Life Sci.*, vol. 69, nº 1, p. 1‑15, mai 2001.
[109] R. Bousselmi, M. A. Lebbi, et M. Ferjani, « Myocardial ischemic conditioning: Physiological aspects and clinical applications in cardiac surgery », *J. Saudi Heart Assoc.*, vol. 26, nº 2, p. 93‑100, avr. 2014.
[110] M. S. Marber, D. S. Latchman, J. M. Walker, et D. M. Yellon, « Cardiac stress protein elevation 24 hours after brief ischemia or heat stress is associated with resistance to myocardial infarction », *Circulation*, vol. 88, nº 3, p. 1264‑1272, sept. 1993.
[111] T. Kuzuya *et al.*, « Delayed effects of sublethal ischemia on the acquisition of tolerance to ischemia », *Circ. Res.*, vol. 72, nº 6, p. 1293‑1299, juin 1993.
[112] G. F. Baxter, M. S. Marber, V. C. Patel, et D. M. Yellon, « Adenosine receptor involvement in a delayed phase of myocardial protection 24 hours after ischemic preconditioning », *Circulation*, vol. 90, nº 6, p. 2993‑3000, déc. 1994.
[113] G. S. Liu, J. Thornton, D. M. Van Winkle, A. W. Stanley, R. A. Olsson, et J. M. Downey, « Protection against infarction afforded by preconditioning is mediated by A1 adenosine receptors in rabbit heart », *Circulation*, vol. 84, nº 1, p. 350‑356, juill. 1991.
[114] T. M. Wall, R. Sheehy, et J. C. Hartman, « Role of bradykinin in myocardial preconditioning », *J. Pharmacol. Exp. Ther.*, vol. 270, nº 2, p. 681‑689, août 1994.
[115] Z.-Q. Zhao *et al.*, « Inhibition of myocardial injury by ischemic postconditioning during reperfusion: comparison with ischemic preconditioning », *Am. J. Physiol.-Heart Circ. Physiol.*, vol. 285, nº 2, p. H579‑H588, août 2003.
[116] H. Kin *et al.*, « Postconditioning attenuates myocardial ischemia-reperfusion injury by inhibiting events in the early minutes of reperfusion », *Cardiovasc. Res.*, vol. 62, nº 1, p. 74‑85, avr. 2004.
[117] Y. Tian, W. Zhang, D. Xia, P. Modi, D. Liang, et M. Wei, « Postconditioning inhibits myocardial apoptosis during prolonged reperfusion via a JAK2-STAT3-Bcl-2 pathway », *J. Biomed. Sci.*, vol. 18, nº 1, p. 53, 2011.
[118] X.-M. Yang, J. B. Proctor, L. Cui, T. Krieg, J. M. Downey, et M. V. Cohen, « Multiple, brief coronary occlusions during early reperfusion protect rabbit hearts by targeting cell signaling pathways », *J. Am. Coll. Cardiol.*, vol. 44, nº 5, p. 1103‑1110, sept. 2004.
[119] L. You, L. Li, Q. Xu, J. Ren, et F. Zhang, « Postconditioning reduces infarct size and cardiac myocyte apoptosis via the opioid receptor and JAK-STAT signaling pathway », *Mol. Biol. Rep.*, vol. 38, nº 1, p. 437‑443, janv. 2011.
[120] Skyschally Andreas *et al.*, « Ischemic Postconditioning in Pigs », *Circ. Res.*, vol. 104, nº 1, p. 15‑18, janv. 2009.
[121] G. Heusch, J. Musiolik, N. Gedik, et A. Skyschally, « Mitochondrial STAT3 activation and cardioprotection by ischemic postconditioning in pigs with regional myocardial ischemia/reperfusion », *Circ. Res.*, vol. 109, nº 11, p. 1302‑1308, nov. 2011.
[122] K. Boengler *et al.*, « Cardioprotection by Ischemic Postconditioning Is Lost in Aged and STAT3-Deficient Mice », *Circ. Res.*, vol. 102, nº 1, p. 131‑135, janv. 2008.

[123] L. Gomez, M. Paillard, H. Thibault, G. Derumeaux, et M. Ovize, « Inhibition of GSK3beta by postconditioning is required to prevent opening of the mitochondrial permeability transition pore during reperfusion », *Circulation*, vol. 117, nº 21, p. 2761‑2768, mai 2008.
[124] Y. Wang, D. Wang, L. Zhang, F. Ye, M. Li, et K. Wen, « Role of JAK-STAT pathway in reducing cardiomyocytes hypoxia/reoxygenation injury induced by S1P postconditioning », *Eur. J. Pharmacol.*, vol. 784, p. 129‑136, août 2016.
[125] G. Heusch, A. Büchert, S. Feldhaus, et R. Schulz, « No loss of cardioprotection by postconditioning in connexin 43-deficient mice », *Basic Res. Cardiol.*, vol. 101, nº 4, p. 354‑356, juill. 2006.
[126] W. Luo, B. Li, G. Lin, et R. Huang, « Postconditioning in cardiac surgery for tetralogy of Fallot », *J. Thorac. Cardiovasc. Surg.*, vol. 133, nº 5, p. 1373‑1374, mai 2007.
[127] V. Sivaraman *et al.*, « Postconditioning protects human atrial muscle through the activation of the RISK pathway », *Basic Res. Cardiol.*, vol. 102, nº 5, p. 453‑459, sept. 2007.
[128] J. Vinten-Johansen, A. Granfeldt, J. Mykytenko, V. V. Undyala, Y. Dong, et K. Przyklenk, « The Multidimensional Physiological Responses to Postconditioning », *Antioxid. Redox Signal.*, vol. 14, nº 5, p. 791‑810, mars 2011.
[129] H.-C. Kim *et al.*, « Sevoflurane Postconditioning Reduces Apoptosis by Activating the JAK-STAT Pathway After Transient Global Cerebral Ischemia in Rats », *J. Neurosurg. Anesthesiol.*, vol. 29, nº 1, p. 37‑45, janv. 2017.
[130] H. Sasaki *et al.*, « Brief ischemia-reperfusion performed after prolonged ischemia (ischemic postconditioning) can terminate reperfusion arrhythmias with no reduction of cardiac function in rats », *Int. Heart. J.*, vol. 48, nº 2, p. 205‑213, mars 2007.
[131] R. A. Kloner, J. Dow, et A. Bhandari, « Postconditioning markedly attenuates ventricular arrhythmias after ischemia-reperfusion », *J. Cardiovasc. Pharmacol. Ther.*, vol. 11, nº 1, p. 55‑63, mars 2006.
[132] L. M. Schwartz et C. J. Lagranha, « Ischemic postconditioning during reperfusion activates Akt and ERK without protecting against lethal myocardial ischemia-reperfusion injury in pigs », *Am. J. Physiol.-Heart Circ. Physiol.*, vol. 290, nº 3, p. H1011‑H1018, mars 2006.
[133] P. R. Crisostomo, M. Wang, G. M. Wairiuko, A. M. Terrell, et D. R. Meldrum, « Postconditioning in females depends on injury severity », *J. Surg. Res.*, vol. 134, nº 2, p. 342‑347, août 2006.
[134] M. Juhaszova *et al.*, « Glycogen synthase kinase-3beta mediates convergence of protection signaling to inhibit the mitochondrial permeability transition pore », *J. Clin. Invest.*, vol. 113, nº 11, p. 1535‑1549, juin 2004.
[135] D. J. Hausenloy et D. M. Yellon, « New directions for protecting the heart against ischaemia-reperfusion injury: targeting the Reperfusion Injury Salvage Kinase (RISK)-pathway », *Cardiovasc. Res.*, vol. 61, nº 3, p. 448‑460, févr. 2004.
[136] S. Lecour, « Activation of the protective Survivor Activating Factor Enhancement (SAFE) pathway against reperfusion injury: Does it go beyond the RISK pathway? », *J. Mol. Cell. Cardiol.*, vol. 47, nº 1, p. 32‑40, juill. 2009.
[137] L. Lacerda, S. Somers, L. H. Opie, et S. Lecour, « Ischaemic postconditioning protects against reperfusion injury via the SAFE pathway », *Cardiovasc. Res.*, vol. 84, nº 2, p. 201‑208, nov. 2009.
[138] D. Schulman, D. S. Latchman, et D. M. Yellon, « Urocortin protects the heart from reperfusion injury via upregulation of p42/p44 MAPK signaling pathway », *Am. J. Physiol. Heart Circ. Physiol.*, vol. 283, nº 4, p. H1481-1488, oct. 2002.

[139] A. Tsang, D. J. Hausenloy, M. M. Mocanu, et D. M. Yellon, « Postconditioning: a form of "modified reperfusion" protects the myocardium by activating the phosphatidylinositol 3-kinase-Akt pathway », *Circ. Res.*, vol. 95, nº 3, p. 230‑232, août 2004.
[140] P. C. Chiari, M. W. Bienengraeber, P. S. Pagel, J. G. Krolikowski, J. R. Kersten, et D. C. Warltier, « Isoflurane protects against myocardial infarction during early reperfusion by activation of phosphatidylinositol-3-kinase signal transduction: evidence for anesthetic-induced postconditioning in rabbits », *Anesthesiology*, vol. 102, nº 1, p. 102‑109, janv. 2005.
[141] C. E. Darling, R. Jiang, M. Maynard, P. Whittaker, J. Vinten-Johansen, et K. Przyklenk, « Postconditioning via stuttering reperfusion limits myocardial infarct size in rabbit hearts: role of ERK1/2 », *Am. J. Physiol.-Heart Circ. Physiol.*, vol. 289, nº 4, p. H1618‑H1626, oct. 2005.
[142] O. C. Manintveld *et al.*, « Cardiac effects of postconditioning depend critically on the duration of index ischemia », *Am. J. Physiol. Heart Circ. Physiol.*, vol. 292, nº 3, p. H1551-1560, mars 2007.
[143] M. Fujita *et al.*, « Prolonged transient acidosis during early reperfusion contributes to the cardioprotective effects of postconditioning », *Am. J. Physiol. Heart Circ. Physiol.*, vol. 292, nº 4, p. H2004-2008, avr. 2007.
[144] O. Bouhidel, S. Pons, R. Souktani, R. Zini, A. Berdeaux, et B. Ghaleb, « Myocardial ischemic postconditioning against ischemia-reperfusion is impaired in ob/ob mice », *Am. J. Physiol. Heart Circ. Physiol.*, vol. 295, nº 4, p. H1580-1586, oct. 2008.
[145] S. Tamareille *et al.*, « Myocardial reperfusion injury management: erythropoietin compared with postconditioning », *Am. J. Physiol. Heart Circ. Physiol.*, vol. 297, nº 6, p. H2035-2043, déc. 2009.
[146] Q.-L. Wu, T. Shen, L.-L. Shao, H. Ma, et J.-K. Wang, « Ischemic postconditioning mediates cardioprotection via PI3K/GSK-3β/β-catenin signaling pathway in ischemic rat myocardium », *Shock Augusta Ga*, vol. 38, nº 2, p. 165‑169, août 2012.
[147] D. J. Hausenloy, S. Lecour, et D. M. Yellon, « Reperfusion Injury Salvage Kinase and Survivor Activating Factor Enhancement Prosurvival Signaling Pathways in Ischemic Postconditioning: Two Sides of the Same Coin », *Antioxid. Redox Signal.*, vol. 14, nº 5, p. 893‑907, mars 2011.
[148] A. J. Zatta *et al.*, « Infarct-sparing effect of myocardial postconditioning is dependent on protein kinase C signalling », *Cardiovasc. Res.*, vol. 70, nº 2, p. 315‑324, mai 2006.
[149] J. Inserte, V. Hernando, Ú. Vilardosa, E. Abad, M. Poncelas-Nozal, et D. Garcia-Dorado, « Activation of cGMP/Protein Kinase G Pathway in Postconditioned Myocardium Depends on Reduced Oxidative Stress and Preserved Endothelial Nitric Oxide Synthase Coupling », *J. Am. Heart Assoc.*, vol. 2, nº 1, janv. 2013.
[150] Z. Chen, X. Zhang, Y. Liu, et Z. Liu, « Morphine Postconditioning Protects against Reperfusion Injury via Inhibiting JNK/p38 MAPK and Mitochondrial Permeability Transition Pores Signaling Pathways », *Cell. Physiol. Biochem.*, vol. 39, nº 1, p. 61‑70, 2016.
[151] M. Yoshizumi, K. Tsuchiya, et T. Tamaki, « Signal transduction of reactive oxygen species and mitogen-activated protein kinases in cardiovascular disease », *J. Med. Investig. JMI*, vol. 48, nº 1‑2, p. 11‑24, févr. 2001.
[152] F. Gao *et al.*, « p38 MAPK inhibition reduces myocardial reperfusion injury via inhibition of endothelial adhesion molecule expression and blockade of PMN accumulation », *Cardiovasc. Res.*, vol. 53, nº 2, p. 414‑422, févr. 2002.

[153] H.-Y. Sun *et al.*, « Postconditioning attenuates cardiomyocyte apoptosis via inhibition of JNK and p38 mitogen-activated protein kinase signaling pathways », *Apoptosis*, vol. 11, nº 9, p. 1583‑1593, sept. 2006.
[154] A. Xia *et al.*, « Naloxone Postconditioning Alleviates Rat Myocardial Ischemia Reperfusion Injury by Inhibiting JNK Activity », *Korean J. Physiol. Pharmacol.*, vol. 18, nº 1, p. 67, 2014.
[155] D. J. Hausenloy et D. M. Yellon, « Reperfusion injury salvage kinase signalling: taking a RISK for cardioprotection », *Heart Fail. Rev.*, vol. 12, nº 3‑4, p. 217‑234, déc. 2007.
[156] D. J. Hausenloy et D. M. Yellon, « Cardioprotective growth factors », *Cardiovasc. Res.*, vol. 83, nº 2, p. 179‑194, juill. 2009.
[157] B. Buchholz, M. Donato, V. D'Annunzio, et R. J. Gelpi, « Ischemic postconditioning: mechanisms, comorbidities, and clinical application », *Mol. Cell. Biochem.*, vol. 392, nº 1‑2, p. 1‑12, juill. 2014.
[158] J.-S. Kim, S. Ohshima, P. Pediaditakis, et J. J. Lemasters, « Nitric oxide: a signaling molecule against mitochondrial permeability transition- and pH-dependent cell death after reperfusion », *Free Radic. Biol. Med.*, vol. 37, nº 12, p. 1943‑1950, déc. 2004.
[159] Y. Abdallah *et al.*, « Insulin protects cardiomyocytes against reoxygenation-induced hypercontracture by a survival pathway targeting SR Ca2+ storage », *Cardiovasc. Res.*, vol. 70, nº 2, p. 346‑353, mai 2006.
[160] D. J. Hausenloy et L. Scorrano, « Targeting cell death », *Clin. Pharmacol. Ther.*, vol. 82, nº 4, p. 370‑373, oct. 2007.
[161] A. K. Jonassen, M. N. Sack, O. D. Mjøs, et D. M. Yellon, « Myocardial protection by insulin at reperfusion requires early administration and is mediated via Akt and p70s6 kinase cell-survival signaling », *Circ. Res.*, vol. 89, nº 12, p. 1191‑1198, déc. 2001.
[162] G. A. Borillo *et al.*, « Pim-1 kinase protects mitochondrial integrity in cardiomyocytes », *Circ. Res.*, vol. 106, nº 7, p. 1265‑1274, avr. 2010.
[163] A. Skyschally *et al.*, « Ischemic Postconditioning in Pigs: No Causal Role for RISK Activation », *Circ. Res.*, vol. 104, nº 1, p. 15‑18, janv. 2009.
[164] Y. Nishino *et al.*, « Glycogen Synthase Kinase-3 Inactivation Is Not Required for Ischemic Preconditioning or Postconditioning in the Mouse », *Circ. Res.*, vol. 103, nº 3, p. 307‑314, août 2008.
[165] S. Lecour *et al.*, « Pharmacological preconditioning with tumor necrosis factor-alpha activates signal transducer and activator of transcription-3 at reperfusion without involving classic prosurvival kinases (Akt and extracellular signal-regulated kinase) », *Circulation*, vol. 112, nº 25, p. 3911‑3918, déc. 2005.
[166] C. Liongue et A. C. Ward, « Evolution of the JAK-STAT pathway », *JAK-STAT*, vol. 2, nº 1, janv. 2013.
[167] J. S. Rawlings, « The JAK/STAT signaling pathway », *J. Cell Sci.*, vol. 117, nº 8, p. 1281‑1283, mars 2004.
[168] Y. T. Xuan, Y. Guo, H. Han, Y. Zhu, et R. Bolli, « An essential role of the JAK-STAT pathway in ischemic preconditioning », *Proc. Natl. Acad. Sci. U. S. A.*, vol. 98, nº 16, p. 9050‑9055, juill. 2001.
[169] M. D. Goodman, S. E. Koch, G. A. Fuller-Bicer, et K. L. Butler, « Regulating RISK: a role for JAK-STAT signaling in postconditioning? », *Am. J. Physiol.-Heart Circ. Physiol.*, vol. 295, nº 4, p. H1649‑H1656, oct. 2008.
[170] B. N. Fuglesteg *et al.*, « Signal transducer and activator of transcription 3 is involved in the cardioprotective signalling pathway activated by insulin therapy at reperfusion », *Basic Res. Cardiol.*, vol. 103, nº 5, p. 444‑453, sept. 2008.

[171] I. Frolkis *et al.*, « Interaction between paracrine tumor necrosis factor-alpha and paracrine angiotensin II during myocardial ischemia », *J. Am. Coll. Cardiol.*, vol. 37, nº 1, p. 316‑322, janv. 2001.
[172] H. Ju, V. J. Venema, H. Liang, M. B. Harris, R. Zou, et R. C. Venema, « Bradykinin activates the Janus-activated kinase/signal transducers and activators of transcription (JAK/STAT) pathway in vascular endothelial cells: localization of JAK/STAT signalling proteins in plasmalemmal caveolae », *Biochem. J.*, vol. 351, nº Pt 1, p. 257‑264, oct. 2000.
[173] L. J. Qin, Y. T. Gu, H. Zhang, et Y. X. Xue, « Bradykinin-induced blood-tumor barrier opening is mediated by tumor necrosis factor-alpha. », *Neurosci. Lett.*, vol. 450, nº 2, p. 172‑175, janv. 2009.
[174] M. V. Cohen et J. M. Downey, « Signalling pathways and mechanisms of protection in pre- and postconditioning: historical perspective and lessons for the future », *Br. J. Pharmacol.*, vol. 172, nº 8, p. 1913‑1932, avr. 2015.
[175] Z. Liu, H. Hsu, D. V. Goeddel, et M. Karin, « Dissection of TNF Receptor 1 Effector Functions: JNK Activation Is Not Linked to Apoptosis While NF-□B Activation Prevents Cell Death », p. 12.
[176] S. J. Somers, M. Frias, L. Lacerda, L. H. Opie, et S. Lecour, « Interplay between SAFE and RISK pathways in sphingosine-1-phosphate-induced cardioprotection », *Cardiovasc. Drugs Ther.*, vol. 26, nº 3, p. 227‑237, juin 2012.
[177] Y. Oshima *et al.*, « STAT3 mediates cardioprotection against ischemia/reperfusion injury through metallothionein induction in the heart », *Cardiovasc. Res.*, vol. 65, nº 2, p. 428‑435, févr. 2005.
[178] K. Szczepanek *et al.*, « Mitochondrial-targeted Signal transducer and activator of transcription 3 (STAT3) protects against ischemia-induced changes in the electron transport chain and the generation of reactive oxygen species », *J. Biol. Chem.*, vol. 286, nº 34, p. 29610‑29620, août 2011.
[179] J. Wu *et al.*, « Sevoflurane postconditioning protects the myocardium against ischemia/reperfusion injury via activation of the JAK2-STAT3 pathway », *PeerJ*, vol. 5, p. e3196, 2017.
[180] S. Pedretti et E. Raddatz, « STAT3α interacts with nuclear GSK3beta and cytoplasmic RISK pathway and stabilizes rhythm in the anoxic-reoxygenated embryonic heart », *Basic Res. Cardiol.*, vol. 106, nº 3, p. 355‑369, mai 2011.
[181] V. Barsukevich *et al.*, « Distinct cardioprotective mechanisms of immediate, early and delayed ischaemic postconditioning », *Basic Res. Cardiol.*, vol. 110, nº 1, janv. 2015.
[182] G. Heusch, J. Musiolik, N. Gedik, et A. Skyschally, « Mitochondrial STAT3 Activation and Cardioprotection by Ischemic Postconditioning in Pigs With Regional Myocardial Ischemia/Reperfusion », *Circ. Res.*, vol. 109, nº 11, p. 1302‑1308, nov. 2011.
[183] A. Das, F. N. Salloum, D. Durrant, R. Ockaili, et R. C. Kukreja, « Rapamycin protects against myocardial ischemia–reperfusion injury through JAK2–STAT3 signaling pathway », *J. Mol. Cell. Cardiol.*, vol. 53, nº 6, p. 858‑869, déc. 2012.
[184] Q.-R. Qi et Z.-M. Yang, « Regulation and function of signal transducer and activator of transcription 3 », *World J. Biol. Chem.*, vol. 5, nº 2, p. 231‑239, mai 2014.
[185] F. A. Zouein, R. Altara, Q. Chen, E. J. Lesnefsky, M. Kurdi, et G. W. Booz, « Pivotal Importance of STAT3 in Protecting the Heart from Acute and Chronic Stress: New Advancement and Unresolved Issues », *Front. Cardiovasc. Med.*, vol. 2, p. 36, 2015.
[186] C. Schindler, « JAK-STAT signaling in human disease », *J. Clin. Invest.*, vol. 109, nº 9, p. 7, 2002.

[187] F. A. Zouein, M. Kurdi, et G. W. Booz, « Dancing rhinos in stilettos: The amazing saga of the genomic and nongenomic actions of STAT3 in the heart », *JAK-STAT*, vol. 2, nº 3, p. e24352, juill. 2013.
[188] K. Boengler, D. Hilfiker-Kleiner, H. Drexler, G. Heusch, et R. Schulz, « The myocardial JAK/STAT pathway: From protection to failure », *Pharmacol. Ther.*, vol. 120, nº 2, p. 172‑185, nov. 2008.
[189] C. P. Lim et X. Cao, « Regulation of Stat3 Activation by MEK Kinase 1 », *J. Biol. Chem.*, vol. 276, nº 24, p. 21004‑21011, juin 2001.
[190] X. Zhang, J. Blenis, H. C. Li, C. Schindler, et S. Chen-Kiang, « Requirement of serine phosphorylation for formation of STAT-promoter complexes », *Science*, vol. 267, nº 5206, p. 1990‑1994, mars 1995.
[191] Z. Wen, Z. Zhong, et J. E. Darnell, « Maximal activation of transcription by statl and stat3 requires both tyrosine and serine phosphorylation », *Cell*, vol. 82, nº 2, p. 241‑250, juill. 1995.
[192] Z. Wen et J. E. Darnell, « Mapping of Stat3 serine phosphorylation to a single residue (727) and evidence that serine phosphorylation has no influence on DNA binding of Stat1 and Stat3 », *Nucleic Acids Res.*, vol. 25, nº 11, p. 2062‑2067, juin 1997.
[193] B. B. Aggarwal *et al.*, « Signal transducer and activator of transcription-3, inflammation, and cancer: how intimate is the relationship? », *Ann. N. Y. Acad. Sci.*, vol. 1171, p. 59‑76, août 2009.
[194] J. Chung, E. Uchida, T. C. Grammer, et J. Blenis, « STAT3 serine phosphorylation by ERK-dependent and -independent pathways negatively modulates its tyrosine phosphorylation. », *Mol. Cell. Biol.*, vol. 17, nº 11, p. 6508‑6516, nov. 1997.
[195] N. Jain, T. Zhang, S. L. Fong, C. P. Lim, et X. Cao, « Repression of Stat3 activity by activation of mitogen-activated protein kinase (MAPK) », *Oncogene*, vol. 17, nº 24, p. 3157‑3167, déc. 1998.
[196] P. Tammineni, C. Anugula, F. Mohammed, M. Anjaneyulu, A. C. Larner, et N. B. V. Sepuri, « The Import of the Transcription Factor STAT3 into Mitochondria Depends on GRIM-19, a Component of the Electron Transport Chain », *J. Biol. Chem.*, vol. 288, nº 7, p. 4723‑4732, févr. 2013.
[197] S. Ray, I. Boldogh, et A. R. Brasier, « STAT3 NH2-terminal acetylation is activated by the hepatic acute-phase response and required for IL-6 induction of angiotensinogen », *Gastroenterology*, vol. 129, nº 5, p. 1616‑1632, nov. 2005.
[198] S. Ray, C. Lee, T. Hou, I. Boldogh, et A. R. Brasier, « Requirement of histone deacetylase1 (HDAC1) in signal transducer and activator of transcription 3 (STAT3) nucleocytoplasmic distribution », *Nucleic Acids Res.*, vol. 36, nº 13, p. 4510‑4520, août 2008.
[199] Z.-L. Yuan, Y.-J. Guan, D. Chatterjee, et Y. E. Chin, « Stat3 dimerization regulated by reversible acetylation of a single lysine residue », *Science*, vol. 307, nº 5707, p. 269‑273, janv. 2005.
[200] J. Schust, B. Sperl, A. Hollis, T. U. Mayer, et T. Berg, « Stattic: a small-molecule inhibitor of STAT3 activation and dimerization », *Chem. Biol.*, vol. 13, nº 11, p. 1235‑1242, nov. 2006.
[201] H. Song, R. Wang, S. Wang, et J. Lin, « A low-molecular-weight compound discovered through virtual database screening inhibits Stat3 function in breast cancer cells », *Proc. Natl. Acad. Sci. U. S. A.*, vol. 102, nº 13, p. 4700‑4705, mars 2005.
[202] K. Siddiquee *et al.*, « Selective chemical probe inhibitor of Stat3, identified through structure-based virtual screening, induces antitumor activity », *Proc. Natl. Acad. Sci. U. S. A.*, vol. 104, nº 18, p. 7391‑7396, mai 2007.

[203] R. Bolli *et al.*, « A murine model of inducible, cardiac-specific deletion of STAT3: its use to determine the role of STAT3 in the upregulation of cardioprotective proteins by ischemic preconditioning », *J. Mol. Cell. Cardiol.*, vol. 50, nº 4, p. 589‑597, avr. 2011.
[204] K. Takeda *et al.*, « Targeted disruption of the mouse Stat3 gene leads to early embryonic lethality », *Proc. Natl. Acad. Sci.*, vol. 94, nº 8, p. 3801‑3804, avr. 1997.
[205] S. Akira, « Functional Roles of STAT Family Proteins: Lessons from Knockout Mice », *STEM CELLS*, vol. 17, nº 3, p. 138‑146, 1999.
[206] J. J. Jacoby *et al.*, « Cardiomyocyte-restricted knockout of STAT3 results in higher sensitivity to inflammation, cardiac fibrosis, and heart failure with advanced age », *Proc. Natl. Acad. Sci.*, vol. 100, nº 22, p. 12929‑12934, oct. 2003.
[207] V. Poli et A. Camporeale, « STAT3-Mediated Metabolic Reprograming in Cellular Transformation and Implications for Drug Resistance », *Front. Oncol.*, vol. 5, juin 2015.
[208] M. Demaria, A. Camporeale, et V. Poli, « STAT3 and metabolism: How many ways to use a single molecule?: STAT3 and Metabolism », *Int. J. Cancer*, vol. 135, nº 9, p. 1997‑2003, nov. 2014.
[209] M. Bernier *et al.*, « Negative regulation of STAT3 protein-mediated cellular respiration by SIRT1 protein », *J. Biol. Chem.*, vol. 286, nº 22, p. 19270‑19279, juin 2011.
[210] J. Wegrzyn *et al.*, « Function of Mitochondrial Stat3 in Cellular Respiration », *Science*, vol. 323, nº 5915, p. 793‑797, févr. 2009.
[211] D. J. Gough, A. Corlett, K. Schlessinger, J. Wegrzyn, A. C. Larner, et D. E. Levy, « Mitochondrial STAT3 supports Ras-dependent oncogenic transformation », *Science*, vol. 324, nº 5935, p. 1713‑1716, juin 2009.
[212] K. Boengler, D. Hilfiker-Kleiner, G. Heusch, et R. Schulz, « Inhibition of permeability transition pore opening by mitochondrial STAT3 and its role in myocardial ischemia/reperfusion », *Basic Res. Cardiol.*, vol. 105, nº 6, p. 771‑785, nov. 2010.
[213] J. McCormick *et al.*, « Free radical scavenging inhibits STAT phosphorylation following *in vivo* ischemia/reperfusion injury », *FASEB J.*, vol. 20, nº 12, p. 2115‑2117, oct. 2006.
[214] S. Negoro, « Activation of JAK/STAT pathway transduces cytoprotective signal in rat acute myocardial infarction », *Cardiovasc. Res.*, vol. 47, nº 4, p. 797‑805, sept. 2000.
[215] D. Hilfiker-Kleiner *et al.*, « Signal transducer and activator of transcription 3 is required for myocardial capillary growth, control of interstitial matrix deposition, and heart protection from ischemic injury », *Circ. Res.*, vol. 95, nº 2, p. 187‑195, juill. 2004.
[216] K. Yamauchi-Takihara et T. Kishimoto, « A Novel Role for STAT3 in Cardiac Remodeling », *Trends Cardiovasc. Med.*, vol. 10, nº 7, p. 298‑303, oct. 2000.
[217] T. Omura *et al.*, « Myocardial ischemia activates the JAK-STAT pathway through angiotensin II signaling in in vivo myocardium of rats », *J. Mol. Cell. Cardiol.*, vol. 33, nº 2, p. 307‑316, févr. 2001.
[218] M. Fuchs *et al.*, « Role of interleukin-6 for LV remodeling and survival after experimental myocardial infarction », *FASEB J. Off. Publ. Fed. Am. Soc. Exp. Biol.*, vol. 17, nº 14, p. 2118‑2120, nov. 2003.
[219] Y. Fujio *et al.*, « Glycoprotein 130 cytokine signal as a therapeutic target against cardiovascular diseases », *J. Pharmacol. Sci.*, vol. 117, nº 4, p. 213‑222, 2011.
[220] P. Fischer et D. Hilfiker-Kleiner, « Survival pathways in hypertrophy and heart failure: The gp130-STAT3 axis », *Basic Res. Cardiol.*, vol. 102, nº 5, p. 393‑411, sept. 2007.
[221] K. E. O'Sullivan, E. P. Breen, H. C. Gallagher, D. J. Buggy, et J. P. Hurley, « Understanding STAT3 signaling in cardiac ischemia », *Basic Res. Cardiol.*, vol. 111, nº 3, p. 27, mai 2016.

[222] S. Negoro *et al.*, « Activation of signal transducer and activator of transcription 3 protects cardiomyocytes from hypoxia/reoxygenation-induced oxidative stress through the upregulation of manganese superoxide dismutase », *Circulation*, vol. 104, nº 9, p. 979‑981, août 2001.
[223] A. Haghikia *et al.*, « Signal transducer and activator of transcription 3-mediated regulation of miR-199a-5p links cardiomyocyte and endothelial cell function in the heart: a key role for ubiquitin-conjugating enzymes », *Eur. Heart J.*, vol. 32, nº 10, p. 1287‑1297, mai 2011.
[224] K. Boengler, E. Ungefug, G. Heusch, et R. Schulz, « The STAT3 inhibitor stattic impairs cardiomyocyte mitochondrial function through increased reactive oxygen species formation », *Curr. Pharm. Des.*, vol. 19, nº 39, p. 6890‑6895, 2013.
[225] Y.-T. Xuan *et al.*, « Mechanism of cyclooxygenase-2 upregulation in late preconditioning », *J. Mol. Cell. Cardiol.*, vol. 35, nº 5, p. 525‑537, mai 2003.
[226] H. Qiu *et al.*, « H11 kinase/heat shock protein 22 deletion impairs both nuclear and mitochondrial functions of STAT3 and accelerates the transition into heart failure on cardiac overload », *Circulation*, vol. 124, nº 4, p. 406‑415, juill. 2011.
[227] D. Enomoto, M. Obana, A. Miyawaki, M. Maeda, H. Nakayama, et Y. Fujio, « Cardiac-specific ablation of the STAT3 gene in the subacute phase of myocardial infarction exacerbated cardiac remodeling », *Am. J. Physiol. Heart Circ. Physiol.*, vol. 309, nº 3, p. H471-480, août 2015.
[228] B. Carow et M. E. Rottenberg, « SOCS3, a Major Regulator of Infection and Inflammation », *Front. Immunol.*, vol. 5, 2014.
[229] D. Hilfiker-Kleiner *et al.*, « Continuous glycoprotein-130-mediated signal transducer and activator of transcription-3 activation promotes inflammation, left ventricular rupture, and adverse outcome in subacute myocardial infarction », *Circulation*, vol. 122, nº 2, p. 145‑155, juill. 2010.
[230] P. J. Murray, « STAT3-mediated anti-inflammatory signalling », *Biochem. Soc. Trans.*, vol. 34, nº 6, p. 1028‑1031, déc. 2006.
[231] A. P. Hutchins, D. Diez, et D. Miranda-Saavedra, « The IL-10/STAT3-mediated anti-inflammatory response: recent developments and future challenges », *Brief. Funct. Genomics*, vol. 12, nº 6, p. 489‑498, nov. 2013.
[232] C. A. Fielding *et al.*, « IL-6 regulates neutrophil trafficking during acute inflammation via STAT3 », *J. Immunol. Baltim. Md 1950*, vol. 181, nº 3, p. 2189‑2195, août 2008.
[233] T.-M. Lee *et al.*, « Preconditioned adipose-derived stem cells ameliorate cardiac fibrosis by regulating macrophage polarization in infarcted rat hearts through the PI3K/STAT3 pathway », *Lab. Invest.*, p. 1, janv. 2019.
[234] T.-M. Lee, N.-C. Chang, et S.-Z. Lin, « Dapagliflozin, a selective SGLT2 Inhibitor, attenuated cardiac fibrosis by regulating the macrophage polarization via STAT3 signaling in infarcted rat hearts », *Free Radic. Biol. Med.*, vol. 104, p. 298‑310, mars 2017.
[235] K. Shirakawa *et al.*, « IL (Interleukin)-10–STAT3–Galectin-3 Axis Is Essential for Osteopontin-Producing Reparative Macrophage Polarization After Myocardial Infarction », *Circulation*, oct. 2018.
[236] T. D. O'Connell, M. C. Rodrigo, et P. C. Simpson, « Isolation and Culture of Adult Mouse Cardiac Myocytes », in *Cardiovascular Proteomics*, vol. 357, New Jersey: Humana Press, 2006, p. 271‑296.
[237] J. Vandesompele *et al.*, « Accurate normalization of real-time quantitative RT-PCR data by geometric averaging of multiple internal control genes », *Genome Biol.*, vol. 3, nº 7, p. RESEARCH0034, juin 2002.

[238] A. Franceschini *et al.*, « STRING v9.1: protein-protein interaction networks, with increased coverage and integration », *Nucleic Acids Res.*, vol. 41, nº Database issue, p. D808-815, janv. 2013.
[239] X. Cheng, C. Peuckert, et S. Wölfl, « Essential role of mitochondrial Stat3 in p38MAPK mediated apoptosis under oxidative stress », *Sci. Rep.*, vol. 7, nov. 2017.
[240] L. M. LaFave et R. L. Levine, « JAK2 the future: therapeutic strategies for JAK-dependent malignancies », *Trends Pharmacol. Sci.*, vol. 33, nº 11, p. 574‑582, nov. 2012.
[241] N. Sato *et al.*, « Physical and functional interactions between STAT3 and ZIP kinase », *Int. Immunol.*, vol. 17, nº 12, p. 1543‑1552, déc. 2005.
[242] Z. Wen, Z. Zhong, et J. E. Darnell, « Maximal activation of transcription by statl and stat3 requires both tyrosine and serine phosphorylation », *Cell*, vol. 82, nº 2, p. 241‑250, juill. 1995.
[243] J. Wegrzyn *et al.*, « Function of mitochondrial Stat3 in cellular respiration », *Science*, vol. 323, nº 5915, p. 793‑797, févr. 2009.
[244] L. Gomez *et al.*, « Inhibition of mitochondrial permeability transition improves functional recovery and reduces mortality following acute myocardial infarction in mice », *Am. J. Physiol.-Heart Circ. Physiol.*, vol. 293, nº 3, p. H1654‑H1661, sept. 2007.
[245] D. J. Hausenloy, H. L. Maddock, G. F. Baxter, et D. M. Yellon, « Inhibiting mitochondrial permeability transition pore opening: a new paradigm for myocardial preconditioning? », *Cardiovasc. Res.*, vol. 55, nº 3, p. 534‑543, août 2002.
[246] S. A. Javadov, S. Clarke, M. Das, E. J. Griffiths, K. H. H. Lim, et A. P. Halestrap, « Ischaemic preconditioning inhibits opening of mitochondrial permeability transition pores in the reperfused rat heart », *J. Physiol.*, vol. 549, nº Pt 2, p. 513‑524, juin 2003.
[247] K. Szczepanek *et al.*, « Cardioprotective function of mitochondrial-targeted and transcriptionally inactive STAT3 against ischemia and reperfusion injury », *Basic Res. Cardiol.*, vol. 110, nº 6, p. 53, nov. 2015.
[248] Q. Zhang *et al.*, « Mitochondrial localized Stat3 promotes breast cancer growth via phosphorylation of serine 727 », *J. Biol. Chem.*, vol. 288, nº 43, p. 31280‑31288, oct. 2013.
[249] L. Avalle *et al.*, « STAT3 localizes to the ER, acting as a gatekeeper for ER-mitochondrion Ca2+ fluxes and apoptotic responses », *Cell Death Differ.*, juill. 2018.
[250] L. Avalle et V. Poli, « Nucleus, Mitochondrion, or Reticulum? STAT3 à La Carte », *Int. J. Mol. Sci.*, vol. 19, nº 9, p. 2820, sept. 2018.
[251] R. Harisseh *et al.*, « Unacylated ghrelin analog prevents myocardial reperfusion injury independently of permeability transition pore », *Basic Res. Cardiol.*, vol. 112, nº 1, p. 4, déc. 2016.
[252] A. Gharib *et al.*, « Opposite and tissue-specific effects of coenzyme Q2 on mPTP opening and ROS production between heart and liver mitochondria: Role of complex I », *J. Mol. Cell. Cardiol.*, vol. 52, nº 5, p. 1091‑1095, mai 2012.
[253] M. R. Wieckowski, C. Giorgi, M. Lebiedzinska, J. Duszynski, et P. Pinton, « Isolation of mitochondria-associated membranes and mitochondria from animal tissues and cells », *Nat. Protoc.*, vol. 4, nº 11, p. 1582‑1590, nov. 2009.
[254] D. De Paulis *et al.*, « Cyclosporine A at reperfusion fails to reduce infarct size in the in vivo rat heart », *Basic Res. Cardiol.*, vol. 108, nº 5, p. 379, août 2013.
[255] G. Bidaux *et al.*, « FRET Image Correlation Spectroscopy Reveals RNAPII-Independent P-TEFb Recruitment on Chromatin », *Biophys. J.*, vol. 114, nº 3, p. 522‑533, févr. 2018.
[256] K. Boengler, « Ischemia/reperfusion injury: The benefit of having STAT3 in the heart », *J. Mol. Cell. Cardiol.*, vol. 50, nº 4, p. 587‑588, avr. 2011.
[257] A. J. Tompkins, L. S. Burwell, S. B. Digerness, C. Zaragoza, W. L. Holman, et P. S. Brookes, « Mitochondrial dysfunction in cardiac ischemia–reperfusion injury: ROS

from complex I, without inhibition », *Biochim. Biophys. Acta BBA - Mol. Basis Dis.*, vol. 1762, nº 2, p. 223‑231, févr. 2006.
[258] D. Phillips *et al.*, « Stoichiometry of STAT3 and mitochondrial proteins: Implications for the regulation of oxidative phosphorylation by protein-protein interactions », *J. Biol. Chem.*, vol. 285, nº 31, p. 23532‑23536, juill. 2010.
[259] I. Sanseverino, C. Purificato, M. C. Gauzzi, et S. Gessani, « Revisiting the specificity of small molecule inhibitors: the example of stattic in dendritic cells », *Chem. Biol.*, vol. 19, nº 10, p. 1213‑1214; author reply 1215-1216, oct. 2012.
[260] R. Yang *et al.*, « Mitochondrial Ca2+ and membrane potential, an alternative pathway for Interleukin 6 to regulate CD4 cell effector function », *eLife*, vol. 4, mai 2015.
[261] K. E. O'Sullivan, E. P. Breen, H. C. Gallagher, D. J. Buggy, et J. P. Hurley, « Understanding STAT3 signaling in cardiac ischemia », *Basic Res. Cardiol.*, vol. 111, nº 3, mai 2016.
[262] M. Dasgupta, J. K. T. Dermawan, B. Willard, et G. R. Stark, « STAT3-driven transcription depends upon the dimethylation of K49 by EZH2 », *Proc. Natl. Acad. Sci. U. S. A.*, vol. 112, nº 13, p. 3985‑3990, mars 2015.
[263] B. B. Ding *et al.*, « Constitutively activated STAT3 promotes cell proliferation and survival in the activated B-cell subtype of diffuse large B-cell lymphomas », *Blood*, vol. 111, nº 3, p. 1515‑1523, oct. 2007.
[264] D. E. Levy et C. Lee, « What does Stat3 do? », *J. Clin. Invest.*, vol. 109, nº 9, p. 1143‑1148, mai 2002.
[265] G. Niu *et al.*, « Signal transducer and activator of transcription 3 is required for hypoxia-inducible factor-1alpha RNA expression in both tumor cells and tumor-associated myeloid cells », *Mol. Cancer Res. MCR*, vol. 6, nº 7, p. 1099‑1105, juill. 2008.
[266] G. Hu, X. Huang, K. Zhang, H. Jiang, et X. Hu, « Anti-inflammatory Effect of B-Type Natriuretic Peptide Postconditioning During Myocardial Ischemia–Reperfusion: Involvement of PI3K/Akt Signaling Pathway », *Inflammation*, vol. 37, nº 5, p. 1669‑1674, oct. 2014.
[267] J. Xiong *et al.*, « Postconditioning with α7nAChR Agonist Attenuates Systemic Inflammatory Response to Myocardial Ischemia–Reperfusion Injury in Rats », *Inflammation*, vol. 35, nº 4, p. 1357‑1364, août 2012.
[268] H. Chen *et al.*, « Ischemic postconditioning attenuates inflammation in rats following renal ischemia and reperfusion injury », *Exp. Ther. Med.*, vol. 10, nº 2, p. 513‑518, août 2015.
[269] Y.-H. Kim, D.-W. Yoon, J.-H. Kim, J.-H. Lee, et C.-H. Lim, « Effect of remote ischemic post-conditioning on systemic inflammatory response and survival rate in lipopolysaccharide-induced systemic inflammation model », *J. Inflamm.*, vol. 11, nº 1, p. 16, mai 2014.
[270] K.-X. Liu *et al.*, « Immediate postconditioning during reperfusion attenuates intestinal injury », *Intensive Care Med.*, vol. 35, nº 5, p. 933, févr. 2009.
[271] B. Xing *et al.*, « Ischemic post-conditioning protects brain and reduces inflammation in a rat model of focal cerebral ischemia/reperfusion », *J. Neurochem.*, vol. 105, nº 5, p. 1737‑1745, 2008.
[272] E. Forte, M. B. Furtado, et N. Rosenthal, « The interstitium in cardiac repair: role of the immune–stromal cell interplay », *Nat. Rev. Cardiol.*, vol. 15, nº 10, p. 601, oct. 2018.
[273] M. Ichiba, K. Nakajima, Y. Yamanaka, N. Kiuchi, et T. Hirano, « Autoregulation of the Stat3 Gene through Cooperation with a cAMP-responsive Element-binding Protein », *J. Biol. Chem.*, vol. 273, nº 11, p. 6132‑6138, mars 1998.

[274] Y. Miyao *et al.*, « Elevated plasma interleukin-6 levels in patients with acute myocardial infarction », *Am. Heart J.*, vol. 126, nº 6, p. 1299‑1304, déc. 1993.